

Completeness of the ZX-calculus



Quanlong Wang
Wolfson College
University of Oxford

A thesis submitted for the degree of

Doctor of Philosophy

Hilary 2018

Acknowledgements

Firstly, I would like to express my sincere gratitude to my supervisor Bob Coecke for all his huge help, encouragement, discussions and comments. I can not imagine what my life would have been like without his great assistance.

Great thanks to my colleague, co-author and friend Kang Feng Ng, for the valuable cooperation in research and his helpful suggestions in my daily life.

My sincere thanks also goes to Amar Hadzihasanovic, who has kindly shared his idea and agreed to cooperate on writing a paper based on his results.

Many thanks to Simon Perdrix, from whom I have learned a lot and received much help when I worked with him in Nancy, while still benefitting from this experience in Oxford.

I would also like to thank Miriam Backens for loads of useful discussions, advertising for my talk in QPL and helping me on latex problems.

Special thanks to Dan Marsden for his patience and generousness in answering my questions and giving suggestions.

I would like to thank Xiaoning Bian for always being ready to help me solve problems in using latex and other softwares.

I also wish to thank all the people who attended the weekly ZX meeting for many interesting discussions.

I am also grateful to my college advisor Jonathan Barrett and department advisor Jamie Vicary, thank you for chatting with me about my research and my life.

I particularly want to thank my examiners, Ross Duncan and Sam Staton, for their very detailed and helpful comments and corrections by which this thesis has been significantly improved.

I am thankful to the Department for Computer Science and Wolfson College, for their kind help and support.

Last but not the least, I would like to thank my family: my parents, my wife and my daughters for supporting me throughout writing this thesis and my life in general.

Abstract

The ZX-calculus is an intuitive but also mathematically strict graphical language for quantum computing, which is especially powerful for the framework of quantum circuits. Completeness of the ZX-calculus means any equality of matrices with size powers of n can be derived purely diagrammatically.

In this thesis, we give the first complete axiomatisation of the ZX-calculus for the overall pure qubit quantum mechanics, via a translation from the completeness result of another graphical language for quantum computing— the ZW-calculus. This paves the way for automated pictorial quantum computing, with the aid of some software like Quantomatic.

Based on this universal completeness, we directly obtain a complete axiomatisation of the ZX-calculus for the Clifford+T quantum mechanics, which is approximately universal for quantum computing, by restricting the ring of complex numbers to its subring corresponding to the Clifford+T fragment resting on the completeness theorem of the ZW-calculus for arbitrary commutative ring.

Furthermore, we prove the completeness of the ZX-calculus (with just 9 rules) for 2-qubit Clifford+T circuits by verifying the complete set of 17 circuit relations in diagrammatic rewriting. This is an important step towards efficient simplification of general n -qubit Clifford+T circuits, considering that we now have all the necessary rules for diagrammatical quantum reasoning and a very simple construction of Toffoli gate within our axiomatisation framework, which is approximately universal for quantum computation together with the Hadamard gate.

In addition to completeness results within the qubit related formalism, we extend the completeness of the ZX-calculus for qubit stabilizer quantum mechanics to the qutrit stabilizer system.

Finally, we show with some examples the application of the ZX-calculus to the proof of generalised supplementarity, the representation of entanglement

classification and Toffoli gate, as well as equivalence-checking for the UMA gate.

Contents

1	Introduction	1
2	Background	5
2.1	Some concepts from category theory	5
2.2	ZX-calculus	9
2.2.1	ZX-calculus in general	9
2.2.2	Qubit ZX-calculus	12
2.2.3	Some known completeness results of the qubit ZX-calculus	17
2.3	ZW-calculus	17
3	Completeness for full qubit quantum mechanics	22
3.1	ZX_{full} -calculus	22
3.2	Simplification of the rules of from the ZX_{full} -calculus	29
3.2.1	Simplified rules for the ZX_{full} -calculus	35
3.3	Interpretations between the ZX_{full} -calculus and the ZW_C -calculus	38
3.4	Completeness	41
3.5	Proof of proposition 3.4.1	43
4	Completeness for Clifford+T qubit quantum mechanics	58
4.1	ZX_{C+T} -calculus	59
4.2	Translations between the ZX_{C+T} -calculus and the ZW_T -calculus	64
4.3	Completeness	68
5	Completeness for 2-qubit Clifford+T circuits	74
5.1	Complete relations for 2-qubit Clifford+T quantum circuits	75
5.2	The ZX-calculus for 2-qubit Clifford+T quantum circuits	77
5.3	Verification of the complete relations in the ZX-calculus	78
5.3.1	Derivation of the (P) rule	78
5.3.2	Proof of completeness for 2-qubit Clifford+T quantum circuits	83

6	Completeness for qutrit stabilizer quantum mechanics	93
6.1	Qutrit Stabilizer quantum mechanics	94
6.1.1	The generalized Pauli group and Clifford group	94
6.1.2	Graph states	95
6.2	Qutrit ZX-calculus	96
6.2.1	The ZX-calculus for general pure state qutrit quantum mechanics	96
6.2.2	Qutrit stabilizer quantum mechanics in the ZX-calculus	102
6.3	Qutrit graph states in the ZX-calculus	112
6.3.1	Stabilizer state diagram and transformations of GS-LC diagrams	112
6.3.2	Rewriting arbitrary stabilizer state diagram into a GS-LC diagram	114
6.3.3	Reduced GS-LC diagrams	126
6.3.4	Transformations of rGS-LC diagrams	134
6.4	Completeness	138
6.4.1	Comparing rGS-LC diagrams	138
6.4.2	Completeness for qutrit stabilizer quantum mechanics	146
7	Some applications of the ZX-calculus	148
7.1	Proof of the generalised supplementarity	148
7.2	3-entanglement qubit states	151
7.3	Representation of Toffoli gate	155
7.4	Equivalence-checking for the UMA gate	158
8	Conclusions and further work	162
	Bibliography	165

Chapter 1

Introduction

There are two paradigms for western metaphysics: substances and processes. The substance metaphysics sees objects as the basic constituents of the universe, while the process metaphysics take processes rather than objects as fundamental [68]. Meanwhile, an influential eastern philosophy—the Madhyamaka philosophy [55], has the key idea that all things (dharmas) are empty of substance or essence (svabhāva) because of dependent arising (Pratītyasamutpāda), thus similar to the opinion of process metaphysics. Following the spirit of the process philosophy and the Madhyamaka philosophy, we think the theory of processes has scientific and philosophical advantages, especially for its application in quantum physics. In fact, if we treat quantum processes as transformations between different types of quantum systems and highlight the compositions of processes, then we arrive at the theory of categorical quantum mechanics (CQM) proposed by Abramsky and Coecke [2]. Therein the theory of processes can be made strict in the mathematical framework of symmetric monoidal categories [50]. It would be of great interest to know how processes could be fundamental while objects being less important in a mathematical formulation of process theory for quantum mechanics. To see this, we need some concepts from category theory. This part will be illustrated in Chapter 2, standard references for which can be found in [50] and [11].

Now we give a introduction to the main theme of this thesis—the ZX-calculus. The ZX-calculus introduced by Coecke and Duncan [14, 15] is an intuitive yet mathematically strict graphical language for quantum computing: it is formulated within the framework of compact closed categories which has a rigorous underpinning for graphical calculus [46], meanwhile being an important branch of CQM [2]. Notably, it has simple rewriting rules to transform diagrams from one to another. Each diagram in the ZX-calculus has a so-called standard interpretation [59], in finite-dimensional Hilbert spaces [63], thus makes it relevant for quantum computing. For the past ten years, the ZX-calculus has enjoyed success in applying to fields of quantum information and quantum computation (QIC) [58],

in particular (topological) measurement-based quantum computing [27, 36] and quantum error correction [25, 13]. Very recently, the ZX-calculus is also used for reducing the cost of implementing quantum programs [40].

It is clear that the usefulness of the ZX-calculus is based on the properties of this theory. There are three main properties of the ZX-calculus: soundness, universality and completeness. Soundness means that all the rules in the ZX-calculus have a correct standard interpretation in the Hilbert spaces. Universality is about if there exists a ZX-calculus diagram for every linear map in Hilbert spaces under the standard interpretation. Completeness refers to whether an equation of diagrams can be derived in the ZX-calculus when their corresponding equation of linear maps under the standard interpretation holds true.

In the framework of category theory, the ZX-calculus is just a PROP [10], and a Hilbert space model of the ZX-calculus is a symmetric monoidal category that is equivalent to a PROP, with objects generated by (tensor powers of) a Hilbert space of dimension $d > 1$ (called qubit model for $d = 2$ and qudit model for $d > 2$). The three main properties of the ZX-calculus are just about the properties of the interpretation from the ZX-calculus to its Hilbert space model : soundness means that this interpretation is a symmetric monoidal functor, while universality and completeness mean this functor is a full and faithful functor respectively.

The property that the ZX-calculus is sound relative to the qubit and qudit model has been shown in [15] and [60] respectively. The universality of the ZX-calculus as to the qubit and qudit model has also been shown in [15] and [70] respectively. The ZX-calculus has been proved to be complete for qubit stabilizer quantum mechanics (qubit model) [3], and recently further axiomatised to be complete for qubit Clifford +T quantum mechanics [42], an approximatively universal fragment of quantum mechanics which has been widely used in quantum computing [12].

The axiomatisation given in [42] relies on a complicated translation from the ZX-calculus to another graphical calculus—the ZW-calculus [32]. As a result that the ZX-calculus is not easy to use for exploring properties of multipartite entangled quantum states, Coecke and Kissinger propose a new graphical calculus called GHZ/W-calculus which is based on the interaction of special commutative Frobenius algebras induced by GHZ-states and anti-special commutative Frobenius algebras induced by W-states [19]. In [32], Hadzihasanovic extends the GHZ/W-calculus into the ZW-calculus with diagrams corresponding to integer matrices, modelling on the ZX-calculus. Most importantly, the ZW-calculus is proved to be complete for pure qubit states with integer coefficients. It was just based on this completeness result that Jeandel, Perdrix and Vilmart were able to give a complete axiomatisation of the ZX-calculus for the Clifford +T quantum mechanics.

However, even with all the rules from the complete axiomatisation for qubit Clifford +T quantum mechanics, the ZX-calculus is still incomplete for the overall qubit quantum mechanics, as suggested in [61] and proved in [43]. On the other hand, the ZW-calculus is generalised to a new version ZW_R -calculus where R is an arbitrary commutative ring, and the ZW_R -calculus is proved to be complete for R -bits (analogues of qubits with coefficients in R) [33].

In this thesis, further to the result of [42], we give the first complete axiomatisation of the ZX-calculus for the overall qubit quantum mechanics (which will be called ZX_{full} -calculus in this thesis) [56], based on the completeness result of $ZW_{\mathbb{C}}$ -calculus, where \mathbb{C} is the field of complex numbers. In view of our results, there comes the paper [43] afterwards which also give an axiomatisation of the ZX-calculus for the entire qubit quantum mechanics, with different generators of diagrams and rewriting rules. Chapter 2 of this thesis will show the details of the complete axiomatisation of the ZX_{full} -calculus.

Given the complete axiomatisation of the ZX_{full} -calculus [56], we also obtain a complete axiomatisation of the ZX-calculus for the Clifford+T quantum mechanics (which will be called ZX_{C+T} -calculus in this thesis) by restricting the ring \mathbb{C} to its subring $\mathbb{Z}[i, \frac{1}{\sqrt{2}}]$ which exactly corresponds to the Clifford+T fragment, resting on the completeness theorem of the ZW_R -calculus. In contrast to the first complete axiomatisation of the ZX-calculus for the Clifford+T fragment [42], we have two new generators—a triangle and a λ box— as features rather than novelties: the triangle can be employed as an essential component to construct a Toffoli gate in a very simple form, while the λ box can be slightly extended to a generalised phase so that the generalised supplementarity (also called cyclotomic supplementarity) [45] is naturally seen as a special case of the generalised spider rule. In addition, due to the introduction of the new generators, our proof for that the Clifford +T fragment of the ZX-calculus exactly corresponds to matrices over the ring $\mathbb{Z}[i, \frac{1}{\sqrt{2}}]$ is much simpler than the corresponding proof given in [42]. These results are shown in detail in Chapter 3.

Considering that Clifford+T quantum circuits are most frequently used in quantum computation, it would be more efficient to use a small set of ZX rules for the purpose of circuit simplification, although the ZX-calculus is complete for both the overall pure qubit quantum mechanics [56] and the Clifford+T pure qubit quantum mechanics [42]. In Chapter 4, we prove the completeness of the ZX-calculus (with just 9 rules) for 2-qubit Clifford+T circuits by verifying the complete set of 17 circuit relations [64] in diagrammatic rewriting. As a consequence, our result can also be seen as a completeness result for single-qubit Clifford+T ZX-calculus [4]. In addition, we are able to give an analytic solution for converting from ZXZ to XZX Euler decompositions of single-qubit unitary gates as suggested by Schröder de Witt and Zamdzhiev [61].

Since there already exist qutrit and general qudit versions of the ZX-calculus [60, 70], it is natural to ask if one could generalise the completeness result of the qubit ZX-calculus to the qudit version for arbitrary dimension d . As for the completeness of the ZX-calculus for the overall and generalised Clifford+T qudit quantum mechanics, there is no result available. Fortunately, the completeness of the ZX-calculus for qubit stabilizer quantum mechanics can be generalised to the qutrit case, which will be shown explicitly in chapter 5.

Having the completeness results established above, it would be interesting to see how it could be applied. In chapter 6, we show by some examples the application of the ZX-calculus to the proof of generalised supplementarity, the representation of entanglement classification and Toffoli gate, as well as equivalence-checking for the UMA gate.

Finally in chapter 7, we conclude this thesis with some open problems.

Chapter 2

Background

In this chapter we give the requisite knowledge of this thesis, which includes the concepts related to category theory, ZX-calculus, and ZW-calculus.

2.1 Some concepts from category theory

In this section, we give some categorical concepts constituting the theoretical framework of this thesis, the standard references for which can be found in [50] and [11].

Category

A category \mathfrak{C} consists of:

- a class of objects $ob(\mathfrak{C})$;
- for each pair of objects A, B , a set $\mathfrak{C}(A, B)$ of morphisms from A to B ;
- for each triple of objects A, B, C , a composition map

$$\begin{array}{ccc} \mathfrak{C}(B, C) \times \mathfrak{C}(A, B) & \longrightarrow & \mathfrak{C}(A, C) \\ (g, f) & \longmapsto & g \circ f; \end{array}$$

- for each object A , an identity morphism $1_A \in \mathfrak{C}(A, A)$,

satisfying the following axioms:

- associativity: for any $f \in \mathfrak{C}(A, B), g \in \mathfrak{C}(B, C), h \in \mathfrak{C}(C, D)$, there holds $(h \circ g) \circ f = h \circ (g \circ f)$;
- identity law: for any $f \in \mathfrak{C}(A, B), 1_B \circ f = f = f \circ 1_A$.

A morphism $f \in \mathfrak{C}(A, B)$ is an *isomorphism* if there exists a morphism $g \in \mathfrak{C}(B, A)$ such that $g \circ f = 1_A$ and $f \circ g = 1_B$. A *product category* $\mathfrak{A} \times \mathfrak{B}$ can be defined componentwise by two categories \mathfrak{A} and \mathfrak{B} .

Functor

Given categories \mathfrak{C} and \mathfrak{D} , a functor $F : \mathfrak{C} \longrightarrow \mathfrak{D}$ consists of:

- a mapping

$$\begin{array}{ccc} \mathfrak{C} & \longrightarrow & \mathfrak{D} \\ A & \mapsto & F(A); \end{array}$$

- for each pair of objects A, B of \mathfrak{C} , a map

$$\begin{array}{ccc} \mathfrak{C}(A, B) & \longrightarrow & \mathfrak{D}(F(A), F(B)) \\ f & \mapsto & F(f), \end{array}$$

satisfying the following axioms:

- preserving composition: for any morphisms $f \in \mathfrak{C}(A, B), g \in \mathfrak{C}(B, C)$, there holds $F(g \circ f) = F(g) \circ F(f)$;
- preserving identity: for any object A of \mathfrak{C} , $F(1_A) = 1_{F(A)}$.

A functor $F : \mathfrak{C} \longrightarrow \mathfrak{D}$ is *faithful (full)* if for each pair of objects A, B of \mathfrak{C} , the map

$$\begin{array}{ccc} \mathfrak{C}(A, B) & \longrightarrow & \mathfrak{D}(F(A), F(B)) \\ f & \mapsto & F(f) \end{array}$$

is injective (surjective).

Natural transformation

Let $F, G : \mathfrak{C} \longrightarrow \mathfrak{D}$ be two functors. A natural transformation $\tau : F \rightarrow G$ is a family $(\tau_A : F(A) \longrightarrow G(A))_{A \in \mathfrak{C}}$ of morphisms in \mathfrak{D} such that the following square commutes:

$$\begin{array}{ccc} F(A) & \xrightarrow{\tau_A} & G(A) \\ F(f) \downarrow & & \downarrow G(f) \\ F(B) & \xrightarrow{\tau_B} & G(B) \end{array}$$

for all morphisms $f \in \mathfrak{C}(A, B)$. A natural isomorphism is a natural transformation where each of the τ_A is an isomorphism.

Strict monoidal category

A strict monoidal category consists of:

- a category \mathfrak{C} ;
- a unit object $I \in \text{ob}(\mathfrak{C})$;
- a bifunctor $- \otimes - : \mathfrak{C} \times \mathfrak{C} \longrightarrow \mathfrak{C}$,

satisfying

- associativity: for each triple of objects A, B, C of \mathfrak{C} , $A \otimes (B \otimes C) = (A \otimes B) \otimes C$; for each triple of morphisms f, g, h of \mathfrak{C} , $f \otimes (g \otimes h) = (f \otimes g) \otimes h$;
- unit law: for each object A of \mathfrak{C} , $A \otimes I = A = I \otimes A$; for each morphism f of \mathfrak{C} , $f \otimes 1_I = f = 1_I \otimes f$.

Strict symmetric monoidal category

A strict monoidal category \mathfrak{C} is symmetric if it is equipped with a natural isomorphism

$$\sigma_{A,B} : A \otimes B \rightarrow B \otimes A$$

for all objects A, B, C of \mathfrak{C} satisfying:

$$\sigma_{B,A} \circ \sigma_{A,B} = 1_{A \otimes B}, \quad \sigma_{A,I} = 1_A, \quad (1_B \otimes \sigma_{A,C}) \circ (\sigma_{A,B} \otimes 1_C) = \sigma_{A,B \otimes C}.$$

Strict monoidal functor

Given two strict monoidal categories \mathfrak{C} and \mathfrak{D} , a strict monoidal functor $F : \mathfrak{C} \longrightarrow \mathfrak{D}$ is a functor $F : \mathfrak{C} \longrightarrow \mathfrak{D}$ such that $F(A) \otimes F(B) = F(A \otimes B)$, $F(f) \otimes F(g) = F(f \otimes g)$, $F(I_{\mathfrak{C}}) = I_{\mathfrak{D}}$, for any objects A, B of \mathfrak{C} , and any morphisms $f \in \mathfrak{C}(A, A_1)$, $g \in \mathfrak{C}(B, B_1)$.

A strict symmetric monoidal functor F is a strict monoidal functor that preserves the symmetry structure, i.e., $F(\sigma_{A,B}) = \sigma_{F(A),F(B)}$.

Self-dual strict compact closed category

A self-dual strict compact closed category is a strict symmetric monoidal category \mathcal{C} such that for each object A of \mathcal{C} , there exists two morphisms

$$\epsilon_A : A \otimes A \rightarrow I, \quad \eta_A : I \rightarrow A \otimes A$$

satisfying:

$$(\epsilon_A \otimes 1_A) \circ (1_A \otimes \eta_A) = 1_A, \quad (1_A \otimes \epsilon_A) \circ (\eta_A \otimes 1_A) = 1_A.$$

Note that here we use the word “self-dual” in the same sense as in [20], instead of the sense in Peter Selinger’s paper [62].

PROP

‘PROP’ is an acronym for ‘products and permutations’, as introduced by Mac Lane [51]. A PROP is a strict symmetric monoidal category having the natural numbers as objects, with the tensor product of objects given by addition. A morphism between two PROPs is a strict symmetric monoidal functor that is the identity on objects [7].

As an example, the category **FinSet** is a PROP whose objects are all finite sets and whose morphisms are all functions between them.

Just as any group can be represented by generators and relations, any PROP can be described as a presentation in terms of generators and relations, which is proved in [7].

Some typical examples of categories in this thesis

- **FdHilb_d**: the category whose objects are complex Hilbert spaces with dimensions d^k , where $d > 1$ is a given integer and k is an arbitrary non-negative integer, and whose morphisms are linear maps between the Hilbert spaces with ordinary composition of linear maps as composition of morphisms. The usual Kronecker tensor product is the monoidal tensor, and the field of complex numbers \mathbb{C} (which is a one-dimensional Hilbert space over itself) is the tensor unit.

For each object of **FdHilb_d**, we can choose an orthonormal basis $\{|i\rangle\}_{0 \leq i \leq d-1}$ denoted in Dirac notation.

- **FdHilb_d/s**: the category which has the same objects as **FdHilb_d** but whose morphisms are equivalence classes of **FdHilb_d**-morphisms, given by the following equivalence relation

$$f \sim g \Leftrightarrow \exists r \in \mathbb{C} \setminus \{0\} \quad \text{such that} \quad f = r \cdot g$$

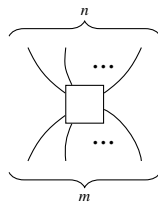
- **Mat $_R$** : the category whose objects are natural numbers and whose morphisms $M : m \rightarrow n$ are $n \times m$ matrices taking values in a given commutative ring R . The composition is matrix multiplication, the monoidal product on objects and morphisms are multiplication of natural numbers and the Kronecker product of matrices respectively.

2.2 ZX-calculus

The ZX-calculus was introduced by Coecke and Duncan in [14, 15] as a graphical language for describing a pair of complementary quantum observables. The key feature of the ZX is that it has intuitive rewriting rules which allow one to transform diagrams from one to another, instead of performing tedious matrix calculations. The original ZX-calculus is designed particularly for qubits [58], then it is generalised to higher dimensions [70, 60]. In this section, we will first give a formal definition of ZX-calculus for arbitrary dimension (called qudit ZX-calculus), then present the details of qubit ZX-calculus and qutrit ZX-calculus, including related properties. Finally we display another graphical language—ZW-calculus in terms of generators and rewriting rules.

2.2.1 ZX-calculus in general

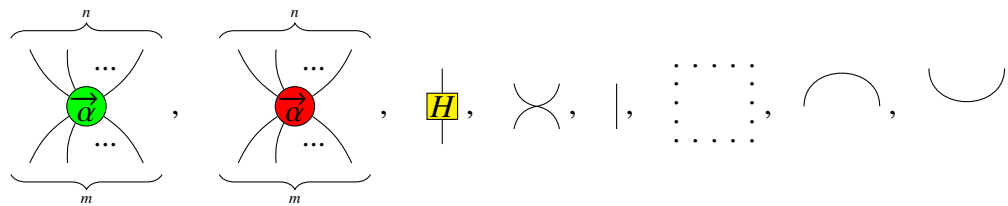
We will describe the ZX-calculus in the framework of PROPs in terms of generators and relations following the way presented in [32]. Explicitly, we build the ZX-calculus in the following way: first we give a set S consisting of basic diagrams including empty diagram and the straight line as generators, where by diagram we mean a picture composed of a vertex, n incoming wires (inputs) and m outgoing wires (outputs):



Note that in this thesis any diagram should be read from top to bottom. Let $ZX[S]$ be the strict monoidal category freely generated by diagrams of S in parallel composition \otimes where any two diagrams D_1 and D_2 are placed side-by-side with D_1 on the left of D_2 ($D_1 \otimes D_2$), or in sequential composition \circ where D_1 has the same number of outputs as the number of inputs of D_2 and D_1 is placed above D_2 with the outputs of D_1 connected to the inputs of D_2 ($D_2 \circ D_1$). It is clear that the empty diagram is a unit of parallel composition

and the diagram of a straight line is a unit of the sequential composition. Then we give an equivalence relation R of diagrams (morphisms) in $ZX[S]$ including the diagrammatical representation (see below) of axioms of a self-dual strict compact closed category. Let $ZX[S]/R$ be the PROP obtained from $ZX[S]$ modulo the equivalence relation R . The pairs in R will be called the rules of $ZX[S]/R$. Furthermore, $ZX[S]/R$ is called a ZX-calculus if

- the generating set S consists of the following basic diagrams:



where $m, n \in \mathbb{N}$, $\vec{\alpha} = (\alpha_1, \dots, \alpha_{d-1})$, $\alpha_i \in [0, 2\pi)$, and the dashed square represents an empty diagram;

- the equivalence relation R consists of two types of rules:

1. the structure rules for a self-dual compact closed category:

$$\cap = \text{loop} \quad \cup = \text{loop} \quad \cup = | = \text{loop} \quad (2.1)$$

$$(2.2)$$

2. non-structural rewriting rules for transforming the generators, typically the spider rule, copy rule, bialgebra rule, Euler decomposition rule, and the colour change rule [15].

For convenience, we have the following short notation:

Since we have the parameter d in the ZX-calculus, we also call it *qudit ZX-calculus* which will be meaningful when we give to it a semantics. It is called *qubit ZX-calculus* if

$d = 2$, and called *qutrit ZX-calculus* if $d = 3$. Also we call a diagram with no inputs and no outputs a *scalar*.

Now we associate to each diagram in the ZX-calculus a standard interpretation $[[\cdot]]$ in \mathbf{FdHilb}_d :

$$\left[\left[\begin{array}{c} \overbrace{}^n \\ \text{---} \\ \text{---} \\ \text{---} \\ \text{---} \\ \text{---} \\ \text{---} \\ \text{---} \\ \underbrace{}_m \end{array} \right] \right] = \sum_{j=0}^{d-1} e^{i\alpha_j} |j\rangle^{\otimes m} \langle j|^{\otimes n}, \alpha_0 = 1,$$

$$\left[\left[\begin{array}{c} \overbrace{}^n \\ \text{---} \\ \text{---} \\ \text{---} \\ \text{---} \\ \text{---} \\ \text{---} \\ \underbrace{}_m \end{array} \right] \right] = \sum_{j=0}^{d-1} e^{i\alpha_j} |h_j\rangle^{\otimes m} \langle h_j|^{\otimes n}, \alpha_0 = 1, |h_j\rangle = \frac{1}{\sqrt{d}} \sum_{k=0}^{d-1} \xi^{jk} |k\rangle, \xi = e^{i\frac{2\pi}{d}},$$

$$\left[\left[\text{---} \right] \right] = \frac{1}{\sqrt{d}} \sum_{i,j=0}^{d-1} \xi^{ji} |j\rangle \langle i|, \quad \left[\left[\begin{array}{c} \vdots \\ \vdots \\ \vdots \\ \vdots \end{array} \right] \right] = 1, \quad \left[\left[\text{---} \right] \right] = \sum_{j=0}^{d-1} |j\rangle \langle j|,$$

$$\left[\left[\text{---} \right] \right] = \sum_{i,j=0}^{d-1} |ji\rangle \langle ij|, \quad \left[\left[\text{---} \right] \right] = \sum_{j=0}^{d-1} |jj\rangle, \quad \left[\left[\text{---} \right] \right] = \sum_{j=0}^{d-1} \langle jj|,$$

$$[[D_1 \otimes D_2]] = [[D_1]] \otimes [[D_2]], \quad [[D_1 \circ D_2]] = [[D_1]] \circ [[D_2]].$$

Now we are ready to define three important properties of the ZX-calculus: soundness, universality and completeness. Note that if a diagram D_1 in the ZX-calculus can be rewritten into another diagram D_2 using the ZX rules, then we denote this as $ZX \vdash D_1 = D_2$.

Definition 2.2.1 The ZX-calculus is called *sound* if for any two diagrams D_1 and D_2 , $ZX \vdash D_1 = D_2$ must imply that $[[D_1]] = [[D_2]]$.

Definition 2.2.2 The ZX-calculus is called *universal* if for any linear map L in \mathbf{FdHilb}_d , there must exist a diagram D in the ZX-calculus such that $[[D]] = L$.

Definition 2.2.3 The ZX-calculus is called *complete* if for any two diagrams D_1 and D_2 , $[[D_1]] = [[D_2]]$ must imply that $ZX \vdash D_1 = D_2$.

Among these three properties, soundness means if an equality of diagrams holds in the ZX-calculus then the corresponding linear maps under the standard interpretation must be the same. Since the derivation of true equalities comes from the rewriting rules, soundness can be checked on a rule-by-rule basis. Secondly, universality means each linear map can be represented by a diagram in the ZX-calculus. Thirdly, completeness means all true equalities of linear maps can be derived graphically.

Proposition 2.2.4 [60] *The qudit ZX-calculus is sound for any $d \geq 2$.*

Proposition 2.2.5 [70] *The qudit ZX-calculus is universal for any $d \geq 2$.*

The proof of the completeness of the ZX-calculus is the main theme of this thesis.

Scalar-free ZX-calculus

A scalar D is called non-zero if $\llbracket D \rrbracket \neq 0$. The ZX-calculus could have a scalar-free version where all the non-zero scalars can be ignored.

Definition 2.2.6 *A scalar-free ZX-calculus is obtained from the ZX-calculus $ZX[S]/R$ modulo an equivalence relation F where two diagrams D_1 and D_2 are in the same equivalent class if there exist non-zero scalars s and t such that $s \otimes D_1 = t \otimes D_2$.*

The standard interpretation $\llbracket \cdot \rrbracket : ZX[S]/R \rightarrow \mathbf{FdHilb}_d$ can be generalised to an interpretation $\llbracket \cdot \rrbracket_{sf} : (ZX[S]/R)/F \rightarrow \mathbf{FdHilb}_d/s$ in a natural way such that the following square commute:

$$\begin{array}{ccc} ZX[S]/R & \twoheadrightarrow & (ZX[S]/R)/F \\ \llbracket \cdot \rrbracket \downarrow & & \downarrow \llbracket \cdot \rrbracket_{sf} \\ \mathbf{FdHilb}_d & \twoheadrightarrow & \mathbf{FdHilb}_d/s \end{array}$$

By the construction of the scalar-free ZX-calculus and the soundness of the qudit ZX-calculus, it is easy to see that the scalar-free ZX-calculus is sound in relative to the interpretation $\llbracket \cdot \rrbracket_{sf}$.

2.2.2 Qubit ZX-calculus

In this subsection, we describe qubit ZX-calculus in detail and give some of its useful properties.

The qubit ZX-calculus has the following generators: where $m, n \in \mathbb{N}$, $\alpha \in [0, 2\pi)$, and e represents an empty diagram.

The qubit ZX-calculus has non-structural rewriting rules as follows:

$R_{Z,\alpha}^{(n,m)} : n \rightarrow m$		$R_{X,\alpha}^{(n,m)} : n \rightarrow m$	
$H : 1 \rightarrow 1$		$\sigma : 2 \rightarrow 2$	
$\mathbb{I} : 1 \rightarrow 1$		$e : 0 \rightarrow 0$	
$C_a : 0 \rightarrow 2$		$C_u : 2 \rightarrow 0$	

Table 2.1: Generators of qubit ZX-calculus

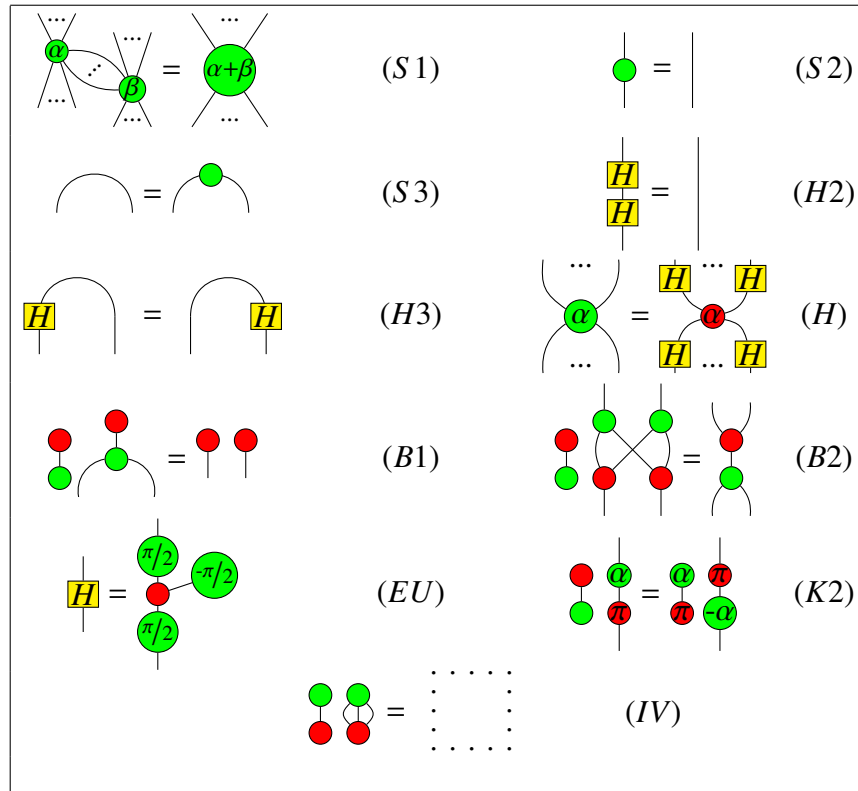


Figure 2.1: Non-structural ZX-calculus rules, where $\alpha, \beta \in [0, 2\pi)$.

Note that all the rules enumerated in Figures 2.1 still hold when they are flipped upside-down. Due to the rule (H) and (H2), the rules in Figure 2.1 have a property that they still hold when the colours green and red swapped. In this thesis, for simplicity, we won't distinguish a rule with its flipped upside-down version or colour swapped version when it

is referred to in a diagrammatic rewriting. The structural rules listed in (2.1) and (2.2) will also be used without being explicitly stated.

If we let $d = 2$ in the standard interpretation of qudit ZX-calculus, then we have the following interpretation for qubit:

$$\left[\begin{array}{c} \overbrace{\quad}^n \\ \diagup \quad \diagdown \\ \text{...} \\ \text{...} \\ \diagdown \quad \diagup \\ \underbrace{\quad}_m \end{array} \right] = |0\rangle^{\otimes m} \langle 0|^{\otimes n} + e^{i\alpha} |1\rangle^{\otimes m} \langle 1|^{\otimes n}, \quad \left[\begin{array}{c} \overbrace{\quad}^n \\ \diagup \quad \diagdown \\ \text{...} \\ \text{...} \\ \diagdown \quad \diagup \\ \underbrace{\quad}_m \end{array} \right] = |+\rangle^{\otimes m} \langle +|^{\otimes n} + e^{i\alpha} |-\rangle^{\otimes m} \langle -|^{\otimes n},$$

$$\left[\begin{array}{c} | \\ \boxed{H} \\ | \end{array} \right] = \frac{1}{\sqrt{2}} \begin{pmatrix} 1 & 1 \\ 1 & -1 \end{pmatrix}, \quad \left[\begin{array}{c} \vdots \\ \vdots \\ \vdots \\ \vdots \end{array} \right] = 1, \quad \left[\begin{array}{c} | \\ | \\ | \end{array} \right] = \begin{pmatrix} 1 & 0 \\ 0 & 1 \end{pmatrix},$$

$$\left[\begin{array}{c} \diagdown \quad \diagup \\ \diagup \quad \diagdown \\ \diagdown \quad \diagup \\ \diagup \quad \diagdown \end{array} \right] = \begin{pmatrix} 1 & 0 & 0 & 0 \\ 0 & 0 & 1 & 0 \\ 0 & 1 & 0 & 0 \\ 0 & 0 & 0 & 1 \end{pmatrix}, \quad \left[\begin{array}{c} \diagup \quad \diagdown \\ \diagdown \quad \diagup \end{array} \right] = \begin{pmatrix} 1 \\ 0 \\ 0 \\ 1 \end{pmatrix}, \quad \left[\begin{array}{c} \diagdown \quad \diagup \\ \diagup \quad \diagdown \end{array} \right] = \begin{pmatrix} 1 & 0 & 0 & 1 \end{pmatrix},$$

$$\llbracket D_1 \otimes D_2 \rrbracket = \llbracket D_1 \rrbracket \otimes \llbracket D_2 \rrbracket, \quad \llbracket D_1 \circ D_2 \rrbracket = \llbracket D_1 \rrbracket \circ \llbracket D_2 \rrbracket,$$

where

$$|0\rangle = \begin{pmatrix} 1 \\ 0 \end{pmatrix}, \quad \langle 0| = \begin{pmatrix} 1 & 0 \end{pmatrix}, \quad |1\rangle = \begin{pmatrix} 0 \\ 1 \end{pmatrix}, \quad \langle 1| = \begin{pmatrix} 0 & 1 \end{pmatrix}, \\ |+\rangle = \frac{1}{\sqrt{2}} \begin{pmatrix} 1 \\ 1 \end{pmatrix}, \quad \langle +| = \frac{1}{\sqrt{2}} \begin{pmatrix} 1 & 1 \end{pmatrix}, \quad |-\rangle = \frac{1}{\sqrt{2}} \begin{pmatrix} 1 \\ -1 \end{pmatrix}, \quad \langle -| = \frac{1}{\sqrt{2}} \begin{pmatrix} 1 & -1 \end{pmatrix}.$$

Below we give some useful properties of the qubit ZX-calculus.

Lemma 2.2.7

$$\begin{array}{c} \begin{array}{c} \bullet \\ \bullet \\ \bullet \end{array} \quad \begin{array}{c} \bullet \\ \diagdown \quad \diagup \\ \bullet \\ \diagup \quad \diagdown \\ \bullet \end{array} = \begin{array}{c} \bullet \\ \bullet \end{array} \end{array} \quad (2.3)$$

Proof: Proof in [6]. The rules used are $S1, S2, S3, H2, H3, H, B1, B2$. □

Lemma 2.2.8

(2.4)

Proof: Proof in [6]. The rules and properties used are $S1, S2, S3, H, H2, H3, B1, B2, EU, IV$. □

Lemma 2.2.9

(2.5)

Proof: Proof in [6]. The rules and properties used are 2.3, $B2, S2, H2, S1, H, B1$. □

Lemma 2.2.10

(2.6)

Proof: Proof in [6]. The rules and properties used are $S1, B1, K2, 2.4, IV$. □

Lemma 2.2.11

(2.7)

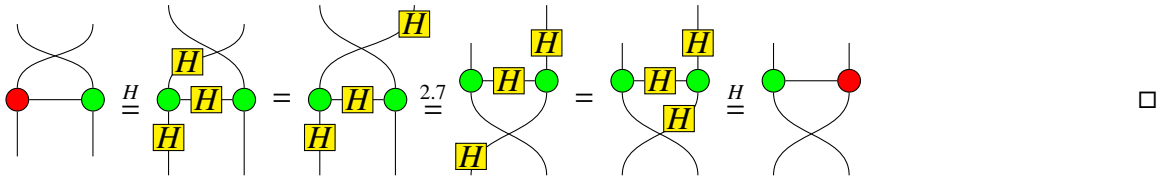
Proof:

□

Lemma 2.2.12

(2.8)

Proof:



Lemma 2.2.13

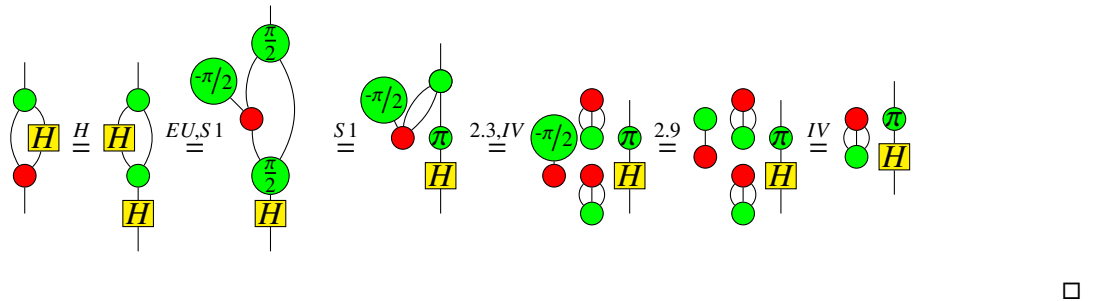
(2.9)

Proof: Proof in [6]. The rules and properties used are $S1$, $B1$, $K2$, 2.4 , IV . □

Lemma 2.2.14

(2.10)

Proof:



Lemma 2.2.15

(2.11)

Proof: The proof can be done by simply sliding the middle line (the line connects the second input and the second output) from the left to the right by naturality. □

2.2.3 Some known completeness results of the qubit ZX-calculus

It has been shown in [61] that the original version of the ZX-calculus [15] plus the Euler decomposition of Hadamard gate is incomplete for the overall pure qubit quantum mechanics (QM). Since then, plenty of efforts have been devoted to the completion of some fragment of qubit QM. In fact, the π -fragment of the ZX-calculus (corresponding to diagrams involving angles multiple of π) has been proved to be complete for real stabilizer QM in [28], and the $\frac{\pi}{2}$ -fragment of the ZX-calculus was shown to be complete for the stabilizer QM in [3]. Moreover, Backens has given the proof of completeness for single qubit Clifford+T ZX-calculus in [4].

The next chapters of this thesis will fill the gap between the above results and the universal completeness of the ZX-calculus for the whole QM.

2.3 ZW-calculus

The ZW-calculus is another graphical language for quantum computing modelled on the ZX-calculus [33]. Let R be an arbitrary commutative ring. The ZW-calculus with all parameters in R is denoted as ZW_R -calculus. Like the ZX-calculus, the ZW_R -calculus is also a self-dual compact closed PROP \mathfrak{F} with a set of rewriting rules. An arbitrary morphism of \mathfrak{F} is a diagram $D : k \rightarrow l$ with source object k and target object l , composed of the following basic components:

$Z : 1 \rightarrow 2$		$R : 1 \rightarrow 1$	
$\tau : 2 \rightarrow 2$		$P : 1 \rightarrow 1$	
$\sigma : 2 \rightarrow 2$		$\mathbb{I} : 1 \rightarrow 1$	
$e : 0 \rightarrow 0$		$W : 1 \rightarrow 2$	
$C_a : 0 \rightarrow 2$		$C_u : 2 \rightarrow 0$	

where $r \in R$, and e represents an empty diagram. With these generators, we can define the following diagrams:

(2.12)

The composition of morphisms is to combine these components in the following two ways: for any two morphisms $D_1 : a \rightarrow b$ and $D_2 : c \rightarrow d$, a *parallel composition* $D_1 \otimes D_2 : a + c \rightarrow b + d$ is obtained by placing D_1 and D_2 side-by-side with D_1 on the left of D_2 ; for any two morphisms $D_1 : a \rightarrow b$ and $D_2 : b \rightarrow c$, a *sequential composition* $D_2 \circ D_1 : a \rightarrow c$ is obtained by placing D_1 above D_2 , connecting the outputs of D_1 to the inputs of D_2 .

There are two kinds of rules for the morphisms of \mathfrak{F} : the structure rules for \mathfrak{F} as an compact closed category shown in (2.1) and (2.2), as well as the rewriting rules listed in Figure 2.2, 2.3, 2.4.

Like the ZX-calculus, all the ZW diagrams should be read from top to bottom.

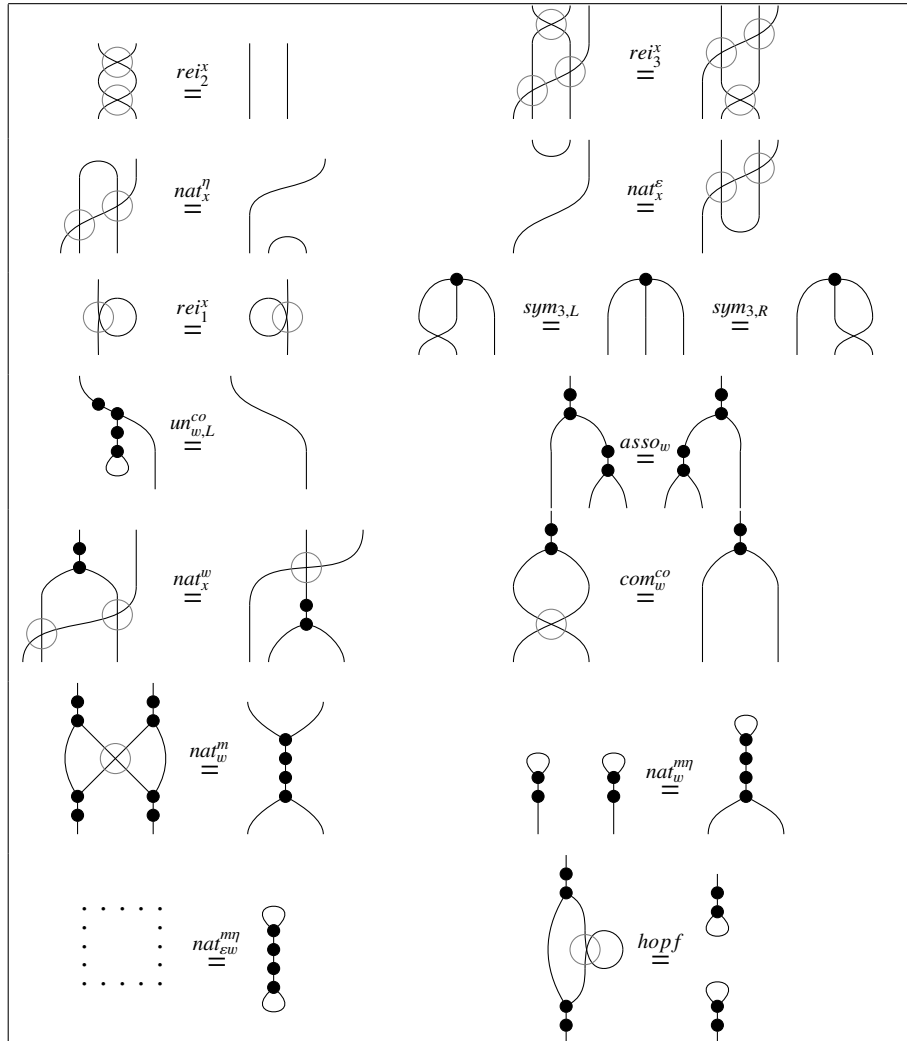


Figure 2.2: ZW_R -calculus rules I

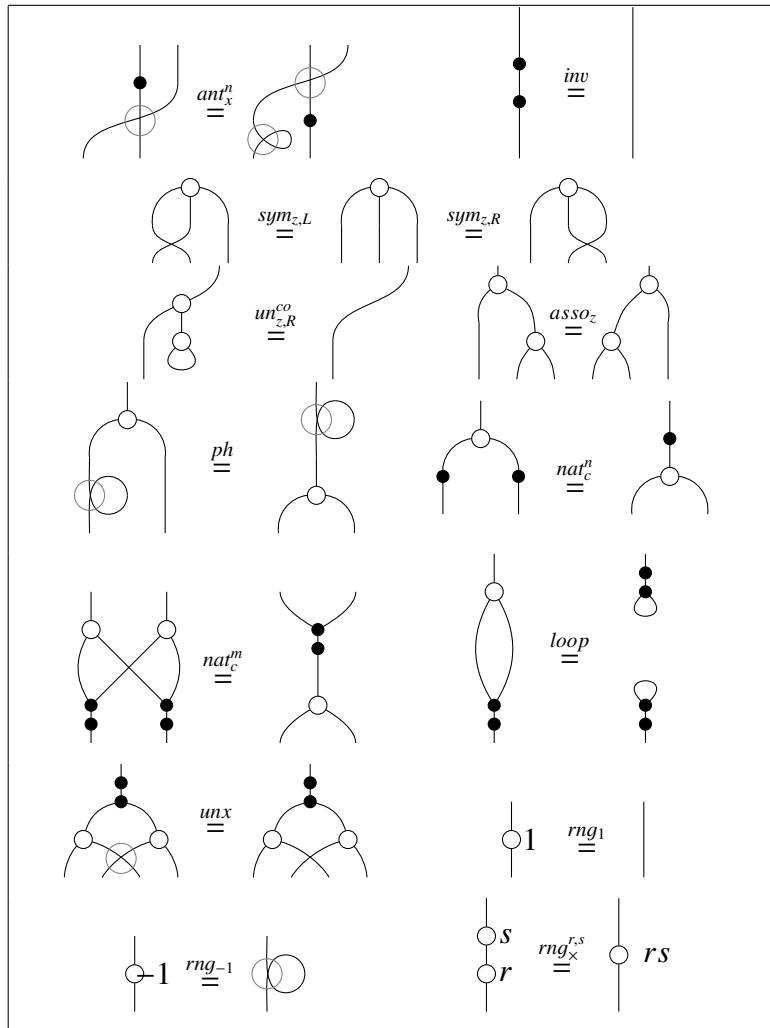


Figure 2.3: ZW_R -calculus rules II

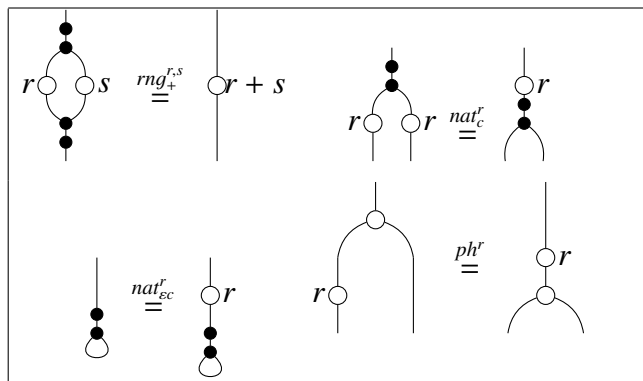


Figure 2.4: ZW_R -calculus rules III

Note that here we presented a ZW_R -calculus generated by a finite set of diagrams. However, there is an equivalent yet more concise presentation generated by an infinite set of diagrams. Both of them are proposed in [33]. We have the following spider form of the white node due to expressions in (2.12) and the rule rng_1 , which will be used for translations between the ZX -calculus and the ZW -calculus.

$$(2.13)$$

By the rules $sym_{z,L}$, $sym_{z,R}$ and $asso_z$ listed in Figure 2.3, this white node spider is commutative.

The diagrams in the ZW_R -calculus have a standard interpretation $[[\cdot]]$ in the category \mathbf{Mat}_R .

$$[[\text{white spider}]] = \begin{pmatrix} 1 & 0 \\ 0 & 0 \\ 0 & 0 \\ 0 & 1 \end{pmatrix}, \quad [[\text{white node with } r \text{ legs}]] = |0\rangle\langle 0| + r|1\rangle\langle 1| = \begin{pmatrix} 1 & 0 \\ 0 & r \end{pmatrix}.$$

$$[[\text{X node}]] = \begin{pmatrix} 1 & 0 & 0 & 0 \\ 0 & 0 & 1 & 0 \\ 0 & 1 & 0 & 0 \\ 0 & 0 & 0 & -1 \end{pmatrix}, \quad [[\text{black node}]] = \begin{pmatrix} 0 & 1 \\ 1 & 0 \\ 0 & 0 \end{pmatrix}, \quad [[\text{black dot}]] = \begin{pmatrix} 0 & 1 \\ 1 & 0 \end{pmatrix}, \quad [[\text{empty box}]] = 1.$$

$$[[\text{empty box}]] = \begin{pmatrix} 1 & 0 \\ 0 & 1 \end{pmatrix}, \quad [[\text{X node}]] = \begin{pmatrix} 1 & 0 & 0 & 0 \\ 0 & 0 & 1 & 0 \\ 0 & 1 & 0 & 0 \\ 0 & 0 & 0 & 1 \end{pmatrix}, \quad [[\text{arc}]] = \begin{pmatrix} 1 \\ 0 \\ 0 \\ 1 \end{pmatrix}, \quad [[\text{cup}]] = (1 \ 0 \ 0 \ 1).$$

$$[[D_1 \otimes D_2]] = [[D_1]] \otimes [[D_2]], \quad [[D_1 \circ D_2]] = [[D_1]] \circ [[D_2]].$$

Soundness, universality and completeness of the ZW_R -calculus can be similarly defined as that for the ZX -calculus. We only recall these properties here.

Theorem 2.3.1 [33] *The ZW_R -calculus is sound and universal.*

Theorem 2.3.2 [33] *The ZW_R -calculus is complete.*

Chapter 3

Completeness for full qubit quantum mechanics

It has been shown in [61] that the original version of the ZX-calculus [15] plus the Euler decomposition of Hadamard gate is incomplete for the overall pure qubit quantum mechanics (QM). Since then, plenty of efforts have been devoted to the completion of some part of QM: real QM [28], stabilizer QM [3], single qubit Clifford+T QM [4] and Clifford+T QM [42]. Amongst them, the completeness of ZX-calculus for Clifford+T QM is especially interesting, since it is approximatively universal for QM. Note that their proof relies on the completeness of ZW-calculus for “qubits with integer coefficients” [32].

In this chapter, we give the first complete axiomatisation of the ZX-calculus for the entire qubit QM, i.e., the ZX_{full} -calculus, based on the completeness result of the ZW_C -calculus [33]. Firstly, we introduce two new generators: a triangle and a series of λ -labeled boxes ($\lambda \geq 0$), which turns out to be expressible in ZX-calculus without these symbols. Then we establish reversible translations from ZX to ZW and vice versa. By checking carefully that all the ZW rewriting rules still hold under translation from ZW to ZX, we finally finished the proof of completeness of ZX_{full} -calculus.

Throughout this chapter, the terms “equation” and “rewriting rule” will be used interchangeably. The proof of the completeness of the full qubit ZX-calculus has been published in [34], with coauthors Amar Hadzihasanovic and Kang Feng Ng.

3.1 ZX_{full} -calculus

The ZX_{full} -calculus has generators as listed in Table 6.1 plus two new generators given in Table 3.1.

$L : 1 \rightarrow 1$	$T : 1 \rightarrow 1$
-----------------------	-----------------------

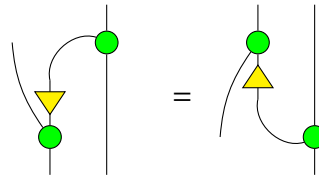
Table 3.1: New generators with $\lambda \geq 0$.

It seems that the ZX_{full} -calculus has more generators than the traditional ZX-calculus. However we will show that they are expressible in red and green nodes in Proposition 3.4.3.

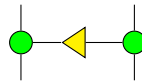
Also we define the following notation:

$$\begin{array}{c} \text{yellow triangle} \end{array} := \begin{array}{c} \text{yellow triangle} \end{array} \quad (3.1)$$

Then it is clear that



Thus it makes sense to draw the following picture:



The ZX_{full} -calculus has the same structural rules as that of the traditional ZX-calculus given in (2.1) and (2.2). Its non-structural rewriting rules are presented in Figures 3.1 (exactly the same as Figure 2.1), 3.2 and 3.3:

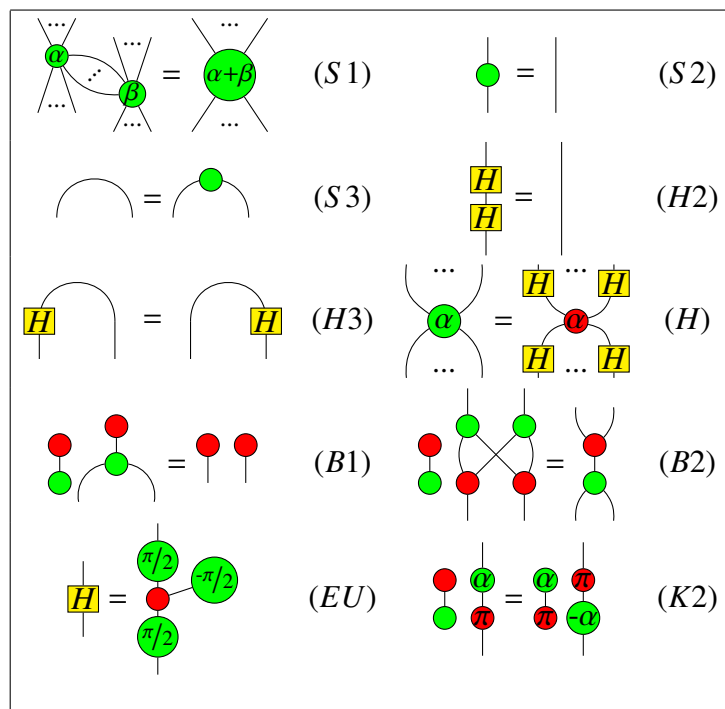


Figure 3.1: Traditional-style ZX-calculus rules, where $\alpha, \beta \in [0, 2\pi)$. The upside-down version and colour swapped version of these rules still hold.

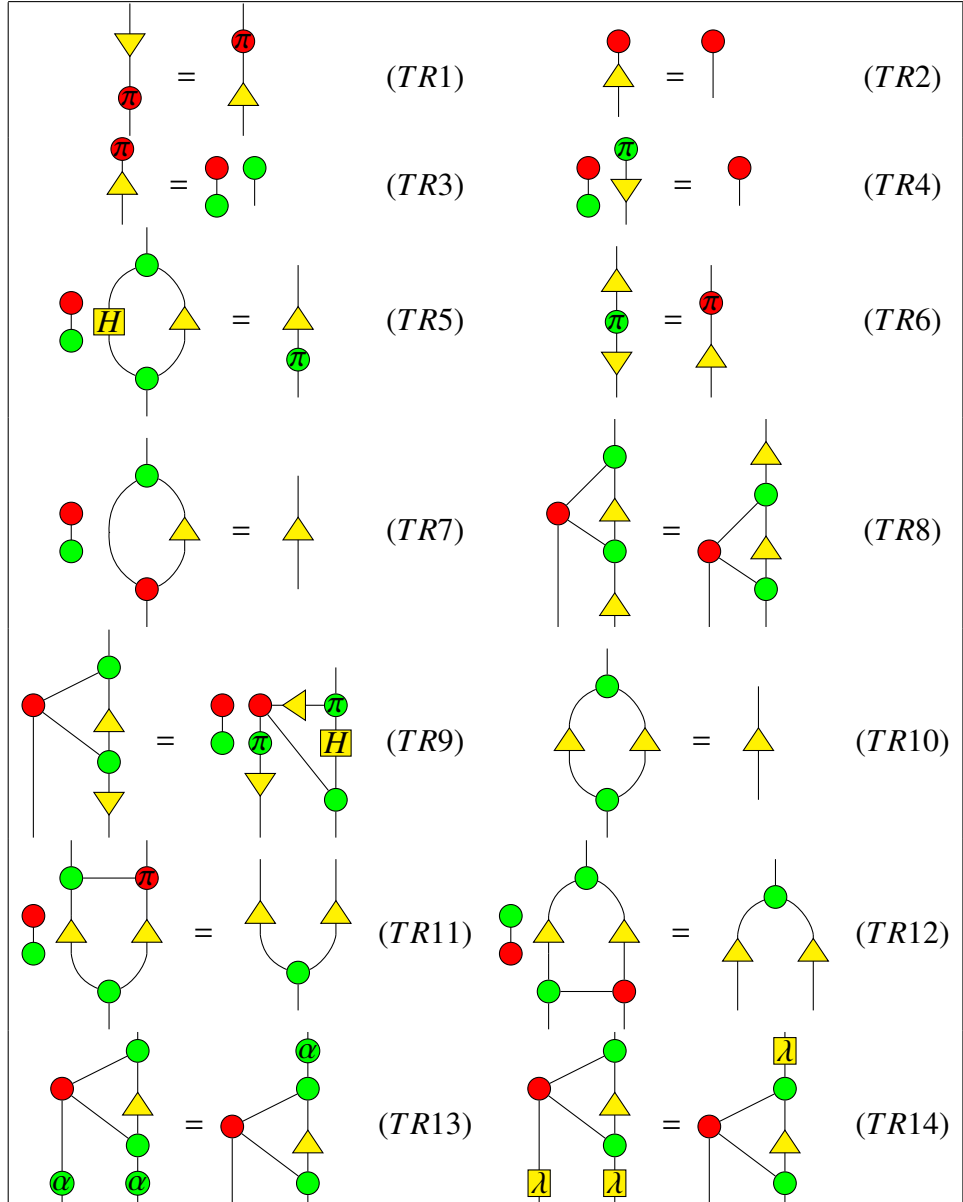


Figure 3.2: Extended ZX-calculus rules for triangle, where $\lambda \geq 0, \alpha \in [0, 2\pi)$. The upside-down version of these rules still hold.

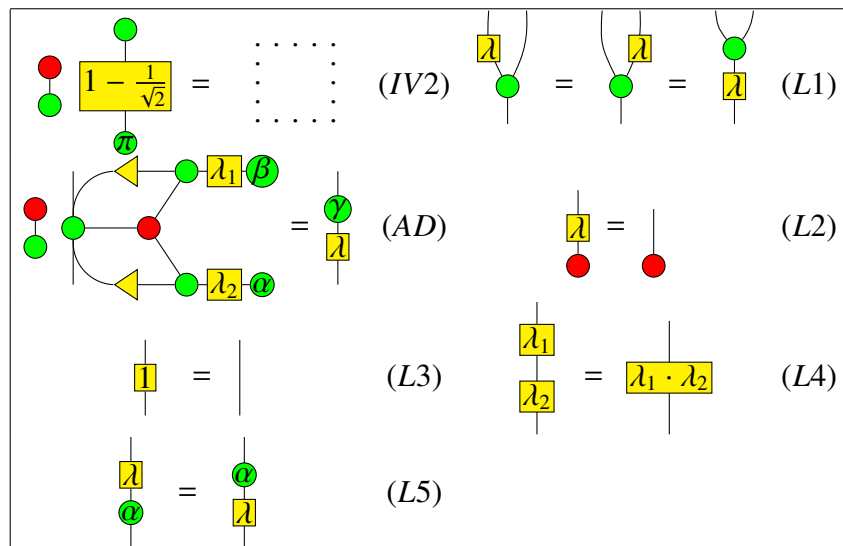


Figure 3.3: Extended ZX-calculus rules for λ and addition, where $\lambda, \lambda_1, \lambda_2 \geq 0, \alpha, \beta, \gamma \in [0, 2\pi)$; in (AD), $\lambda e^{i\gamma} = \lambda_1 e^{i\beta} + \lambda_2 e^{i\alpha}$. The upside-down version of these rules still hold.

The diagrams in the ZX_{full} -calculus have a standard interpretation composed of two parts: the standard interpretation of the traditional qubit ZX-calculus described in Section 2.2.2 as well as the interpretation of the new generators triangle and λ box to be given below. For simplicity, we still use the notation $\llbracket \cdot \rrbracket$ to denote the standard interpretation for the ZX_{full} -calculus.

$$\llbracket \begin{array}{c} \triangle \\ | \\ | \end{array} \rrbracket = \begin{pmatrix} 1 & 1 \\ 0 & 1 \end{pmatrix}, \quad \llbracket \begin{array}{c} \lambda \\ | \\ | \end{array} \rrbracket = \begin{pmatrix} 1 & 0 \\ 0 & \lambda \end{pmatrix}. \quad (3.2)$$

Useful derivable results

Now we derive some identities that will be useful in this thesis.

Lemma 3.1.1

$$\begin{array}{c} \bullet \bullet \\ | \quad | \\ \bullet \bullet \end{array} = \begin{array}{c} \cdot \cdot \cdot \\ \cdot \cdot \cdot \end{array} \quad (3.3)$$

Proof:

First we have

$$\begin{array}{c} \bullet \bullet \bullet \\ | \quad | \quad | \\ \bullet \bullet \bullet \end{array} \stackrel{S1}{=} \begin{array}{c} \bullet \bullet \bullet \\ | \quad | \quad | \\ \bullet \bullet \bullet \end{array} \stackrel{2.3}{=} \begin{array}{c} \bullet \\ | \\ \bullet \end{array} \quad (3.4)$$

Then

$$\begin{array}{c} \bullet \bullet \\ | \quad | \\ \bullet \bullet \end{array} = \begin{array}{c} \cdot \cdot \cdot \\ \cdot \cdot \cdot \end{array} \stackrel{IV2}{=} \begin{array}{c} \bullet \\ | \\ \text{box} \end{array} \begin{array}{c} \bullet \bullet \bullet \\ | \quad | \quad | \\ \bullet \bullet \bullet \end{array} \stackrel{3.4}{=} \begin{array}{c} \bullet \\ | \\ \text{box} \end{array} \begin{array}{c} \bullet \\ | \\ \bullet \end{array} \stackrel{IV2}{=} \begin{array}{c} \cdot \cdot \cdot \\ \cdot \cdot \cdot \end{array} \quad \square$$

Lemma 3.1.2

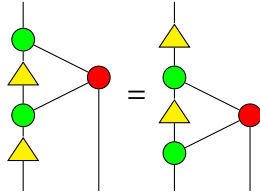
$$\begin{array}{c} \bullet \\ | \\ \triangle \\ | \\ \bullet \bullet \end{array} = \begin{array}{c} \bullet \\ | \\ \triangle \\ | \\ \bullet \bullet \end{array} \quad (3.5)$$

Proof:

$$\begin{array}{c} \bullet \\ | \\ \triangle \\ | \\ \bullet \bullet \end{array} \stackrel{B2}{=} \begin{array}{c} \bullet \\ | \\ \triangle \\ | \\ \bullet \bullet \end{array} \stackrel{S1,2.8}{=} \begin{array}{c} \bullet \\ | \\ \triangle \\ | \\ \bullet \bullet \end{array} \stackrel{TR7}{=} \begin{array}{c} \bullet \\ | \\ \triangle \\ | \\ \bullet \bullet \end{array} \stackrel{2.8}{=} \begin{array}{c} \bullet \\ | \\ \triangle \\ | \\ \bullet \bullet \end{array} \stackrel{2.5}{=} \begin{array}{c} \bullet \\ | \\ \triangle \\ | \\ \bullet \bullet \end{array} = \begin{array}{c} \bullet \\ | \\ \triangle \\ | \\ \bullet \bullet \end{array}$$

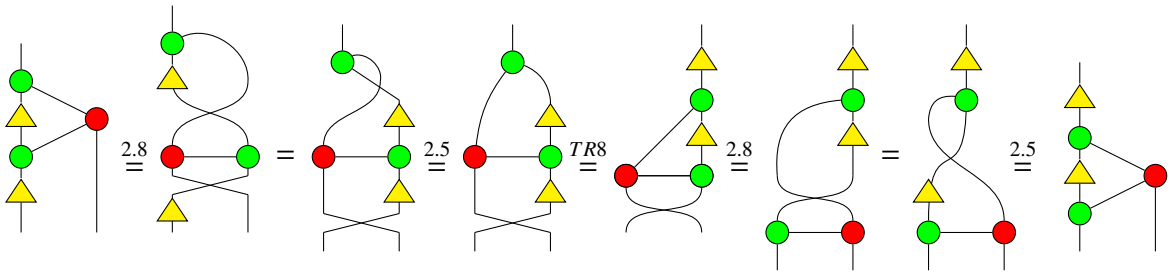
□

Lemma 3.1.3



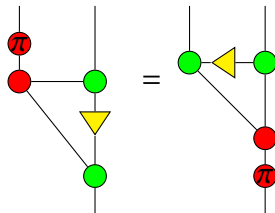
(3.6)

Proof:



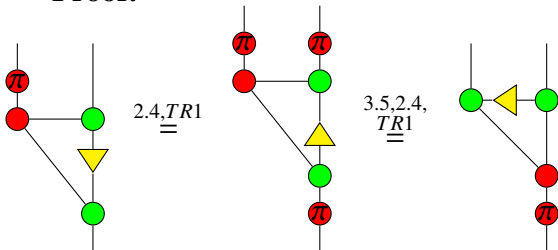
□

Lemma 3.1.4



(3.7)

Proof:



□

3.2 Simplification of the rules of from the ZX_{full} -calculus

The rules for the ZX_{full} -calculus as listed in Figure 3.2, and Figure 3.3 can be further simplified, and some rules can be derived from others. We did not introduce the simplified version of rules at the beginning because we want to show the developing process of the theory of the ZX-calculus. In this section, we will exhibit how rules could be simplified or derived.

First we show that the addition rule (AD) in Figure 3.3 can be simplified:

(3.8)

This means

(3.9)

From now on, we will call the simplified addition rule (AD'):

(3.10)

As a consequence, we have the following commutativity of addition:

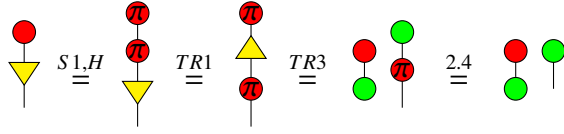
(3.11)

Next we prove that some rules in Figure 3.2 are derivable.

Lemma 3.2.1

(3.11)

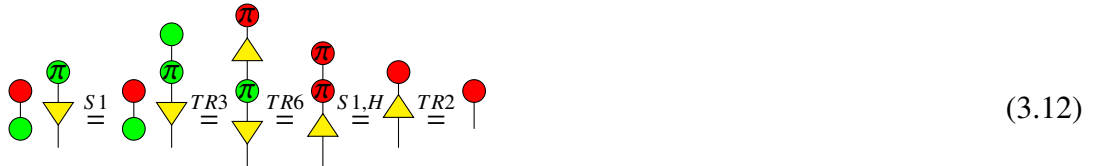
Proof:



□

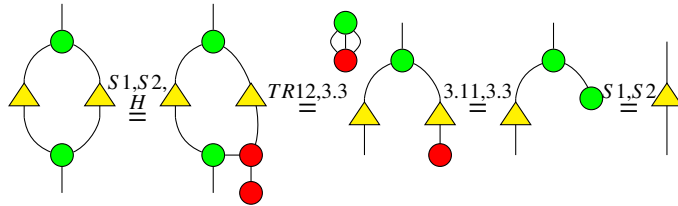
Lemma 3.2.2 *The rules (TR4), (TR10), and (TR11) can be derived from other rules.*

Proof: For the derivation of (TR4), we have



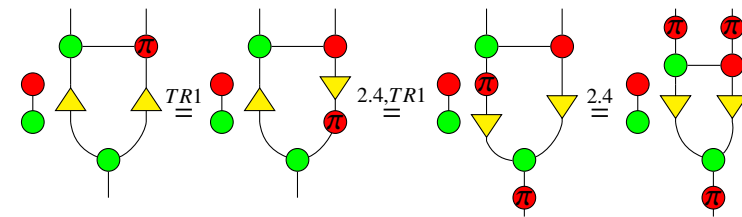
(3.12)

For the derivation of (TR10), we have

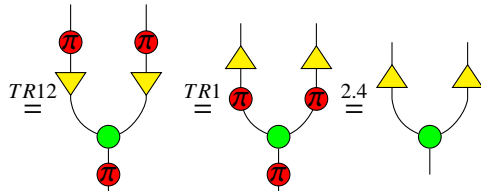


(3.13)

For the derivation of (TR11), we have



(3.14)



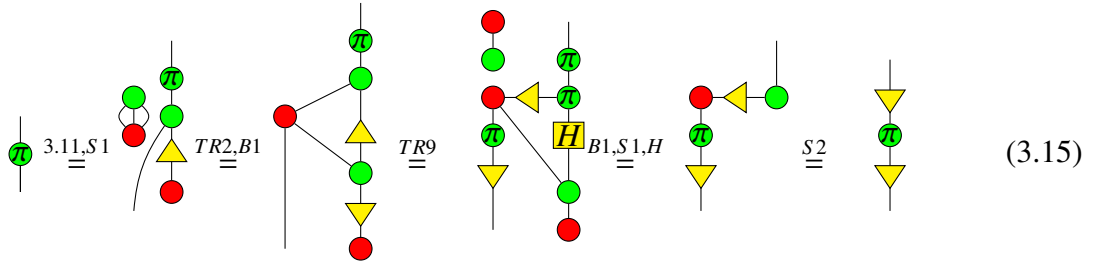
□

The following property will be very useful for deriving (TR5) here and in later sections:

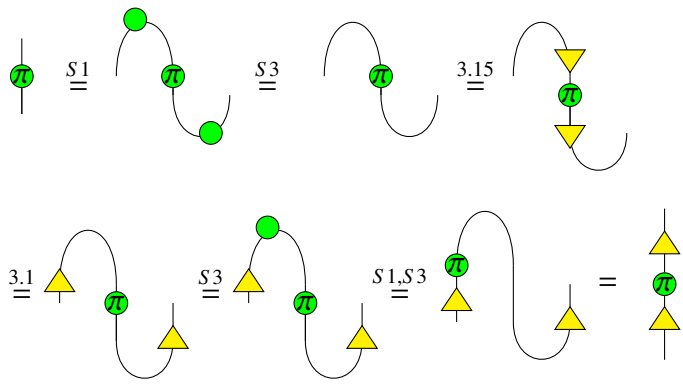
Lemma 3.2.3

$$\begin{array}{c} \triangleup \\ | \\ \pi \\ | \\ \triangleup \end{array} = \begin{array}{c} | \\ \pi \\ | \end{array} \quad (TR10')$$

Proof:



Then

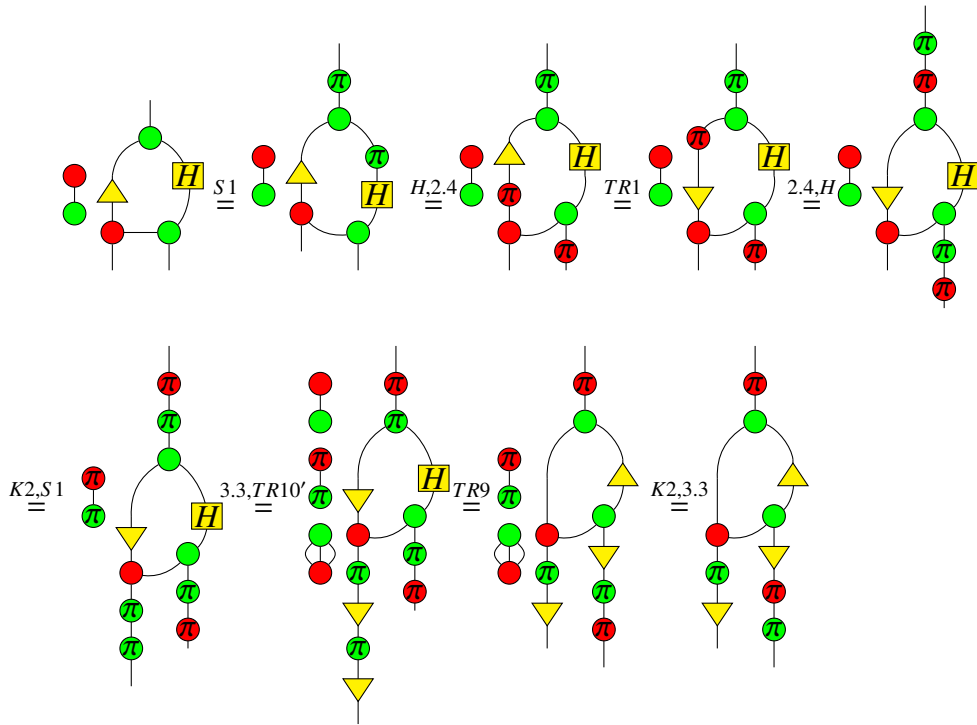


□

Lemma 3.2.4

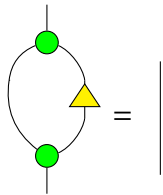


Proof:



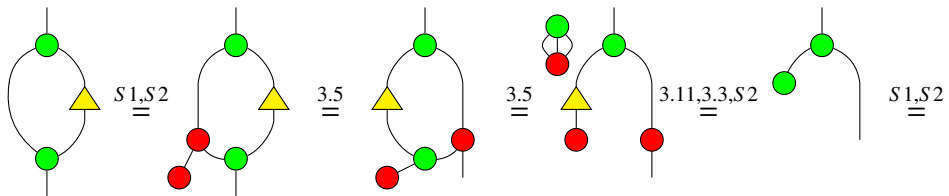
□

Lemma 3.2.5



(3.17)

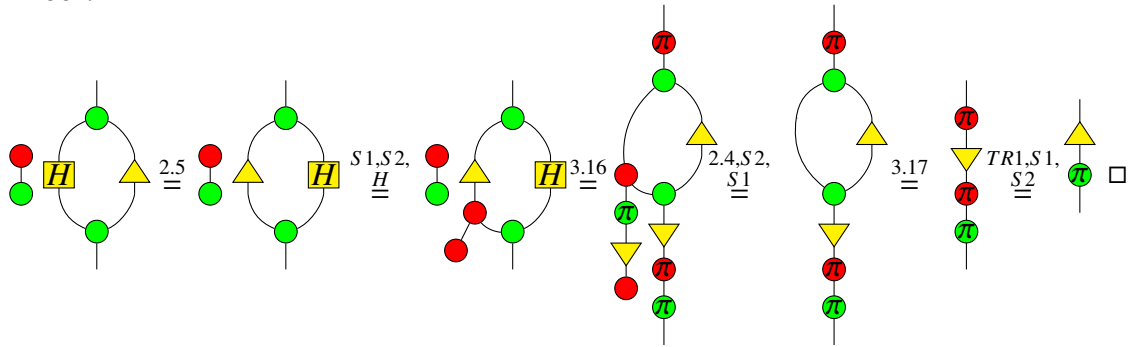
Proof:



□

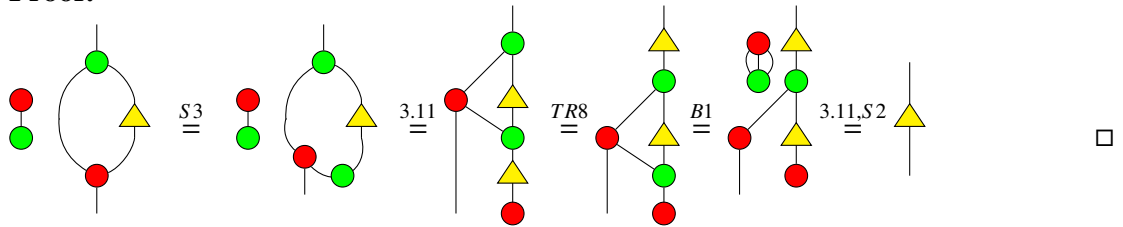
Lemma 3.2.6 *The rule (TR5) can be derived.*

Proof:



Lemma 3.2.7 *The rule (TR7) can be derived.*

Proof:



Lemma 3.2.8 *The rules (TR13) and (TR14) can be combined.*

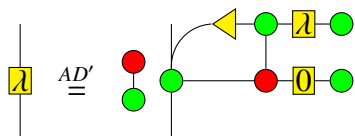
Proof: Obviously, (TR13) and (TR14) can be combined into a single rule called (TR13') as follows:



□

Lemma 3.2.9 *The rule (L1) can be derived.*

Proof: By the addition rule, we have



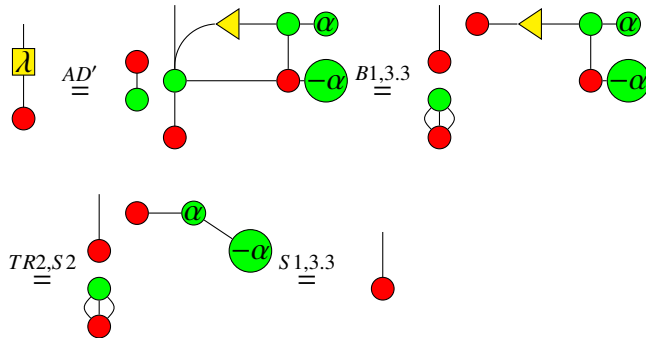
Then (L1) directly follows from the spider rule (S1).

□

Lemma 3.2.10 *The rule (L2) can be derived.*

Proof:

First we can write the non-negative number λ as a sum of its integer part and remainder part: $\lambda = [\lambda] + \{\lambda\}$, where $[\lambda]$ is a non-negative integer and $0 \leq \{\lambda\} < 1$. Let $n = [\lambda]$, $\alpha = \arccos \frac{\{\lambda\}}{2}$. It follows that $\{\lambda\} = 2 \cos \alpha = e^{i\alpha} + e^{-i\alpha}$. If $n = 0$, then we have



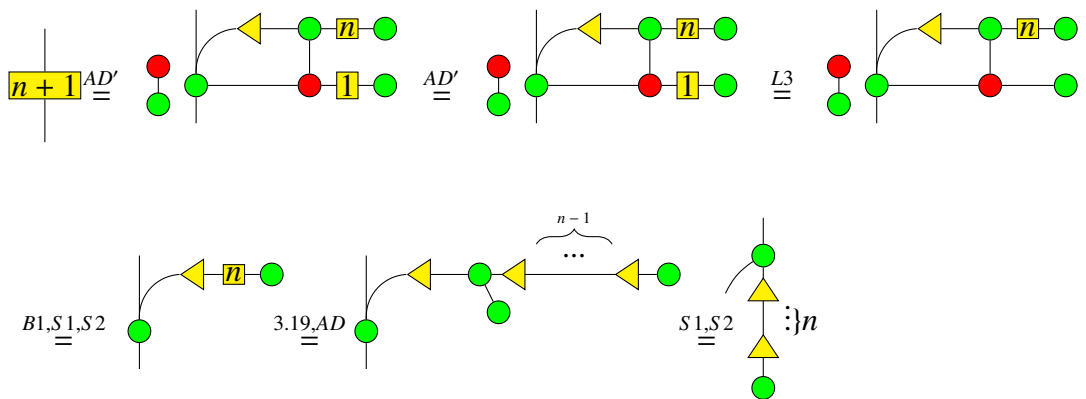
If $n > 0$, then we have

$$[n] = \begin{array}{c} \text{---} \\ | \\ \text{---} \\ | \\ \text{---} \\ | \\ \text{---} \\ | \\ \text{---} \end{array} = \begin{array}{c} \text{---} \\ | \\ \text{---} \\ | \\ \text{---} \\ | \\ \text{---} \\ | \\ \text{---} \end{array} \quad \left. \vphantom{\begin{array}{c} \text{---} \\ | \\ \text{---} \\ | \\ \text{---} \\ | \\ \text{---} \\ | \\ \text{---} \end{array}} \right\} n-1 \quad (3.19)$$

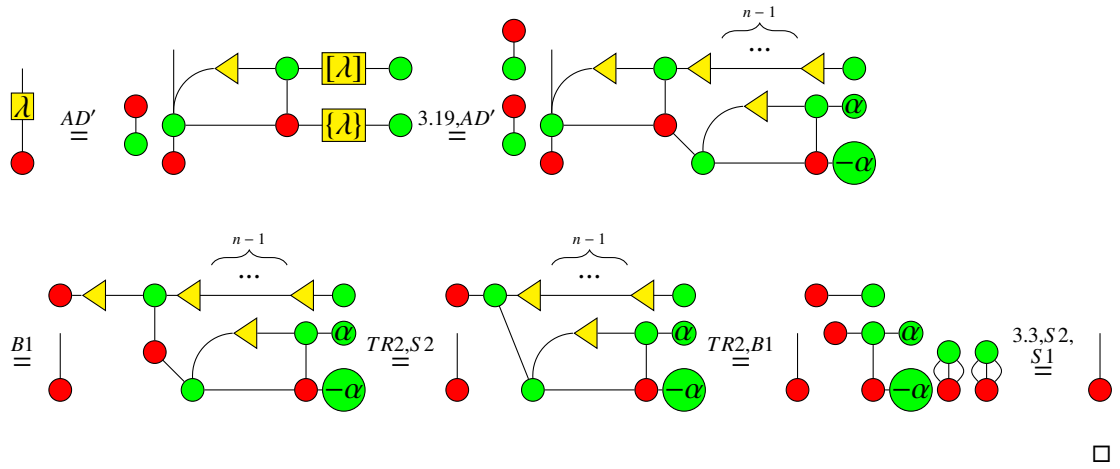
We show this by induction on n . When $n = 1$, we have

$$[1] \stackrel{L3}{=} \left| \begin{array}{c} \text{---} \\ | \\ \text{---} \\ | \\ \text{---} \end{array} \right| \stackrel{S1,S2}{=} \begin{array}{c} \text{---} \\ | \\ \text{---} \\ | \\ \text{---} \end{array}$$

Suppose (3.19) holds for n . Then for $n + 1$ we have

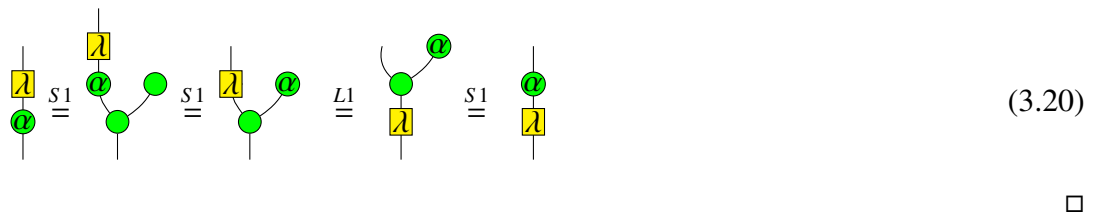


This completes the induction. Therefore,



Lemma 3.2.11 *The rule (L5) can be derived.*

Proof:



3.2.1 Simplified rules for the ZX_{full} -calculus

Now can summarise the results obtained in Section 3.2 and give the simplified version of all the non-structural rewriting rules for the ZX_{full} -calculus in the following Figures 3.4 and 3.5 .

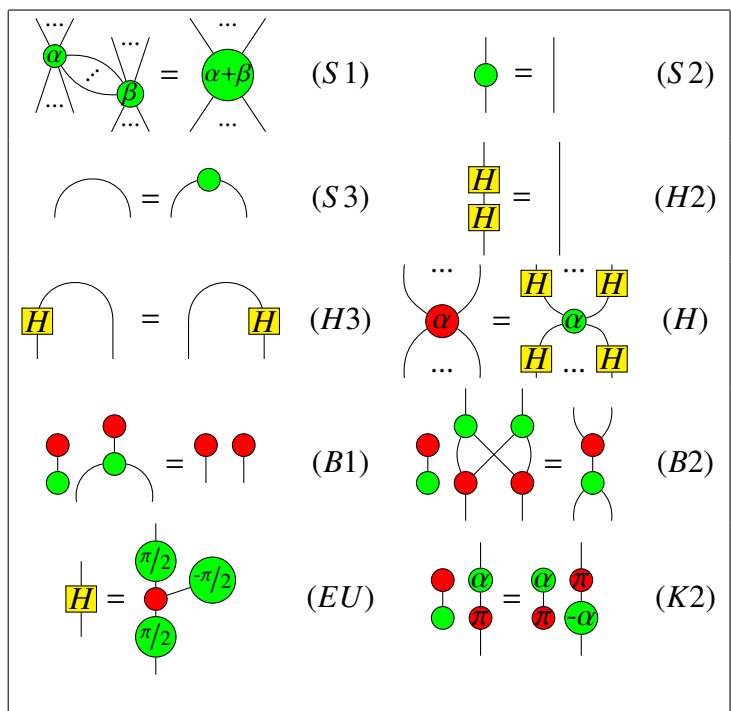


Figure 3.4: Traditional ZX-calculus rules, where $\alpha, \beta \in [0, 2\pi)$. The upside-down version and colour swapped version of these rules still hold.

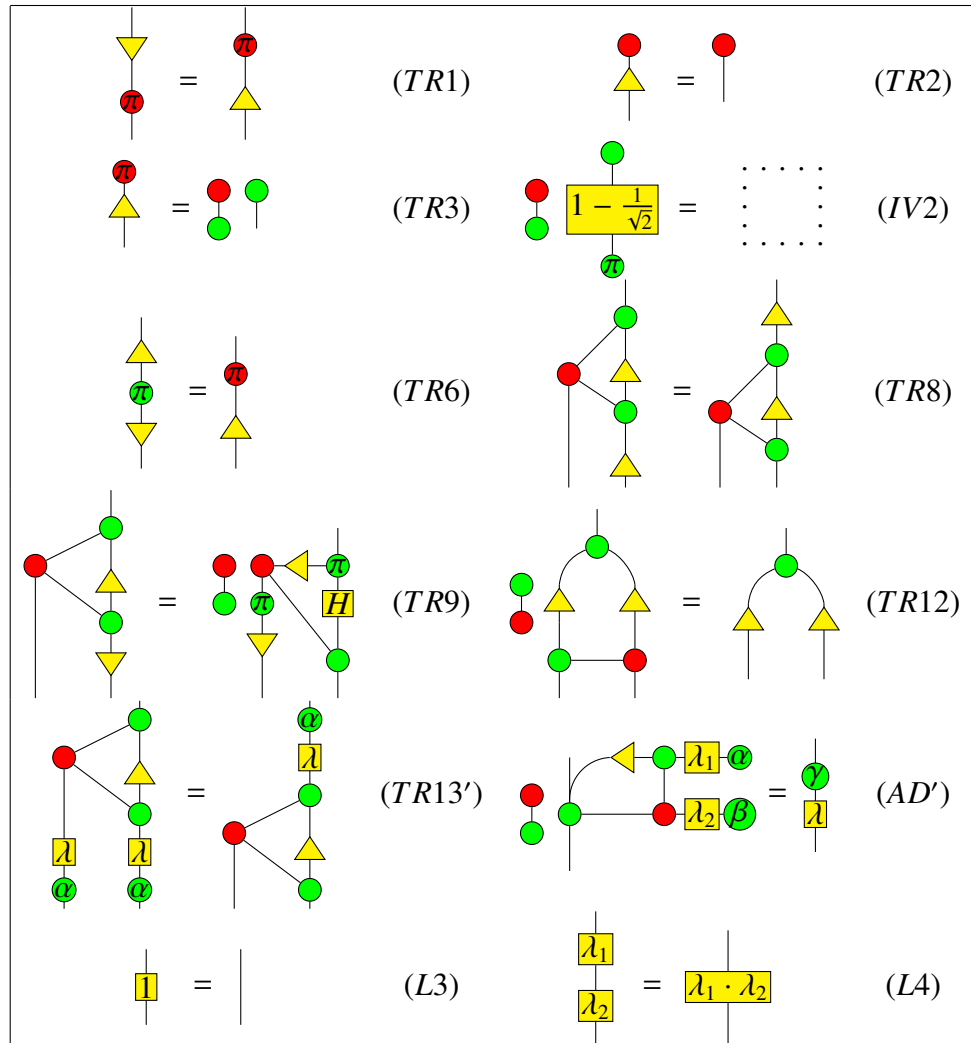


Figure 3.5: Extended ZX-calculus rules, where $\lambda, \lambda_1, \lambda_2 \geq 0, \alpha, \beta, \gamma \in [0, 2\pi)$; in (AD'), $\lambda e^{i\gamma} = \lambda_1 e^{i\beta} + \lambda_2 e^{i\alpha}$. The upside-down version of these rules still hold.

With these simplified rules, we have

Proposition 3.2.12 *The ZX_{full} -calculus is sound.*

Proof: By the construction of general ZX-calculus described in Section 2.2.1, any two diagrams D_1 and D_2 of the ZX_{full} -calculus are equal modulo the equivalence relations given in (2.1) and (2.2) as structural rules and in Figures 3.4 and 3.5 as non-structural rewriting rules. That is, $D_1 = D_2$ if and only if D_1 can be rewritten into D_2 using finitely many of these rules. In addition, $\llbracket D_1 \otimes D_2 \rrbracket = \llbracket D_1 \rrbracket \otimes \llbracket D_2 \rrbracket$, $\llbracket D_1 \circ D_2 \rrbracket = \llbracket D_1 \rrbracket \circ \llbracket D_2 \rrbracket$. Therefore, to prove the soundness of the ZX_{full} -calculus, it suffices to verify that all the rules listed in (2.1) and (2.2) and Figures 3.4 and 3.5 still hold under the standard interpretation $\llbracket \cdot \rrbracket$ including (3.2). The structural rules have been proved to be sound in [15]. It is a routine check that the rules in Figures 3.4 and 3.5 are sound. □

3.3 Interpretations between the ZX_{full} -calculus and the $ZW_{\mathbb{C}}$ -calculus

The ZX_{full} -calculus and the $ZW_{\mathbb{C}}$ -calculus are not irrelevant to each other. In fact, there exists an invertible translation between them. Note that a spider can be decomposed into a form consisting of a phase-free spider and a pure phase gate, which will be used for translation between the ZX-calculus and the ZW-calculus:

$$\begin{array}{c}
 \begin{array}{ccc}
 \begin{array}{c} \dots \\ \diagdown \quad \diagup \\ \circ \\ \diagup \quad \diagdown \\ \dots \end{array} & = & \begin{array}{c} \dots \\ \diagdown \quad \diagup \\ \circ \\ \diagup \quad \diagdown \\ \dots \\ \circ \\ \dots \end{array} \\
 \begin{array}{c} \dots \\ \diagdown \quad \diagup \\ \circ \\ \diagup \quad \diagdown \\ \dots \end{array} & = & \begin{array}{c} \dots \\ \diagdown \quad \diagup \\ \circ \\ \diagup \quad \diagdown \\ \dots \\ \circ \\ \dots \end{array}
 \end{array}
 \end{array} \tag{3.21}$$

First we define the interpretation $\llbracket \cdot \rrbracket_{XW}$ from ZX_{full} -calculus to $ZW_{\mathbb{C}}$ -calculus as follows:

$$\begin{array}{c}
 \begin{array}{ccc}
 \llbracket \begin{array}{c} \dots \\ \vdots \\ \dots \end{array} \rrbracket_{XW} = \begin{array}{c} \dots \\ \vdots \\ \dots \end{array}, & \llbracket \begin{array}{c} \vdots \\ \vdots \\ \vdots \end{array} \rrbracket_{XW} = \begin{array}{c} | \\ | \\ | \end{array}, & \llbracket \begin{array}{c} \frown \\ \smile \end{array} \rrbracket_{XW} = \begin{array}{c} \frown \\ \smile \end{array}, & \llbracket \begin{array}{c} \smile \\ \frown \end{array} \rrbracket_{XW} = \begin{array}{c} \smile \\ \frown \end{array}, \\
 \llbracket \begin{array}{c} \diagdown \quad \diagup \\ \diagup \quad \diagdown \end{array} \rrbracket_{XW} = \begin{array}{c} \diagdown \quad \diagup \\ \diagup \quad \diagdown \end{array}, & \llbracket \begin{array}{c} \dots \\ \diagdown \quad \diagup \\ \circ \\ \diagup \quad \diagdown \\ \dots \end{array} \rrbracket_{XW} = \begin{array}{c} \dots \\ \diagdown \quad \diagup \\ \circ \\ \diagup \quad \diagdown \\ \dots \end{array}, & \llbracket \begin{array}{c} \circ \\ \vdots \end{array} \rrbracket_{XW} = \begin{array}{c} \circ \\ \vdots \end{array} e^{i\alpha}, & \llbracket \begin{array}{c} \square \\ \vdots \end{array} \rrbracket_{XW} = \begin{array}{c} \square \\ \vdots \end{array} \lambda, \\
 \llbracket \begin{array}{c} \square \\ \vdots \end{array} \rrbracket_{XW} = \frac{\sqrt{2}-2}{2} \begin{array}{c} \circ \\ \diagdown \quad \diagup \\ \circ \\ \diagup \quad \diagdown \\ \circ \end{array}, & \llbracket \begin{array}{c} \triangle \\ \vdots \end{array} \rrbracket_{XW} = \begin{array}{c} \bullet \\ \diagdown \quad \diagup \\ \bullet \\ \diagup \quad \diagdown \\ \bullet \end{array}, & \llbracket \begin{array}{c} \circ \\ \vdots \end{array} \rrbracket_{XW} = \llbracket \begin{array}{c} \square \\ \vdots \end{array} \rrbracket_{XW} \circ \left(\begin{array}{c} \circ \\ \vdots \end{array} e^{i\alpha} \right) \circ \llbracket \begin{array}{c} \square \\ \vdots \end{array} \rrbracket_{XW},
 \end{array}$$

$$\left[\left[\begin{array}{c} \overbrace{\quad\quad\quad}^n \\ \vdots \\ \text{---} \\ \vdots \\ \underbrace{\quad\quad\quad}_m \end{array} \right] \right]_{XW} = \left[\left[\left(\begin{array}{c} \vdots \\ \text{---} \\ \vdots \end{array} \right)^{\otimes m} \right] \right]_{XW} \circ \left[\left[\begin{array}{c} \overbrace{\quad\quad\quad}^n \\ \vdots \\ \text{---} \\ \vdots \\ \underbrace{\quad\quad\quad}_m \end{array} \right] \right] \circ \left[\left[\left(\begin{array}{c} \vdots \\ \text{---} \\ \vdots \end{array} \right)^{\otimes n} \right] \right]_{XW},$$

$$\llbracket D_1 \otimes D_2 \rrbracket_{XW} = \llbracket D_1 \rrbracket_{XW} \otimes \llbracket D_2 \rrbracket_{XW}, \quad \llbracket D_1 \circ D_2 \rrbracket_{XW} = \llbracket D_1 \rrbracket_{XW} \circ \llbracket D_2 \rrbracket_{XW},$$

where $\alpha \in [0, 2\pi)$, $\lambda \geq 0$.

The interpretation $\llbracket \cdot \rrbracket_{XW}$ preserves the standard interpretation:

Lemma 3.3.1 *Suppose D is an arbitrary diagram in the ZX_{full} -calculus. Then $\llbracket \llbracket D \rrbracket_{XW} \rrbracket = \llbracket D \rrbracket$.*

Proof: Since each diagram in the ZX_{full} -calculus is generated in parallel composition \otimes and sequential composition \circ by generators in Table 6.1 and Table 3.1, and the interpretation $\llbracket \cdot \rrbracket_{XW}$ respects these two compositions, it suffices to prove $\llbracket \llbracket D \rrbracket_{XW} \rrbracket = \llbracket D \rrbracket$ when D is a generator diagram. This is a routine check, we omit the verification details here. \square

Next we define the interpretation $\llbracket \cdot \rrbracket_{WX}$ from ZW_C -calculus to ZX_{full} -calculus as follows:

$$\begin{array}{l} \left[\left[\begin{array}{c} \vdots \\ \vdots \\ \vdots \end{array} \right] \right]_{WX} = \begin{array}{c} \vdots \\ \vdots \\ \vdots \end{array}, \quad \left[\left[\begin{array}{c} \vdots \\ \vdots \\ \vdots \end{array} \right] \right]_{WX} = \begin{array}{c} \vdots \\ \vdots \\ \vdots \end{array}, \quad \left[\left[\begin{array}{c} \text{---} \\ \text{---} \end{array} \right] \right]_{WX} = \text{---}, \quad \left[\left[\begin{array}{c} \text{---} \\ \text{---} \end{array} \right] \right]_{WX} = \text{---}, \\ \left[\left[\begin{array}{c} \text{---} \\ \text{---} \end{array} \right] \right]_{WX} = \text{---}, \quad \left[\left[\begin{array}{c} \overbrace{\quad\quad\quad}^n \\ \vdots \\ \text{---} \\ \vdots \\ \underbrace{\quad\quad\quad}_m \end{array} \right] \right]_{WX} = \begin{array}{c} \text{---} \\ \vdots \\ \text{---} \\ \vdots \\ \text{---} \end{array}, \quad \left[\left[\begin{array}{c} \text{---} \\ \text{---} \end{array} \right] \right]_{WX} = \begin{array}{c} \text{---} \\ \text{---} \end{array}, \quad \left[\left[\begin{array}{c} \text{---} \\ \text{---} \end{array} \right] \right]_{WX} = \begin{array}{c} \text{---} \\ \text{---} \end{array}, \\ \left[\left[\begin{array}{c} \text{---} \\ \text{---} \end{array} \right] \right]_{WX} = \begin{array}{c} \text{---} \\ \text{---} \end{array}, \quad \left[\left[\begin{array}{c} \text{---} \\ \text{---} \end{array} \right] \right]_{WX} = \begin{array}{c} \text{---} \\ \text{---} \end{array}, \quad \left[\left[\begin{array}{c} \text{---} \\ \text{---} \end{array} \right] \right]_{WX} = \begin{array}{c} \text{---} \\ \text{---} \end{array}, \\ \left[\left[\begin{array}{c} \text{---} \\ \text{---} \end{array} \right] \right]_{WX} = \begin{array}{c} \text{---} \\ \text{---} \end{array}, \quad \left[\left[\begin{array}{c} \text{---} \\ \text{---} \end{array} \right] \right]_{WX} = \begin{array}{c} \text{---} \\ \text{---} \end{array}, \quad \left[\left[\begin{array}{c} \text{---} \\ \text{---} \end{array} \right] \right]_{WX} = \begin{array}{c} \text{---} \\ \text{---} \end{array}, \end{array}$$

$$\llbracket D_1 \otimes D_2 \rrbracket_{WX} = \llbracket D_1 \rrbracket_{WX} \otimes \llbracket D_2 \rrbracket_{WX}, \quad \llbracket D_1 \circ D_2 \rrbracket_{WX} = \llbracket D_1 \rrbracket_{WX} \circ \llbracket D_2 \rrbracket_{WX}.$$

where $r = \lambda e^{i\alpha}$, $\alpha \in [0, 2\pi)$, $\lambda \geq 0$.

The interpretation $\llbracket \cdot \rrbracket_{WX}$ preserves the standard interpretation as well:

Lemma 3.3.2 *Suppose D is an arbitrary diagram in $ZW_{\mathbb{C}}$ -calculus. Then $\llbracket \llbracket D \rrbracket_{WX} \rrbracket = \llbracket D \rrbracket$.*

Proof: The proof is similar to that of Lemma 3.3.1. \square

Thus both $\llbracket \cdot \rrbracket_{WX}$ and $\llbracket \cdot \rrbracket_{XW}$ preserve the standard interpretation. Combining with the completeness of the $ZW_{\mathbb{C}}$ -calculus, we have

Lemma 3.3.3 *If $ZX_{full} \vdash D_1 = D_2$, then $ZW_{\mathbb{C}} \vdash \llbracket D_1 \rrbracket_{XW} = \llbracket D_2 \rrbracket_{XW}$.*

Proof: Suppose $ZX_{full} \vdash D_1 = D_2$, Then by the soundness of the ZX_{full} , we have $\llbracket D_1 \rrbracket = \llbracket D_2 \rrbracket$. Therefore $\llbracket \llbracket D_1 \rrbracket_{XW} \rrbracket = \llbracket D_1 \rrbracket = \llbracket D_2 \rrbracket = \llbracket \llbracket D_2 \rrbracket_{XW} \rrbracket$ by Lemma 3.3.1. Then it follows that $ZW_{\mathbb{C}} \vdash \llbracket D_1 \rrbracket_{XW} = \llbracket D_2 \rrbracket_{XW}$ by the completeness of the $ZW_{\mathbb{C}}$ -calculus. \square

This means the interpretation $\llbracket \cdot \rrbracket_{XW}$ is a well-defined functor from the PROP ZX_{full} to the PROP $ZW_{\mathbb{C}}$.

Moreover, we have

Lemma 3.3.4 *For any diagram $G \in ZW_{\mathbb{C}}$,*

$$ZW_{\mathbb{C}} \vdash \llbracket \llbracket G \rrbracket_{WX} \rrbracket_{XW} = G \quad (3.22)$$

Proof: By Lemma 3.3.1 and Lemma 3.3.2, the interpretations $\llbracket \cdot \rrbracket_{XW}$ and $\llbracket \cdot \rrbracket_{WX}$ preserve the standard interpretation $\llbracket \cdot \rrbracket$. Thus $\llbracket G \rrbracket = \llbracket \llbracket G \rrbracket_{WX} \rrbracket = \llbracket \llbracket \llbracket G \rrbracket_{WX} \rrbracket_{XW} \rrbracket$. By the completeness of the $ZW_{\mathbb{C}}$ -calculus, it must be that $ZW_{\mathbb{C}} \vdash \llbracket \llbracket G \rrbracket_{WX} \rrbracket_{XW} = G$. \square

On the other hand, we have

Lemma 3.3.5 *Suppose D is an arbitrary diagram in the ZX_{full} -calculus. Then $ZX_{full} \vdash \llbracket \llbracket D \rrbracket_{XW} \rrbracket_{WX} = D$.*

Proof: By the construction of $\llbracket \cdot \rrbracket_{XW}$ and $\llbracket \cdot \rrbracket_{WX}$, we only need to prove for the generators of the ZX_{full} -calculus. Here we consider all the generators translated at the beginning of this section. The first six generators are the same as the first six generators in the $ZW_{\mathbb{C}}$ -calculus, so we just need to check for the last six generators. Since the red phase gate and the red spider are translated in terms of the translation of Hadamard gate, green phase gate and green spider, we only need to care for the four generators: Hadamard gate, green phase gate, λ box and the triangle.

Firstly,

$$\llbracket \llbracket \text{Green Circle} \rrbracket_{XW} \rrbracket = \text{Green Circle} e^{i\alpha},$$

so we have

$$\llbracket \llbracket \llbracket \text{Z} \rrbracket \rrbracket_{XW} \rrbracket_{WX} = \llbracket \llbracket e^{i\alpha} \rrbracket \rrbracket_{WX} = \llbracket \text{Z} \rrbracket,$$

by the definition of $\llbracket \cdot \rrbracket_{WX}$ and the ZX rule (L3). Similarly, we can easily check that

$$\llbracket \llbracket \llbracket \text{Z} \rrbracket \rrbracket_{XW} \rrbracket_{WX} = \llbracket \text{Z} \rrbracket.$$

Finally,

$$\begin{aligned} \llbracket \llbracket \llbracket \text{H} \rrbracket \rrbracket_{XW} \rrbracket_{WX} &= \llbracket \llbracket \frac{\sqrt{2}-2}{2} \text{ (diagram) } \rrbracket \rrbracket_{WX} = \llbracket \llbracket 1 - \frac{1}{\sqrt{2}} \text{ (diagram) } \rrbracket \rrbracket_{WX} \stackrel{IV}{=} \llbracket \llbracket \text{H} \rrbracket \rrbracket_{WX} \stackrel{S1,S2}{=} \llbracket \text{H} \rrbracket, \\ \llbracket \llbracket \llbracket \text{H} \rrbracket \rrbracket_{XW} \rrbracket_{WX} &= \llbracket \llbracket \text{ (diagram) } \rrbracket \rrbracket_{WX} = \llbracket \llbracket \text{ (diagram) } \rrbracket \rrbracket_{WX} \stackrel{B1,S1,S2}{=} \llbracket \text{H} \rrbracket. \end{aligned}$$

□

Therefore, by Lemma 3.3.4 and Lemma 3.3.5, the interpretations between the ZX_{full} -calculus and the ZW_C -calculus are mutually invertible to each other.

3.4 Completeness

Proposition 3.4.1 *If $ZW_C \vdash D_1 = D_2$, then $ZX_{full} \vdash \llbracket D_1 \rrbracket_{WX} = \llbracket D_2 \rrbracket_{WX}$.*

Proof: By the construction of the ZW -calculus, any two ZW diagrams are equal if and only if one of them can be rewritten into another. So here we need only to prove that $ZX_{full} \vdash \llbracket D_1 \rrbracket_{WX} = \llbracket D_2 \rrbracket_{WX}$ where $D_1 = D_2$ is a rewriting rule of ZW_C -calculus. This proof is quite lengthy, we put it at the end of this chapter for the convenience of reading. □

This proposition means the interpretation $\llbracket \cdot \rrbracket_{WX}$ is a well-defined functor from the PROP ZW_C to the PROP ZX_{full} . Together with lemma 3.3.4 and lemma 3.3.5, now we can say that there are invertible functors between the PROP ZW_C and the PROP ZX_{full} , which means the two calculi ZW_C and ZX_{full} are isomorphic.

At last, we prove the main theorem of this chapter.

Theorem 3.4.2 *The ZX_{full} -calculus is complete for the entire pure qubit quantum mechanics: If $\llbracket D_1 \rrbracket = \llbracket D_2 \rrbracket$, then $ZX_{full} \vdash D_1 = D_2$,*

Proof: Suppose $D_1, D_2 \in ZX_{full}$ and $\llbracket D_1 \rrbracket = \llbracket D_2 \rrbracket$. Then by lemma 3.3.1, $\llbracket \llbracket D_1 \rrbracket_{xw} \rrbracket = \llbracket D_1 \rrbracket = \llbracket D_2 \rrbracket = \llbracket \llbracket D_2 \rrbracket_{xw} \rrbracket$. Thus by the completeness of the ZW_C -calculus [33], $ZW_C \vdash \llbracket D_2 \rrbracket_{xw} = \llbracket D_2 \rrbracket_{xw}$. Now by proposition 3.4.1, $ZX_{full} \vdash \llbracket \llbracket D_1 \rrbracket_{xw} \rrbracket_{wx} = \llbracket \llbracket D_2 \rrbracket_{xw} \rrbracket_{wx}$. Finally, by lemma 3.3.5, $ZX_{full} \vdash D_1 = D_2$. \square

Now we can express the new generators in terms of green and red nodes.

Proposition 3.4.3 *The triangle \triangle and the lambda box λ are expressible in Z and X phases.*

Proof: The semantic representation of the triangle \triangle in terms of Z and X phases in the ZX-calculus has been clearly described in [42]. Interestingly, another representation of the triangle was implicitly given in [20] by a slash-labeled box in the following form:

$$\triangle_{[20]} = \text{Diagram with green and red nodes and phases} \quad (3.23)$$

It can be directly verified that the two diagrams on both sides of (3.23) have the same standard interpretation. Thus by Theorem 3.4.2 the identity (3.23) can be derived in the ZX_{full} -calculus.

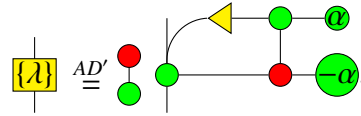
Now we consider the representation of the lambda box. Since λ is a non-negative real number, we can write λ as a sum of its integer part and remainder part: $\lambda = \llbracket \lambda \rrbracket + \{\lambda\}$, where $\llbracket \lambda \rrbracket$ is a non-negative integer and $0 \leq \{\lambda\} < 1$. Let $n = \llbracket \lambda \rrbracket$. If $n = 0$, then

$$\lambda_{[0]} = \text{Diagram sequence} \quad (3.24)$$

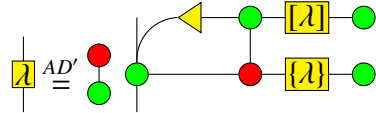
If $n \geq 1$, then by (3.19), we have

$$\lambda_{[n]} = \text{Diagram with stack of triangle gates and nodes}$$

Since $0 \leq \{\lambda\} < 1$, we could let $\alpha = \arccos \frac{\{\lambda\}}{2}$. Then $\{\lambda\} = 2 \cos \alpha = e^{i\alpha} + e^{-i\alpha}$, and



Therefore, we have



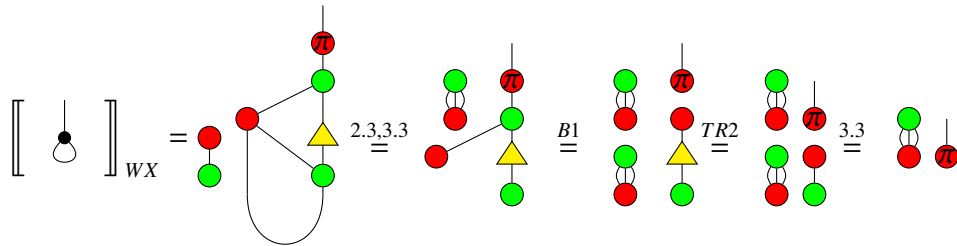
□

3.5 Proof of proposition 3.4.1

Lemma 3.5.1

$$\left[\begin{array}{c} \text{loop} \\ \text{WX} \end{array} \right] = \begin{array}{c} \text{green dot} \\ \text{red dot} \end{array} \pi \quad (3.25)$$

Proof:

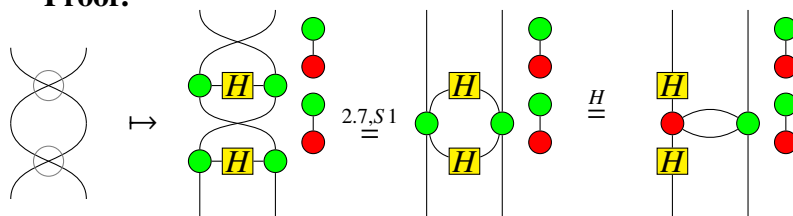


□

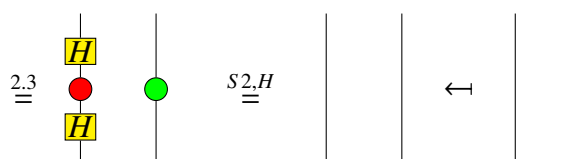
Proposition 3.5.2 (*ZW rule rei_2^x*)

$$ZX \vdash \left[\begin{array}{c} \text{crossing} \\ \text{WX} \end{array} \right] = \left[\begin{array}{c} \text{H} \\ \text{WX} \end{array} \right]$$

Proof:



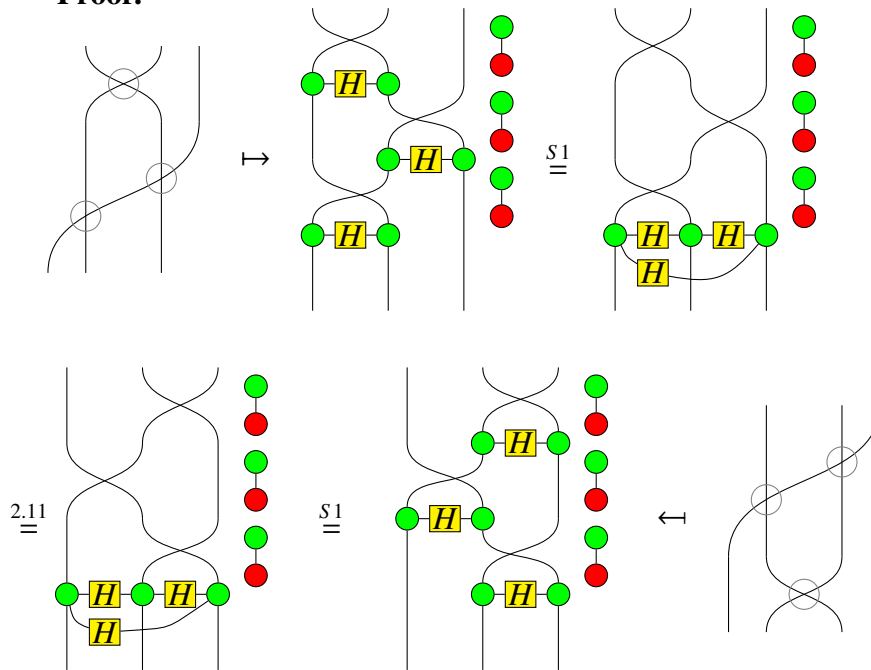
□



Proposition 3.5.3 (ZW rule rei_3^x)

$$ZX \vdash \left[\begin{array}{c} \text{Diagram 1} \\ \text{Diagram 2} \end{array} \right]_{WX} = \left[\begin{array}{c} \text{Diagram 3} \\ \text{Diagram 4} \end{array} \right]_{WX}$$

Proof:

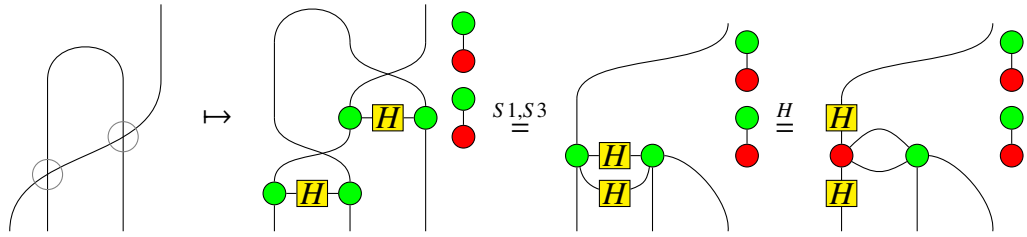


□

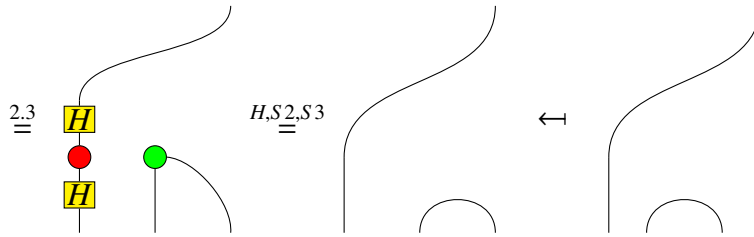
Proposition 3.5.4 (ZW rule nat_x^n)

$$ZX \vdash \left[\begin{array}{c} \text{Diagram 1} \\ \text{Diagram 2} \end{array} \right]_{WX} = \left[\begin{array}{c} \text{Diagram 3} \\ \text{Diagram 4} \end{array} \right]_{WX}$$

Proof:



□



Proposition 3.5.5 (*ZW rule nat_x^ε*)

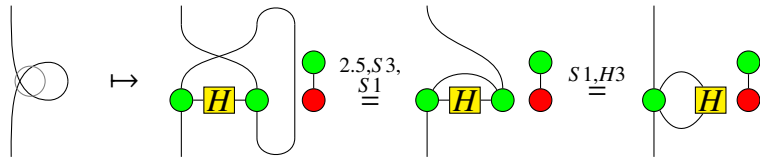
$$ZX \vdash \left[\begin{array}{c} \text{strand} \\ \text{strand} \end{array} \right]_{WX} = \left[\begin{array}{c} \text{crossing} \\ \text{strand} \end{array} \right]_{WX}$$

Proof: This is the upside-down version of Proposition 3.5.4, thus the proof is similar. We omit the proof but note that the rules and properties used are *S 1, S 2, S 3, H, 2.3*. □

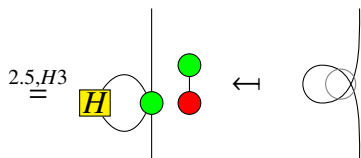
Proposition 3.5.6 (*ZW rule rei₁^x*)

$$ZX \vdash \left[\begin{array}{c} \text{circle} \\ \text{strand} \end{array} \right]_{WX} = \left[\begin{array}{c} \text{strand} \\ \text{strand} \end{array} \right]_{WX}$$

Proof:



(3.26)

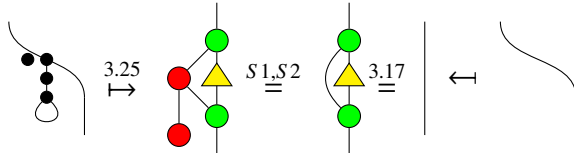


□

Proposition 3.5.7 (ZW rule $un_{w,L}^{co}$)

$$ZX \vdash \left[\begin{array}{c} \text{Diagram 1} \\ \hline \end{array} \right]_{WX} = \left[\begin{array}{c} \text{Diagram 2} \\ \hline \end{array} \right]_{WX}$$

Proof:

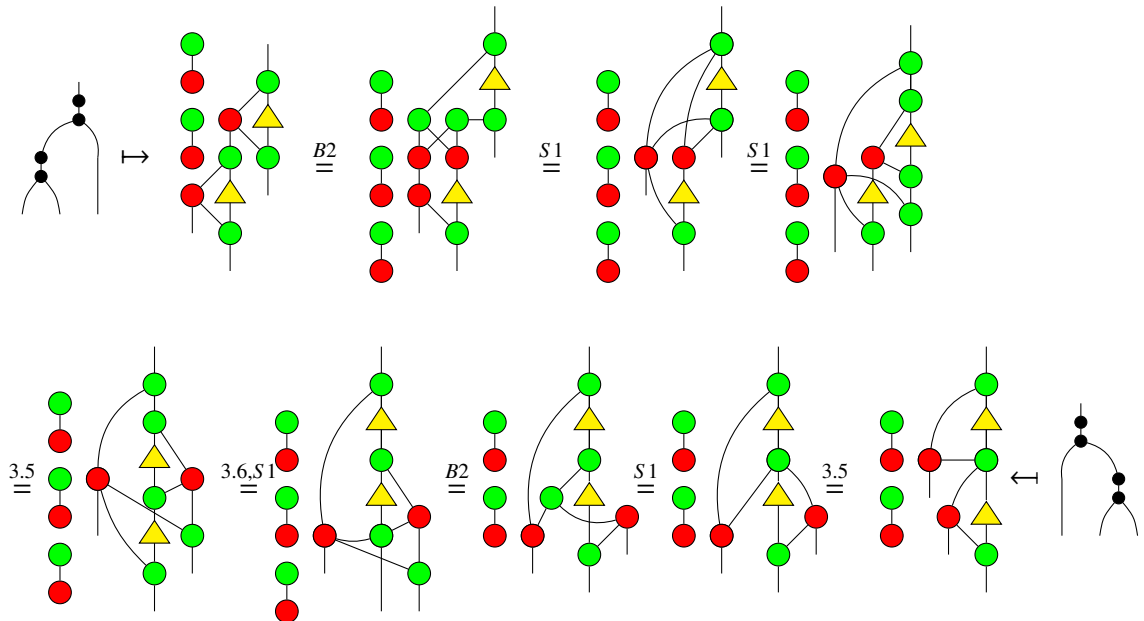


□

Proposition 3.5.8 (ZW rule $asso_w$)

$$ZX \vdash \left[\begin{array}{c} \text{Diagram 1} \\ \hline \end{array} \right]_{WX} = \left[\begin{array}{c} \text{Diagram 2} \\ \hline \end{array} \right]_{WX}$$

Proof:

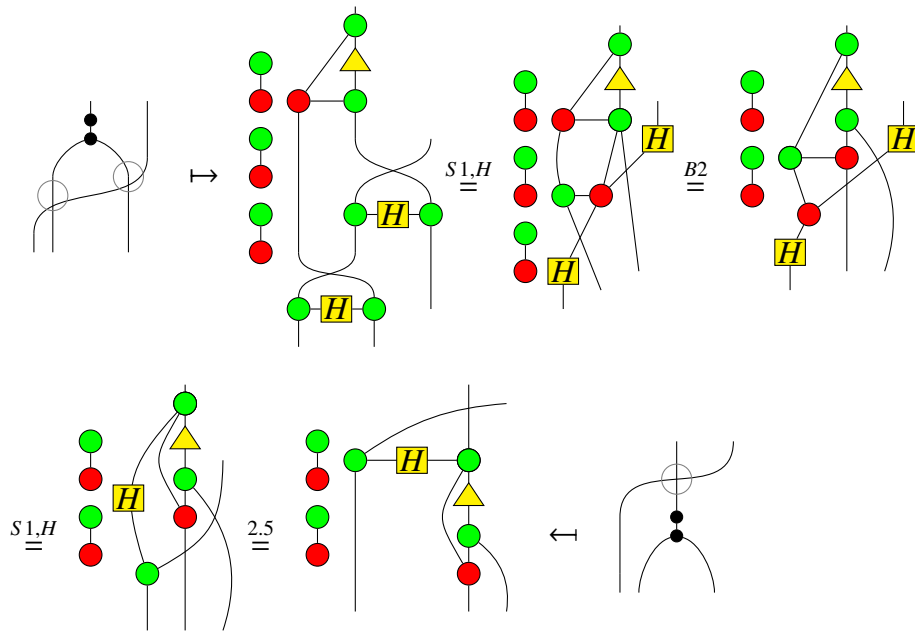


□

Proposition 3.5.9 (*ZW rule nat_x^w*)

$$\text{ZX} \vdash \left[\begin{array}{c} \text{Diagram 1} \\ \text{WX} \end{array} \right] = \left[\begin{array}{c} \text{Diagram 2} \\ \text{WX} \end{array} \right]$$

Proof:

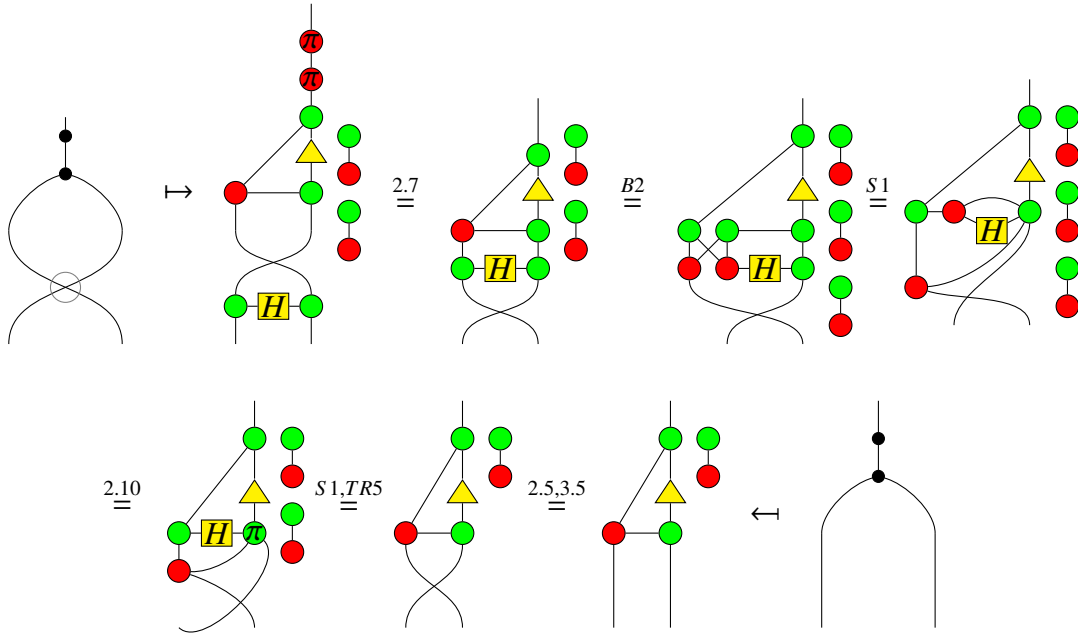


□

Proposition 3.5.10 (*ZW rule com_w^{co}*)

$$\text{ZX} \vdash \left[\begin{array}{c} \text{Diagram 1} \\ \text{WX} \end{array} \right] = \left[\begin{array}{c} \text{Diagram 2} \\ \text{WX} \end{array} \right]$$

Proof:



□

Proposition 3.5.11 (*ZW rule nat_w^m*)

$$\text{ZX} \vdash \left[\begin{array}{c} \bullet \\ \bullet \\ \bullet \\ \bullet \\ \bullet \\ \bullet \\ \bullet \\ \bullet \end{array} \right]_{\text{WX}} = \left[\begin{array}{c} \bullet \\ \bullet \\ \bullet \\ \bullet \\ \bullet \\ \bullet \\ \bullet \\ \bullet \end{array} \right]_{\text{WX}}$$

Proof: This has been proved in [42], proposition 7, part 5a. The proof is quite complicated, lots of rules and lemmas are employed. Fortunately, all the rules used for this proof in [42] are either a part of the rules in the ZX_{full} -calculus or derivatives from the rules of the ZX_{full} -calculus. Also, all the lemmas applied to this proof are either a part of the rules in the ZX_{full} -calculus or derived properties from the rules of the ZX_{full} -calculus. Therefore, we need not to repeat the proof here, but just indicate part by part the rules and lemmas used in [42], proposition 7, part 5a, with the correspondence between lemmas in [42] and rules and properties in the ZX_{full} -calculus shown in brackets.

There are eight parts in the proof: (i), (ii), (iii), (iv), (v), (vi), (vii), (viii), as well as a final derivation at the end.

The rules used in part (i) are $B2$, $S1$, H , lemma 23 (3.2.6 in this thesis), lemma 3 (2.4 in this thesis).

The rules used in part (ii) are lemma 26 (3.5 in this thesis), $S1$, $B2$, $S1$, lemma 32 (3.14 in this thesis), lemma 3 (2.4 in this thesis), lemma 16 ($TR1$ in this thesis).

The rules used in part (iii) are lemma 24 (TR6 in this thesis), lemma 26 (3.5 in this thesis), S1, lemma 27 (TR8 in this thesis), lemma 3 (2.4 in this thesis).

The rules used in part (iv) are lemma 26 (3.5 in this thesis), S1, B2, lemma 3 (2.4 in this thesis), lemma 32 (3.14 in this thesis).

The rules used in part (v) are lemma 3 (2.4 in this thesis), part (v).

The rules used in part (vi) are part (i), lemma 26 (3.5 in this thesis), lemma 28 (TR9 in this thesis), S1, lemma 3 (2.4 in this thesis), lemma 2 (2.3 in this thesis), lemma 16 (TR1 in this thesis), K2, part (iii), part (v), part (iv), part (ii).

The rules used in part (vii) are lemma 3 (2.4 in this thesis), S1, lemma 16 (TR1 in this thesis), B2, lemma 25 (TR7 in this thesis), lemma 26 (3.5 in this thesis), lemma 32 (3.14 in this thesis).

The rules used in part (viii) are lemma 3 (2.4 in this thesis), H, B2, S1, lemma 2 (2.3 in this thesis), lemma 8 (2.10 in this thesis).

The final derivation of the proof of this proposition uses lemma 26 (3.5 in this thesis), S1, part (viii), lemma 2 (2.3 in this thesis), part (vii), part (vi), B2, 2.5 and 3.7 in this thesis, lemma 3 (2.4 in this thesis), lemma 16 (TR1 in this thesis).

□

Proposition 3.5.12 (ZW rule nat_w^{mn})

$$ZX \vdash \left[\begin{array}{c} \text{Diagram: A vertical line with four black dots and a loop at the top, with a horizontal line branching to the left from the second dot.} \end{array} \right]_{WX} = \left[\begin{array}{c} \text{Diagram: Two vertical lines, each with a black dot and a loop at the top.} \end{array} \right]_{WX}$$

Proof:

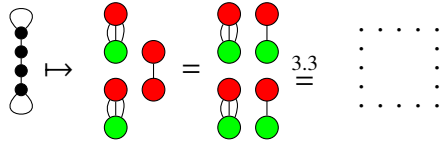
$$\begin{array}{c} \text{Diagram: Same as left side of Prop 3.5.12} \end{array} \mapsto \begin{array}{c} \text{Diagram: A complex diagram with red and green dots and yellow triangles.} \end{array} \stackrel{B1,3.3}{=} \begin{array}{c} \text{Diagram: Similar to previous, with different dot connections.} \end{array} \stackrel{TR2}{=} \begin{array}{c} \text{Diagram: Further simplified diagram.} \end{array} \stackrel{B1,3.3}{=} \begin{array}{c} \text{Diagram: Two vertical lines, each with a green dot and a loop at the top.} \end{array} \leftrightarrow \begin{array}{c} \text{Diagram: Two vertical lines, each with a black dot and a loop at the top.} \end{array}$$

□

Proposition 3.5.13 (ZW rule $\text{nat}_{\varepsilon,w}^{mn}$)

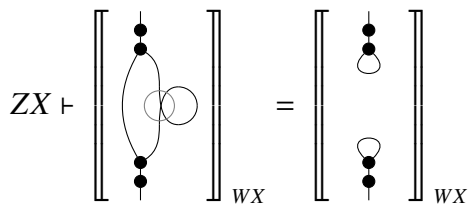
$$ZX \vdash \left[\begin{array}{c} \text{Diagram: A vertical line with four black dots and a loop at the bottom.} \end{array} \right]_{WX} = \left[\begin{array}{c} \text{Diagram: A square grid of dots with arrows indicating a path from the top-left to the bottom-right corner.} \end{array} \right]_{WX}$$

Proof:

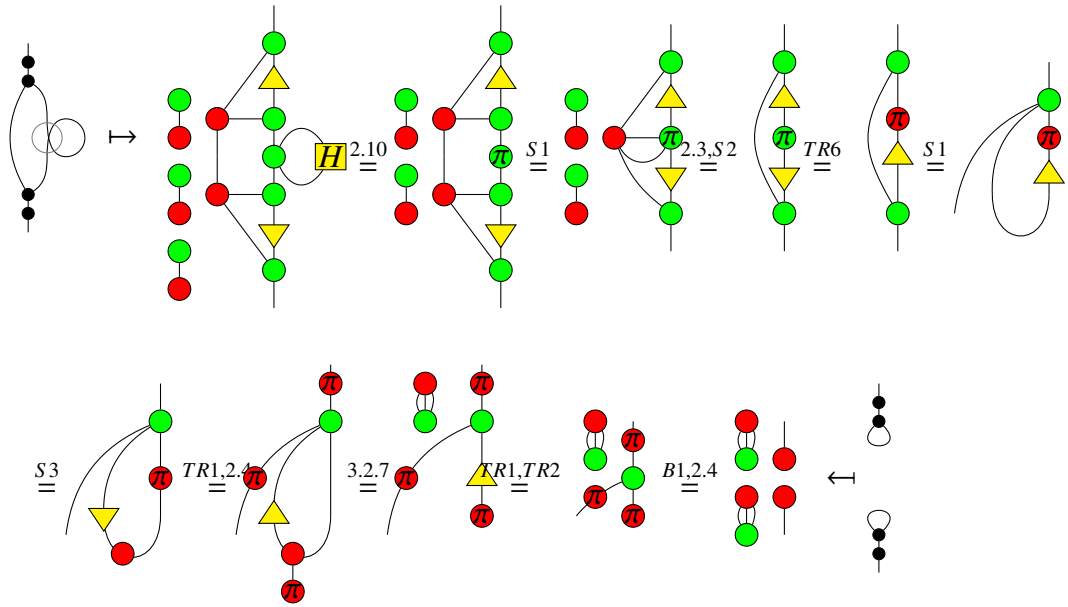


□

Proposition 3.5.14 (*ZW rule hopf*)

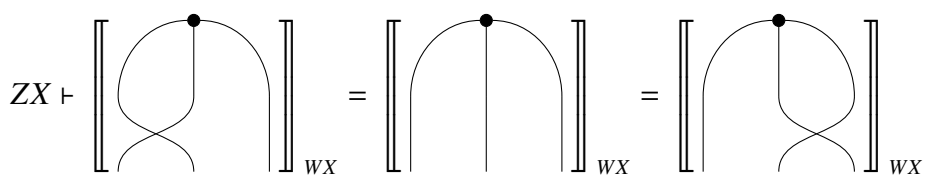


Proof:

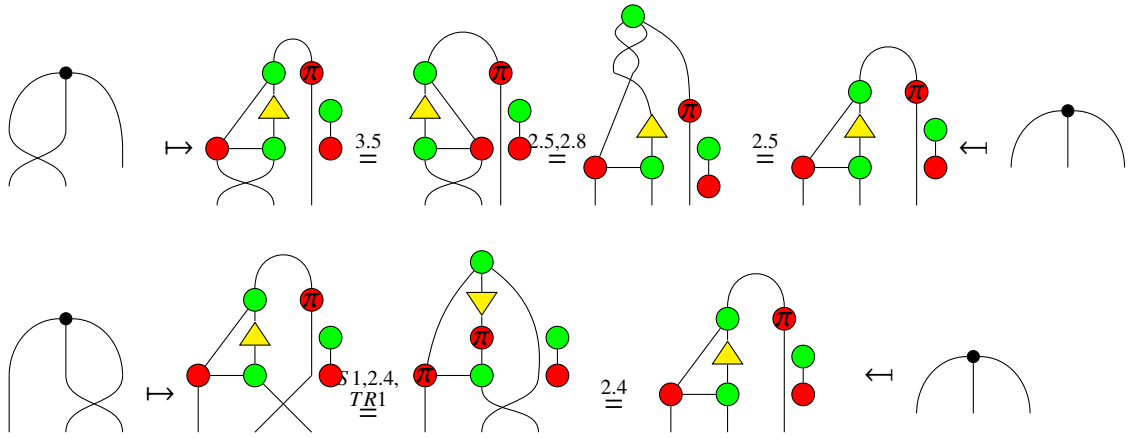


□

Proposition 3.5.15 (*ZW rules sym_{3,L} and sym_{3,R}*)

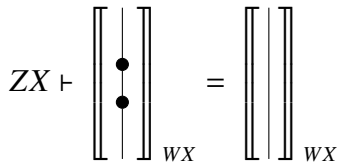


Proof:

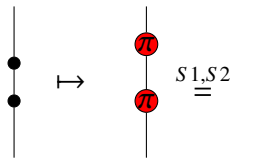


□

Proposition 3.5.16 (*ZW rule inv*)

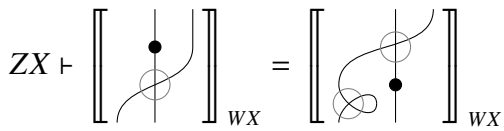


Proof:

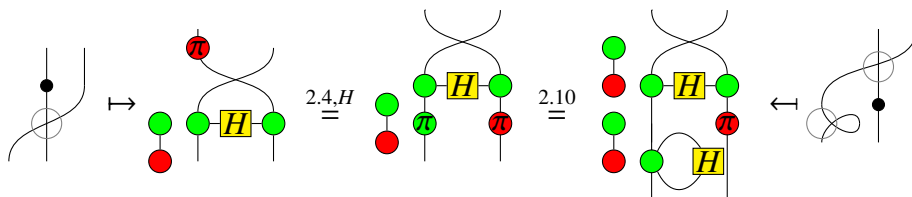


□

Proposition 3.5.17 (*ZW rule ant_x^l*)



Proof:

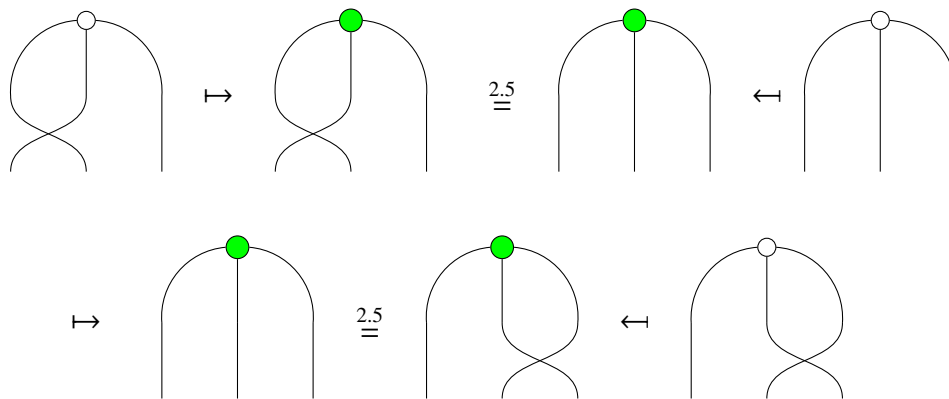


□

Proposition 3.5.18 (ZW rules $\text{sym}_{z,L}$ and $\text{sym}_{z,R}$)

$$\text{ZX} \vdash \left[\begin{array}{c} \text{Diagram 1} \\ \text{Diagram 2} \end{array} \right]_{WX} = \left[\begin{array}{c} \text{Diagram 3} \\ \text{Diagram 4} \end{array} \right]_{WX} = \left[\begin{array}{c} \text{Diagram 5} \\ \text{Diagram 6} \end{array} \right]_{WX}$$

Proof:

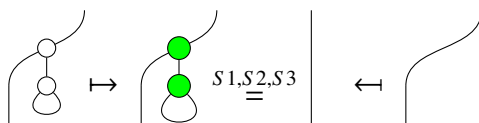


□

Proposition 3.5.19 (ZW rule $\text{un}_{z,R}^{co}$)

$$\text{ZX} \vdash \left[\begin{array}{c} \text{Diagram 1} \\ \text{Diagram 2} \end{array} \right]_{WX} = \left[\begin{array}{c} \text{Diagram 3} \\ \text{Diagram 4} \end{array} \right]_{WX}$$

Proof:

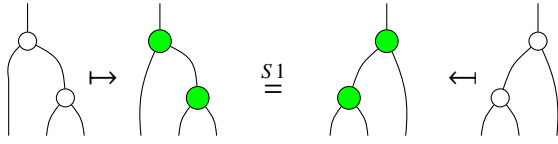


□

Proposition 3.5.20 (ZW rule asso_z)

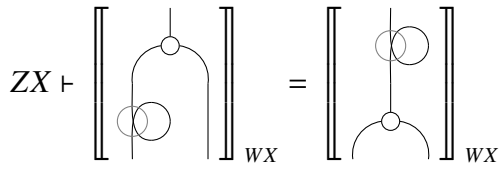
$$\text{ZX} \vdash \left[\begin{array}{c} \text{Diagram 1} \\ \text{Diagram 2} \end{array} \right]_{WX} = \left[\begin{array}{c} \text{Diagram 3} \\ \text{Diagram 4} \end{array} \right]_{WX}$$

Proof:

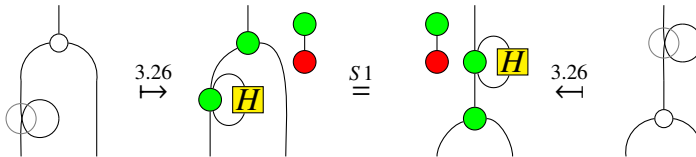


□

Proposition 3.5.21 (*ZW rule ph*)

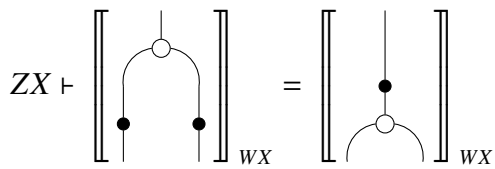


Proof:

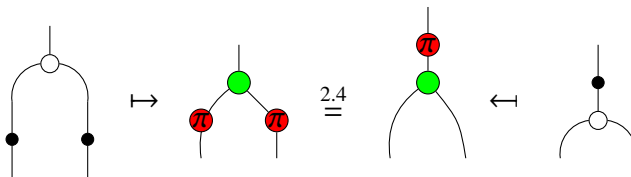


□

Proposition 3.5.22 (*ZW rule nat_cⁿ*)

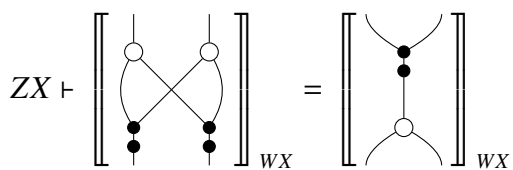


Proof:

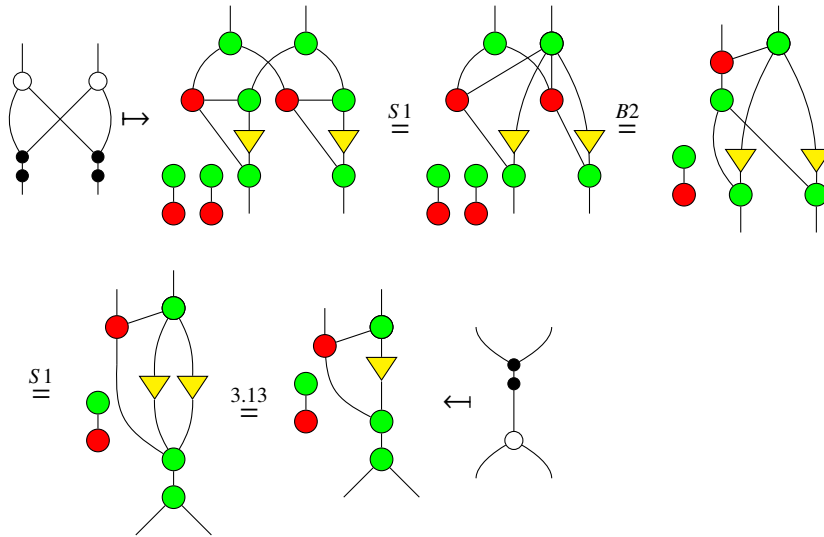


□

Proposition 3.5.23 (*ZW rule nat_c^m*)

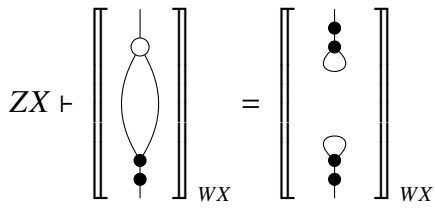


Proof:

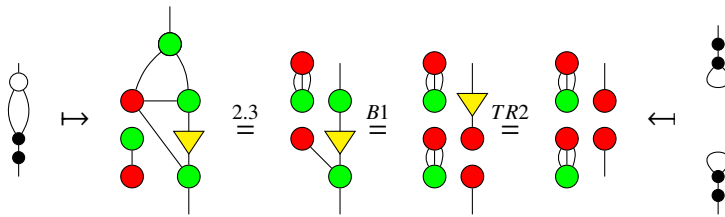


□

Proposition 3.5.24 (*ZW rule loop*)

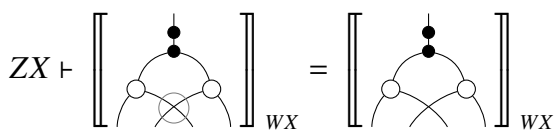


Proof:

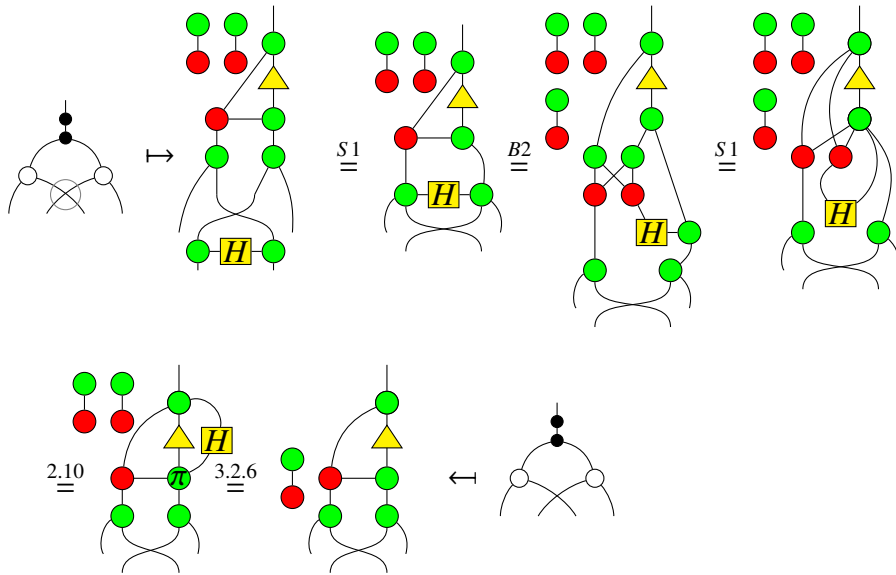


□

Proposition 3.5.25 (*ZW rule unx*)



Proof:

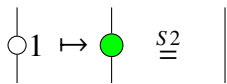


□

Proposition 3.5.26 (ZW rule rng_1)

$$ZX \vdash \left[\begin{array}{c} \circlearrowleft 1 \\ \hline \end{array} \right]_{WX} = \left[\begin{array}{c} | \\ | \\ | \\ \hline \end{array} \right]_{WX}$$

Proof:

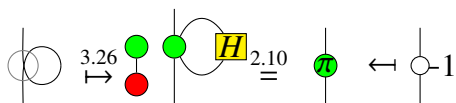


□

Proposition 3.5.27 (ZW rule rng_{-1})

$$ZX \vdash \left[\begin{array}{c} \circlearrowright \\ \hline \end{array} \right]_{WX} = \left[\begin{array}{c} \circlearrowleft 1 \\ \hline \end{array} \right]_{WX}$$

Proof:

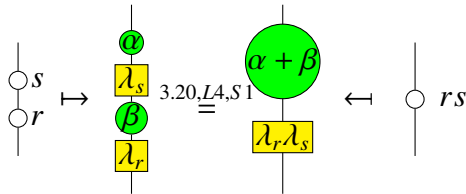


□

Proposition 3.5.28 (ZW rule $\text{rng}_\times^{r,s}$)

$$\text{ZX} \vdash \left[\begin{array}{c} \circ^s \\ | \\ \circ^r \end{array} \right]_{\text{WX}} = \left[\begin{array}{c} \circ \\ | \\ \circ \end{array} \right]_{\text{WX}}^{rs}$$

Proof:

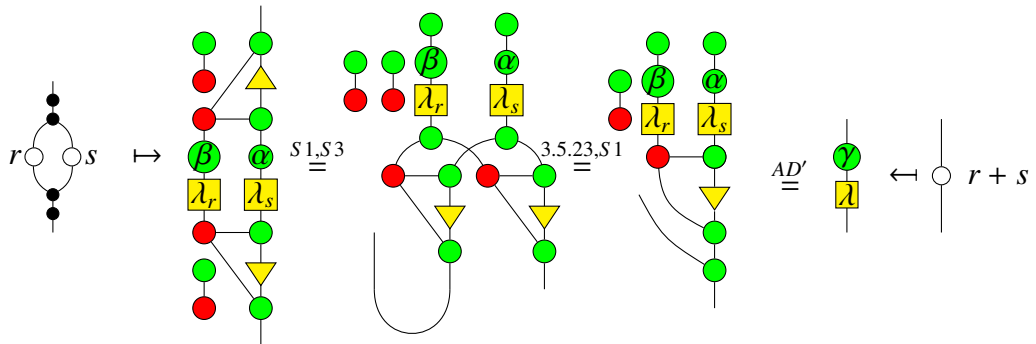


where $s = \lambda_s e^{i\alpha}$, $r = \lambda_r e^{i\beta}$. □

Proposition 3.5.29 (ZW rule $\text{rng}_+^{r,s}$)

$$\text{ZX} \vdash \left[\begin{array}{c} \bullet \\ | \\ \circ^r \circ^s \\ | \\ \bullet \end{array} \right]_{\text{WX}} = \left[\begin{array}{c} \circ \\ | \\ \circ \end{array} \right]_{\text{WX}}^{r+s}$$

Proof:

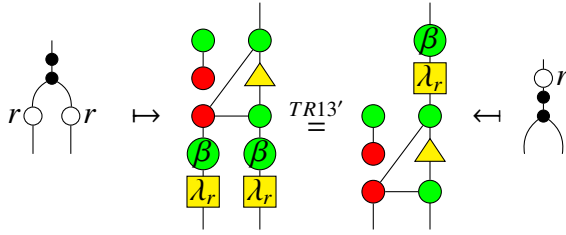


where $s = \lambda_s e^{i\alpha}$, $r = \lambda_r e^{i\beta}$, $r + s = \lambda e^{i\gamma}$. □

Proposition 3.5.30 (ZW rule nat_c^r)

$$\text{ZX} \vdash \left[\begin{array}{c} \bullet \\ | \\ \circ^r \circ^r \\ | \\ \bullet \end{array} \right]_{\text{WX}} = \left[\begin{array}{c} \circ^r \\ | \\ \bullet \end{array} \right]_{\text{WX}}$$

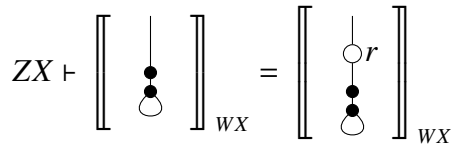
Proof:



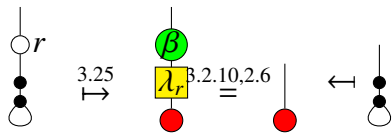
where $r = \lambda_r e^{i\beta}$.

□

Proposition 3.5.31 (ZW rule nat_{ec}^r)



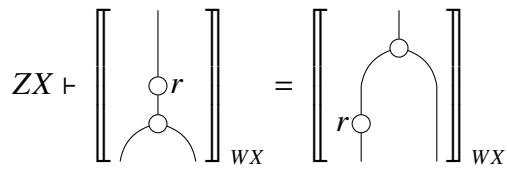
Proof:



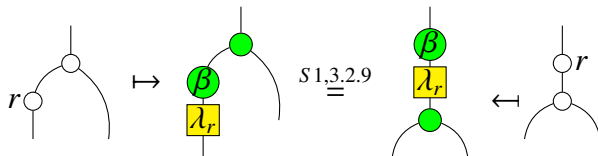
where $r = \lambda_r e^{i\beta}$.

□

Proposition 3.5.32 (ZW rule ph^r)



Proof:



where $r = \lambda_r e^{i\beta}$.

□

Chapter 4

Completeness for Clifford+T qubit quantum mechanics

Clifford+T qubit quantum mechanics (QM) is an approximately universal fragment of QM, which has been widely used in quantum computing. One of the main open problems of the ZX-calculus is to give a complete axiomatisation for the Clifford+T QM [1]. After the first completeness result on this fragment—the completeness of the ZX-calculus for single qubit Clifford+T QM [4], there finally comes an completion of the ZX-calculus for the whole Clifford+T QM [42], which contributes a solution to the above mentioned open problem. However, this complete axiomatisation for the Clifford+T QM relies on a very complicated translation from the ZX-calculus to the ZW-calculus.

Further to this complete axiomatisation for the Clifford+T fragment QM [42], we have given a complete axiomatisation of the ZX-calculus for the overall pure qubit QM (i.e., the ZX_{full} -calculus) in the previous chapter. Then a natural question arises: can we just make a restriction on the generators and rules of the ZX_{full} -calculus obtained in Chapter 3 to trivially get a complete axiomatisation of the ZX-calculus for the Clifford+T QM (called ZX_{C+T} -calculus)? The answer is negative: we will show in this chapter that we can have a complete ZX_{C+T} -calculus by restricting on the generators and rules of the ZX_{full} -calculus, but some modifications like changing or adding rules have to be made. We will illustrate this by a counterexample. To do this, we need to determine the range of the value of λ in a λ box which will be used as a generator in the ZX_{C+T} -calculus. Let $\mathbb{T} := \mathbb{Z}[\frac{1}{2}, e^{i\frac{\pi}{4}}]$ be the ring extension of \mathbb{Z} in \mathbb{C} generated by $\frac{1}{2}, e^{i\frac{\pi}{4}}$. Similarly we can define the ring $\mathbb{Z}[i, \frac{1}{\sqrt{2}}]$. It is not difficult to see that \mathbb{T} is a commutative ring and $\mathbb{Z}[\frac{1}{2}, e^{i\frac{\pi}{4}}] = \mathbb{Z}[i, \frac{1}{\sqrt{2}}]$.

Denote by $ZX_{\frac{\pi}{4}}$ the ZX-calculus which has only traditional generators as given in Table 6.1 and angles multiple of $\frac{\pi}{4}$ in any green or red spider. Now we recall a result on the relation between $ZX_{\frac{\pi}{4}}$ diagrams and their corresponding matrices (we will give a simpler proof later in this Chapter):

Proposition 4.0.1 [42] *The diagrams of the $ZX_{\frac{\pi}{4}}$ -calculus exactly corresponds to the matrices over the ring \mathbb{T} .*

This means if we want to introduce the λ box as a generator in the the same way (λ being the magnitude of a complex number) as in Chapter 3 to make a ZX_{C+T} -calculus, then it must be that each λ is a non-negative real number and $\lambda \in \mathbb{T}$. Furthermore, as pointed out in [42], each element r of \mathbb{T} can be uniquely written as the form $r = a_0 + a_1 e^{i\frac{\pi}{4}} + a_2 (e^{i\frac{\pi}{4}})^2 + a_3 (e^{i\frac{\pi}{4}})^3$, $a_j \in \mathbb{Z}[\frac{1}{2}]$. Equivalently, $r = a_0 e^{i\alpha_0} + a_1 e^{i\alpha_1} + a_2 e^{i\alpha_2} + a_3 e^{i\alpha_3}$, $0 \leq a_j \in \mathbb{Z}[\frac{1}{2}]$, $\alpha_j = j\frac{\pi}{4}$ or $j\frac{\pi}{4} + \pi$, $j = 0, 1, 2, 3$. Therefore, if an arbitrary complex number in \mathbb{T} has phase restricted to multiple of $\frac{\pi}{4}$, then its magnitude λ must satisfy that $0 \leq \lambda \in \mathbb{Z}[\frac{1}{2}]$. On the other hand, we have the following identity in the ZX_{full} -calculus by the rule (AD’):

$$(4.1)$$

The left side of (4.1) is already in the range of ZX_{C+T} -calculus, but the right side of (4.1) is beyond the ZX_{C+T} -calculus ($\lambda = \sqrt{2} \notin \mathbb{Z}[\frac{1}{2}]$). This means we can not have a ZX_{C+T} -calculus that is complete for the Clifford+T QM just by restricting on the generators and rules of the ZX_{full} -calculus.

In this chapter, we propose a complete axiomatisation of the ZX-calculus for the Clifford+T quantum mechanics (the ZX_{C+T} -calculus), not only making a restriction on the generators and rules of the ZX_{full} -calculus, but also modifying and adding some rules. As before, we still need the completeness result of the ZW-calculus, but will restrict the parameter ring \mathbb{C} to its subring \mathbb{T} in the ZW-calculus (will be called $ZW_{\mathbb{T}}$ -calculus afterwards in this thesis) [33].

The results of this chapter are collected from the arXiv paper [57] coauthored with Kang Feng Ng. The proof of the completeness of the ZX_{C+T} -calculus has been published in [34], with coauthors Amar Hadzihasanovic and Kang Feng Ng.

4.1 ZX_{C+T} -calculus

In this section, we give for the ZX_{C+T} -calculus all the rewriting rules which will be shown to be sufficient for the completeness with regard to the Clifford+T QM.

The ZX_{C+T} -calculus is still a kind of ZX-calculus as described in the previous chapter. Its generators are listed in Table 6.1 and Table 3.1, with the restriction that $\alpha \in \{\frac{k\pi}{4} | k = 0, 1, \dots, 7\}$, $0 \leq \lambda, \in \mathbb{Z}[\frac{1}{2}]$.

There are two kinds of rules for the ZX_{C+T} -calculus: the categorical structure rules as listed in (2.1) and (2.2), and the non-structural rewriting rules including the traditional rules in Figure 4.1 and the extended rules in Figure 4.2.

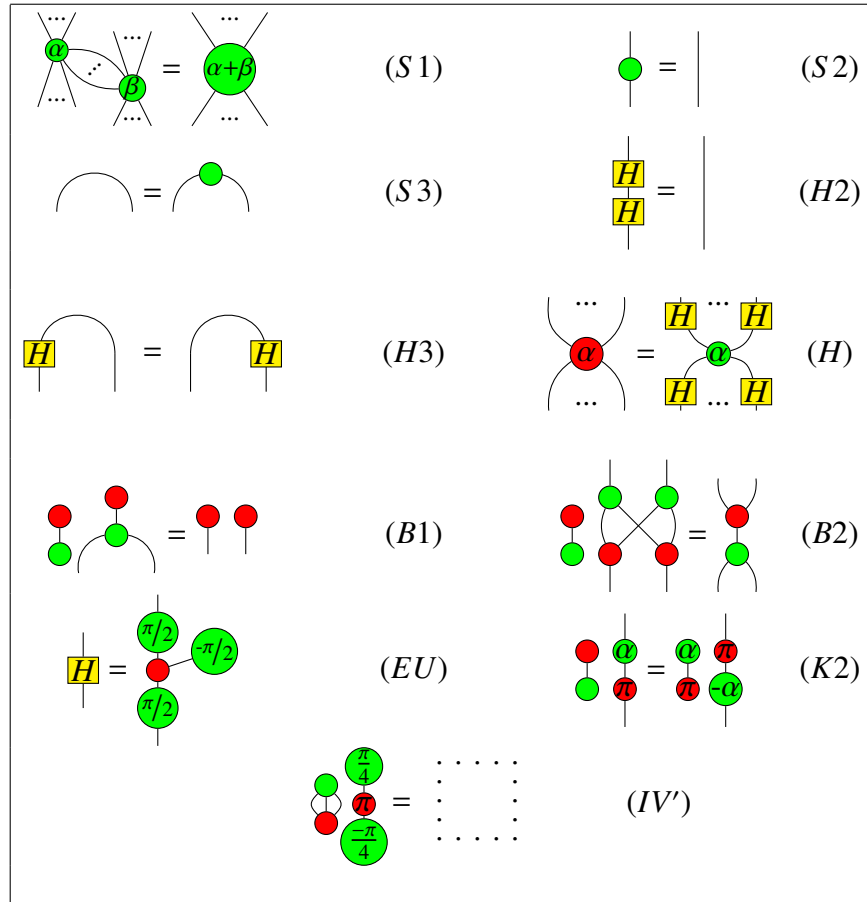


Figure 4.1: Traditional-style ZX_{C+T} -calculus rules, where $\alpha, \beta \in \{\frac{k\pi}{4} | k = 0, 1, \dots, 7\}$. The upside-down version and colour swapped version of these rules still hold.

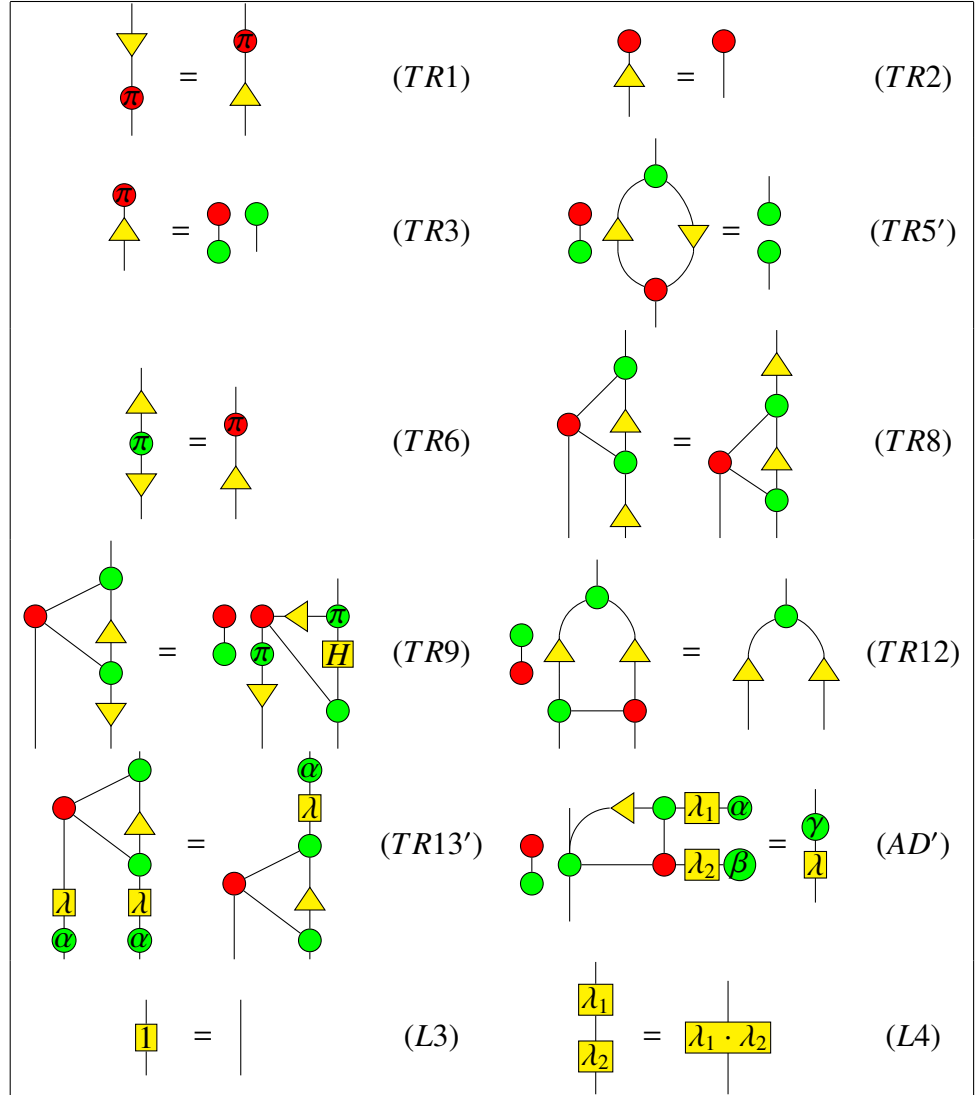


Figure 4.2: ZX_{C+T} -calculus rules with triangle and λ box, where $0 \leq \lambda, \lambda_1, \lambda_2 \in \mathbb{Z}[\frac{1}{2}]$, $\alpha \in \{\frac{k\pi}{4} | k = 0, 1, \dots, 7\}$, $\alpha \equiv \beta \equiv \gamma \pmod{\pi}$ in (AD'). The upside-down version of these rules still hold.

In comparison to the rules of the ZX_{full} -calculus, except for the restrictions described above, we made the following modifications in the ZX_{C+T} -calculus:

- The empty rule (IV2) for the ZX_{full} -calculus shown in Figure 3.5 is changed to the form of rule (IV') in Figure 4.1.
- The rule (TR5') is added in Figure 4.1.
- The condition $\lambda e^{i\gamma} = \lambda_1 e^{i\beta} + \lambda_2 e^{i\alpha}$ for the rule (AD') of the ZX_{full} -calculus shown in

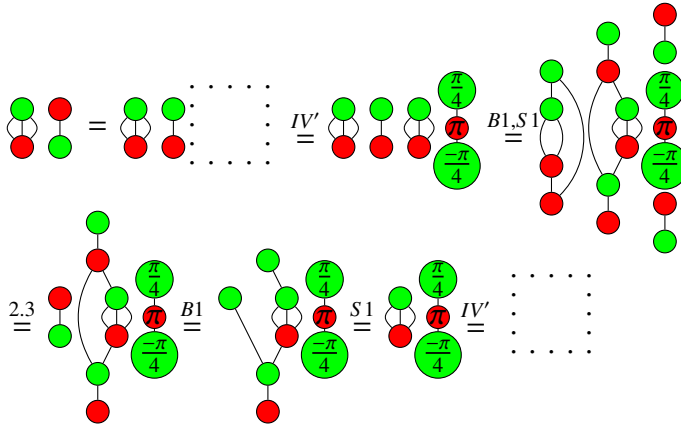
Figure 3.5 has been changed to an equivalence condition $\alpha \equiv \beta \equiv \gamma \pmod{\pi}$ for the rule (AD') of the ZX_{C+T} -calculus shown in Figure 4.2.

Next we explain these modifications are needed. Firstly, the complex number $1 - \frac{1}{\sqrt{2}}$ in the λ box of the rule (IV2) does not exist in the ZX_{C+T} -calculus, so a modified empty rule is required for the ZX_{C+T} -calculus satisfying that the translation of the Hadamard gate to a ZW diagram is reversible. Therefore we have the rule (IV') and the following useful property.

Lemma 4.1.1 *The frequently used empty rule can be derived from the $ZX_{\frac{\pi}{4}}$ -calculus:*


(4.2)

Proof:



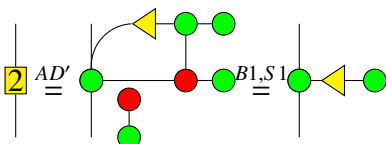
□

Secondly, the rule (TR5') is introduced to make the $\frac{1}{2}$ -box expressible in the ZX_{C+T} -calculus:

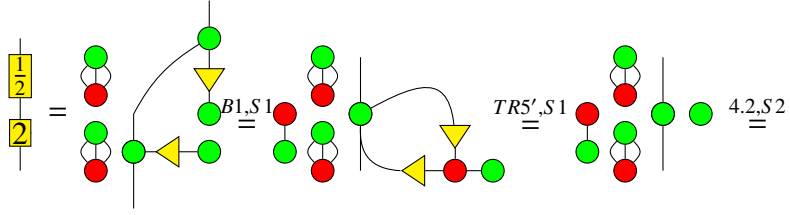
Lemma 4.1.2


(4.3)

Proof: First, it is clear that



Then



□

Finally, it is easy to check that the condition $\lambda e^{i\gamma} = \lambda_1 e^{i\beta} + \lambda_2 e^{i\alpha}$ is equivalent to the condition $\alpha \equiv \beta \equiv \gamma \pmod{\pi}$, when $0 \leq \lambda, \lambda_1, \lambda_2 \in \mathbb{Z}[\frac{1}{2}]$, $\alpha, \beta, \gamma \in \{\frac{k\pi}{4} | k = 0, 1, \dots, 7\}$.

Following the soundness of the ZX_{full} -calculus, it suffice to check that the rules (IV') and (TR5') are sound in order to have the soundness of ZX_{C+T} -calculus. This is just a routine verification, we omit the details here.

Also we mention that the rules (TR10'), (TR5) and (L5) proved in Chapter 3 for the ZX_{full} -calculus still hold for the ZX_{C+T} -calculus, since each rule applied in those proofs resides in the ZX_{C+T} -calculus as well.

In the previous chapter, the lambda box has been described in terms of triangle, green nodes and red nodes with angles in $[0, 2\pi)$. While for the ZX_{C+T} -calculus, we have

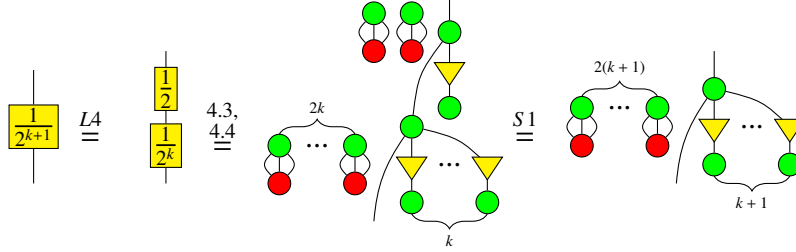
Lemma 4.1.3 *The lambda box λ is expressible in terms of triangle, green nodes and red nodes with angles in $\{\frac{k\pi}{4} | k = 0, 1, \dots, 7\}$.*

Proof:

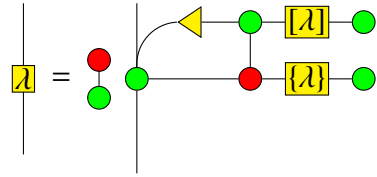
First we can write λ as a sum of its integer part and remainder part: $\lambda = [\lambda] + \{\lambda\}$, where $[\lambda]$ is a non-negative integer and $0 \leq \{\lambda\} < 1$. Since $\lambda \in \mathbb{Z}[\frac{1}{2}]$, $\{\lambda\}$ can be uniquely written as a binary expansion of the form $a_1 \frac{1}{2} + \dots + a_s \frac{1}{2^s}$, where $a_i \in \{0, 1\}$, $i = 1, \dots, s$. For the integer part $[\lambda]$, the corresponding λ box has been represented in terms of triangle, green nodes and red nodes with angles multiples of $\frac{k\pi}{4}$ as shown in Lemma 3.4.3. For the remainder part $\{\lambda\}$, it is sufficient to express the λ box for $\lambda = \frac{1}{2^k}$ in terms of triangle and Z, X phases for any positive integer k , since one can apply the addition rule (AD') recursively. In fact, we have

(4.4)

We prove this by induction on k . When $k = 1$, it is just the identity (4.3) proved in Lemma 4.1.2. Suppose (4.4) holds for k . Then for $k + 1$ we have



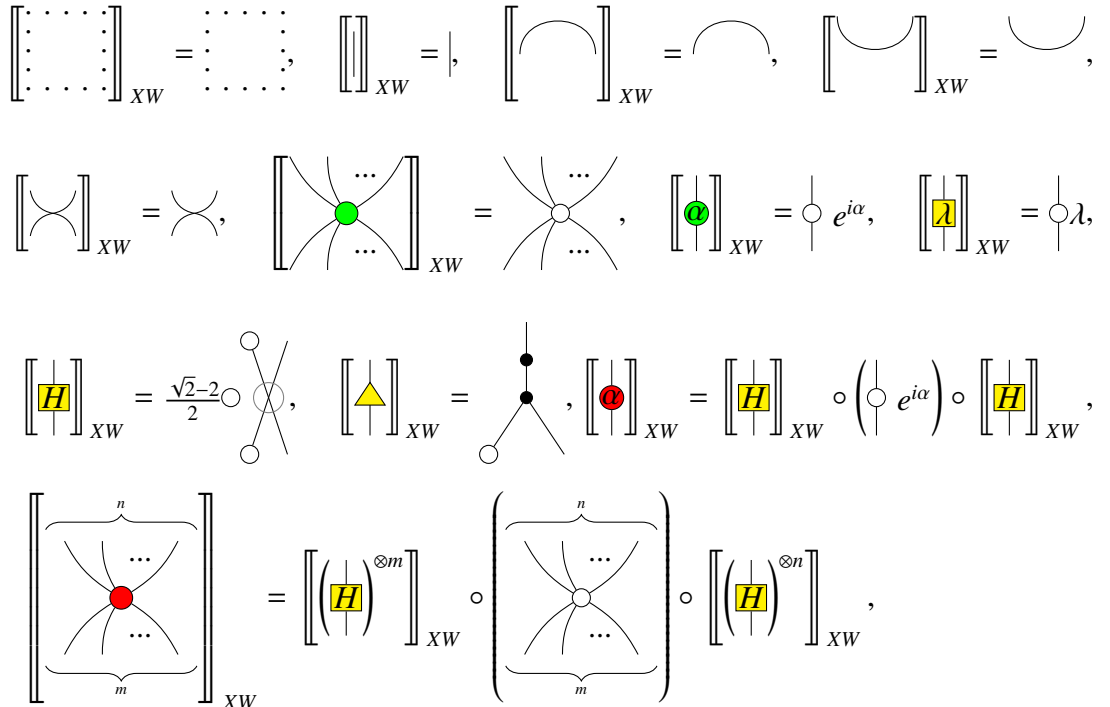
This completes the induction. Therefore,



□

4.2 Translations between the ZX_{C+T} -calculus and the $ZW_{\mathbb{T}}$ -calculus

The interpretation $[\cdot]_{XW}$ from the ZX_{C+T} -calculus to the $ZW_{\mathbb{T}}$ -calculus is just a restriction of the interpretation $[\cdot]_{XW}$ from the ZX_{full} -calculus to the $ZW_{\mathbb{C}}$ -calculus:



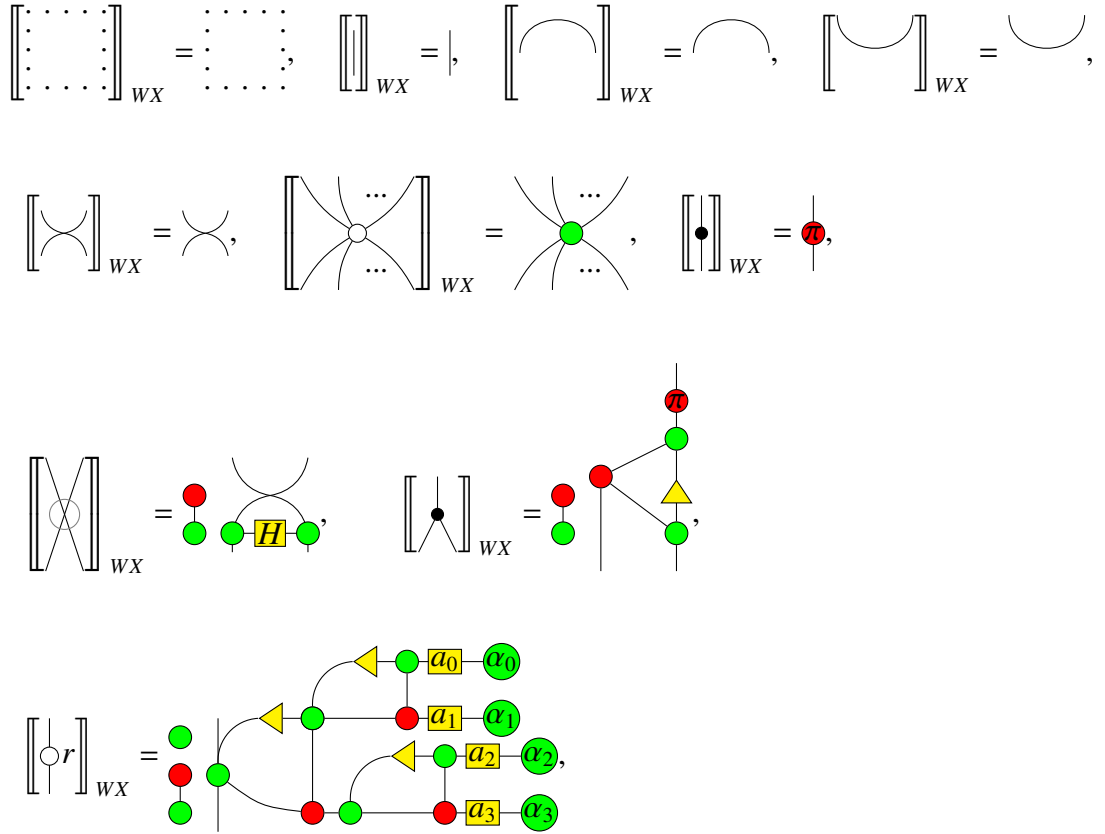
$$[[D_1 \otimes D_2]]_{XW} = [[D_1]]_{XW} \otimes [[D_2]]_{XW}, \quad [[D_1 \circ D_2]]_{XW} = [[D_1]]_{XW} \circ [[D_2]]_{XW},$$

where $0 \leq \lambda \in \mathbb{Z}[\frac{1}{2}], \alpha \in \{\frac{k\pi}{4} | k = 0, 1, \dots, 7\}$.

Since $\mathbb{T} = \mathbb{Z}[\frac{1}{2}, e^{i\frac{\pi}{4}}] = \mathbb{Z}[i, \frac{1}{\sqrt{2}}]$, we have $\frac{\sqrt{2}-2}{2} \in \mathbb{T}$. Then it is clear that this restricted translation will always result in a well-defined $ZW_{\mathbb{T}}$ diagram.

By Lemma 3.3.1 the interpretation $[[\cdot]]_{XW}$ preserves the standard interpretation.

On the other hand, the interpretation $[[\cdot]]_{WX}$ from the $ZW_{\mathbb{T}}$ -calculus to the ZX_{C+T} -calculus is the same as the interpretation $[[\cdot]]_{WX}$ from the ZX_{full} -calculus to the ZW_C -calculus except for the r -phase part:



$$[[D_1 \otimes D_2]]_{WX} = [[D_1]]_{WX} \otimes [[D_2]]_{WX}, \quad [[D_1 \circ D_2]]_{WX} = [[D_1]]_{WX} \circ [[D_2]]_{WX},$$

where $r = a_0 e^{i\alpha_0} + a_1 e^{i\alpha_1} + a_2 e^{i\alpha_2} + a_3 e^{i\alpha_3}$, $0 \leq a_j \in \mathbb{Z}[\frac{1}{2}]$, $\alpha_j = j\frac{\pi}{4}$ or $j\frac{\pi}{4} + \pi$, $j = 0, 1, 2, 3$. Note that the representation of a_j box is described in Lemma 4.1.3.

It seems that the interpretation of the r -phase is somehow complicated. However, the corresponding interpreted ZX diagram is actually the result of three applications of the addition rule (AD') according to the identity $r = a_0 e^{i\alpha_0} + a_1 e^{i\alpha_1} + a_2 e^{i\alpha_2} + a_3 e^{i\alpha_3}$, which clearly has the same standard interpretation as that of the r -phase if we take this as happened in

the ZX_{full} -calculus. Then by Lemma 3.3.2, the interpretation $[\cdot]_{WX}$ from the ZW_T -calculus to the ZX_{C+T} -calculus preserves the standard interpretation.

Next we will prove that the effect of successive translations from ZX to ZW and then back to ZX is the same as no translations.

Lemma 4.2.1

$$\text{Diagram} = \text{Diagram} \tag{4.5}$$

Proof:

$$\text{Diagram} \stackrel{S1,4.2}{=} \text{Diagram} \stackrel{S1}{=} \text{Diagram} \stackrel{TR10'}{=} \text{Diagram} \stackrel{2.4}{=} \text{Diagram} \stackrel{S1,2.3}{=} \text{Diagram} \stackrel{S1,4.2}{=} \text{Diagram} \tag{4.5}$$

□

Lemma 4.2.2

$$\text{Diagram} = \text{Diagram} \tag{4.6}$$

Proof:

$$\text{Diagram} \stackrel{S1}{=} \text{Diagram} \stackrel{TR1}{=} \text{Diagram} \stackrel{TR2}{=} \text{Diagram} \tag{4.6}$$

□

Lemma 4.2.3

$$\text{Diagram} = \text{Diagram} \tag{4.7}$$

Proof:

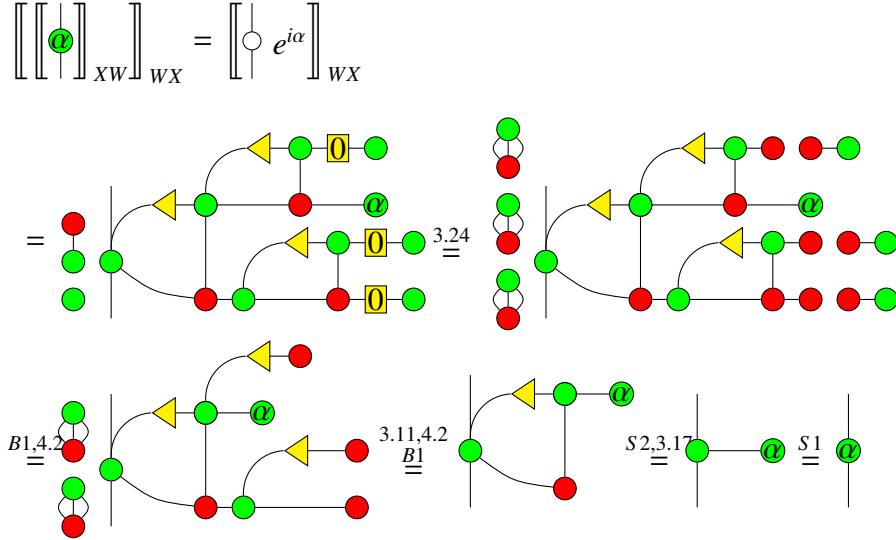
$$\text{Diagram} \stackrel{2.4,B1, 4.2}{=} \text{Diagram} \stackrel{2.3,S1}{=} \text{Diagram} \stackrel{2.4,S1}{=} \text{Diagram} \stackrel{B1,4.2}{=} \text{Diagram} \stackrel{IV'}{=} \text{Diagram} \tag{4.7}$$

□

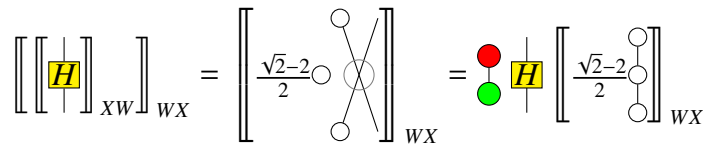
Lemma 4.2.4 Suppose D is an arbitrary diagram in the ZX_{C+T} -calculus. Then $ZX_{C+T} \vdash \llbracket \llbracket D \rrbracket_{XW} \rrbracket_{WX} = D$.

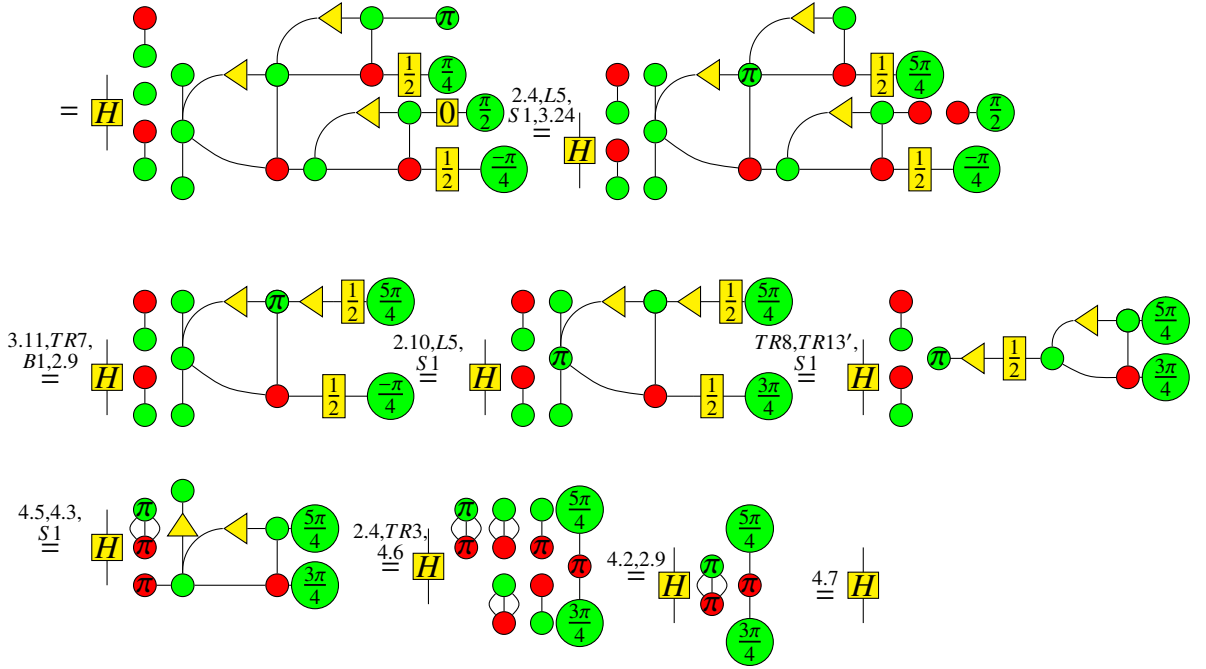
Proof: By the construction of $\llbracket \cdot \rrbracket_{XW}$ and $\llbracket \cdot \rrbracket_{WX}$, we only need to prove for the generators of the ZX_{C+T} -calculus. Here we consider all the generators translated at the beginning of this section. The first six generators are the same as the first six generators in the ZW_T -calculus, so we just need to check for the last six generators. Since the red phase gate and the red spider are translated in terms of the translation of Hadamard gate, green phase gate and green spider, we only need to care for the four generators: Hadamard gate, green phase gate, λ box and the triangle.

For the green phase gate, if we write $e^{i\alpha}$ in the form $r = a_0 + a_1e^{i\frac{\pi}{4}} + a_2e^{i\frac{2\pi}{4}} + a_3e^{i\frac{3\pi}{4}}$, there is exactly one a_i which is non-zero. By commutative property of addition 3.10, we have



For the Hadamard gate, we write $\frac{\sqrt{2}-2}{2} = -1 + \frac{1}{2}e^{i\frac{\pi}{4}} + 0e^{i\frac{2\pi}{4}} - \frac{1}{2}e^{i\frac{3\pi}{4}} = -1 + \frac{1}{2}e^{i\frac{\pi}{4}} + 0e^{i\frac{2\pi}{4}} + \frac{1}{2}e^{i\frac{-\pi}{4}}$, then





Finally, it is easy to check that

$$\llbracket \llbracket \lambda \rrbracket_{XW} \rrbracket_{WX} = \lambda, \quad \llbracket \llbracket \triangle \rrbracket_{XW} \rrbracket_{WX} = \triangle.$$

□

For the same reason as we have shown in Section 3.3 of Chapter 3, the translations $\llbracket \cdot \rrbracket_{XW}$ and $\llbracket \cdot \rrbracket_{WX}$ are mutually invertible to each other.

4.3 Completeness

Proposition 4.3.1 *If $ZW_{\mathbb{T}} \vdash D_1 = D_2$, then $ZX_{C+T} \vdash \llbracket D_1 \rrbracket_{WX} = \llbracket D_2 \rrbracket_{WX}$.*

Proof: Since the derivation of equalities in ZW and ZX is made by rewriting rules, we need only to prove that $ZX_{C+T} \vdash \llbracket D_1 \rrbracket_{WX} = \llbracket D_2 \rrbracket_{WX}$ where $D_1 = D_2$ is a rewriting rule of the $ZW_{\mathbb{T}}$ -calculus. Most proofs of this proposition have been done in the proof for completeness of the ZX_{full} -calculus in the previous chapter, we only need to check for the last 5 rules $rng_{\times}^{r,s}$, $rng_{+}^{r,s}$, nat_c^r , nat_{ec}^r , ph^r , which involve white phases in the $ZW_{\mathbb{T}}$ -calculus. The rules nat_{ec}^r and ph^r are easy to check, we just deal with the rules $rng_{\times}^{r,s}$, $rng_{+}^{r,s}$ and nat_c^r at the end of this section, for the sake of easy reading. □

Theorem 4.3.2 *The ZX_{C+T} -calculus is complete for Clifford+T QM: if $\llbracket D_1 \rrbracket = \llbracket D_2 \rrbracket$, then $ZX_{C+T} \vdash D_1 = D_2$.*

Proof: Suppose $D_1, D_2 \in ZX$ and $\llbracket D_1 \rrbracket = \llbracket D_2 \rrbracket$. Then by lemma ??, $\llbracket \llbracket D_1 \rrbracket_{XW} \rrbracket = \llbracket D_1 \rrbracket = \llbracket D_2 \rrbracket = \llbracket \llbracket D_2 \rrbracket_{XW} \rrbracket$. Thus by the completeness of the $ZW_{\mathbb{T}}$ -calculus [33], $ZW_{\mathbb{T}} \vdash \llbracket D_2 \rrbracket_{XW} = \llbracket D_2 \rrbracket_{XW}$. Now by proposition 4.3.1, $ZX_{C+T} \vdash \llbracket \llbracket D_1 \rrbracket_{XW} \rrbracket_{WX} = \llbracket \llbracket D_2 \rrbracket_{XW} \rrbracket_{WX}$. Finally, by lemma 4.2.4, $ZX_{C+T} \vdash D_1 = D_2$. \square

Now we can give a new proof for Proposition 4.0.1.

Proposition 4.3.3 *The diagrams of the ZX_{C+T} -calculus exactly corresponds to the matrices over the ring $\mathbb{Z}[i, \frac{1}{\sqrt{2}}]$.*

Proof: The triangle \triangle has been represented in the $ZX_{\frac{\mathbb{T}}{4}}$ -calculus in [20] as follows:

$$\triangle \stackrel{[20]}{=} \text{circuit diagram} \quad (4.8)$$

It can be directly verified that the two diagrams on both sides of (4.8) have the same standard interpretation. Thus by Theorem 4.3.2 the identity (4.8) can be derived in the ZX_{C+T} -calculus.

Obviously each traditional generator of the ZX_{C+T} -calculus corresponds to a matrix over the ring $\mathbb{Z}[i, \frac{1}{\sqrt{2}}]$ via the standard interpretation. By lemma 4.1.3, the new generators can also be represented by traditional generators and the triangle (described in terms of green and red nodes in (4.8)), thus correspond to matrices over $\mathbb{Z}[i, \frac{1}{\sqrt{2}}]$ as well. Therefore, each diagram of the ZX_{C+T} -calculus which is composed of those generators must correspond to a matrix over the ring $\mathbb{Z}[i, \frac{1}{\sqrt{2}}]$.

Conversely, since $\mathbb{Z}[i, \frac{1}{\sqrt{2}}] = \mathbb{Z}[\frac{1}{2}, e^{i\frac{\pi}{4}}]$, each matrix over the ring \mathbb{T} can be first turned into a non-normalized quantum state by map-state duality, then represented by a normal form in the $ZW_{\mathbb{T}}$ -calculus with phases belong to the ring $\mathbb{Z}[\frac{1}{2}, e^{i\frac{\pi}{4}}]$ [33]. Furthermore, by the interpretation $\llbracket \cdot \rrbracket_{WX}$ given in section 4.2, this ZW normal form can be translated to a diagram in the ZX_{C+T} -calculus. \square

In [30], Giles and Selinger have established a correspondence between Clifford +T quantum circuits with some finite number of ancillas and the ring $\mathbb{Z}[i, \frac{1}{\sqrt{2}}]$. Here we generalise this result to the case of the ZX_{C+T} -calculus which is not restrained by unitarity. Our proof here is more direct thus simpler than the one presented in [42].

Proof of proposition 4.3.1

First we note that all the ZX diagrams translated by $\llbracket \cdot \rrbracket_{WX}$ won't be given in this proof for the sake of readability. For simplicity, we will use ZW rules in the diagrammatic reasoning instead of listing all the ZX rules which are used to derive the ZW rules under the interpretation $\llbracket \cdot \rrbracket_{WX}$. All the ZW rules used in this proof are $cut_w, cut_z, ba_{zw}, sym_w^x, ba_w$, where $cut_w, cut_z, ba_{zw}, ba_w$ are just the spider forms of the rules $asso_w, asso_z, nat_c^m, nat_w^m$ respectively as presented in Figure 2.2 and Figure 2.3. We use these spider forms to avoid plenty of repetitive application of their corresponding non-spider forms [33].

Proposition 4.3.4 (ZW rule nat_c^r)

$$ZX \vdash \left[\left[\begin{array}{c} \bullet \\ \diagup \quad \diagdown \\ \circ \quad \circ \\ \text{\scriptsize } r \quad \text{\scriptsize } r \end{array} \right] \right]_{WX} = \left[\left[\begin{array}{c} \circ \\ \text{\scriptsize } r \\ \bullet \end{array} \right] \right]_{WX}, \quad (4.9)$$

where $r = a_0 e^{i\alpha_0} + a_1 e^{i\alpha_1} + a_2 e^{i\alpha_2} + a_3 e^{i\alpha_3}$, $0 \leq a_j \in \mathbb{Z}[\frac{1}{2}]$, $\alpha_j = j\frac{\pi}{4}$ or $j\frac{\pi}{4} + \pi$, $j = 0, 1, 2, 3$.

Proof: Let $c_k = a_k e^{i\alpha_k}$, $k = 0, 1, 2, 3$. Then

$$\begin{aligned} \left[\left[\begin{array}{c} \circ \\ \text{\scriptsize } r \end{array} \right] \right]_{WX} &= \left[\left[\begin{array}{c} \bullet \\ \diagup \quad \diagdown \\ \circ \quad \circ \\ \text{\scriptsize } a_0 \alpha_0 \\ \text{\scriptsize } a_1 \alpha_1 \\ \text{\scriptsize } a_2 \alpha_2 \\ \text{\scriptsize } a_3 \alpha_3 \end{array} \right] \right]_{WX} \stackrel{cut_w}{=} \left[\left[\begin{array}{c} \circ_0 \\ \circ_1 \\ \circ_2 \\ \circ_3 \\ \bullet \end{array} \right] \right]_{WX} \\ &\stackrel{cut_z}{=} \left[\left[\begin{array}{c} \circ_0 \quad \circ_1 \quad \circ_2 \quad \circ_3 \\ \bullet \\ \bullet \end{array} \right] \right]_{WX} \stackrel{ba_{zw}}{=} \left[\left[\begin{array}{c} \circ_0 \quad \circ_1 \quad \circ_2 \quad \circ_3 \\ \bullet \quad \bullet \\ \bullet \end{array} \right] \right]_{WX} \stackrel{cut_z}{=} \left[\left[\begin{array}{c} \bullet \\ \diagup \quad \diagdown \\ \circ_0 \quad \circ_1 \\ \circ_2 \quad \circ_3 \end{array} \right] \right]_{WX} \end{aligned} \quad (4.10)$$

Thus

$$\begin{aligned}
 \left[\begin{array}{c} \bullet \\ | \\ \circ r \\ | \\ \bullet \\ \cup \\ | \\ \bullet \end{array} \right]_{WX} &\stackrel{(4.10)}{=} \left[\begin{array}{c} \bullet \\ | \\ \circ c_0 \quad \circ c_1 \quad \circ c_2 \quad \circ c_3 \\ | \\ \bullet \\ | \\ \bullet \end{array} \right]_{WX} \stackrel{ba_w}{=} \left[\begin{array}{c} \bullet \\ | \\ \circ c_0 \quad \circ c_1 \quad \circ c_2 \quad \circ c_3 \\ | \\ \bullet \\ | \\ \bullet \\ | \\ \bullet \\ | \\ \bullet \end{array} \right]_{WX} \\
 &\stackrel{cut_w, sym_0^x, TR13, TR14}{=} \left[\begin{array}{c} \bullet \\ | \\ \circ c_0 \quad \circ c_1 \quad \circ c_2 \quad \circ c_3 \quad \circ c_0 \quad \circ c_1 \quad \circ c_2 \quad \circ c_3 \\ | \\ \bullet \\ | \\ \bullet \end{array} \right]_{WX} \stackrel{(4.10)}{=} \left[\begin{array}{c} \bullet \\ | \\ \circ r \quad \circ r \\ | \\ \bullet \end{array} \right]_{WX}
 \end{aligned} \tag{4.11}$$

□

Proposition 4.3.5 (ZW rule $rng_+^{r,s}$)

$$ZX \vdash \left[\begin{array}{c} \bullet \\ | \\ \circ r \quad \circ s \\ | \\ \bullet \end{array} \right]_{WX} = \left[\begin{array}{c} | \\ | \\ \circ r + s \\ | \\ | \end{array} \right]_{WX}, \tag{4.12}$$

where $r = a_0 e^{i\alpha_0} + a_1 e^{i\alpha_1} + a_2 e^{i\alpha_2} + a_3 e^{i\alpha_3}$, $s = b_0 e^{i\beta_0} + b_1 e^{i\beta_1} + b_2 e^{i\beta_2} + b_3 e^{i\beta_3}$, $0 \leq a_j, b_j \in \mathbb{Z}[\frac{1}{2}]$, $\alpha_j, \beta_j = j\frac{\pi}{4}$ or $j\frac{\pi}{4} + \pi$, $j = 0, 1, 2, 3$.

Proof: Let $c_k = a_k e^{i\alpha_k}$, $d_k = b_k e^{i\alpha_k}$, $k = 0, 1, 2, 3$. Then we have

$$\begin{aligned}
& \left[\left[\begin{array}{c} \bullet \\ | \\ \circ \text{---} \circ \\ | \\ \bullet \end{array} \right]_{WX} \right] \stackrel{(4.10)}{=} \left[\left[\begin{array}{c} \bullet \\ | \\ \bullet \\ | \\ \circ \text{---} \circ \text{---} \circ \text{---} \circ \\ | \\ \bullet \\ | \\ \bullet \end{array} \right]_{WX} \right] \stackrel{cut_w}{=} \left[\left[\begin{array}{c} \bullet \\ | \\ \bullet \\ | \\ \circ \text{---} \circ \text{---} \circ \text{---} \circ \\ | \\ \bullet \\ | \\ \bullet \end{array} \right]_{WX} \right] \\
& \stackrel{cut_w}{=} \left[\left[\begin{array}{c} \bullet \\ | \\ \bullet \\ | \\ \circ \text{---} \circ \text{---} \circ \text{---} \circ \\ | \\ \bullet \\ | \\ \bullet \end{array} \right]_{WX} \right] \stackrel{(AD')}{=} \left[\left[\begin{array}{c} \bullet \\ | \\ \bullet \\ | \\ \circ + d_0 \text{---} \circ + d_1 \text{---} \circ + d_2 \text{---} \circ + d_3 \\ | \\ \bullet \\ | \\ \bullet \end{array} \right]_{WX} \right] \stackrel{(4.10)}{=} \left[\left[\begin{array}{c} | \\ | \\ \circ \text{---} \circ \\ | \\ | \end{array} \right]_{WX} \right] \\
& \hspace{15em} \square
\end{aligned} \tag{4.13}$$

Proposition 4.3.6 (*ZW rule $rng_{\times}^{r,s}$*)

$$ZX \vdash \left[\left[\begin{array}{c} \circ \text{---} \circ \\ | \\ \circ \text{---} \circ \end{array} \right]_{WX} \right] = \left[\left[\begin{array}{c} | \\ | \\ \circ \text{---} \circ \\ | \\ | \end{array} \right]_{WX} \right], \tag{4.14}$$

where $r = a_0 e^{i\alpha_0} + a_1 e^{i\alpha_1} + a_2 e^{i\alpha_2} + a_3 e^{i\alpha_3}$, $s = b_0 e^{i\beta_0} + b_1 e^{i\beta_1} + b_2 e^{i\beta_2} + b_3 e^{i\beta_3}$, $0 \leq a_j, b_j \in \mathbb{Z}[\frac{1}{2}]$, $\alpha_j, \beta_j = j\frac{\pi}{4}$ or $j\frac{\pi}{4} + \pi$, $j = 0, 1, 2, 3$.

Proof: Let $c_k = a_k e^{i\alpha_k}$, $d_k = b_k e^{i\alpha_k}$, $k = 0, 1, 2, 3$. Then by (4.10) we have

$$\left[\left[\begin{array}{c} | \\ | \\ \circ \text{---} \circ \\ | \\ | \end{array} \right]_{WX} \right] = \left[\left[\begin{array}{c} \bullet \\ | \\ \bullet \\ | \\ \circ \text{---} \circ \text{---} \circ \text{---} \circ \\ | \\ \bullet \\ | \\ \bullet \end{array} \right]_{WX} \right], \quad \left[\left[\begin{array}{c} | \\ | \\ \circ \text{---} \circ \\ | \\ | \end{array} \right]_{WX} \right] = \left[\left[\begin{array}{c} \bullet \\ | \\ \bullet \\ | \\ \circ \text{---} \circ \text{---} \circ \text{---} \circ \\ | \\ \bullet \\ | \\ \bullet \end{array} \right]_{WX} \right] \tag{4.15}$$

Therefore,

$$\begin{array}{c}
 \left[\begin{array}{c} \circ s \\ \circ r \end{array} \right]_{WX} \stackrel{(4.10)}{=} \left[\begin{array}{c} d_0, d_1, d_2, d_3 \\ \circ \bullet \\ \circ \bullet \\ \circ \bullet \\ \circ \bullet \\ c_0, c_1, c_2, c_3 \end{array} \right]_{WX} \stackrel{ba_w}{=} \left[\begin{array}{c} d_0, d_1, d_2, d_3 \\ \bullet \bullet \bullet \bullet \\ \bullet \bullet \bullet \bullet \\ \bullet \bullet \bullet \bullet \\ c_0, c_1, c_2, c_3 \end{array} \right]_{WX} \stackrel{TR13, TR14, cut_w}{=} \left[\begin{array}{c} d_0, d_1, d_2, d_3, d_0, d_1, d_2, d_3, d_0, d_1, d_2, d_3, d_0, d_1, d_2, d_3 \\ \bullet \bullet \bullet \bullet \\ \bullet \bullet \bullet \bullet \\ c_0, c_1, c_2, c_3 \end{array} \right]_{WX} \stackrel{TR13, TR14, cut_w}{=} \left[\begin{array}{c} c_0, c_1, c_2, c_3, c_0, c_1, c_2, c_3, c_0, c_1, c_2, c_3, c_0, c_1, c_2, c_3, c_0, c_1, c_2, c_3 \\ \bullet \bullet \bullet \bullet \\ \bullet \bullet \bullet \bullet \\ d_0, d_1, d_2, d_3 \end{array} \right]_{WX} \stackrel{(4.12)}{=} \left[\circ rs \right]_{WX}
 \end{array}$$

(4.16) □

Chapter 5

Completeness for 2-qubit Clifford+T circuits

Quantum computing is powerful in outperforming classical computing at solving important problems like factoring large numbers by quantum algorithms. But before implementing a quantum algorithm, one needs to turn an algorithm into elementary gates. In principle, one could use any approximately universal set of elementary gates for gate-synthesis purpose. However, the most widely used approximately universal set of elementary gates is the Clifford+T gate set, which means any unitary transformation can be approximated with an arbitrary precision by a Clifford+T gate. And a useful cost measure for realising Clifford+T circuits is the T count — the number of T gates in the circuit.

With the motivation to minimise the T count, Selinger and Bian set up a set of relations of circuits which is complete for Clifford+T 2-qubit circuits [64]. Here by complete it means any two 2-qubit Clifford+T circuits that are equal in their corresponding matrices can be proved to be equal circuits only using the set of relations. Unlike the single-qubit case, there is no known algorithm that is both optimal and efficient for multi-qubit unitary synthesis.

As evident from the main theorem in [64], it is not a simple task to use the circuit relations to simplify the quantum circuits. In contrast, the ZX-calculus has intuitive and simple rewriting rules to transform diagrams from one to another. It is possible to use the ZX-calculus to efficiently simplify Clifford+T circuits. Although the ZX-calculus is complete for both the overall pure qubit quantum mechanics(QM) and the Clifford+T pure qubit QM as we have shown in the last two chapters, it would be more efficient to use a small set of ZX rules for the purpose of circuit simplification.

The first step towards this goal is from Backens' work on completeness of the ZX-calculus for the single-qubit Clifford+T group [4]. However, the strategy for the single-qubit Clifford+T group does not apply to multi-qubit circuits.

In this chapter, we verify all the circuit relations (17 equations) in [64] by a small set of simple ZX-calculus rules (9 rules). Since the 17 relations are complete for 2-qubit Clifford+T circuits, so is the ZX-calculus with the 9 rules. Obviously, any single-qubit Clifford+T group can be seen as a 2-qubit Clifford+T circuit with one line empty of quantum gates. Therefore, our result can also be seen as a completeness result for single-qubit Clifford+T ZX-calculus. In comparing to the normal ZX rules [15, 6], we just added the (P) rule, which is a property of the general Euler decomposition in ZXZ and XZX forms. The problem of giving an analytic solution for converting from ZXZ to XZX Euler decompositions of single-qubit unitary gates has been proposed by Schröder de Witt and Zamdzhiev in [61]. Here we first give an explicit formula for the relation of ZXZ and XZX Euler decompositions of generalised Z and X phases, then obtain as a corollary the formula for normal Z and X phases. Note that we do not have to know the precise values of the angles in the (P) rule to verify those circuit relations, which makes it much simpler for simplifying circuits. Also, in the ZX computation at intermediate stages, we have gone beyond the range of Clifford+T and broken through the constraint of unitarity. These can be seen as the advantages of the ZX-calculus in comparison to quantum circuits.

Given that the ZX-calculus is universally complete, our result here is an important step towards efficient simplification of arbitrary n-qubit Clifford+T circuits.

For convenience, in this chapter we use the scalar-free version of the ZX-calculus as described in Section 2.2.1.

The results of this chapter has been published in the paper [21], with the coauthor Bob Coecke.

5.1 Complete relations for 2-qubit Clifford+T quantum circuits

In 2015, a set of relations that is complete for 2-qubit Clifford+T quantum circuits was given by Selinger and Bian [64]. We list these relations in Theorem 5.1.1 in the language of ZX-calculus ignoring the non-zero scalars. Note that given a 2-qubit Clifford+T quantum circuit, it is easy to translate it into a ZX diagram. On the contrary, given an arbitrary ZX diagram with two inputs and two outputs, it is usually hard to decide whether it is a 2-qubit circuit.

Theorem 5.1.1 ([64]) *The following set of relations is complete for 2-qubit Clifford+T circuits:*

$$\text{---} \boxed{H} \boxed{H} \text{---} = \text{---} \quad (5.1)$$

$$\text{---} \begin{matrix} \circlearrowleft \frac{\pi}{2} \\ \circlearrowleft \frac{\pi}{2} \\ \circlearrowleft \frac{\pi}{2} \\ \circlearrowleft \frac{\pi}{2} \end{matrix} \text{---} = \text{---} \quad (5.2)$$

$$\text{---} \begin{matrix} \circlearrowleft \frac{\pi}{2} \\ H \\ \circlearrowleft \frac{\pi}{2} \\ H \\ \circlearrowleft \frac{\pi}{2} \\ H \end{matrix} \text{---} = \text{---} \quad (5.3)$$

$$\begin{matrix} \circlearrowleft \\ H \\ \circlearrowleft \end{matrix} \begin{matrix} \circlearrowleft \\ H \\ \circlearrowleft \end{matrix} = \text{---} \quad (5.4)$$

$$\begin{matrix} \circlearrowleft \frac{\pi}{2} \\ H \\ \circlearrowleft \end{matrix} = \begin{matrix} \circlearrowleft \\ H \\ \circlearrowleft \frac{\pi}{2} \end{matrix} \quad (5.5)$$

$$\begin{matrix} \circlearrowleft \\ H \\ \circlearrowleft \frac{\pi}{2} \end{matrix} = \begin{matrix} \circlearrowleft \\ H \\ \circlearrowleft \frac{\pi}{2} \end{matrix} \quad (5.6)$$

$$\begin{matrix} H \\ \circlearrowleft \frac{\pi}{2} \\ \circlearrowleft \frac{\pi}{2} \\ H \\ \circlearrowleft \frac{\pi}{2} \end{matrix} = \begin{matrix} \circlearrowleft \\ H \\ \circlearrowleft \frac{\pi}{2} \\ \circlearrowleft \frac{\pi}{2} \\ H \end{matrix} \quad (5.7)$$

$$\begin{matrix} \circlearrowleft \\ H \\ \circlearrowleft \frac{\pi}{2} \\ \circlearrowleft \frac{\pi}{2} \\ H \\ \circlearrowleft \frac{\pi}{2} \end{matrix} = \begin{matrix} \circlearrowleft \frac{\pi}{2} \\ \circlearrowleft \frac{\pi}{2} \\ H \\ \circlearrowleft \frac{\pi}{2} \\ \circlearrowleft \frac{\pi}{2} \\ H \end{matrix} \quad (5.8)$$

$$\begin{matrix} \circlearrowleft \\ H \\ \circlearrowleft \\ H \\ \circlearrowleft \\ H \end{matrix} = \begin{matrix} \circlearrowleft \frac{\pi}{2} \\ H \\ \circlearrowleft \frac{\pi}{2} \\ H \\ \circlearrowleft \frac{\pi}{2} \\ H \end{matrix} \quad (5.9)$$

$$\begin{matrix} \circlearrowleft \\ H \\ \circlearrowleft \\ H \\ \circlearrowleft \\ H \end{matrix} = \begin{matrix} \circlearrowleft \frac{\pi}{2} \\ H \\ \circlearrowleft \frac{\pi}{2} \\ H \\ \circlearrowleft \frac{\pi}{2} \\ H \end{matrix} \quad (5.10)$$

$$\begin{matrix} \circlearrowleft \frac{\pi}{4} \\ \circlearrowleft \frac{\pi}{4} \end{matrix} = \begin{matrix} \circlearrowleft \frac{\pi}{2} \end{matrix} \quad (5.11)$$

$$\begin{array}{c} \frac{\pi}{4} \text{H} \frac{\pi}{2} \frac{\pi}{2} \text{H} \\ \frac{\pi}{4} \text{H} \frac{\pi}{2} \frac{\pi}{2} \text{H} \end{array} = \text{---} \quad (5.12)$$

$$\begin{array}{c} \frac{\pi}{4} \\ \text{H} \\ \bullet \end{array} = \begin{array}{c} \bullet \frac{\pi}{4} \\ \text{H} \\ \bullet \end{array} \quad (5.13)$$

$$\begin{array}{c} \bullet \text{H} \bullet \text{H} \frac{\pi}{4} \\ \text{H} \bullet \text{H} \\ \text{H} \bullet \text{H} \bullet \end{array} = \begin{array}{c} \bullet \text{H} \bullet \text{H} \\ \text{H} \bullet \text{H} \\ \frac{\pi}{4} \text{H} \bullet \text{H} \bullet \end{array} \quad (5.14)$$

$$\left(\begin{array}{c} \pi \bullet \pi \\ \frac{-\pi}{4} \frac{-\pi}{2} \text{H} \frac{-\pi}{4} \bullet \frac{\pi}{4} \text{H} \frac{\pi}{2} \frac{\pi}{4} \bullet \end{array} \right)^2 = \text{---} \quad (5.15)$$

$$\left(\begin{array}{c} \bullet \pi \bullet \pi \\ \bullet \frac{\pi}{4} \text{H} \frac{\pi}{4} \text{H} \frac{-\pi}{4} \bullet \frac{\pi}{4} \text{H} \frac{-\pi}{4} \text{H} \frac{-\pi}{4} \bullet \end{array} \right)^2 = \text{---} \quad (5.16)$$

$$\begin{array}{c} \pi \bullet \pi \bullet \frac{-\pi}{2} \text{H} \frac{-\pi}{4} \bullet \frac{\pi}{4} \text{H} \frac{\pi}{4} \text{H} \frac{-\pi}{4} \bullet \frac{\pi}{4} \text{H} \frac{\pi}{2} \frac{-\pi}{4} \dots \\ \bullet \frac{\pi}{4} \text{H} \frac{\pi}{4} \text{H} \frac{-\pi}{4} \bullet \frac{\pi}{4} \text{H} \frac{\pi}{2} \frac{-\pi}{4} \pi \bullet \pi \bullet \frac{\pi}{4} \frac{-\pi}{2} \text{H} \frac{-\pi}{4} \dots \\ \dots \bullet \pi \bullet \frac{\pi}{4} \text{H} \frac{-\pi}{4} \text{H} \frac{-\pi}{4} \bullet \frac{\pi}{4} \text{H} \frac{-\pi}{4} \text{H} \frac{-\pi}{4} \bullet \frac{\pi}{4} \text{H} \frac{\pi}{2} \bullet \\ \dots \bullet \frac{\pi}{4} \text{H} \frac{-\pi}{4} \text{H} \frac{-\pi}{4} \bullet \frac{\pi}{4} \text{H} \frac{\pi}{2} \bullet \bullet \pi \bullet \frac{-\pi}{2} \text{H} \frac{-\pi}{4} \end{array} = \text{---} \quad (5.17)$$

5.2 The ZX-calculus for 2-qubit Clifford+T quantum circuits

Although we have several complete axiomatisations of the ZX-calculus for both entire qubit quantum mechanics and the Clifford +T fragment, it is more practical to have a small set of rewriting rules just for 2-qubit Clifford+T quantum circuits. In this section, we use the scalar-free version of the ZX-calculus which was described in Section 2.2.1. The generators of the ZX-calculus for 2-qubit Clifford+T quantum circuits is the traditional generators of the qubit ZX-calculus as given in Table 6.1. The structural rules are just those given in (2.1) and (2.2). The non-structural rewriting rules of the ZX-calculus for 2-qubit Clifford+T quantum circuits are listed in the following:

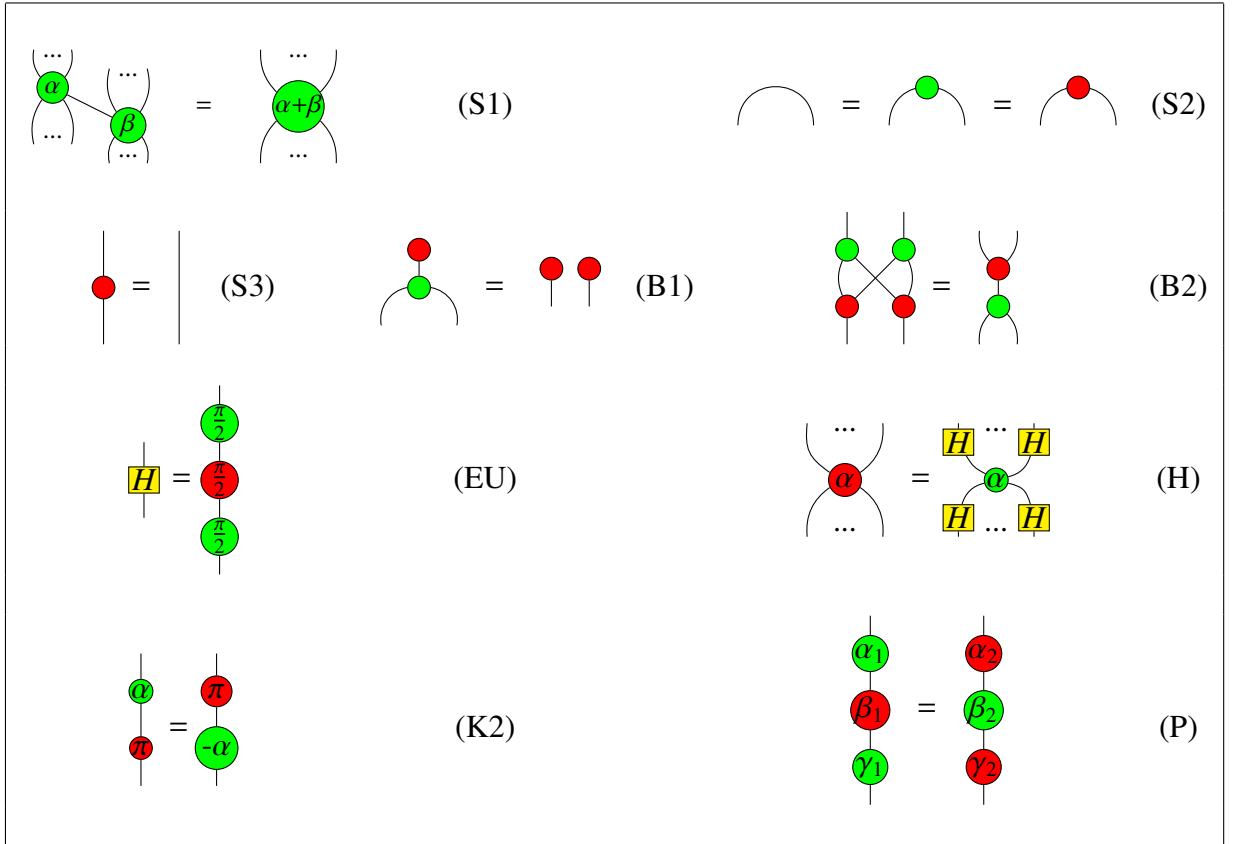


Figure 5.1: Rules of ZX-calculus for 2-qubit Clifford+T quantum circuits, where $\alpha, \beta \in [0, 2\pi)$. The exact formula for the rule (P) is given in (5.21). The red-green colour swapped version and upside-down flipped version of these rules still hold.

The main difference between the rules in Figure 5.1 for 2-qubit Clifford+T quantum circuits and the traditional rules in Figure 3.4 for the ZX_{full} -calculus is that the former has a new identity called (P) rule. The soundness of the (P) rule is proved in Corollary 5.3.2, however in this thesis we only need to know that the (P) rule hold and to use the property given in Corollary 5.3.2 that if $\alpha_1 = \gamma_1$, then $\alpha_2 = \gamma_2$, and if $\alpha_1 = -\gamma_1$, then $\alpha_2 = \pi + \gamma_2$. The exact values of the angles in the (P) rule need not to be known for the proof of the last three equations in the previous section. We add this (P) rule of the ZX-calculus for 2-qubit Clifford+T quantum circuits because we have no efficient way to prove equations (5.15), (5.16), (5.17) in the ZX-calculus.

5.3 Verification of the complete relations in the ZX-calculus

5.3.1 Derivation of the (P) rule

Firstly, we explain how the ZX rule (P) is obtained.

For arbitrary complex numbers a, b , define $\begin{array}{|c|} \hline a \\ \hline \end{array}$ as a general green phase which has the matrix form

$$\begin{pmatrix} 1 & 0 \\ 0 & a \end{pmatrix},$$

define $\begin{array}{|c|} \hline b \\ \hline \end{array} = \begin{array}{|c|} \hline H \\ \hline \end{array}$ as a general red phase which has the matrix form

$$\begin{pmatrix} 1+b & 1-b \\ 1-b & 1+b \end{pmatrix}.$$

Lemma 5.3.1 (*General phases colour-swap law*)

Let

$$\begin{aligned} \tau &= (1 - \lambda_2)(\lambda_1 + \lambda_3) + (1 + \lambda_2)(1 + \lambda_1\lambda_3), \\ U &= (1 + \lambda_2)(\lambda_1\lambda_3 - 1), & V &= (1 - \lambda_2)(\lambda_1 - \lambda_3), \\ S &= (1 - \lambda_2)(\lambda_1 + \lambda_3) - (1 + \lambda_2)(1 + \lambda_1\lambda_3), & T &= \tau(U^2 - V^2). \end{aligned} \quad (5.18)$$

Then

$$\begin{array}{|c|} \hline \lambda_1 \\ \hline \end{array} = \begin{array}{|c|} \hline \sigma_1 \\ \hline \end{array} \quad \begin{array}{|c|} \hline \lambda_2 \\ \hline \end{array} = \begin{array}{|c|} \hline \sigma_2 \\ \hline \end{array} \quad \begin{array}{|c|} \hline \lambda_3 \\ \hline \end{array} = \begin{array}{|c|} \hline \sigma_3 \\ \hline \end{array} \quad (5.19)$$

where

$$\sigma_1 = -i(U + V)\sqrt{\frac{S}{T}}, \quad \sigma_2 = \frac{\tau + i\sqrt{\frac{T}{S}}}{\tau - i\sqrt{\frac{T}{S}}}, \quad \sigma_3 = -i(U - V)\sqrt{\frac{S}{T}}.$$

Epecially, if $\lambda_1 = \lambda_3$, then $\sigma_1 = \sigma_3$; if $\lambda_1\lambda_3 = 1$, then $\sigma_1 = -\sigma_3$; if $\lambda_1\lambda_3 = -1$, then $\sigma_1\sigma_3 = -1$; if $\lambda_1 = -\lambda_3$, then $\sigma_1\sigma_3 = 1$.

Proof: The matrix of the left-hand-side of (5.19) is

$$\begin{pmatrix} 1 & 0 \\ 0 & \lambda_3 \end{pmatrix} \begin{pmatrix} 1 + \lambda_2 & 1 - \lambda_2 \\ 1 - \lambda_2 & 1 + \lambda_2 \end{pmatrix} \begin{pmatrix} 1 & 0 \\ 0 & \lambda_1 \end{pmatrix} = \begin{pmatrix} 1 + \lambda_2 & \lambda_1(1 - \lambda_2) \\ \lambda_3(1 - \lambda_2) & \lambda_1\lambda_3(1 + \lambda_2) \end{pmatrix}$$

The matrix of the right-hand-hand-side of (5.19) is

$$\begin{aligned} & \begin{pmatrix} 1 + \sigma_3 & 1 - \sigma_3 \\ 1 - \sigma_3 & 1 + \sigma_3 \end{pmatrix} \begin{pmatrix} 1 & 0 \\ 0 & \sigma_2 \end{pmatrix} \begin{pmatrix} 1 + \sigma_1 & 1 - \sigma_1 \\ 1 - \sigma_1 & 1 + \sigma_1 \end{pmatrix} \\ &= \begin{pmatrix} (1 + \sigma_3)(1 + \sigma_1) + (1 - \sigma_3)\sigma_2(1 - \sigma_1) & (1 + \sigma_3)(1 - \sigma_1) + (1 - \sigma_3)\sigma_2(1 + \sigma_1) \\ (1 - \sigma_3)(1 + \sigma_1) + (1 + \sigma_3)\sigma_2(1 - \sigma_1) & (1 - \sigma_3)(1 - \sigma_1) + (1 + \sigma_3)\sigma_2(1 + \sigma_1) \end{pmatrix} := \begin{pmatrix} X & Y \\ Z & W \end{pmatrix} \end{aligned}$$

To let the equality (5.19) hold, there must exist a non-zero complex number k such that

$$\begin{pmatrix} X & Y \\ Z & W \end{pmatrix} = k \begin{pmatrix} 1 + \lambda_2 & \lambda_1(1 - \lambda_2) \\ \lambda_3(1 - \lambda_2) & \lambda_1\lambda_3(1 + \lambda_2) \end{pmatrix} \quad (5.20)$$

Then

$$X + Y = 2(1 + \sigma_2 + \sigma_3 - \sigma_2\sigma_3) = k[1 + \lambda_2 + \lambda_1(1 - \lambda_2)]$$

$$Z + W = [(1 - \sigma_3)2 + (1 + \sigma_3)\sigma_2] = 2(1 + \sigma_2 - \sigma_3 + \sigma_2\sigma_3) = k[\lambda_3(1 - \lambda_2) + \lambda_1\lambda_3(1 + \lambda_2)]$$

Thus

$$X + Y + Z + W = 4(1 + \sigma_2) = k[(1 + \lambda_2)(1 + \lambda_1\lambda_3) + (1 - \lambda_2)(\lambda_1 + \lambda_3)],$$

i.e.,

$$\sigma_2 = \frac{k}{4}[(1 + \lambda_2)(1 + \lambda_1\lambda_3) + (1 - \lambda_2)(\lambda_1 + \lambda_3)] - 1 = \frac{k}{4}\tau - 1,$$

and

$$Z + W - (X + Y) = 4\sigma_3(\sigma_2 - 1) = k[(1 + \lambda_2)(\lambda_1\lambda_3 - 1) + (1 - \lambda_2)(\lambda_3 - \lambda_1)],$$

i.e.,

$$\sigma_3 = \frac{\frac{k}{4}[(1 + \lambda_2)(\lambda_1\lambda_3 - 1) + (1 - \lambda_2)(\lambda_3 - \lambda_1)]}{\frac{k}{4}\tau - 2} = \frac{k[(1 + \lambda_2)(\lambda_1\lambda_3 - 1) + (1 - \lambda_2)(\lambda_3 - \lambda_1)]}{k\tau - 8}.$$

Similarly,

$$X + Z = 2(1 + \sigma_1 + \sigma_2 - \sigma_1\sigma_2) = k[1 + \lambda_2 + \lambda_3(1 - \lambda_2)]$$

$$Y + W = 2(1 + \sigma_2 - \sigma_1 + \sigma_2\sigma_1) = k[\lambda_1(1 - \lambda_2) + \lambda_1\lambda_3(1 + \lambda_2)]$$

$$Y + W - (X + Z) = 4\sigma_1(\sigma_2 - 1) = k[(1 + \lambda_2)(\lambda_1\lambda_3 - 1) + (1 - \lambda_2)(\lambda_1 - \lambda_3)],$$

i.e.,

$$\sigma_1 = \frac{\frac{k}{4}[(1 + \lambda_2)(\lambda_1\lambda_3 - 1) + (1 - \lambda_2)(\lambda_1 - \lambda_3)]}{\frac{k}{4}\tau - 2} = \frac{k[(1 + \lambda_2)(\lambda_1\lambda_3 - 1) + (1 - \lambda_2)(\lambda_1 - \lambda_3)]}{k\tau - 8},$$

Now we decide the value of k . Let $U = (1 + \lambda_2)(\lambda_1\lambda_3 - 1)$, $V = (1 - \lambda_2)(\lambda_1 - \lambda_3)$. Then

$$\sigma_1 + \sigma_3 = \frac{2kU}{k\tau - 8}, \quad \sigma_1\sigma_3 = \frac{k^2(U^2 - V^2)}{(k\tau - 8)^2},$$

Furthermore,

$$X = (1 + \sigma_3)(1 + \sigma_1) + (1 - \sigma_3)\sigma_2(1 - \sigma_1) = k(1 + \lambda_2),$$

i.e.,

$$1 + \sigma_1 + \sigma_2 + \sigma_3 + \sigma_1\sigma_3 - \sigma_1\sigma_2 - \sigma_2\sigma_3 + \sigma_1\sigma_2\sigma_3 = k(1 + \lambda_2),$$

by rearrangement, we have

$$(\sigma_1 + \sigma_3)(1 - \sigma_2) + (1 + \sigma_2)(1 + \sigma_1\sigma_3) = k(1 + \lambda_2).$$

Therefore,

$$\frac{2kU}{k\tau - 8} \left(2 - \frac{k}{4}\tau\right) + \frac{k}{4}\tau \left(1 + \frac{k^2(U^2 - V^2)}{(k\tau - 8)^2}\right) = k(1 + \lambda_2).$$

Divide by k on both sides, then multiply by $(k\tau - 8)^2$ on both sides, we obtain a quadratic equation of k :

$$2U(k\tau - 8) \left(2 - \frac{k}{4}\tau\right) + \frac{1}{4}\tau[(k\tau - 8)^2 + k^2(U^2 - V^2)] = (k\tau - 8)^2(1 + \lambda_2).$$

By rearrangement, we have

$$(k\tau - 8)^2[\tau - 2U - 4(1 + \lambda_2)] + k^2\tau(U^2 - V^2) = 0.$$

Let

$$\begin{aligned} S &= \tau - 2U - 4(1 + \lambda_2) \\ &= (1 + \lambda_2)(1 + \lambda_1\lambda_3) + (1 - \lambda_2)(\lambda_1 + \lambda_3) - 2[(1 + \lambda_2)(\lambda_1\lambda_3 - 1) + 2(1 + \lambda_2)] \\ &= (1 - \lambda_2)(\lambda_1 + \lambda_3) - (1 + \lambda_2)(1 + \lambda_1\lambda_3), \\ T &= \tau(U^2 - V^2). \end{aligned}$$

Then the equation can be rewritten as

$$(S\tau^2 + T)k^2 - 16S\tau k + 64S = 0.$$

Solving this equation, we have

$$k = \frac{8S\tau \pm 8\sqrt{-ST}}{S\tau^2 + T}.$$

When we calculate the square root, we do not have to consider its sign, hence we can write k as

$$k = \frac{8S\tau + 8\sqrt{-ST}}{S\tau^2 + T}.$$

Now

$$\frac{8}{k} = \frac{8}{\frac{8S\tau + 8\sqrt{-ST}}{S\tau^2 + T}} = \frac{S\tau^2 + T}{S\tau + \sqrt{-ST}} = \frac{(\sqrt{S}\tau + i\sqrt{T})(\sqrt{S}\tau - i\sqrt{T})}{\sqrt{S}(\sqrt{S}\tau + i\sqrt{T})} = \tau - i\sqrt{\frac{T}{S}},$$

i.e.,

$$k = \frac{8}{\tau - i\sqrt{\frac{T}{S}}}.$$

Then

$$\sigma_1 = \frac{k(U+V)}{k\tau - 8} = \frac{U+V}{\tau - \frac{8}{k}} = \frac{U+V}{i\sqrt{\frac{T}{S}}} = -i(U+V)\sqrt{\frac{S}{T}}.$$

$$\sigma_3 = -i(U-V)\sqrt{\frac{S}{T}}, \quad \sigma_2 = \frac{\tau + i\sqrt{\frac{T}{S}}}{\tau - i\sqrt{\frac{T}{S}}}.$$

If $\lambda_1\lambda_3 = -1$, then clearly $\tau = S, T = S(U^2 - V^2)$. Thus $\frac{S}{T} = \frac{1}{U^2 - V^2}$. Therefore, $\sigma_1\sigma_3 = [-i(U+V)\sqrt{\frac{S}{T}}][-i(U-V)\sqrt{\frac{S}{T}}] = -(U^2 - V^2)\frac{S}{T} = -1$. Similarly, if $\lambda_1 = -\lambda_3$, then $\sigma_1\sigma_3 = 1$. \square

Corollary 5.3.2 For $\alpha_1, \beta_1, \gamma_1 \in (0, 2\pi)$ we have:

$$\begin{array}{c} \alpha_1 \\ \beta_1 \\ \gamma_1 \end{array} = \begin{array}{c} \alpha_2 \\ \beta_2 \\ \gamma_2 \end{array} \quad \text{with} \quad \begin{cases} \alpha_2 = \arg z + \arg z_1 \\ \beta_2 = 2 \arg(|\frac{z}{z_1}| + i) \\ \gamma_2 = \arg z - \arg z_1 \end{cases} \quad (5.21)$$

where:

$$z = \cos \frac{\beta_1}{2} \cos \frac{\alpha_1 + \gamma_1}{2} + i \sin \frac{\beta_1}{2} \cos \frac{\alpha_1 - \gamma_1}{2} \quad z_1 = \cos \frac{\beta_1}{2} \sin \frac{\alpha_1 + \gamma_1}{2} - i \sin \frac{\beta_1}{2} \sin \frac{\alpha_1 - \gamma_1}{2}$$

So if $\alpha_1 = \gamma_1$, then $\alpha_2 = \gamma_2$, and if $\alpha_1 = -\gamma_1$, then $\alpha_2 = \pi + \gamma_2$.

Proof: In (5.19), let $\lambda_1 = e^{i\alpha_1}, \lambda_2 = e^{i\beta_1}, \lambda_3 = e^{i\gamma_1}$. Then for the values of U, V, S, τ in (5.18) we have

$$\begin{aligned} U &= 4ie^{i\frac{\alpha_1 + \beta_1 + \gamma_1}{2}} \cos \frac{\beta_1}{2} \sin \frac{\alpha_1 + \gamma_1}{2}, & V &= 4e^{i\frac{\alpha_1 + \beta_1 + \gamma_1}{2}} \sin \frac{\beta_1}{2} \sin \frac{\alpha_1 - \gamma_1}{2}, \\ S &= 4e^{i\frac{\alpha_1 + \beta_1 + \gamma_1}{2}} z, & \tau &= 4e^{i\frac{\alpha_1 + \beta_1 + \gamma_1}{2}} \bar{z}, \end{aligned}$$

where $z = \cos \frac{\beta_1}{2} \cos \frac{\alpha_1 + \gamma_1}{2} + i \sin \frac{\beta_1}{2} \cos \frac{\alpha_1 - \gamma_1}{2}$, \bar{z} is the complex conjugate of z . Also, if we let $z_1 = \cos \frac{\beta_1}{2} \sin \frac{\alpha_1 + \gamma_1}{2} - i \sin \frac{\beta_1}{2} \sin \frac{\alpha_1 - \gamma_1}{2}$, then

$$U + V = 4ie^{i\frac{\alpha_1 + \beta_1 + \gamma_1}{2}} z_1, \quad U - V = 4ie^{i\frac{\alpha_1 + \beta_1 + \gamma_1}{2}} \bar{z}_1.$$

Thus

$$\frac{U+V}{U-V} = \frac{z_1}{\bar{z}_1} = \frac{z_1^2}{|z_1|^2}, \quad \sqrt{\frac{U+V}{U-V}} = \frac{z_1}{|z_1|} = e^{i\theta}.$$

where $|z_1|$ is the magnitude of the complex number z_1 , and $\theta = \arg z_1 \in [0, 2\pi)$ is the phase of z_1 . Similarly, we have

$$\sqrt{\frac{z}{\bar{z}}} = \frac{z}{|z|} = e^{i\phi},$$

where $\phi = \arg z \in [0, 2\pi)$ is the phase of z . Therefore,

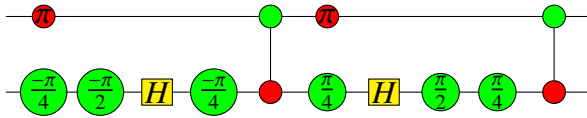
$$\begin{aligned} \sigma_1 &= -i(U+V)\sqrt{\frac{S}{T}} = -i(U+V)\sqrt{\frac{S}{\tau(U+V)(U-V)}} \\ &= -i\sqrt{\frac{S(U+V)}{\tau(U-V)}} = -i\sqrt{-\frac{z}{\bar{z}}\frac{z_1}{\bar{z}_1}} = -ie^{i\phi}e^{i\theta} = e^{i(\phi+\theta)}, \\ \sigma_3 &= -i(U-V)\sqrt{\frac{S}{T}} = -i(U-V)\sqrt{\frac{S}{\tau(U+V)(U-V)}} \\ &= -i\sqrt{\frac{S(U-V)}{\tau(U+V)}} = -i\sqrt{-\frac{z}{\bar{z}}\frac{\bar{z}_1}{z_1}} = -ie^{i\phi}e^{-i\theta} = e^{i(\phi-\theta)}, \\ \sigma_2 &= \frac{\tau+i\sqrt{\frac{T}{S}}}{\tau-i\sqrt{\frac{T}{S}}} = \frac{\tau\sqrt{\frac{S}{T}}+i}{\tau\sqrt{\frac{S}{T}}-i} = \frac{\sqrt{\frac{S\tau^2}{\tau(U^2-V^2)}+i}}{\sqrt{\frac{S\tau^2}{\tau(U^2-V^2)}-i}} \\ &= \frac{\sqrt{\frac{S\tau}{(U+V)(U-V)}+i}}{\sqrt{\frac{S\tau}{(U+V)(U-V)}-i}} = \frac{\sqrt{\frac{z\bar{z}_2}{z_1\bar{z}_1}+i}}{\sqrt{\frac{z\bar{z}_2}{z_1\bar{z}_1}-i}} = \frac{|z_2|+i}{|z_2|-i} = \frac{z_2}{\bar{z}_2} = \left(\frac{z_2}{|z_2|}\right)^2 = e^{i2\varphi}, \end{aligned}$$

where $z_2 = \frac{z}{z_1} + i$, $\varphi = \arg z_2$ is the phase of z_2 . Let $\alpha_2 = \phi + \theta, \beta_2 = 2\varphi, \gamma_2 = \phi - \theta$. Apparently, if $\alpha_1 = \gamma_1$, then $V = 0$, i.e., $e^{i\theta} = 1$, thus $\theta = 0$. It follows that $\alpha_2 = \gamma_2$. If $\alpha_1 = -\gamma_1$, then $U = 0$, thus $e^{i(\phi+\theta)} = -e^{i(\phi-\theta)} = e^{i(\pi+\phi-\theta)}$, i.e., $e^{i\alpha_2} = e^{i(\pi+\gamma_2)}$. Thus $\alpha_2 = \pi + \gamma_2$. \square

5.3.2 Proof of completeness for 2-qubit Clifford+T quantum circuits

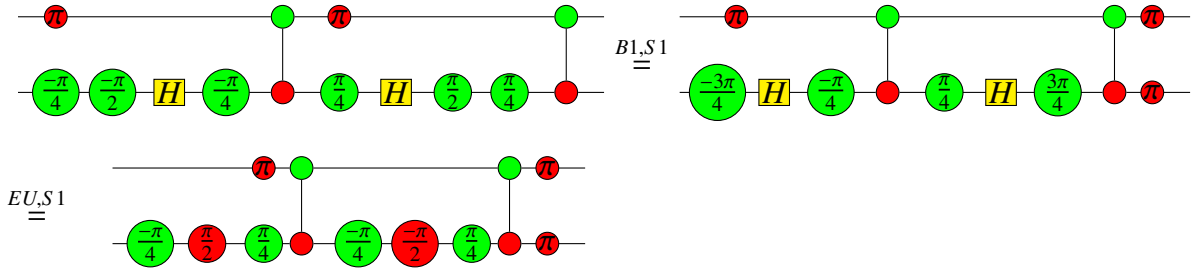
In this subsection we show that the ZX-calculus with rules in Figure 5.1 is complete for 2-qubit Clifford+T quantum circuits. First we prove as lemmas the correctness of the three complicated circuit relations (5.15), (5.16) and (5.17) within the ZX-calculus.

Lemma 5.3.3 *Let $A =$*



then $A^2 = I$.

Proof: First we have $A =$



By the rule (P), we can assume that

$$\text{---} \begin{array}{c} \text{---} \pi \\ \text{---} \frac{-\pi}{4} \quad \frac{\pi}{2} \quad \frac{\pi}{4} \end{array} \text{---} = \text{---} \begin{array}{c} \alpha \quad \beta \quad \gamma \end{array} \text{---} \quad (5.22)$$

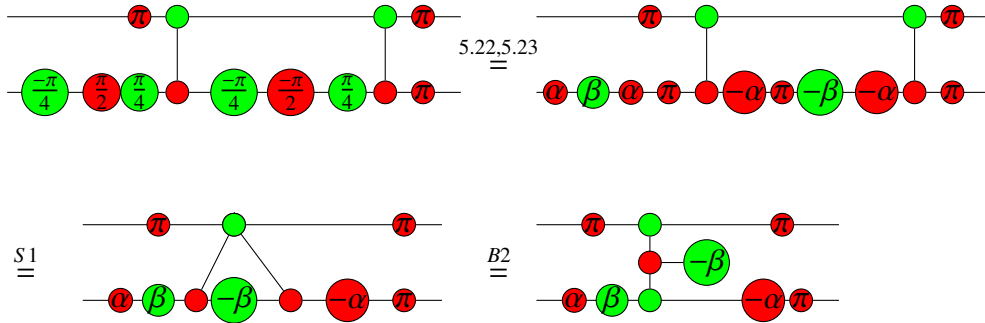
Since $e^{i\frac{-\pi}{4}} e^{i\frac{\pi}{4}} = 1$, we could let $\gamma = \alpha + \pi$. Also note that

$$\text{---} \begin{array}{c} \text{---} \pi \\ \text{---} \frac{-\pi}{4} \quad \frac{\pi}{2} \quad \frac{\pi}{4} \end{array} \text{---} = \left(\text{---} \begin{array}{c} \text{---} \pi \\ \text{---} \frac{-\pi}{4} \quad \frac{\pi}{2} \quad \frac{\pi}{4} \end{array} \text{---} \right)^{-1}$$

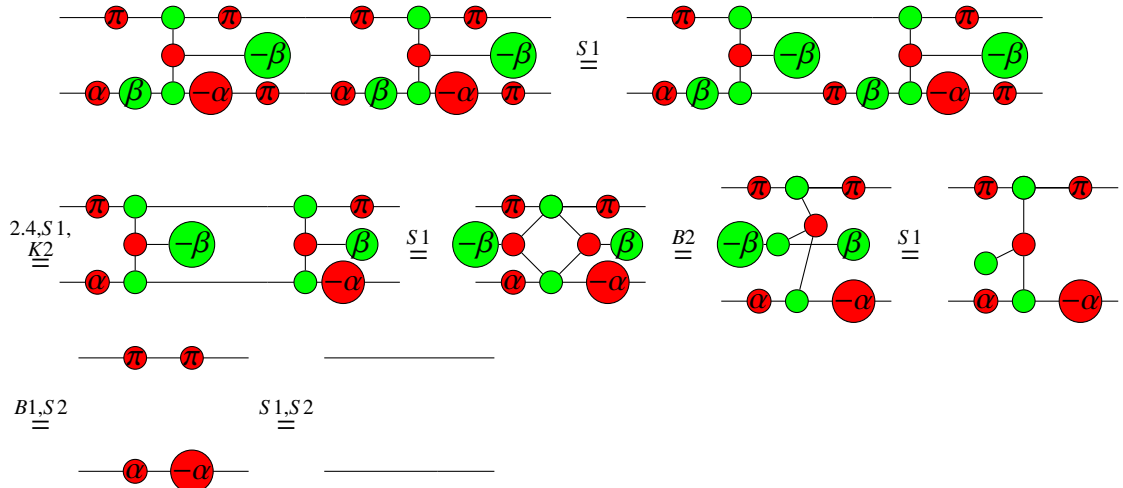
Thus

$$\text{---} \begin{array}{c} \text{---} \pi \\ \text{---} \frac{-\pi}{4} \quad \frac{\pi}{2} \quad \frac{\pi}{4} \end{array} \text{---} = \text{---} \begin{array}{c} -\gamma \quad -\beta \quad -\alpha \end{array} \text{---} \quad (5.23)$$

Therefore, $A =$

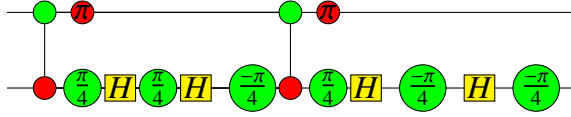


Finally, $A^2 =$



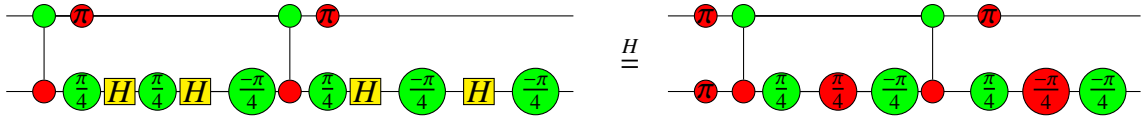
□

Lemma 5.3.4 Let $B =$



then $B^2 = I$.

Proof: Firstly we have



By the rule (P), we can assume that

$$\begin{array}{c} \pi/4 \\ \pi/4 \\ -\pi/4 \end{array} = \begin{array}{c} \alpha \\ \beta \\ \gamma \end{array} \quad (5.24)$$

Since $e^{i\frac{-\pi}{4}} e^{i\frac{\pi}{4}} = 1$, we could let $\gamma = \alpha + \pi$.

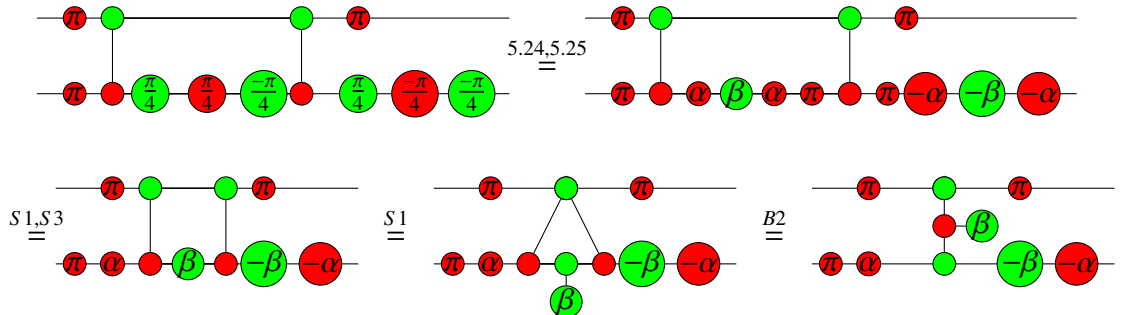
Also note that

$$\begin{array}{c} \pi/4 \\ -\pi/4 \\ -\pi/4 \end{array} = \left(\begin{array}{c} \pi/4 \\ \pi/4 \\ -\pi/4 \end{array} \right)^{-1}$$

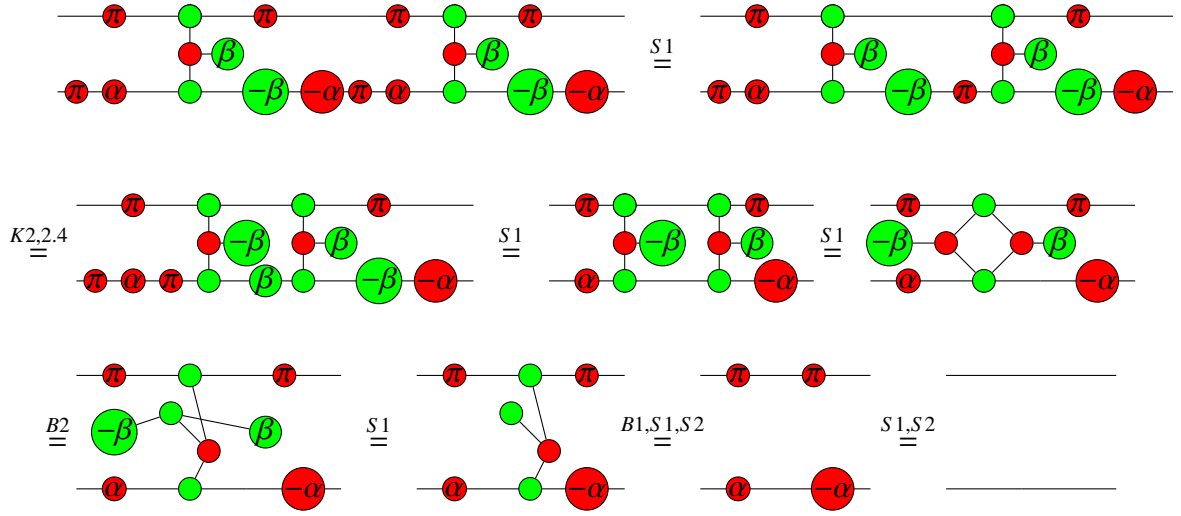
Thus

$$\begin{array}{c} \pi/4 \\ -\pi/4 \\ -\pi/4 \end{array} = \begin{array}{c} -\gamma \\ -\beta \\ -\alpha \end{array} \quad (5.25)$$

Therefore, $B =$

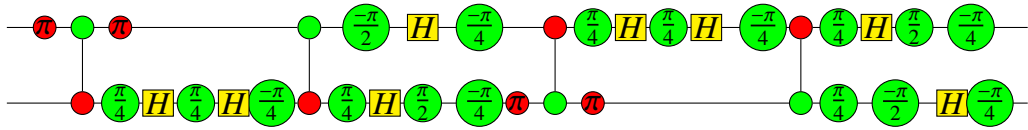


Finally, $B^2 =$

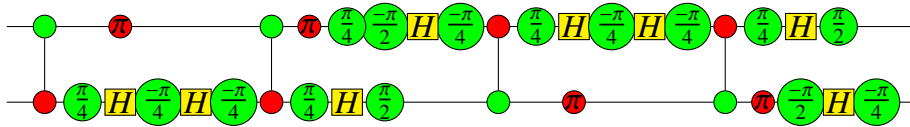


□

Lemma 5.3.5 Let $C =$

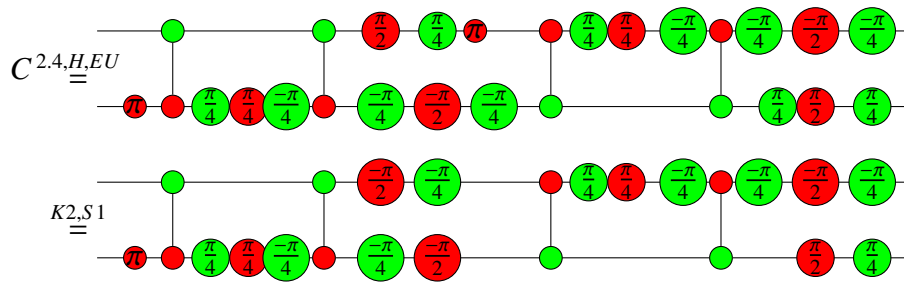


$D =$



then $D \circ C = I$.

Proof: Firstly we simplify the circuit C as follows:



By the rule (P), we can assume that

$$\begin{array}{c} \pi/4 \\ \pi/4 \\ \pi/4 \end{array} = \begin{array}{c} \alpha \\ \pi \\ \beta \\ \alpha \end{array} \quad (5.26)$$

(5.30)

By Corollary 5.3.2, we can assume that

$$\alpha \quad \frac{-\pi}{4} \quad \frac{-\pi}{2} = \sigma_1 \quad \sigma \quad \sigma_3 \quad (5.31)$$

Then for its inverse, we have

$$\frac{\pi}{2} \quad \frac{\pi}{4} \quad -\alpha = -\sigma_3 \quad -\sigma \quad -\sigma_1 \quad (5.32)$$

Also we can obtain that

$$\begin{aligned} & \alpha \quad \frac{-\pi}{4} \quad \frac{-\pi}{2} \stackrel{K2,S1}{=} \pi \quad \alpha \quad \frac{-\pi}{4} \quad \pi \quad \frac{-\pi}{2} \\ & \stackrel{K2,S1}{=} \pi \quad \alpha \quad \frac{-\pi}{4} \quad \frac{-\pi}{2} \quad \pi \quad \pi \stackrel{5.31}{=} \pi \quad \sigma_1 \quad \sigma \quad \sigma_3 \quad \pi \quad \pi \\ & \stackrel{K2,S1}{=} \sigma_1 \quad -\sigma \quad \pi \quad -\sigma_3 \end{aligned} \quad (5.33)$$

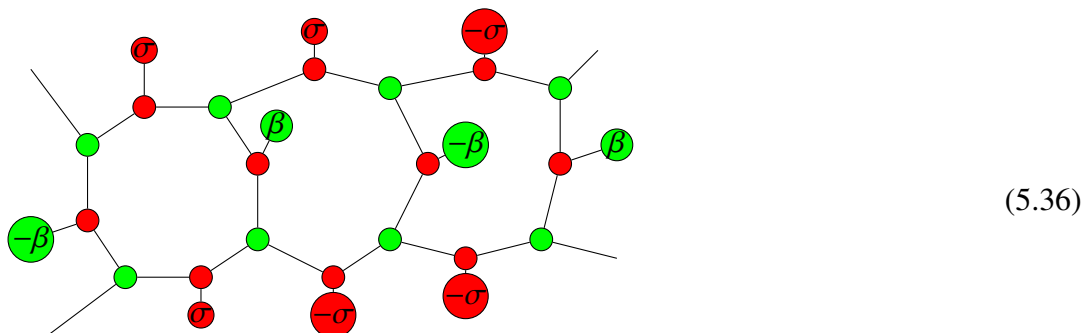
As a consequence, we have the inverse for both sides of (5.33):

$$\frac{\pi}{2} \quad \frac{\pi}{4} \quad -\alpha \stackrel{5.33}{=} -\sigma_3 \quad -\sigma \quad \pi \quad -\sigma_1 \quad (5.34)$$

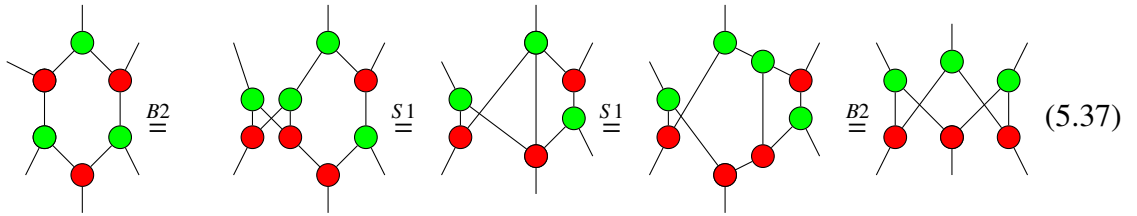
Now we can rewrite $D \circ C$ as

$$\begin{aligned} & \begin{array}{c} \sigma_3 \quad \sigma \quad \pi \quad -\sigma_1 \quad \sigma_1 \quad \sigma \quad \sigma_3 \quad -\sigma_3 \quad -\sigma \quad -\sigma_1 \quad \sigma_1 \quad -\sigma \quad \pi \quad -\sigma_3 \\ \beta \quad \beta \quad -\beta \quad -\beta \\ \alpha \quad \sigma_1 \quad \sigma \quad \sigma_3 \quad -\sigma_3 \quad -\sigma \quad -\sigma_1 \quad \sigma_1 \quad -\sigma \quad \pi \quad -\sigma_3 \quad \frac{\pi}{2} \quad \frac{\pi}{4} \end{array} \\ & = \begin{array}{c} \sigma_3 \quad \pi \quad \sigma \quad \sigma \quad -\sigma \quad -\sigma \quad -\sigma \quad \pi \quad -\sigma_3 \\ \beta \quad \beta \quad -\beta \quad -\beta \\ \alpha \quad \sigma_1 \quad \sigma \quad \sigma \quad -\sigma \quad -\sigma \quad \sigma_3 \quad \frac{\pi}{2} \quad \frac{\pi}{4} \end{array} \end{aligned} \quad (5.35)$$

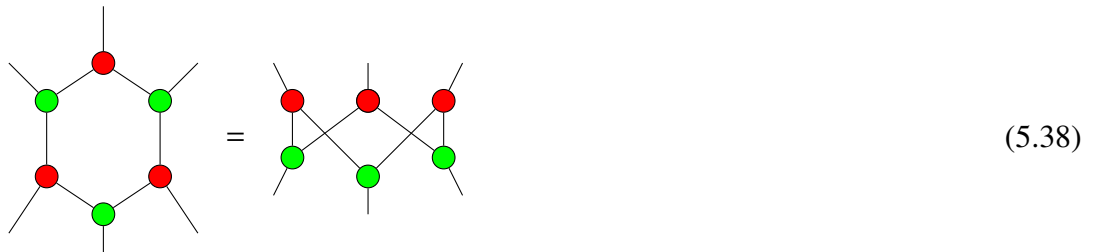
We can depict the dashed part of (5.35) in a form of connected octagons:



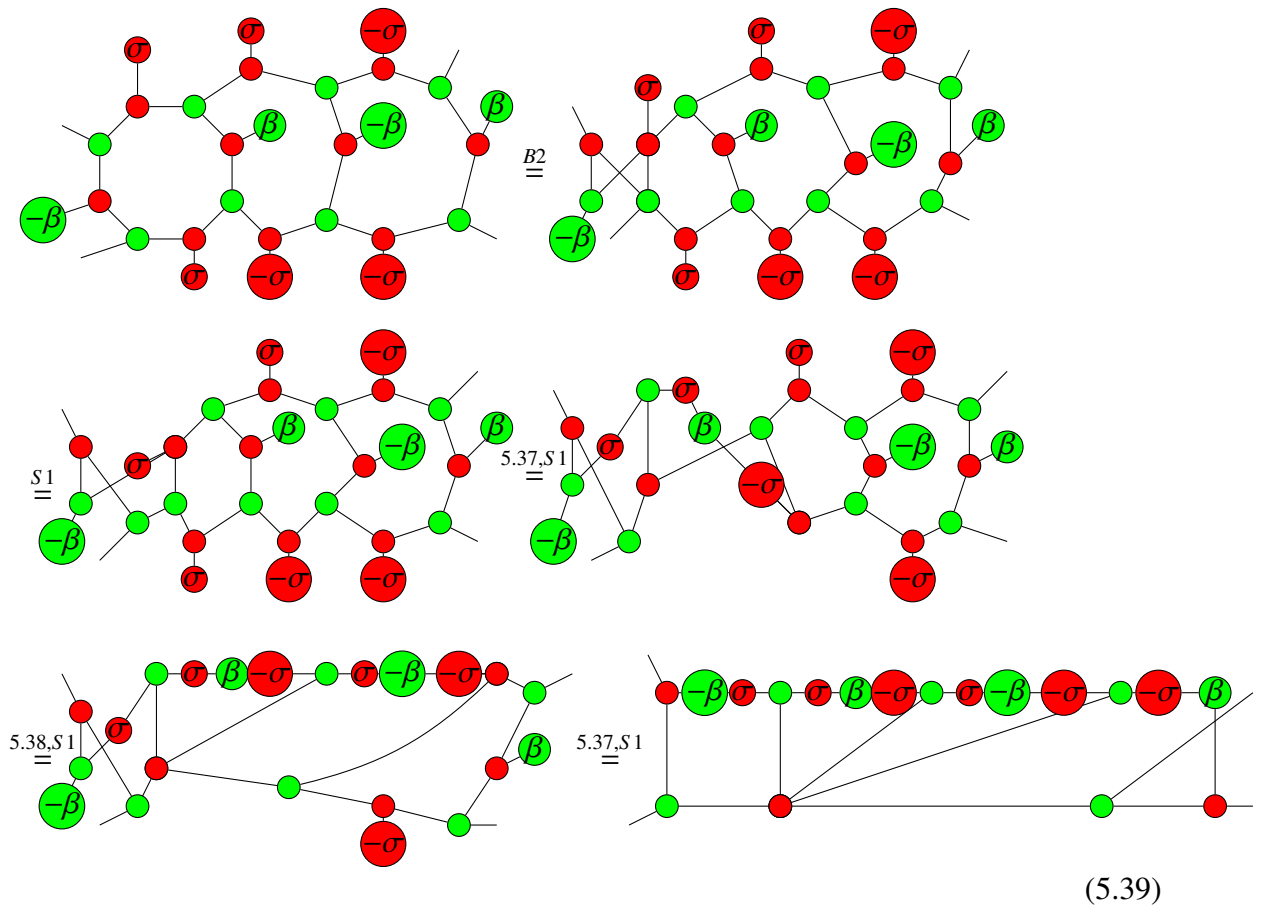
To deal with these octagons, we need to cope with hexagons. The following property of hexagons was first given in [26]:



By colour change rule (H), we have



Then we can rewrite (5.36) as follows:



By the (P) rule, we have

$$\text{---} \sigma \beta \text{---} \sigma \text{---} = \text{---} x y z \text{---} \quad (5.40)$$

where $z = x + \pi$. Then we take inverse for each side of (5.40) and obtain that

$$\text{---} \sigma \text{---} \beta \text{---} \sigma \text{---} = \text{---} z \text{---} y \text{---} x \text{---} \quad (5.41)$$

By rearranging the phases on both sides of (5.40), we have

$$\text{---} \sigma \text{---} x y \text{---} \stackrel{5.40}{=} \text{---} \sigma \text{---} \sigma \beta \text{---} \sigma \text{---} z \text{---} \stackrel{5.40, S1}{=} \text{---} \beta \text{---} \sigma \text{---} x \pi \text{---} \quad (5.42)$$

Thus

$$\begin{aligned} & \text{---} \sigma \text{---} x \text{---} y \text{---} \stackrel{K2, S1}{=} \text{---} \pi \text{---} \sigma \text{---} x y \text{---} \pi \text{---} \\ & \stackrel{5.42}{=} \text{---} \pi \text{---} \beta \text{---} \sigma \text{---} x \text{---} \pi \text{---} \pi \text{---} \stackrel{S1}{=} \text{---} \pi \text{---} \beta \text{---} \sigma \text{---} x \text{---} \end{aligned} \quad (5.43)$$

Therefore,

$$\begin{aligned} & \text{---} \beta \text{---} \sigma \text{---} x \text{---} y \text{---} \stackrel{5.43}{=} \text{---} \beta \text{---} \pi \text{---} \beta \text{---} \sigma \text{---} x \text{---} \\ & \stackrel{S1}{=} \text{---} \pi \text{---} \sigma \text{---} x \text{---} \stackrel{K2}{=} \text{---} \sigma \text{---} x \text{---} \pi \text{---} \end{aligned} \quad (5.44)$$

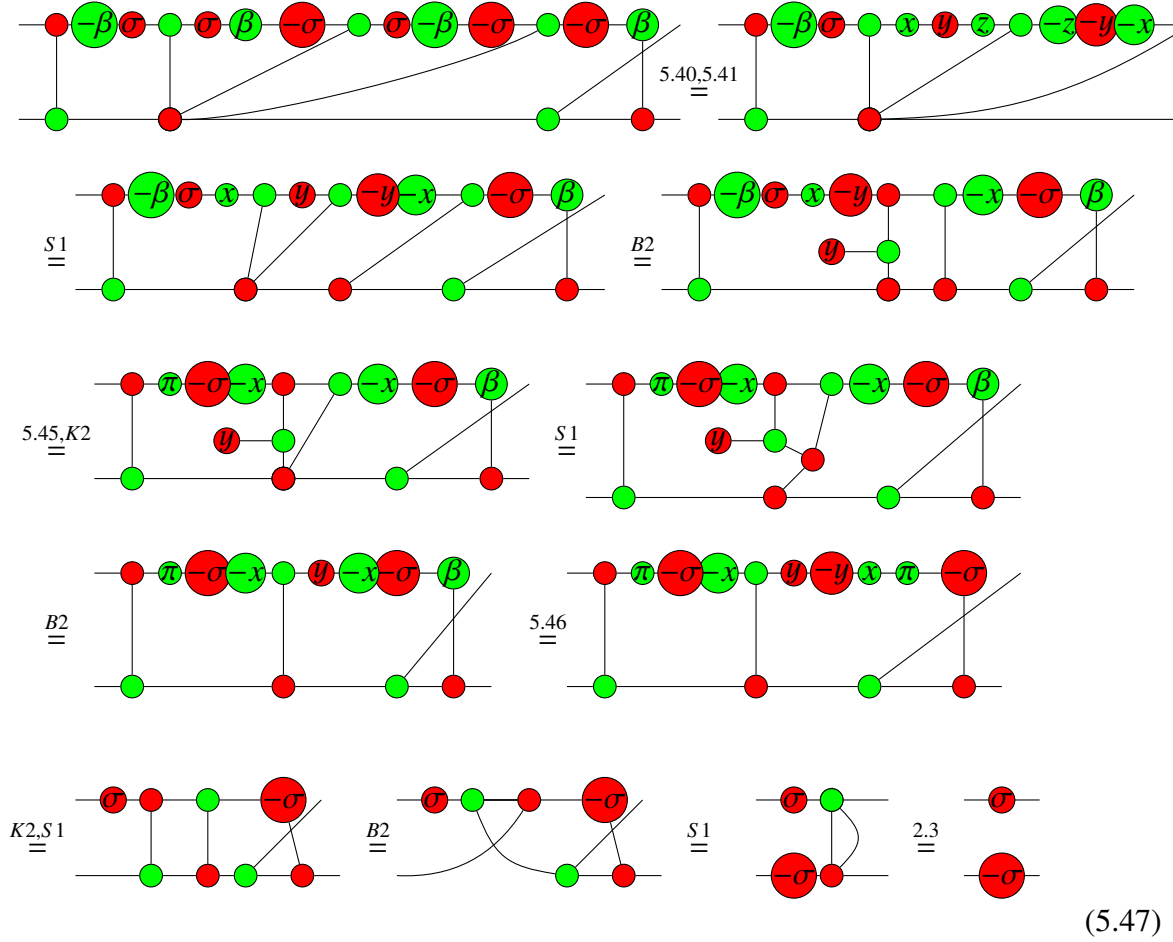
It then follows that

$$\text{---} \beta \text{---} \sigma \text{---} x \text{---} \stackrel{5.44}{=} \text{---} \sigma \text{---} x \text{---} \pi \text{---} y \text{---} \quad (5.45)$$

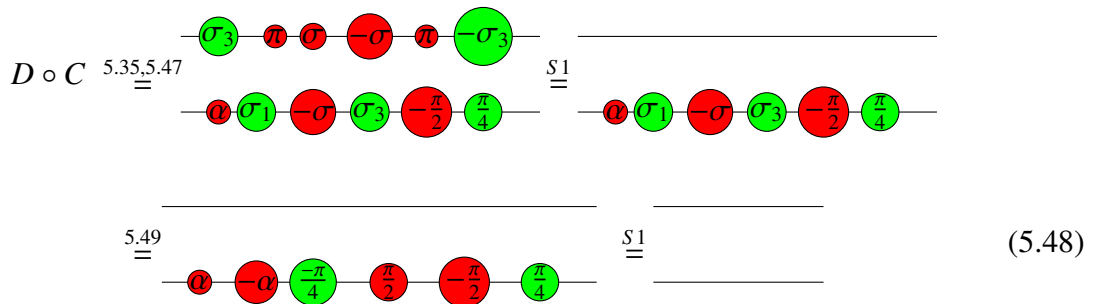
If we take the inverse of the left-hand-side of (5.45), then we have

$$\text{---} x \text{---} \sigma \text{---} \beta \text{---} = \text{---} y \text{---} x \text{---} \pi \text{---} \sigma \text{---} \quad (5.46)$$

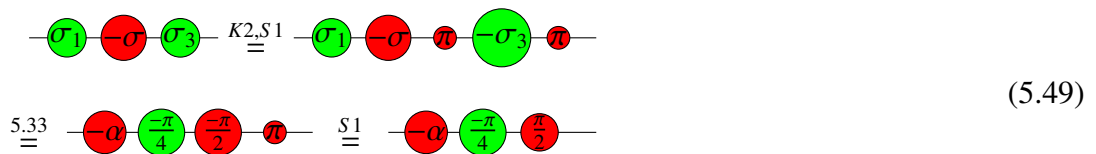
Now we can further simplify the final diagram in (5.39) as follows:



Finally, the composite circuit $D \circ C$ as can be simplified as follows:



where we used the following property:



□

The other relations are easy to be verified by the ZX-calculus, we omit those verification here. Since the circuit relations are proved to be complete for 2-qubit Clifford+T quantum circuits [64], we have the following

Theorem 5.3.6 *The ZX-calculus is complete for 2-qubit Clifford+T quantum circuits.*

In this chapter, the essential technique we employed is that we go beyond the range of Clifford+T and broke thorough the constraint of unitarity at intermediate stages by using the new (P) rule. Although we do not have a general general strategy for simplifying arbitrary quantum circuits by the ZX-calculus, we would expect the (P) rule to have more utilities in quantum computing and information.

Chapter 6

Completeness for qutrit stabilizer quantum mechanics

The theory of quantum information and quantum computation (QIC) is traditionally based on binary logic (qubits). However, multi-valued logic has been recently proposed for quantum computing, using linear ion traps [54], cold atoms [67], and entangled photons [52]. In particular, metaplectic non-Abelian anyons were shown to be naturally connected to ternary (qutrit) logic in contrast to binary logic in topological quantum computing, based on which there comes the Metaplectic Topological Quantum Computer platform [23].

Taking into consideration the practicality of qutrits and the fruitful results on completeness of the ZX-calculus that have been obtained in the previous chapters, it is natural to give a qutrit version of the ZX-calculus. However, the generalisation from qubits to qutrits is not trivial, since the qutrit-based structures are usually much more complicated than the qubit-based structures. For instance, the local Clifford group for qubits has only 24 elements, while the local Clifford group for qutrits has 216 elements. Thus it is no surprise that, as presented in [31], the rules of qutrit ZX-calculus are significantly different from that of the qubit case: each phase gate has a pair of phase angles, the operator commutation rule is more complicated, the Hadamard gate is not self-adjoint, the colour-change rule is doubled, and the dualiser has a much richer structure than being just an identity. Despite being already well established in [9, 70] and independently introduced as a typical special case of qudit ZX-calculus in [60], to the best of our knowledge, there are no completeness results available for qutrit ZX-calculus. Without this kind of results, how can we even know that the rules of a so-called ZX-calculus are useful enough for quantum computing?

In this chapter, based on the rules and results in [31], we show that the qutrit ZX-calculus is complete for pure qutrit stabilizer quantum mechanics (QM). The strategy we used here mirrors that of the qubit case in [3], although it is technically more complicated, especially for the completeness of the single qutrit Clifford group C_1 . Firstly, we show

that any stabilizer state diagram is equal to some GS-LC diagram within the ZX-calculus, where a GS-LC diagram consists of a graph state diagram with arbitrary single-qutrit Clifford operators applied to each output. We then show that any stabilizer state diagram can be further brought into a reduced form of the GS-LC diagram. Finally, for any two stabilizer state diagrams on the same number of qutrits, we make them into a simplified pair of reduced GS-LC diagram such that they are equal under the standard interpretation in Hilbert spaces if and only if they are identical in the sense that they are constructed by the same element constituents in the same way. By the map-state duality, the case for operators represented by diagrams are also covered, thus we have shown the completeness of the ZX-calculus for all pure qutrit stabilizer QM.

The results of this chapter are collected from the paper [69] without any coauthor. In addition, all of the proofs are included here.

6.1 Qutrit Stabilizer quantum mechanics

6.1.1 The generalized Pauli group and Clifford group

The notions of Pauli group and Clifford group for qubits can be generalised to qutrits in a natural way: In the 3-dimensional Hilbert space H_3 , we define the *generalised Pauli operators* X and Z as follows

$$X|j\rangle = |j+1\rangle, \quad Z|j\rangle = \omega^j|j\rangle, \quad (6.1)$$

where $j \in \mathbb{Z}_3$ (the ring of integers modulo 3), $\omega = e^{i\frac{2}{3}\pi}$, and the addition is a modulo 3 operation. We will use the same denotation for tensor products of these operators as is presented in [37]: for $v, w \in \mathbb{Z}_3^n$ (n -dimensional vector space over \mathbb{Z}_3), let

$$v = \begin{pmatrix} v_1 \\ \vdots \\ v_n \end{pmatrix}, \quad w = \begin{pmatrix} w_1 \\ \vdots \\ w_n \end{pmatrix}, \quad a = \begin{pmatrix} v \\ w \end{pmatrix} \in \mathbb{Z}_3^{2n},$$

$$XZ(a) = X^{v_1}Z^{w_1} \otimes \cdots \otimes X^{v_n}Z^{w_n}. \quad (6.2)$$

We define the *generalized Pauli group* \mathcal{P}_n on n qutrits as

$$\mathcal{P}_n = \{\omega^\delta XZ(a) | a \in \mathbb{Z}_3^{2n}, \delta \in \mathbb{Z}_3\}.$$

Definition 6.1.1 *The generalized Clifford group C_n on n qutrits is defined as the normalizer of \mathcal{P}_n in the group of unitaries: $C_n = \{Q | Q^\dagger = Q^{-1}, Q\mathcal{P}_nQ^\dagger = \mathcal{P}_n\}$. Especially, for $n = 1$, C_1 is called the generalized local Clifford group.*

Similar to the qubit case, it can be shown that the generalized Clifford group is generated by the gate $\mathcal{S} = |0\rangle\langle 0| + |1\rangle\langle 1| + \omega|2\rangle\langle 2|$, the generalized Hadamard gate $H = \frac{1}{\sqrt{3}} \sum_{k,j=0}^2 \omega^{kj} |k\rangle\langle j|$, and the SUM gate $\Lambda = \sum_{i,j=0}^2 |i, i+j(\text{mod}3)\rangle\langle ij|$ [37, 23]. In particular, the local Clifford group C_1 is generated by the gate \mathcal{S} and the generalized Hadamard gate H [37], with the group order being $3^3(3^2 - 1) = 216$, up to global phases [38].

We define the *stabilizer code* as the non-zero joint eigenspace to the eigenvalue 1 of a subgroup of the generalized Pauli group \mathcal{P}_n [8]. A *stabilizer state* $|\psi\rangle$ is a stabilizer code of dimension 1, which is therefore stabilized by an abelian subgroup of order 3^n of the Pauli group excluding multiples of the identity other than the identity itself [37]. We call this subgroup the *stabilizer* \mathfrak{S} of $|\psi\rangle$.

Finally, the *qutrit stabilizer quantum mechanics* can be described as the fragment of the pure qutrit quantum theory where only states represented in computational basis, Clifford unitaries and measurements in computational basis are considered.

6.1.2 Graph states

Graph states are special stabilizer states which are constructed based on undirected graphs without loops. However, it turns out that they are not far from stabilizer states.

Definition 6.1.2 [39] A \mathbb{Z}_3 -weighted graph is a pair $G = (V, E)$ where V is a set of n vertices and E is a collection of weighted edges specified by the adjacency matrix Γ , which is a symmetric n by n matrix with zero diagonal entries, each matrix element $\Gamma_{lm} \in \mathbb{Z}_3$ representing the weight of the edge connecting vertex l with vertex m .

Definition 6.1.3 [49] Given a \mathbb{Z}_3 -weighted graph $G = (V, E)$ with n vertices and adjacency matrix Γ , the corresponding qutrit graph state can be defined as

$$|G\rangle = \mathcal{U} |+\rangle^{\otimes n},$$

where $|+\rangle = \frac{1}{\sqrt{3}}(|0\rangle + |1\rangle + |2\rangle)$, $\mathcal{U} = \prod_{\{l,m\} \in E} (C_{lm})^{\Gamma_{lm}}$, $C_{lm} = \sum_{j=0}^2 \sum_{k=0}^2 \omega^{jk} |j\rangle\langle j|_l \otimes |k\rangle\langle k|_m$, subscripts indicate to which qutrit the operator is applied.

Lemma 6.1.4 [39] The qutrit graph state $|G\rangle$ is the unique (up to a global phase) joint +1 eigenstate of the group generated by the operators

$$X_v \prod_{u \in V} (Z_u)^{\Gamma_{uv}} \text{ for all } v \in V.$$

Therefore, graph states must be stabilizer states. On the contrary, stabilizer states are equivalent to graph states in the following sense.

Definition 6.1.5 [3] *Two n -qutrit stabilizer states $|\psi\rangle$ and $|\phi\rangle$ are equivalent with respect to the local Clifford group if there exists $U \in C_1^{\otimes n}$ such that $|\psi\rangle = U|\phi\rangle$.*

Lemma 6.1.6 [8] *Every qutrit stabilizer state is equivalent to a graph state with respect to the local Clifford group.*

Below we describe some operations on graphs corresponding to graph states. These operations will play a central role in the proof of the completeness of ZX-calculus for qutrit stabilizer quantum mechanics.

Definition 6.1.7 [8] *Let $G = (V, E)$ be a \mathbb{Z}_3 -weighted graph with n vertices and adjacency matrix Γ . For every vertex v , and $0 \neq b \in \mathbb{Z}_3$, define the operator $\circ_b v$ on the graph as follows: $G \circ_b v$ is the graph on the same vertex set, with adjacency matrix $I(v, b)\Gamma I(v, b)$, where $I(v, b) = \text{diag}(1, 1, \dots, b, \dots, 1)$, b being on the v -th entry. For every vertex v and $a \in \mathbb{Z}_3$, define the operator $*_a v$ on the graph as follows: $G *_a v$ is the graph on the same vertex set, with adjacency matrix Γ' , where $\Gamma'_{jk} = \Gamma_{jk} + a\Gamma_{vj}\Gamma_{vk}$ for $j \neq k$, and $\Gamma'_{jj} = 0$ for all j . The operator $*_a v$ is also called the a -local complementation at the vertex v [53].*

Now the equivalence of graph states can be described in terms of these operations on graphs.

Theorem 6.1.8 [8] *Two graph states $|G\rangle$ and $|H\rangle$ with adjacency matrices M and N over \mathbb{Z}_3 , are equivalent under local Clifford group if and only if there exists a sequence of $*$ and \circ operators acting on one of them to obtain the other.*

6.2 Qutrit ZX-calculus

6.2.1 The ZX-calculus for general pure state qutrit quantum mechanics

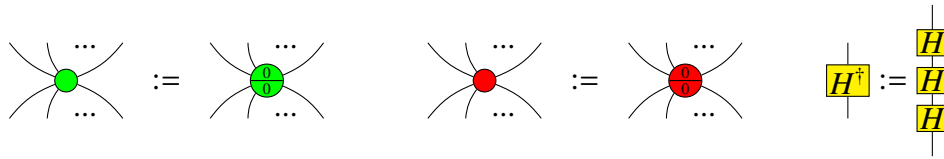
As described in Section 2.2.1, the qutrit ZX-calculus is a special case of the qudit ZX-calculus where $d = 3$. Especially, we use the scalar-free version of the the qutrit ZX-calculus throughout this chapter. The generators of the qutrit ZX-calculus is explicitly given as follows:

$R_Z^{(n,m)}(\frac{\alpha}{\beta}) : n \rightarrow m$		$R_X^{(n,m)}(\frac{\alpha}{\beta}) : n \rightarrow m$	
$H : 1 \rightarrow 1$		$\sigma : 2 \rightarrow 2$	
$\mathbb{I} : 1 \rightarrow 1$		$e : 0 \rightarrow 0$	
$C_a : 0 \rightarrow 2$		$C_u : 2 \rightarrow 0$	

Table 6.1: Generators of qubit ZX-calculus

where $m, n \in \mathbb{N}$, $\alpha, \beta \in [0, 2\pi)$, and e is denoted by an empty diagram.

For simplicity, we have the following notations:



The qubit ZX-calculus has the structural rules as given in (2.1) and (2.2). Its non-structural rewriting rules are presented in Figure 6.1.

Note that all the diagrams should be read from top to bottom.

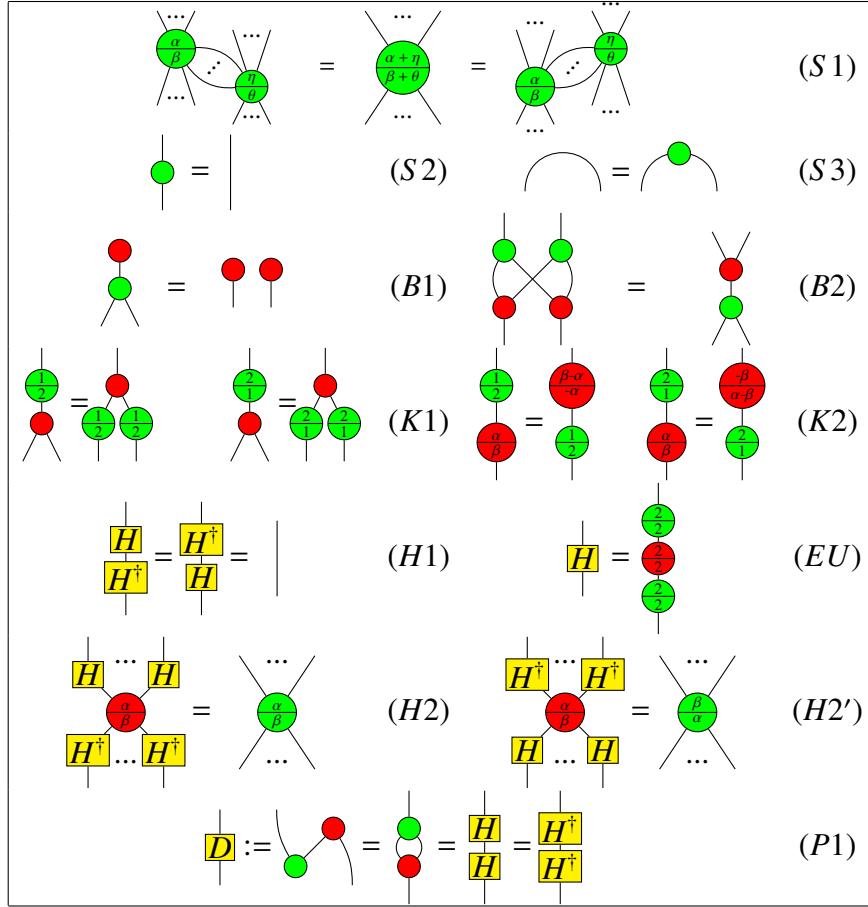


Figure 6.1: Qutrit ZX-calculus rewriting rules

For the easiness of reading, we will denote the frequently used angles $\frac{2\pi}{3}$ and $\frac{4\pi}{3}$ by 1 and 2 respectively. Note that the red spider rule still holds, for simplicity, we also refer to it as rule (S1).

The diagrams in Qutrit ZX-calculus have a standard interpretation (up to a non-zero scalar) $[[\cdot]]$ in the Hilbert spaces:

$$\left[\left[\begin{array}{c} \overbrace{\quad\quad\quad}^n \\ \text{---} \\ \text{---} \\ \text{---} \\ \text{---} \\ \text{---} \\ \text{---} \\ \underbrace{\quad\quad\quad}_m \end{array} \right] \right] = |0\rangle^{\otimes m} \langle 0|^{\otimes n} + e^{i\alpha} |1\rangle^{\otimes m} \langle 1|^{\otimes n} + e^{i\beta} |2\rangle^{\otimes m} \langle 2|^{\otimes n}$$

$$\left[\begin{array}{c} \overbrace{\quad\quad\quad}^n \\ \vdots \\ \text{---} \\ \text{---} \\ \text{---} \\ \vdots \\ \underbrace{\quad\quad\quad}_m \end{array} \right] = |+\rangle^{\otimes m} \langle +|^{\otimes n} + e^{i\alpha} |\omega\rangle^{\otimes m} \langle \omega|^{\otimes n} + e^{i\beta} |\bar{\omega}\rangle^{\otimes m} \langle \bar{\omega}|^{\otimes n}$$

$$\left[\begin{array}{c} \boxed{H} \\ \vdots \\ \vdots \\ \vdots \end{array} \right] = |+\rangle \langle 0| + |\omega\rangle \langle 1| + |\bar{\omega}\rangle \langle 2| = |0\rangle \langle +| + |1\rangle \langle \bar{\omega}| + |2\rangle \langle \omega|$$

$$\left[\begin{array}{c} \boxed{H^\dagger} \\ \vdots \\ \vdots \\ \vdots \end{array} \right] = |0\rangle \langle +| + |1\rangle \langle \omega| + |2\rangle \langle \bar{\omega}| = |+\rangle \langle 0| + |\omega\rangle \langle 2| + |\bar{\omega}\rangle \langle 1|$$

where $\bar{\omega} = e^{\frac{4}{3}\pi i} = \omega^2$, and

$$\begin{cases} |+\rangle = |0\rangle + |1\rangle + |2\rangle \\ |\omega\rangle = |0\rangle + \omega |1\rangle + \bar{\omega} |2\rangle \\ |\bar{\omega}\rangle = |0\rangle + \bar{\omega} |1\rangle + \omega |2\rangle \end{cases}$$

with ω satisfying $\omega^3 = 1$, $1 + \omega + \bar{\omega} = 0$.

For convenience, we also use the following matrix form:

$$\left[\begin{array}{c} \text{---} \\ \text{---} \\ \text{---} \\ \text{---} \\ \text{---} \end{array} \right] = \begin{pmatrix} 1 & 0 & 0 \\ 0 & e^{i\alpha} & 0 \\ 0 & 0 & e^{i\beta} \end{pmatrix} \quad (6.3)$$

$$\left[\begin{array}{c} \text{---} \\ \text{---} \\ \text{---} \\ \text{---} \\ \text{---} \end{array} \right] = \begin{pmatrix} 1 + e^{i\alpha} + e^{i\beta} & 1 + \bar{\omega}e^{i\alpha} + \omega e^{i\beta} & 1 + \omega e^{i\alpha} + \bar{\omega}e^{i\beta} \\ 1 + \omega e^{i\alpha} + \bar{\omega}e^{i\beta} & 1 + e^{i\alpha} + e^{i\beta} & 1 + \bar{\omega}e^{i\alpha} + \omega e^{i\beta} \\ 1 + \bar{\omega}e^{i\alpha} + \omega e^{i\beta} & 1 + \omega e^{i\alpha} + \bar{\omega}e^{i\beta} & 1 + e^{i\alpha} + e^{i\beta} \end{pmatrix} \quad (6.4)$$

$$\left[\begin{array}{c} \boxed{H} \\ \vdots \\ \vdots \\ \vdots \end{array} \right] = \begin{pmatrix} 1 & 1 & 1 \\ 1 & \omega & \bar{\omega} \\ 1 & \bar{\omega} & \omega \end{pmatrix} \quad (6.5)$$

Like the qubit case, there are three important properties about the qutrit ZX-calculus, i.e. universality, soundness, and completeness: Universality is about if there exists a ZX-calculus diagram for every corresponding linear map in Hilbert spaces under the standard interpretation. Soundness means that all the rules in the qutrit ZX-calculus have a correct standard interpretation in the Hilbert spaces. Completeness is concerned with whether an equation of diagrams can be derived in the ZX-calculus when their corresponding equation

of linear maps under the standard interpretation holds true. Among these properties, universality is proved in [70]. Soundness can easily be checked with the standard interpretation $\llbracket \cdot \rrbracket$.

To represent qutrit graph states in the ZX-calculus, we first show that the horizontal nodes H and H^\dagger make sense when connected to two green nodes.

Lemma 6.2.1 [31]

$$\begin{array}{c} \text{Green} \\ | \\ \text{H} \\ | \\ \text{Green} \end{array} = \begin{array}{c} \text{Green} \\ | \\ \text{H} \\ | \\ \text{Green} \end{array} =: \begin{array}{c} \text{Green} \\ | \\ \text{H} \\ | \\ \text{Green} \end{array}, \quad \begin{array}{c} \text{Green} \\ | \\ \text{H}^\dagger \\ | \\ \text{Green} \end{array} = \begin{array}{c} \text{Green} \\ | \\ \text{H}^\dagger \\ | \\ \text{Green} \end{array} =: \begin{array}{c} \text{Green} \\ | \\ \text{H}^\dagger \\ | \\ \text{Green} \end{array}. \quad (6.6)$$

Proof: We will only prove the first equation, since the proof for the second one is similar.

$$\begin{array}{c} \text{Green} \\ | \\ \text{H} \\ | \\ \text{Green} \end{array} \stackrel{H2}{=} \begin{array}{c} \text{Green} \\ | \\ \text{H} \\ | \\ \text{H} \\ | \\ \text{H}^\dagger \end{array} \stackrel{P1}{=} \begin{array}{c} \text{Green} \\ | \\ \text{H} \\ | \\ \text{H}^\dagger \end{array} \stackrel{S1}{=} \begin{array}{c} \text{Green} \\ | \\ \text{H} \\ | \\ \text{H}^\dagger \end{array} \stackrel{S1}{=} \begin{array}{c} \text{Green} \\ | \\ \text{H} \\ | \\ \text{H}^\dagger \end{array} \stackrel{H2'}{=} \begin{array}{c} \text{H} \\ | \\ \text{H}^\dagger \\ | \\ \text{H} \\ | \\ \text{H}^\dagger \end{array} \stackrel{H1}{=} \begin{array}{c} \text{Green} \\ | \\ \text{H} \\ | \\ \text{Green} \end{array}. \quad \square$$

We also list some useful properties which have been proved in [31] or [70]:

$$\begin{array}{c} \text{D} \\ | \\ \text{D} \end{array} = \begin{array}{c} \text{D} \\ | \\ \text{Green} \\ | \\ \text{D} \end{array} = \begin{array}{c} \text{D} \\ | \\ \text{Green} \end{array} \quad \begin{array}{c} \text{D} \\ | \\ \text{Green} \\ \left(\begin{array}{c} \beta \\ \alpha \end{array} \right) \\ | \\ \text{D} \end{array} = \begin{array}{c} \text{D} \\ | \\ \text{Green} \\ \left(\begin{array}{c} \alpha \\ \beta \end{array} \right) \\ | \\ \text{D} \end{array} \quad (6.7)$$

$$\begin{array}{c} \text{Green} \\ | \\ \text{Red} \end{array} = \begin{array}{c} \text{Green} \\ | \\ \text{Red} \\ \left(\begin{array}{c} \alpha \\ \beta \end{array} \right) \end{array} = \begin{array}{c} \text{Green} \\ | \\ \text{Red} \\ \left(\begin{array}{c} \beta \\ \alpha \end{array} \right) \end{array} \quad (6.8)$$

$$\begin{array}{c} \text{Green} \\ | \\ \text{Red} \end{array} = \begin{array}{c} \text{Green} \\ | \\ \text{Red} \\ \text{Curve} \end{array} \quad \begin{array}{c} \text{Green} \\ | \\ \text{Red} \end{array} = \begin{array}{c} \text{Green} \\ | \\ \text{Red} \\ \text{Curve} \end{array} \quad (6.9)$$

$$\begin{array}{c} \text{Red} \\ | \\ \text{Green} \end{array} = \begin{array}{c} \text{Red} \\ | \\ \text{Green} \\ \text{Curve} \end{array} \quad \begin{array}{c} \text{Red} \\ | \\ \text{Green} \end{array} = \begin{array}{c} \text{Red} \\ | \\ \text{Green} \\ \text{Curve} \end{array}$$

$$(6.10)$$

$$(6.11)$$

$$(6.12)$$

$$(6.13)$$

$$(6.14)$$

Note that the red-green colour swap version of these properties also holds.

Remark 6.2.2 *In the qubit ZX-calculus, all its diagrams obey a meta-rule which has been formalized as a well-known slogan: “only the topology matters” [15], or more recently as “only connectedness matters” [21]. This means, any diagram of the qubit ZX-calculus can be transformed into a semantically equal diagram (representing the same matrix) by moving the components around without changing their connections, thus rendering the qubit ZX-calculus unoriented. However, as one can see in (6.9), this meta-rule does not hold for all diagrams in the qutrit ZX-calculus. Therefore, one should be careful with the orientation of a qutrit ZX diagram, especially when there is a connection between green and red nodes.*

6.2.2 Qutrit stabilizer quantum mechanics in the ZX-calculus

In this subsection, we represent in ZX-calculus the qutrit stabilizer QM, which consists of state preparations and measurements based on the computational basis $\{|0\rangle, |1\rangle, |2\rangle\}$, as well as unitary operators belonging to the generalized Clifford group C_n . Furthermore, we give the unique form for single qutrit Clifford operators.

Firstly, the states and effects in computational basis can be represented as:

$$|0\rangle = \begin{array}{|c|} \hline \bullet \\ \hline \end{array}, \quad |1\rangle = \begin{array}{|c|} \hline \oplus \\ \hline \end{array}, \quad |2\rangle = \begin{array}{|c|} \hline \oplus \\ \hline \end{array}, \quad \langle 0| = \begin{array}{|c|} \hline \bullet \\ \hline \end{array}, \quad \langle 1| = \begin{array}{|c|} \hline \oplus \\ \hline \end{array}, \quad \langle 2| = \begin{array}{|c|} \hline \oplus \\ \hline \end{array}. \quad (6.15)$$

The generators of the generalized Clifford group C_n are denoted by the following diagrams:

$$S = \begin{array}{|c|} \hline \oplus \\ \hline \end{array}, \quad H = \begin{array}{|c|} \hline H \\ \hline \end{array}, \quad \Lambda = \begin{array}{|c|} \hline \bullet \\ \hline \end{array} \begin{array}{|c|} \hline \bullet \\ \hline \end{array}. \quad (6.16)$$

Lemma 6.2.3 *A pure n-qutrit quantum state $|\psi\rangle$ is a stabilizer state if and only if there exists an n-qutrit Clifford unitary U such that $|\psi\rangle = U|0\rangle^{\otimes n}$.*

Proof: If a pure n-qutrit quantum state $|\psi\rangle$ is a stabilizer state, then by Lemma 6.1.6, there exists a Clifford operator U' such that $|\psi\rangle = U'|G\rangle$, where $|G\rangle = \mathcal{U}|+\rangle^{\otimes n}$ is a graph state, $\mathcal{U} = \prod_{\{l,m\} \in E} (C_{lm})^{\Gamma_{lm}}$, and $C_{lm} = \sum_{j=0}^2 \sum_{k=0}^2 \omega^{jk} |j\rangle \langle j|_l \otimes |k\rangle \langle k|_m$. It is shown in [31] that

$$C_{lm} = \begin{array}{|c|} \hline \bullet \\ \hline \end{array} \begin{array}{|c|} \hline H \\ \hline \end{array} \begin{array}{|c|} \hline \bullet \\ \hline \end{array} = \begin{array}{|c|} \hline \bullet \\ \hline \end{array} \begin{array}{|c|} \hline H^\dagger \\ \hline \end{array} \begin{array}{|c|} \hline \bullet \\ \hline \end{array},$$

which means C_{lm} is a Clifford operator, so is \mathcal{U} . Let $V = \mathcal{U}H^{\otimes n}$, then V is also a Clifford operator, and $|G\rangle = V|0\rangle^{\otimes n}$. Therefore, $|\psi\rangle = U'|G\rangle = U'V|0\rangle^{\otimes n}$. Let $U = U'V$, then $|\psi\rangle = U|0\rangle^{\otimes n}$, and U is a Clifford unitary.

On the contrary, assume $|\psi\rangle = U|0\rangle^{\otimes n}$, where U is a Clifford unitary. Let $|G\rangle = \mathcal{U}|+\rangle^{\otimes n}$ be an n-qutrit graph state, $V = \mathcal{U}H^{\otimes n}$, and $W = UV^\dagger$. Then $|\psi\rangle = WV|0\rangle^{\otimes n} = W|G\rangle$. Suppose \mathfrak{S} is the stabilizer group of $|G\rangle$. Since $WSW^\dagger|\psi\rangle = WSW^\dagger W|G\rangle = WS|G\rangle = W|G\rangle = |\psi\rangle, \forall S \in \mathfrak{S}$, it follows that $W\mathfrak{S}W^\dagger$ is the stabilizer group of $|\psi\rangle$, i.e., $|\psi\rangle$ is a stabilizer state. \square

Lemma 6.2.4 *In the qutrit formalism, any stabilizer state, Clifford unitary, or post-selected measurement can be represented by a ZX-calculus diagram with phase angles just integer multiples of $\frac{2}{3}\pi$.*

Proof: Firstly, by Lemma 6.2.3, each stabilizer state can be obtained by applying an n-qutrit Clifford unitary to the computational basis state $|0\rangle^{\otimes n}$. Secondly, any Clifford unitary can be generated by the gates \mathcal{S}, H and Λ [37, 23], which are clearly composed of phases with angles integer multiples of $\frac{2}{3}\pi$. Since the generators are composed of phases with angles integer multiples of $\frac{2}{3}\pi$, so are Clifford unitaries generated by these generators. Thirdly, computational basis states and post-selected computational basis measurements are clearly with phase angles integer multiples of $\frac{2}{3}\pi$. Therefore, by (6.15) and (6.16), any stabilizer state, Clifford unitary, or post-selected measurement can be represented by a ZX-calculus diagram with phase angles just integer multiples of $\frac{2}{3}\pi$. \square

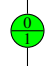

Lemma 6.2.5 *Each qutrit ZX-calculus diagram can be represented by a combination of the following components:*


(6.17)

where $\alpha, \beta \in [0, 2\pi)$.

The proof follows directly from the qutrit spider rule (S1) and the colour change rules (H2) and (H2').

Lemma 6.2.6 *Each qutrit ZX-calculus diagram with phase angles integer multiples of $\frac{2}{3}\pi$ corresponds to an element of the qutrit stabilizer QM.*

Proof: By Lemma 6.2.5, each ZX-calculus diagram can be decomposed into basic components as shown in (6.17). Since composition of diagrams corresponds to composition of corresponding matrices in QM, we only need to consider those basic components where the phase angles are integer multiples of $\frac{2}{3}\pi$, in such a way that turns the standard interpretation of each basic component into a composition of Clifford unitaries, computational basis states, and computational basis effects. We have tackled the basic components  and  in (6.16), the remaining components are dealt with as follows:

$$\left[\begin{array}{c} \bullet \\ | \\ | \end{array} \right] = \left[\begin{array}{c} \bullet \\ \boxed{H} \\ | \end{array} \right] = H |0\rangle \quad (6.18)$$

$$\left[\begin{array}{c} | \\ | \\ \bullet \end{array} \right] = \left[\begin{array}{c} | \\ | \\ \boxed{H} \\ \bullet \end{array} \right] = \langle 0 | H \quad (6.19)$$

$$\left[\begin{array}{c} | \\ | \\ \bullet \\ | \\ | \\ \bullet \end{array} \right] = \left[\begin{array}{c} | \\ | \\ \bullet \\ | \\ | \\ \bullet \end{array} \right] = \Lambda \circ (I \otimes |0\rangle) \quad (6.20)$$

$$\left[\begin{array}{c} | \\ | \\ \bullet \\ | \\ | \\ \bullet \\ | \\ | \\ \bullet \end{array} \right] = \left[\begin{array}{c} | \\ | \\ \bullet \\ | \\ | \\ \bullet \\ | \\ | \\ \bullet \end{array} \right] = (I \otimes \langle 0 |) \circ \Lambda(I \otimes (H \circ H)) \quad (6.21)$$

Thus we conclude the proof. \square

bringing together

Bringing together Lemmas 6.2.4 and 6.2.6, we have

Theorem 6.2.7 *The ZX-calculus for pure qutrit stabilizer QM comprises exactly the diagrams with phase angles integer multiples of $\frac{2}{3}\pi$.*

In the sequel, a diagram in which all phase angles are integer multiples of $\frac{2}{3}\pi$ will be called a stabilizer diagram. Now we denote $\frac{2\pi}{3}$ and $\frac{4\pi}{3}$ by 1 and 2 (or -1) respectively, and let

$$\mathcal{P} = \left\{ \frac{1}{1}, \frac{2}{2} \right\}, \quad \mathcal{N} = \left\{ \frac{1}{0}, \frac{0}{1}, \frac{2}{0}, \frac{0}{2} \right\}, \quad \mathcal{M} = \left\{ \frac{0}{0}, \frac{2}{1}, \frac{1}{2} \right\}, \quad \mathcal{Q} = \mathcal{P} \cup \mathcal{N}, \quad \mathcal{A} = \mathcal{Q} \cup \mathcal{M},$$

where the symbol $\frac{a}{b}$ is just the denotation of the pair (a, b) , instead of the fraction $\frac{a}{b}$. Then each green or red node in a stabilizer diagram has its phase angles denoted as elements in the set \mathcal{A} . Define the addition $+$ in \mathcal{A} as $\frac{a}{b} + \frac{c}{d} := \frac{a+c(\text{mod}3)}{b+d(\text{mod}3)}$. Then \mathcal{A} is an abelian group, with $\mathcal{P} \cup \{ \frac{0}{0} \}$ and \mathcal{M} as subgroups. Note that the elements in \mathcal{P} resemble to the phases $\frac{\pi}{2}$ and $-\frac{\pi}{2}$ in the qubit ZX-calculus, and the non-zero elements in \mathcal{M} are analogous to the phase π in the qubit ZX-calculus.

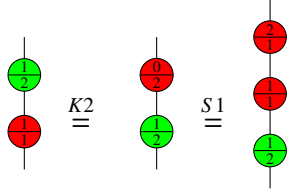
With the notation of $\frac{a}{b}$ and the addition defined above, the commutation rule (K2) has a special form for elements in \mathcal{P} :

Lemma 6.2.8

$$\left[\begin{array}{c} \frac{m_1}{m_2} \\ \frac{p_1}{p_1} \end{array} \right] = \left[\begin{array}{c} \frac{p_3}{p_4} \\ \frac{p_1}{p_1} \\ \frac{m_1}{m_2} \end{array} \right] \quad (6.22)$$

where $\frac{m_1}{m_2}, \frac{m_3}{m_4} \in \mathcal{M}, \frac{p_1}{p_1} \in \mathcal{P}$.

Proof: There are several similar cases to be verified here. We only show one case where $\frac{m_1}{m_2} = \frac{1}{2}, \frac{p_1}{p_2} = \frac{1}{1}$.



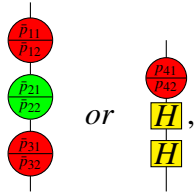
□

Lemma 6.2.9 Any single qutrit stabilizer diagram of form



(6.23)

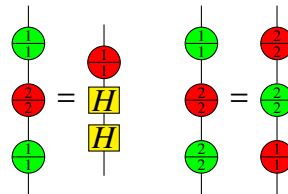
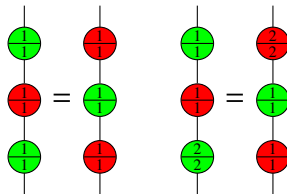
can be rewritten as



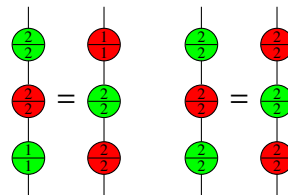
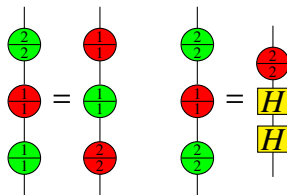
(6.24)

where $\frac{p_{i1}}{p_{i2}}, \frac{\bar{p}_{j1}}{\bar{p}_{j2}} \in \mathcal{P}, \forall i \in \{1, 2, 3, 4\}, \forall j \in \{1, 2, 3\}$.

Proof: First we list all the possible forms of (6.23) and their rewritten forms of (6.24) as follows:

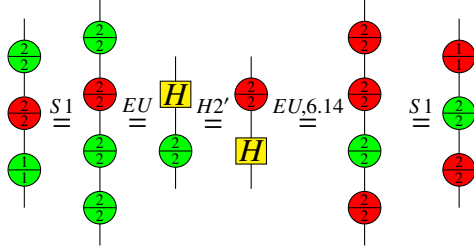


(6.25)



(6.26)

For simplicity, we just show one derivation here:

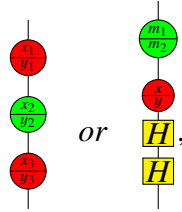


□

Lemma 6.2.10 Any single qutrit stabilizer diagram of form

$$K = \begin{array}{c} \text{green } \frac{a_1}{b_1} \\ \text{red } \frac{a_2}{b_2} \\ \text{green } \frac{a_3}{b_3} \end{array} \quad (6.27)$$

can be rewritten as

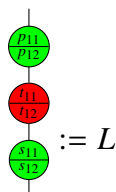


where $\frac{m_1}{m_2} \in \mathcal{M}$.

Proof: If $\frac{a_1}{b_1} \in \mathcal{M}$, then by rule (S2) or (K2), this green node can be pushed down and merges with another green node thus K is rewritten as

$$K = \begin{array}{c} \text{red } \frac{a}{b} \\ \text{green } \frac{a}{b} \end{array} \quad (6.28)$$

Otherwise, $\frac{a_1}{b_1} \in \mathcal{Q}$, then $\frac{a_1}{b_1} = \frac{p_{11}}{p_{12}} + \frac{m_{11}}{m_{12}}$, where $\frac{p_{11}}{p_{12}} \in \mathcal{P}$, $\frac{m_{11}}{m_{12}} \in \mathcal{M}$ (e.g., $\frac{0}{1} = \frac{2}{2} + \frac{1}{2}$). Therefore, by the spider rule (S1) and the commutation rule (K2), the \mathcal{M} part can be separated from the $\frac{a_1}{b_1}$ node and pushed down to the bottom to merge with the other green node, thus K can be rewritten as



Furthermore, if $\frac{t_{11}}{t_{12}} \in \mathcal{M}$, then the red node in L can be pushed up, thus L is rewritten as

$$\begin{array}{c} \text{red} \\ \text{green} \end{array} \quad (6.29)$$

Otherwise, $\frac{t_{11}}{t_{12}} \in \mathcal{Q}$, then use the same trick as for $\frac{a_1}{b_1} \in \mathcal{Q}$, L can be rewritten as

$$\begin{array}{c} \text{green} \\ \text{red} \\ \text{green} \\ \text{red} \end{array} := R$$

where $\frac{p_{21}}{p_{22}} \in \mathcal{P}$, $\frac{m_{21}}{m_{22}} \in \mathcal{M}$. We continue the similar analysis on $\frac{s_{31}}{s_{32}}$ in R . If $\frac{s_{31}}{s_{32}} = \frac{m_{31}}{m_{32}} \in \mathcal{M}$, then

$$R = \begin{array}{c} \text{green} \\ \text{red} \\ \text{green} \\ \text{red} \end{array} \stackrel{K2, S1}{=} \begin{array}{c} \text{green} \\ \text{red} \end{array} \quad (6.30)$$

where by commutation rule ($K2$) we push the $\frac{m_{31}}{m_{32}}$ node up and merge nodes with same colours. Otherwise, $\frac{s_{31}}{s_{32}} \in \mathcal{Q}$, then by the same trick as for $\frac{a_1}{b_1} \in \mathcal{Q}$, R can be rewritten as

$$\begin{array}{c} \text{green} \\ \text{red} \\ \text{green} \\ \text{red} \\ \text{green} \end{array} := J \quad (6.31)$$

where $\frac{p_{31}}{p_{32}} \in \mathcal{P}$, $\frac{m_{41}}{m_{42}} \in \mathcal{M}$, and we used the fact that a green node with phase angles in \mathcal{M} must commute with a red node with phase angles also in \mathcal{M} .

By Lemma 6.2.9, J can be rewritten as

$$\begin{array}{c}
\begin{array}{c}
\textcircled{p_{11}} \\
\textcircled{p_{12}} \\
\textcircled{p_{21}} \\
\textcircled{p_{22}} \\
\textcircled{p_{31}} \\
\textcircled{p_{32}} \\
\textcircled{m_{21}} \\
\textcircled{m_{22}} \\
\textcircled{m_{41}} \\
\textcircled{m_{42}}
\end{array}
\equiv^{K2, S1}
\begin{array}{c}
\textcircled{p_1} \\
\textcircled{p_2} \\
\textcircled{p_3}
\end{array},
\end{array}
\quad (6.32)
\quad \text{or} \quad
\begin{array}{c}
\begin{array}{c}
\textcircled{p_{31}} \\
\textcircled{p_{32}} \\
\textcircled{m_{21}} \\
\textcircled{m_{22}} \\
\textcircled{m_{41}} \\
\textcircled{m_{42}}
\end{array}
\equiv^{6.7, S1}
\begin{array}{c}
\textcircled{m_1} \\
\textcircled{m_2} \\
\textcircled{p} \\
\textcircled{H} \\
\textcircled{H} \\
\textcircled{H}
\end{array}
\end{array}
\quad (6.33)$$

where we used the commutation rule (K2) to push the nodes with phase angles in \mathcal{M} and the property (6.7).

Now we finish the proof by pointing out that the single qutrit stabilizer diagrams (6.28), (6.29), (6.30) are just special forms of (6.32). \square

Corollary 6.2.11 *Any ZX diagram for single qutrit Clifford operator can be rewritten in one of the forms*

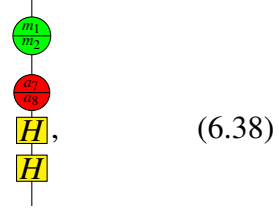
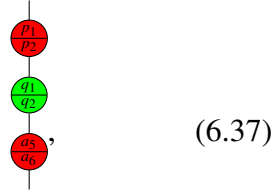
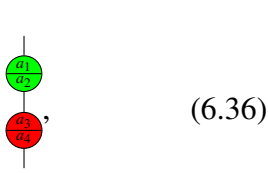
$$\begin{array}{c}
\begin{array}{c}
\textcircled{p_1} \\
\textcircled{p_2} \\
\textcircled{p_3}
\end{array},
\end{array}
\quad (6.34)
\quad \text{or} \quad
\begin{array}{c}
\begin{array}{c}
\textcircled{p_1} \\
\textcircled{p_2} \\
\textcircled{p_3} \\
\textcircled{H} \\
\textcircled{H}
\end{array}
\end{array}
\quad (6.35)$$

Proof: Because of the spider rule (S1), we only consider the case where any two adjacent nodes are of different colours. First note that single qutrit stabilizer diagram with one node or two nodes is a special form of (6.34). If there are only three aligned nodes in the diagram, then they are either the form of (6.34) or (6.27), the later can be rewritten into one of the forms (6.34) and (6.35) by Lemma 6.2.10. We can now proceed by induction: Suppose that any single qutrit stabilizer diagram D_n with $n(n \geq 3)$ nodes can be rewritten into one of the forms (6.34) and (6.35). For single qutrit stabilizer diagram D_{n+1} with $n + 1$ nodes, we consider its toppest node called t . If t is a red node, then by the spider rule (S1), it merges with a red node in D_n , thus D_{n+1} is still of form (6.34) or (6.35). If t is a green node, after rewriting the remaining n nodes into a form of (6.34) or (6.35) by the induction hypothesis, D_{n+1} now has 4 interlaced green and red nodes except for Hadamard nodes. The first 3 nodes then consist a diagram of form (6.27), applying the induction hypothesis again, D_{n+1} can be reduced to a form of (6.34) or (6.35), noting that we used $H^4 = 1$ derived from rules

(H1) and (P1) in the case that 4 Hadamard notes appear in one diagram. □

Now we can give a normal form for the single qutrit Clifford group C_1 .

Theorem 6.2.12 *In the ZX-calculus, each element of the single qutrit Clifford group C_1 can be uniquely represented in one of the following forms*



where $\frac{a_1}{a_2}, \frac{a_3}{a_4}, \frac{a_5}{a_6}, \frac{a_7}{a_8} \in \mathcal{A}, \frac{p_1}{p_2} \in \mathcal{P}, \frac{q_1}{q_2} \in \mathcal{Q}, \frac{m_1}{m_2} \in \mathcal{M}$.

Proof: By Corollary 6.2.11, any single qutrit Clifford operator is of form (6.34) or (6.35). Furthermore, if $\frac{x_1}{y_1} \in \mathcal{M}$, then the corresponding red node can be pushed down and merge with the other red node at the bottom, thus diagram (6.34) becomes the form (6.36).

If otherwise $\frac{x_1}{y_1} \in \mathcal{Q}$, then we can use the same trick as in the proof of Lemma 6.2.10: separate the \mathcal{M} part and push it down to be merged. Thus diagram (6.34) becomes the form



where $\frac{p_1}{p_2} \in \mathcal{P}$. If furthermore $\frac{s_1}{s_2} \in \mathcal{M}$, then the corresponding green node can be pushed up and diagram (6.39) becomes the form (6.36). Otherwise, $\frac{s_1}{s_2} \in \mathcal{Q}$, and diagram (6.39) is of the form (6.37), where $\frac{q_1}{q_2} \in \mathcal{Q}$. To sum up, the diagram (6.34) can be rewritten into the form (6.36) or (6.37). As a consequence, the diagram (6.35) can be rewritten into one of the forms



where $\frac{p_1}{p_2} \in \mathcal{P}$, $\frac{q_1}{q_2} \in \mathcal{Q}$.

Next we show that the diagrams (6.40) and (6.41) can be rewritten into the form (6.36), (6.37) or (6.38). For (6.40), if $\frac{a_1}{a_2} \in \mathcal{M}$, it is just the form (6.38). Otherwise, $\frac{a_1}{a_2} \in \mathcal{Q}$, thus $\frac{a_2}{a_1} \in \mathcal{Q}$. Let $\frac{a_2}{a_1} = \frac{m_1}{m_2} + \frac{p_1}{p_1}$, where $\frac{m_1}{m_2} \in \mathcal{M}$, $\frac{p_1}{p_1} \in \mathcal{P}$. It is clear from (6.25) and (6.26) that

$$\begin{array}{c} \boxed{H} \\ \boxed{H} \\ \textcircled{p} \end{array} = \begin{array}{c} \textcircled{\frac{p}{p}} \\ \textcircled{\frac{p'}{p''}} \\ \textcircled{\frac{p}{p}} \\ \textcircled{\frac{p}{p}} \end{array}, \quad (6.42)$$

where $\frac{p}{p}$, $\frac{p'}{p'} \in \mathcal{P}$. Combining with (6.7), we have

$$\begin{array}{c} \textcircled{\frac{a_1}{a_2}} \\ \textcircled{\frac{a_3}{a_4}} \\ \boxed{H} \\ \boxed{H} \end{array} \stackrel{6.7}{=} \begin{array}{c} \boxed{H} \\ \boxed{H} \\ \textcircled{\frac{a_2}{a_1}} \\ \textcircled{\frac{a_3}{a_3}} \end{array} \stackrel{S1}{=} \begin{array}{c} \textcircled{\frac{p_1}{p_1}} \\ \textcircled{\frac{m_1}{m_2}} \\ \textcircled{\frac{a_4}{a_3}} \end{array} \stackrel{6.25}{=} \begin{array}{c} \textcircled{\frac{p_1}{p_1}} \\ \textcircled{\frac{p_2}{p_2}} \\ \textcircled{\frac{m_1}{m_2}} \\ \textcircled{\frac{a_4}{a_3}} \end{array} \stackrel{6.26}{=} \begin{array}{c} \textcircled{\frac{p_1}{p_1}} \\ \textcircled{\frac{p_2}{p_2}} \\ \textcircled{\frac{m_1}{m_2}} \\ \textcircled{\frac{a_5}{a_6}} \end{array} \stackrel{K2}{=} \begin{array}{c} \textcircled{\frac{p_1}{p_1}} \\ \textcircled{\frac{p_2}{p_2}} \\ \textcircled{\frac{a_1}{a_2}} \\ \textcircled{\frac{a_5}{a_6}} \end{array} \stackrel{S1}{=} \begin{array}{c} \textcircled{\frac{p_1}{p_1}} \\ \textcircled{\frac{a_1}{a_2}} \\ \textcircled{\frac{a_5}{a_6}} \end{array}, \quad (6.43)$$

which is just of form (6.37).

For (6.41), except for the top red node of phase $\frac{p_1}{p_2}$, the remaining part is exactly the same as the case of (6.40) when $\frac{a_1}{a_2} \in \mathcal{Q}$, thus can be rewritten into the form of (6.37). Composing with the red node $\frac{p_1}{p_2}$, we obtain a diagram of form (6.36) or (6.37).

By now we have shown that each single qutrit Clifford operator can be represented by a ZX-calculus diagram in one of the forms (6.36), (6.37) and (6.38). Next we show that these forms are unique. First we prove that all the forms presented in (6.36), (6.37) and (6.38) are not equal to each other. There are several cases to be considered, we first compare the form of (6.36) with the form of (6.38). Suppose that

$$\begin{array}{c} \textcircled{\frac{a_1}{a_2}} \\ \textcircled{\frac{a_3}{a_4}} \\ \boxed{H} \\ \boxed{H} \end{array} = \begin{array}{c} \textcircled{\frac{a_1}{a_2}} \\ \textcircled{\frac{a_3}{a_4}} \\ \textcircled{\frac{a_3}{a_4}} \end{array} \quad (6.44)$$

Then

$$\begin{array}{c} \text{green circle} \\ \frac{a_1 - a_1}{a_2 - a_2} \\ \text{yellow box } H \\ \text{yellow box } H \end{array} = \begin{array}{c} \text{red circle} \\ \frac{a_3 - a_4}{a_4 - a_3} \\ \text{red circle} \end{array} \quad (6.45)$$

which can be written in a matrix form as follows:

$$\begin{pmatrix} 1 & 1 & 1 \\ 1 & \omega & \bar{\omega} \\ 1 & \bar{\omega} & \omega \end{pmatrix} \begin{pmatrix} 1 & 1 & 1 \\ 1 & \omega & \bar{\omega} \\ 1 & \bar{\omega} & \omega \end{pmatrix} \begin{pmatrix} 1 & 0 & 0 \\ 0 & e^{i\alpha} & 0 \\ 0 & 0 & e^{i\beta} \end{pmatrix} \simeq \begin{pmatrix} u & v & w \\ w & u & v \\ v & w & u \end{pmatrix} \quad (6.46)$$

where \simeq means equal up to a non-zero scalar and the matrix on the right hand side of \simeq comes from (6.5). After simplification on the left hand side, we have

$$\begin{pmatrix} 1 & 0 & 0 \\ 0 & 0 & e^{i\beta} \\ 0 & e^{i\alpha} & 0 \end{pmatrix} \simeq \begin{pmatrix} u & v & w \\ w & u & v \\ v & w & u \end{pmatrix} \quad (6.47)$$

From the first row of the above matrices, $u \neq 0, v = w = 0$, while from the third row, $w \neq 0, u = 0$, a contradiction. Therefore the equality (6.44) is impossible, i.e., the form of (6.36) will never equal to the form of (6.38).

Then we compare the form of (6.37) with the form of (6.38). Suppose that

$$\begin{array}{c} \text{green circle} \\ \frac{a_1}{a_2} \\ \text{red circle} \\ \frac{a_3}{a_4} \\ \text{yellow box } H \\ \text{yellow box } H \end{array} = \begin{array}{c} \text{red circle} \\ \frac{p_1}{p_2} \\ \text{green circle} \\ \frac{a_1}{a_2} \\ \text{red circle} \\ \frac{a_2}{a_4} \end{array} \quad (6.48)$$

Then

$$\begin{array}{c} \text{red circle} \\ \frac{a_3 - a_4}{a_4 - a_3} \\ \text{yellow box } H \\ \text{yellow box } H \end{array} = \begin{array}{c} \text{green circle} \\ \frac{a_1}{a_2} \\ \text{red circle} \\ \frac{p_1}{p_2} \\ \text{green circle} \\ \frac{a_1}{a_2} \end{array} \quad (6.49)$$

When $\frac{p_1}{p_2} = \frac{1}{1}$, the matrix form of (6.49) is as follows:

$$\begin{pmatrix} 1 & 0 & 0 \\ 0 & 0 & 1 \\ 0 & 1 & 0 \end{pmatrix} \begin{pmatrix} a & b & c \\ c & a & b \\ b & c & a \end{pmatrix} \simeq \begin{pmatrix} 1 & 0 & 0 \\ 0 & e^{i\alpha} & 0 \\ 0 & 0 & e^{i\beta} \end{pmatrix} \begin{pmatrix} \omega & 1 & 1 \\ 1 & \omega & 1 \\ 1 & 1 & \omega \end{pmatrix} \begin{pmatrix} 1 & 0 & 0 \\ 0 & e^{i\alpha} & 0 \\ 0 & 0 & e^{i\tau} \end{pmatrix} \quad (6.50)$$

where $\alpha, \beta, \sigma, \tau \in [0, 2\pi)$. That is,

$$\begin{pmatrix} a & b & c \\ c & a & b \\ b & c & a \end{pmatrix} \simeq \begin{pmatrix} \omega & e^{i\sigma} & e^{i\tau} \\ e^{i\beta} & e^{i(\beta+\sigma)} & \omega e^{i(\beta+\tau)} \\ e^{i\alpha} & \omega e^{i(\alpha+\sigma)} & e^{i(\alpha+\tau)} \end{pmatrix} \quad (6.51)$$

Therefore,

$$\begin{cases} e^{i\sigma} = e^{i\alpha} = \omega e^{i(\beta+\tau)} \\ e^{i\tau} = e^{i\beta} = \omega e^{i(\alpha+\sigma)} \\ \omega = e^{i(\alpha+\tau)} = e^{i(\beta+\sigma)} \end{cases}$$

Solving this system, we have $\sigma = \alpha, \tau = \beta$,

$$\begin{cases} \alpha = 0 \\ \beta = \frac{2\pi}{3} \end{cases} \quad \begin{cases} \alpha = \frac{2\pi}{3} \\ \beta = 0 \end{cases} \quad \begin{cases} \alpha = \frac{4\pi}{3} \\ \beta = \frac{4\pi}{3} \end{cases} \quad (6.52)$$

Return to the equation (6.49). For $\alpha = 0, \beta = \frac{2\pi}{3}$, we have $\frac{q_1}{q_2} = \frac{0}{1}, \frac{a_1}{a_2} = \frac{0}{2}, \frac{a_3-a_6}{a_4-a_5} = \frac{0}{1}$. For $\alpha = \frac{2\pi}{3}, \beta = 0$, we have $\frac{q_1}{q_2} = \frac{1}{0}, \frac{a_1}{a_2} = \frac{2}{0}, \frac{a_3-a_6}{a_4-a_5} = \frac{1}{0}$. For $\alpha = \frac{4\pi}{3}, \beta = \frac{4\pi}{3}$, we have $\frac{q_1}{q_2} = \frac{2}{2}, \frac{a_1}{a_2} = \frac{1}{1}, \frac{a_3-a_6}{a_4-a_5} = \frac{2}{2}$. To sum up, when $\frac{p_1}{p_2} = \frac{1}{1}$, it must be that $\frac{a_1}{a_2} \in \{\frac{2}{0}, \frac{0}{2}, \frac{1}{1}\}$ for (6.48) to hold.

Similarly, it can be shown that when $\frac{p_1}{p_2} = \frac{2}{2}$, it must be that $\frac{a_1}{a_2} \in \{\frac{1}{0}, \frac{0}{1}, \frac{2}{2}\}$ for (6.48) to hold. Thus for $\frac{a_1}{a_2} \in \mathcal{M}$, (6.48) does not hold, i.e., the form of (6.37) will never equal to the form of (6.38).

In the same way, we can show that the form of (6.36) is not equal to the form of (6.37), and different elements (with different parameters) of the same form (be it (6.36), (6.37), or (6.38)) must not be equal to each other.

Now we can prove the uniqueness of these forms. By direct calculation, (6.36) has $9 \times 9 = 81$ elements, (6.37) has $2 \times 6 \times 9 = 108$ elements, and (6.38) has $3 \times 9 = 27$ elements. So the total number elements is $81 + 108 + 27 = 216$, which is exactly equal to the order $|C_1|$ of the group of single qutrit Clifford operators. Since each element of C_1 has been shown to be representable by forms (6.36), (6.37) or (6.38), there should be enough members belonging to these kind of forms, thus no common elements are allowed. Therefore the representation of single qutrit Clifford operators is unique. \square


6.3 Qutrit graph states in the ZX-calculus

6.3.1 Stabilizer state diagram and transformations of GS-LC diagrams

The qutrit graph states have a nice representation in the ZX-calculus.

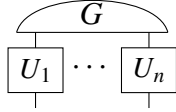
Lemma 6.3.1 [31] A qutrit graph state $|G\rangle$, where $G = (E; V)$ is an n -vertex graph, is represented in the graphical calculus as follows:

- for each vertex $v \in V$, a green node with one output, and
- for each 1-weighted edge $\{u, v\} \in E$, an H node connected to the green nodes representing vertices u and v ,
- for each 2-weighted edge $\{u, v\} \in E$, an H^\dagger node connected to the green nodes representing vertices u and v .

A graph state $|G\rangle$ is also denoted by the diagram .

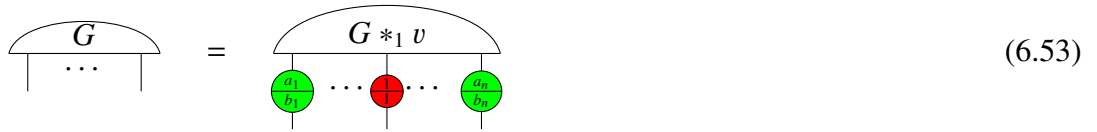
Definition 6.3.2 [5] A diagram in the stabilizer ZX-calculus is called a GS-LC diagram if it consists of a graph state diagram with arbitrary single-qutrit Clifford operators applied to each output. These associated Clifford operators are called vertex operators.

An n -qutrit GS-LC diagram is represented as



where $G = (V, E)$ is a graph and $U_v \in C_1$ for $v \in V$.

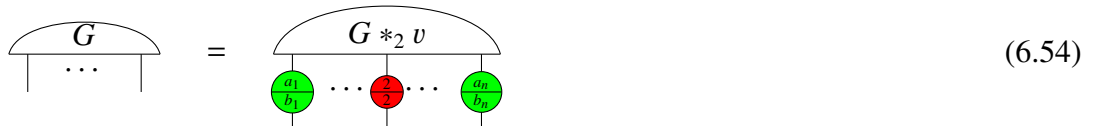
Theorem 6.3.3 [31] Let $G = (V, E)$ be a graph with adjacency matrix Γ and $G *_1 v$ be the graph that results from applying to G a 1-local complementation about some $v \in V$. Then the corresponding graph states $|G\rangle$ and $|G *_1 v\rangle$ are related as follows:

$$\begin{array}{c} \text{Diagram of } |G\rangle \\ \text{---} \end{array} = \begin{array}{c} \text{Diagram of } |G *_1 v\rangle \\ \text{---} \end{array} \quad (6.53)$$


where for $1 \leq i \leq n$, $i \neq v$,

$$\frac{a_i}{b_i} = \begin{cases} \frac{2}{2}, & \text{if } \Gamma_{iv} \neq 0 \\ \frac{0}{0}, & \text{if } \Gamma_{iv} = 0 \end{cases}$$

Corollary 6.3.4 Let $G = (V, E)$ be a graph with adjacency matrix Γ and $G *_2 v$ be the graph that results from applying to G a 2-local complementation about some $v \in V$. Then the corresponding graph states $|G\rangle$ and $|G *_2 v\rangle$ are related as follows:

$$\begin{array}{c} \text{Diagram of } |G\rangle \\ \text{---} \end{array} = \begin{array}{c} \text{Diagram of } |G *_2 v\rangle \\ \text{---} \end{array} \quad (6.54)$$


where for $1 \leq i \leq n$, $i \neq v$,

$$\frac{a_i}{b_i} = \begin{cases} \frac{1}{1}, & \text{if } \Gamma_{iv} \neq 0 \\ \frac{0}{0}, & \text{if } \Gamma_{iv} = 0 \end{cases}$$

Proof: Note that $G *_2 v = (G *_1 v) *_1 v$. □

Theorem 6.3.5 Let $G = (V, E)$ be a graph with adjacency matrix Γ and let $G \circ_2 v$ be the graph that results from applying the transformation $\circ_2 v$ about some $v \in V$. Then the corresponding graph states $|G\rangle$ and $|G \circ_2 v\rangle$ are related as follows:

$$\begin{array}{c} \text{---} \\ \text{---} \end{array} \overset{G}{\text{---}} = \begin{array}{c} \text{---} \\ \text{---} \end{array} \overset{G \circ_2 v}{\text{---}} \begin{array}{c} \boxed{H} \\ \vdots \\ \boxed{H} \end{array} \quad (6.55)$$

where the Hadamard nodes are on the output of the vertex v .

Proof: According to the definition of $G \circ_2 v$, we only need to consider the vertices that are connected to v . The effect of applying the operator $G \circ_2 v$ is to replace the H node connected to v with an $H^\dagger (= H^{-1})$ node, and vice versa, i.e., changing from $H^{\pm 1}$ to $H^{\mp 1}$. By the rewriting rule (P1), we have $\boxed{H^{\pm 1}} = \frac{\boxed{H^{\mp 1}}}{\boxed{D}}$. That means $G \circ_2 v$ can be seen as having one more D node on each edge connected to v than on the corresponding edge in G . The equality (6.55) then follows immediately from pushing these D nodes to the output of v by the property (6.7). □

6.3.2 Rewriting arbitrary stabilizer state diagram into a GS-LC diagram

In this subsection we show that any stabilizer state diagram can be rewritten into a GS-LC diagram by rules of the ZX-calculus. We give the proof of this result following [3, 5].

Theorem 6.3.6 Any stabilizer state diagram can be rewritten into a GS-LC diagram by rules of the ZX-calculus.

Proof: By lemma 6.2.5, any ZX-calculus diagram can be written as composed of four basic spiders together with phase shifts and Hadamard and Hadamard dagger nodes. Thus we can proceed with the proof by induction: \bullet is the initial GS-LC diagram, if it can be shown that applying any basic component of the ZX-calculus diagrams to a GS-LC diagram still

results in a GS-LC diagram, then any stabilizer state diagram can be rewritten into a GS-LC diagram. The following lemmas 6.3.7, 6.3.8, 6.3.13, 6.3.14 and 6.3.15 exactly give the inductive steps, hence completes the proof. \square

Lemma 6.3.7 A GS-LC diagram associated with \bullet is still a GS-LC diagram.

Proof: It follows directly from the definition of GS-LC diagrams and lemma 6.3.1. \square

Lemma 6.3.8 Applying a basic single qutrit Clifford unitary to a GS-LC diagram still results in a GS-LC diagram.

Proof: This follows directly from the definition of GS-LC diagrams. \square

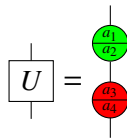
Lemma 6.3.9 If a vertex in a GS-LC diagram has no neighbours, then it must be a single-qutrit pure stabilizer state as one of the follows:

$$\begin{array}{cccccccccccc}
 \bullet & \frac{1}{2} & \frac{2}{1} & \frac{1}{1} & \frac{2}{2} & \frac{0}{1} & \frac{0}{1} & \frac{0}{2} & \frac{2}{0} & \bullet & \frac{1}{2} & \frac{1}{2} \\
 | & | & | & | & | & | & | & | & | & | & | & | \\
 \hline
 \end{array} \tag{6.56}$$

Proof: A vertex with no neighbours in a GS-LC diagram must be written as



where U is of one of the forms (6.36), (6.37) and (6.38). If



then

$$\begin{array}{c}
 \bullet \\
 | \\
 \boxed{U} = \\
 | \\
 \frac{a_1}{a_2} \\
 | \\
 \frac{a_3}{a_4} \\
 | \\
 \hline
 \end{array}
 \stackrel{S1}{=}
 \begin{array}{c}
 \bullet \\
 | \\
 \frac{a_1}{a_2} \\
 | \\
 \frac{a_3}{a_4} \\
 | \\
 \hline
 \end{array}
 \tag{6.57}$$

For $\frac{a_1}{a_2} = \frac{0}{0}$,

$$\begin{array}{c}
 \frac{a_1}{a_2} \\
 | \\
 \frac{a_3}{a_4} \\
 | \\
 \hline
 \end{array}
 =
 \begin{array}{c}
 \bullet \\
 | \\
 \frac{a_3}{a_4} \\
 | \\
 \hline
 \end{array}
 \stackrel{S1}{=}
 \begin{array}{c}
 \bullet \\
 | \\
 \frac{a_3}{a_4} \\
 | \\
 \hline
 \end{array}
 \stackrel{B1}{=}
 \begin{array}{c}
 \bullet \\
 | \\
 \hline
 \end{array}
 \tag{6.58}$$

For $\frac{a_1}{a_2} = \frac{1}{2}$,

$$\begin{array}{c} \begin{array}{c} \text{green} \\ \frac{a_1}{a_2} \\ \text{red} \\ \frac{a_3}{a_4} \end{array} = \begin{array}{c} \text{green} \\ \frac{1}{2} \\ \text{red} \\ \frac{a_3}{a_4} \end{array} \stackrel{K2}{=} \begin{array}{c} \text{green} \\ \frac{a_4 - a_3}{-a_3} \\ \text{red} \\ \frac{1}{2} \end{array} \stackrel{B1, S1}{=} \begin{array}{c} \text{green} \\ \frac{1}{2} \\ \text{red} \\ \frac{1}{2} \end{array} \end{array} \quad (6.59)$$

For $\frac{a_1}{a_2} = \frac{2}{1}$,

$$\begin{array}{c} \begin{array}{c} \text{green} \\ \frac{a_1}{a_2} \\ \text{red} \\ \frac{a_3}{a_4} \end{array} = \begin{array}{c} \text{green} \\ \frac{2}{1} \\ \text{red} \\ \frac{a_3}{a_4} \end{array} \stackrel{K2}{=} \begin{array}{c} \text{green} \\ \frac{-a_4}{2a_3 - a_4} \\ \text{red} \\ \frac{2}{1} \end{array} \stackrel{B1, S1}{=} \begin{array}{c} \text{green} \\ \frac{2}{1} \\ \text{red} \\ \frac{2}{1} \end{array} \end{array} \quad (6.60)$$

For $\frac{a_1}{a_2} = \frac{1}{1}$,

$$\begin{array}{c} \begin{array}{c} \text{green} \\ \frac{a_1}{a_2} \\ \text{red} \\ \frac{a_3}{a_4} \end{array} = \begin{array}{c} \text{green} \\ \frac{1}{1} \\ \text{red} \\ \frac{a_3}{a_4} \end{array} \stackrel{6.62}{=} \begin{array}{c} \text{red} \\ \frac{2}{2} \\ \text{red} \\ \frac{a_3}{a_4} \end{array} \stackrel{S1}{=} \begin{array}{c} \text{red} \\ \frac{2+a_3}{2+a_4} \\ \text{red} \\ \frac{a_3}{a_4} \end{array} \end{array} \quad (6.61)$$

where we used the property proved in [31] that

$$\begin{array}{c} \text{green} \\ \frac{1}{1} \\ \text{red} \\ \frac{a_3}{a_4} \end{array} = \begin{array}{c} \text{red} \\ \frac{2}{2} \\ \text{red} \\ \frac{a_3}{a_4} \end{array} \quad \begin{array}{c} \text{green} \\ \frac{2}{2} \\ \text{red} \\ \frac{a_3}{a_4} \end{array} = \begin{array}{c} \text{red} \\ \frac{1}{1} \\ \text{red} \\ \frac{a_3}{a_4} \end{array} \quad (6.62)$$

Now we consider $\frac{a_3}{a_4}$ in (6.61). For $\frac{a_3}{a_4} \in \{0, \frac{1}{1}, \frac{2}{2}, \frac{2}{0}, \frac{0}{2}\}$, by (6.62), we have

$$\begin{array}{c} \text{green} \\ \frac{a_1}{a_2} \\ \text{red} \\ \frac{a_3}{a_4} \end{array} \in \left\{ \begin{array}{c} \text{red} \\ \frac{1}{1} \\ \text{red} \\ \frac{a_3}{a_4} \end{array}, \begin{array}{c} \text{green} \\ \frac{2}{2} \\ \text{red} \\ \frac{a_3}{a_4} \end{array}, \begin{array}{c} \text{red} \\ \frac{2}{2} \\ \text{red} \\ \frac{a_3}{a_4} \end{array}, \begin{array}{c} \text{red} \\ \frac{1}{1} \\ \text{red} \\ \frac{a_3}{a_4} \end{array}, \begin{array}{c} \text{red} \\ \frac{2}{2} \\ \text{red} \\ \frac{a_3}{a_4} \end{array} \right\}.$$

For $\frac{a_3}{a_4} = \frac{0}{1}$, we have

$$\begin{array}{c} \begin{array}{c} \text{red} \\ \frac{2}{2} \\ \text{red} \\ \frac{a_3}{a_4} \end{array} \stackrel{S1}{=} \begin{array}{c} \text{red} \\ \frac{2+0}{2+1} \\ \text{red} \\ \frac{0}{1} \end{array} = \begin{array}{c} \text{red} \\ \frac{2}{0} \\ \text{red} \\ \frac{0}{1} \end{array} \stackrel{S1}{=} \begin{array}{c} \text{red} \\ \frac{1}{1} \\ \text{red} \\ \frac{0}{2} \end{array} \stackrel{6.62}{=} \begin{array}{c} \text{green} \\ \frac{2}{2} \\ \text{red} \\ \frac{0}{2} \end{array} \stackrel{S1}{=} \begin{array}{c} \text{green} \\ \frac{2}{2} \\ \text{red} \\ \frac{0}{2} \end{array} \stackrel{K2}{=} \begin{array}{c} \text{green} \\ \frac{1}{1} \\ \text{red} \\ \frac{0}{2} \end{array} \stackrel{B1, S1}{=} \begin{array}{c} \text{green} \\ \frac{1}{1} \\ \text{red} \\ \frac{0}{2} \end{array} \end{array} \quad (6.63)$$

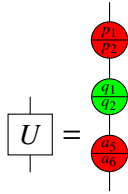
Similarly, we have

$$\begin{array}{c} \begin{array}{c} \text{red} \\ \frac{2}{2} \\ \text{red} \\ \frac{0}{1} \end{array} = \begin{array}{c} \text{red} \\ \frac{0}{2} \\ \text{red} \\ \frac{0}{1} \end{array} = \begin{array}{c} \text{green} \\ \frac{1}{0} \\ \text{red} \\ \frac{0}{1} \end{array}, \quad \begin{array}{c} \text{red} \\ \frac{2}{2} \\ \text{red} \\ \frac{2}{1} \end{array} = \begin{array}{c} \text{red} \\ \frac{1}{0} \\ \text{red} \\ \frac{2}{1} \end{array} = \begin{array}{c} \text{green} \\ \frac{2}{0} \\ \text{red} \\ \frac{2}{1} \end{array}, \quad \begin{array}{c} \text{red} \\ \frac{2}{2} \\ \text{red} \\ \frac{0}{2} \end{array} = \begin{array}{c} \text{red} \\ \frac{0}{1} \\ \text{red} \\ \frac{0}{2} \end{array} = \begin{array}{c} \text{green} \\ \frac{0}{2} \\ \text{red} \\ \frac{0}{2} \end{array}. \end{array} \quad (6.64)$$

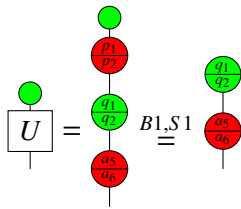
In the same way, for $\frac{a_1}{a_2} \in \{0, \frac{1}{1}, \frac{2}{2}, \frac{2}{0}, \frac{0}{2}\}$, and $\frac{a_3}{a_4} \in \mathcal{A}$, we can prove that

$$\begin{array}{c} \text{green} \\ \frac{a_1}{a_2} \\ \text{red} \\ \frac{a_3}{a_4} \end{array} \in \left\{ \begin{array}{c} \text{green} \\ \frac{1}{2} \\ \text{green} \\ \frac{2}{1} \\ \text{green} \\ \frac{1}{1} \\ \text{green} \\ \frac{2}{2} \\ \text{green} \\ \frac{0}{1} \\ \text{green} \\ \frac{1}{0} \\ \text{green} \\ \frac{0}{2} \\ \text{red} \\ \frac{1}{1} \\ \text{red} \\ \frac{2}{1} \end{array} \right\}.$$

If

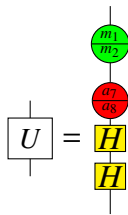


then

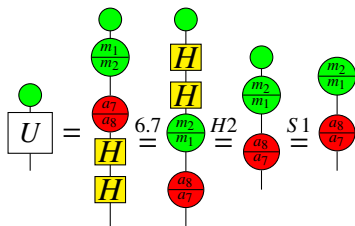


which is reduced to the case (6.57).

If



then



which is also reduced to the case (6.57).

□

Definition 6.3.10 [5] A vertex in a GS-LC diagram that is being acted upon by some operation is called a *operand vertex*.

Definition 6.3.11 [5] A neighbour of an operand vertex in a GS-LC diagram is called a *swapping partner of the operand vertex*.

Lemma 6.3.12 *If in some GS-LC diagram an operand vertex has at least one neighbour, it is always possible to change the vertex operator on the operand vertex to the following form using 1-local (2-local) complementations:*

$$\begin{array}{c} \textcircled{m_3} \\ \textcircled{m_4} \\ \textcircled{m_1} \\ \textcircled{m_2} \end{array} \quad (6.65)$$

where $\frac{m_1}{m_2}, \frac{m_3}{m_4} \in \mathcal{M}$.

Proof: We can pick one neighbour of the operand vertex as the swapping partner. A 1-local complementation about the operand vertex adds $\textcircled{+}$ to its vertex operator, while a 1-local complementation about the swapping partner adds $\textcircled{-}$ to the vertex operator on the operand vertex. Note that local complementations about the operand vertex or its swapping partner do not remove the edge between these two vertices. Therefore, after each local complementation, the operand vertex still has a neighbour, enabling further local complementations. By Theorem 6.2.12, the vertex operator U must be in one of the form (6.36), (6.37) or (6.38). For

$$\boxed{U} = \begin{array}{c} \textcircled{a_1} \\ \textcircled{a_2} \\ \textcircled{a_3} \\ \textcircled{a_4} \end{array} \quad (6.66)$$

if $\frac{a_1}{a_2} \in \mathcal{Q}$, and $\frac{a_3}{a_4} \in \mathcal{Q}$, similar to the trick used in the proof of Lemma 6.2.10, we have $\frac{a_1}{a_2} = \frac{p_1}{p_2} + \frac{m_1}{m_2}, \frac{a_3}{a_4} = \frac{p_3}{p_4} + \frac{m_3}{m_4}$, where $\frac{p_1}{p_2}, \frac{p_3}{p_4} \in \mathcal{P}, \frac{m_1}{m_2}, \frac{m_3}{m_4} \in \mathcal{M}$. Therefore,

$$\begin{array}{c} \textcircled{p_1} \\ \textcircled{p_2} \\ \textcircled{a_1} \\ \textcircled{a_2} \\ \textcircled{a_3} \\ \textcircled{a_4} \end{array} = \begin{array}{c} \textcircled{p_1} \\ \textcircled{p_2} \\ \textcircled{m_3} \\ \textcircled{m_4} \\ \textcircled{m_1} \\ \textcircled{m_2} \end{array} \quad (6.67)$$

where $\frac{\tilde{m}_3}{\tilde{m}_4} \in \mathcal{M}$. Applying the 1-local complementation about the operand vertex or its swapping partner, the nodes $\frac{p_1}{p_2}, \frac{p_3}{p_4}$ can be removed, and the remaining part is of the form (6.65). The case for $\frac{a_1}{a_2} \in \mathcal{Q}, \frac{a_3}{a_4} \in \mathcal{M}$ or $\frac{a_1}{a_2} \in \mathcal{M}, \frac{a_3}{a_4} \in \mathcal{Q}$ is similar as above, yet simpler.

For

$$\boxed{U} = \begin{array}{c} \textcircled{p_1} \\ \textcircled{p_2} \\ \textcircled{a_1} \\ \textcircled{a_2} \\ \textcircled{a_3} \\ \textcircled{a_4} \end{array} \quad (6.68)$$

the node $\frac{p_1}{p_2}$ can be removed by the 1-local complementation about the operand vertex or its swapping partner, then we are in the case of (6.66).

For

$$\begin{array}{c}
 \begin{array}{|c} \hline U \\ \hline \end{array} = \begin{array}{c} \textcircled{\frac{m_1}{m_2}} \\ \textcircled{\frac{a_1}{a_s}} \\ \boxed{H} \\ \boxed{H} \end{array}
 \end{array} \tag{6.69}$$

the two Hadamard nodes can be pushed up to the top and removed by the 1-local complementation about the operand vertex or its swapping partner, then we are in the case of (6.66).

The proof is similar for 2-local complementations. □

Lemma 6.3.13 Applying $\textcircled{\bullet}$ to a GS-LC diagram results in a GS-LC diagram or a zero diagram.

Proof: There are two cases for the operand vertex when applying $\textcircled{\bullet}$ to a GS-LC diagram.

Firstly, if the operand vertex has no neighbours, then by lemma 6.3.14, it is just one of the 12 single qutrit pure stabilizer states. If the operand vertex is in state $\textcircled{\frac{1}{2}}$ or $\textcircled{\frac{2}{1}}$, the result of applying $\textcircled{\bullet}$ is the scalar zero. Otherwise the result is a non-zero global factor, which can be ignored.


Secondly, we consider the case that the operand vertex has at least one neighbour. Note that we have the following property:

$$\begin{array}{c}
 \begin{array}{c} \dots \\ \boxed{H^{a_1}} \end{array} \dots \begin{array}{c} \dots \\ \boxed{H^{a_s}} \end{array} \\
 \begin{array}{c} \textcircled{\frac{a}{b}} \\ \textcircled{\frac{a_1}{a_s}} \\ \textcircled{\frac{m_1}{m_2}} \end{array} \stackrel{S1}{=} \begin{array}{c} \dots \\ \boxed{H^{a_1}} \end{array} \dots \begin{array}{c} \dots \\ \boxed{H^{a_s}} \end{array} \\
 \begin{array}{c} \textcircled{\frac{a}{b}} \\ \textcircled{\frac{a_1}{a_s}} \\ \textcircled{\frac{m_1}{m_2}} \end{array} \stackrel{K1}{=} \begin{array}{c} \dots \\ \boxed{H^{a_1}} \end{array} \dots \begin{array}{c} \dots \\ \boxed{H^{a_s}} \end{array} \\
 \begin{array}{c} \textcircled{\frac{a}{b}} \\ \textcircled{\frac{a_1}{a_s}} \\ \textcircled{\frac{m_1}{m_2}} \end{array} \stackrel{B1, K1}{=} \begin{array}{c} \dots \\ \boxed{H^{a_1}} \end{array} \dots \begin{array}{c} \dots \\ \boxed{H^{a_s}} \end{array} \\
 \begin{array}{c} \dots \\ \boxed{H^2} \end{array} \dots \begin{array}{c} \dots \\ \textcircled{\frac{m_1}{m_2}} \end{array} \dots \begin{array}{c} \dots \\ \textcircled{\frac{m_1}{m_2}} \end{array}
 \end{array} \tag{6.70}$$

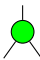
where $a_i \in \{1, -1\}$, $i = 1, \dots, s$, $\frac{a}{b} \in \mathcal{A}$, $\frac{m_1}{m_2} \in \mathcal{M}$, $\frac{m_{i1}}{m_{i2}} \in \{\frac{m_1}{m_2}, \frac{m_2}{m_1}\}$, $i = 1, \dots, s$.

Therefore, if the vertex operator of the operand vertex is

$$\begin{array}{c}
 \textcircled{\frac{a}{b}} \\
 \textcircled{\frac{m_1}{m_2}} \\
 \boxed{H^{\pm 1}}
 \end{array} \tag{6.71}$$

then the operand vertex will be removed from the graph state when the operator  is applied.

Otherwise, we can pick one neighbour of the operand vertex as the swapping partner. By Lemma 6.3.12, it is always possible to change the vertex operator on the operand vertex to the form of (6.71) using 1-local complementations. Then we get back to the above case. This completes the proof. \square

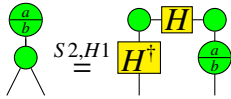
Lemma 6.3.14 Applying  to an GS-LC diagram will still result in a GS-LC diagram.

Proof: There are two cases for the operand vertex.

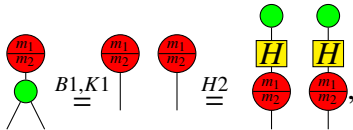
First, if the operand vertex has no neighbours, then by lemma 6.3.14, it is just one of the 12 single qutrit pure stabilizer states which can be written as



where $\frac{a}{b} \in \mathcal{A}$, $\frac{m_1}{m_2} \in \mathcal{M}$. Then



and

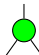


where the right hand side of each equation is clearly a GS-LC diagram.

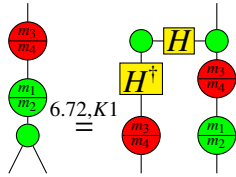
Second, if the operand vertex has at least one neighbour, we can write the green copy as



Thus if there is no vertex operator on the operand vertex, then we just add a new vertex and edge to the diagram.

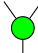
Otherwise, by Lemma 6.3.12, the vertex operator U on the operand vertex can be changed to the form (6.65) using 1-local complementations. Now applying  to the

operand vertex, we have




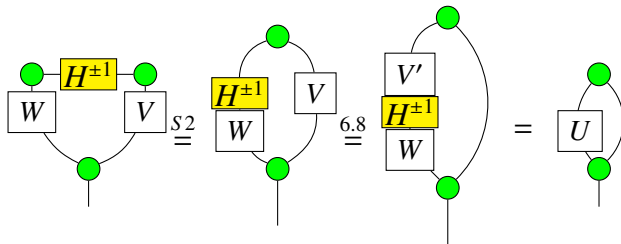
which still means we just add a new vertex and edge to the graph. This completes the proof.

□

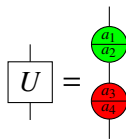
Lemma 6.3.15 Applying  to an GS-LC diagram will result in a GS-LC diagram or a zero diagram.

Proof: Now there are two operand vertices, and we have four cases to deal with.

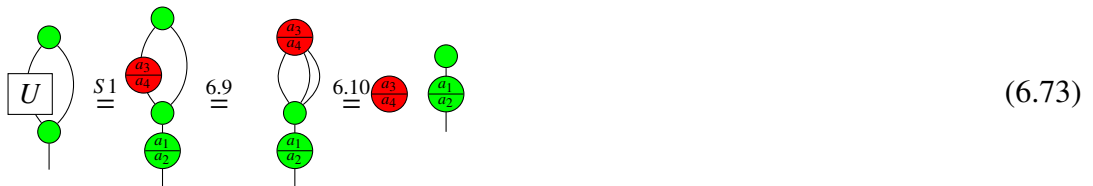
Firstly, if the two operand vertices are connected only to each other, then we do not need to care about all non-operand vertices. Now applying  to the operand vertices, we have



where $W, V, V' \in C_1$, $U = W \circ H^{\pm 1} \circ V' \in C_1$. By Theorem 6.2.12, U must be in one of the form (6.36), (6.37) or (6.38). For

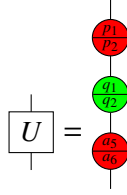


we have

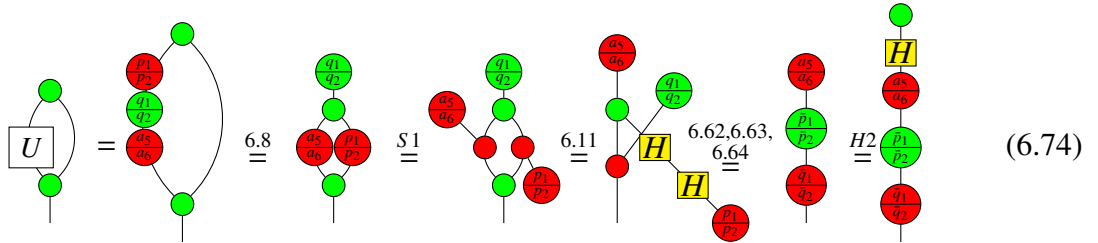


The result is either a zero diagram or a GS-LC diagram.

For

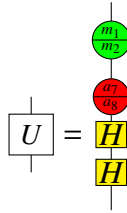


we have

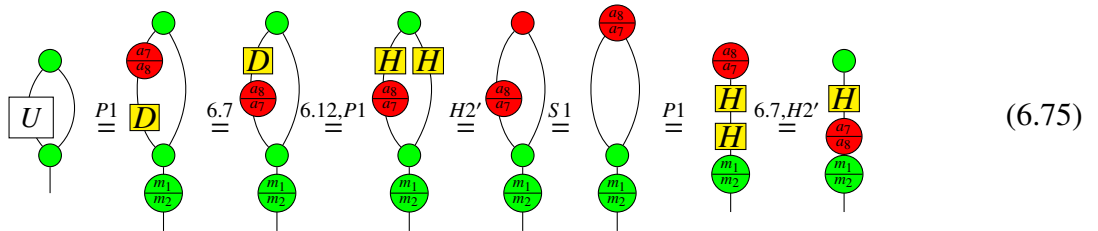


The result is a GS-LC diagram, where we used property (6.8) for the second equality, property (6.11) for the fourth equality, and (6.62), (6.63) and (6.64) for the fifth equality.

For

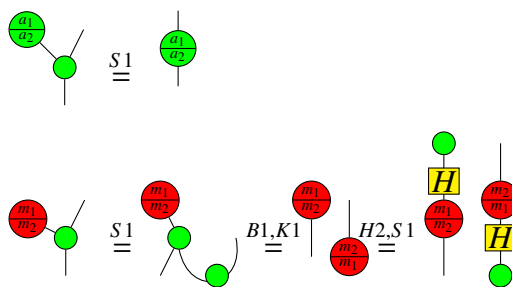


we have



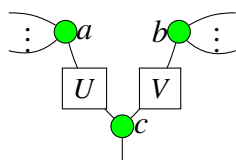
The result is a GS-LC diagram. This complete the first case.

Secondly, if one operand vertex has no neighbours, then it must be one of the 12 single qutrit states given in (6.56). For $\frac{a_1}{a_2} \in \mathcal{A}$ and $\frac{m_1}{m_2} \in \mathcal{M}$,

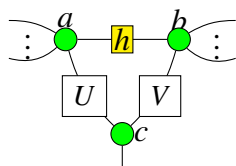


Thus we are back into the application situation of lemma 6.3.8 and lemma 6.3.13, which means the resulting diagram is still a GS-LC diagram.

Thirdly, if both operand vertices have non-operand neighbours, denoted by a and b respectively, then by applying ⊗ to a and b , we have

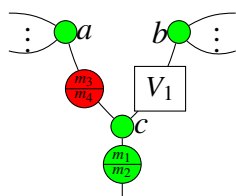


or

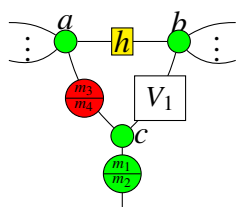


where $U, V \in C_1$. From now on, we will always denote by h the node H or H^\dagger when it is unnecessary to state explicitly.

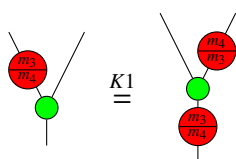
By lemma 6.3.12, applying local complementations to a and its swapping partner, the vertex operator U can be changed to the form (6.65). So we have



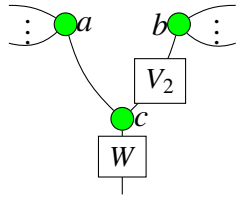
or



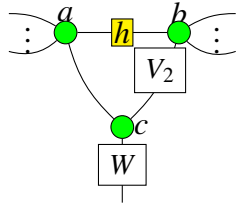
where $V_1 \in C_1$. Note that



Therefore we have

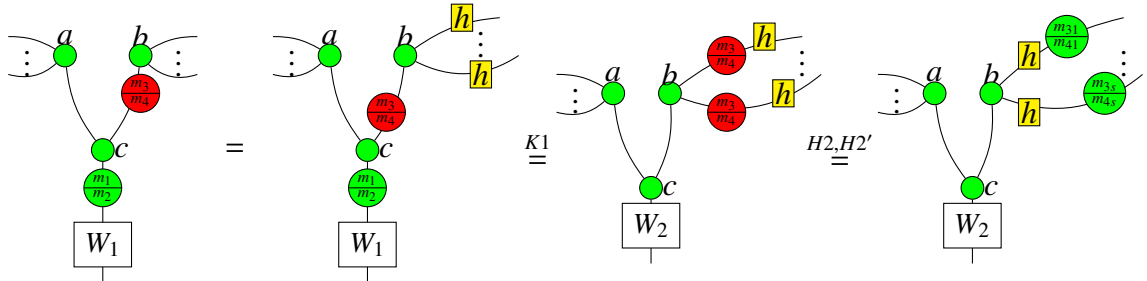


or

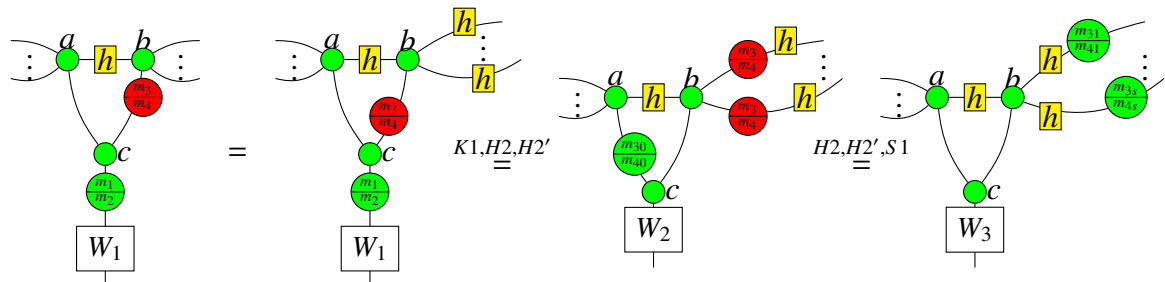


(6.76)

where $W, V_2 \in C_1$. In the same way as we just did for a , we can repeat the procedure for b by choosing its own swapping partner. Note that we will get extra phases of the form $\begin{matrix} \bullet \\ \oplus \\ \bullet \end{matrix}$ or $\begin{matrix} \oplus \\ \bullet \end{matrix}$ added to a 's vertex operator thus merging into the operator W to be W_1 , in the case that a is connected to b or to b 's swapping partner. Now we have



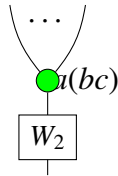
or



where $W_1, W_2, W_3 \in C_1$, $\frac{m_3}{m_4}, \frac{m_{30}}{m_{40}}, \frac{m_{31}}{m_{41}}, \dots, \frac{m_{3s}}{m_{4s}} \in \mathcal{M}$. Note that these green nodes $\frac{m_{31}}{m_{41}}, \dots, \frac{m_{3s}}{m_{4s}}$ can be merged with the vertex operators of b 's neighbours by the spider rule.

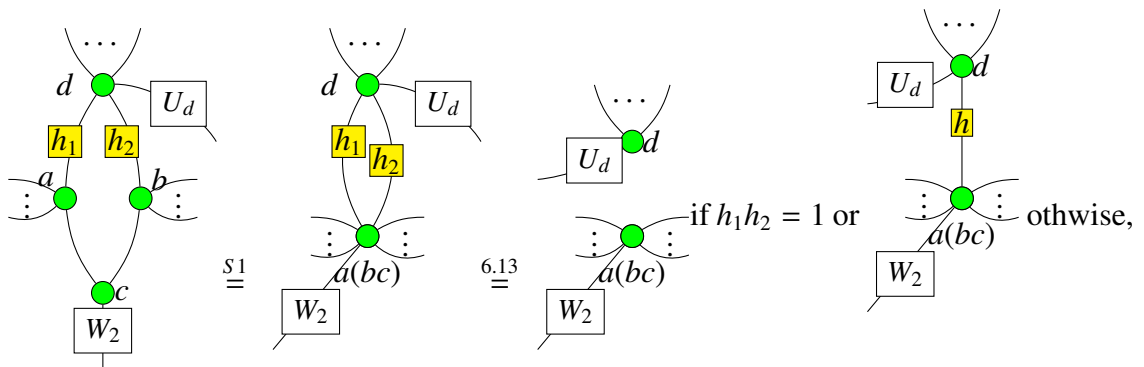
Furthermore, we can merge the nodes a, b and c to get a GS-LC diagram. In fact, there are three cases.

1) Neither a and b are connected by a Hadamard node nor they have common non-operand neighbours. In this case a , b and c can be directly merged, thus we have



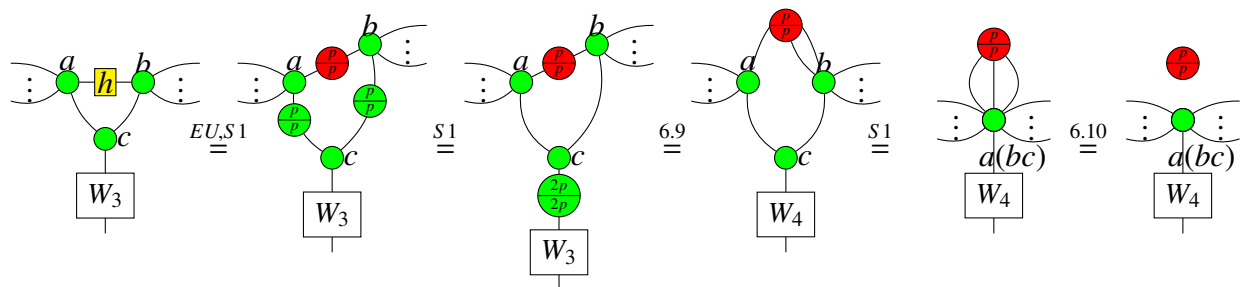
which is a GS-LC diagram.

2) a and b are not connected but they have common non-operand neighbours. For any common non-operand neighbour d we have



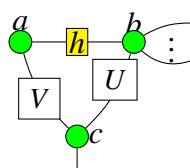
where in either sub-case we get a GS-LC diagram.

3) a and b are connected. Then we have

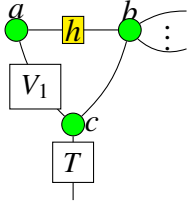


where $W_4 \in C_1$, $\frac{p}{p} = \frac{1}{1}$ or $\frac{2}{2}$, and we used the rule (EU), property (6.9) and property (6.10). Clearly the result is a GS-LC diagram.

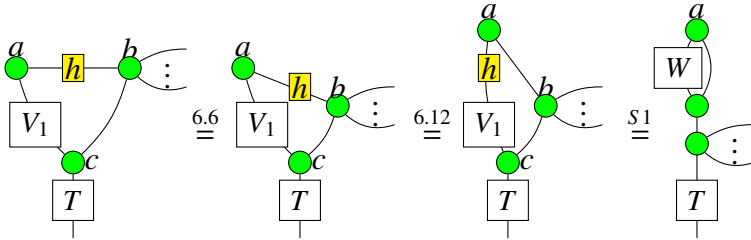
Finally, if one operand vertex is connected only to the other, but the latter has a non-operand neighbour, then we have



where $V, U \in C_1$. We can use the same strategy as we have applied for (6.76) in the third case to cancel out the vertex operator U of the second operand vertex b . Therefore we have



where $V_1, T \in C_1$. If in this process the operand vertex a gains one or more non-operand neighbours, then we can proceed as above. Otherwise,



where $W = V_1 \circ h \in C_1$. By equalities (6.73), (6.74) and (6.75), and lemma 6.3.14, $K = \text{\textcircled{W}}$ is either a zero diagram or a stabilizer state of the form (6.56). If K is a stabilizer state represented by a green node in (6.56), then the green phase operator is added to the operator T by the spider rule (S1), thus we get a GS-LC diagram. Otherwise, by the copy rule (B1) and the rule (K1), K can be copied, and it is easy to see that we still get a GS-LC diagram. This completes the proof. \square

6.3.3 Reduced GS-LC diagrams

Further to GS-LC diagrams, we can define a more reduced form as in [5].

Definition 6.3.16 *A stabilizer state diagram is called to be in a reduced GS-LC (or rGS-LC) form if it is a GS-LC diagram satisfying the following conditions:*

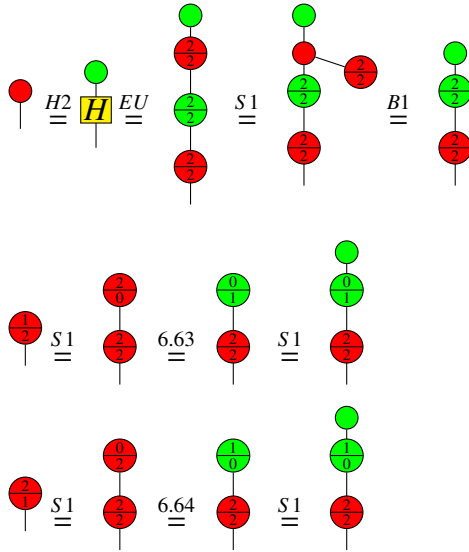
- All vertex operators belong to the set

$$\mathcal{R} = \left\{ \begin{array}{c} \left| \begin{array}{cccccccccccccccc} \textcircled{1/2} & \textcircled{2/1} & \textcircled{0/1} & \textcircled{2/2} & \textcircled{0/1} & \textcircled{1/0} & \textcircled{0/2} & \textcircled{2/0} & \textcircled{2/3} & \textcircled{0/1} & \textcircled{0/0} & \textcircled{1/1} & \textcircled{1/2} & \textcircled{2/0} \\ \textcircled{1/2} & \textcircled{2/1} & \textcircled{0/1} & \textcircled{2/2} & \textcircled{0/1} & \textcircled{1/0} & \textcircled{0/2} & \textcircled{2/0} & \textcircled{2/3} & \textcircled{0/1} & \textcircled{0/0} & \textcircled{1/1} & \textcircled{1/2} & \textcircled{2/0} \end{array} \right. \end{array} \right\}. \quad (6.77)$$

- Two adjacent vertices must not both have vertex operators including red nodes.

Theorem 6.3.17 *In the qutrit ZX-calculus, each qutrit stabilizer state diagram can be rewritten into some rGS-LC diagram.*

Proof: By theorem 6.3.6, any stabilizer state diagram can be rewrite into a GS-LC diagram. If a vertex in the GS-LC diagram has no neighbours, by Lemma 6.3.14, it can be brought into one of the forms in (6.56), where the nine green nodes can be clearly seen as having vertex operators belong to the set \mathcal{R} . For the other three red nodes, note that



Therefore, the vertex operators on these three red nodes can be brought into elements of \mathcal{R} .

From now on, we can assume that each vertex in the GS-LC diagram has at least one neighbour. Our strategy is to prove the theorem in three steps: First we prove that each vertex operator in the GS-LC diagram can be brought into the following form:

$$\mathcal{R}' = \left\{ \left| \begin{array}{cccccccccccc} \frac{1}{2} & \frac{2}{1} & \frac{1}{1} & \frac{2}{2} & \frac{0}{1} & \frac{1}{0} & \frac{0}{2} & \frac{2}{0} & \frac{q_1}{q_2} & \frac{p_1}{p_2} \\ \hline \text{Green} & \text{Green} & \text{Green} & \text{Green} & \text{Green} & \text{Green} & \text{Green} & \text{Green} & \text{Green} & \text{Red} \end{array} \right. \right\}. \quad (6.78)$$

where $\frac{q_1}{q_2} \in \mathcal{Q}$, $\frac{p_1}{p_2} \in \mathcal{P}$. Then we show that any GS-LC diagram with vertex operators all belonging to \mathcal{R}' can be further brought into a form where any two adjacent vertices must not both have vertex operators including red nodes while the vertex operators still resides in \mathcal{R}' . Finally we prove that the GS-LC diagram obtained in the second step can be rewritten into a rGS-LC diagram.

For the first step of the strategy, we pick an arbitrary node v that has at least one neighbour. By theorem 6.2.12, the vertex operator U of the vertex v has the form (6.36), (6.37) or (6.38). We deal with these three forms separately.

Firstly consider that U has the form (6.36):

$$\begin{array}{c} \boxed{U} \\ \hline \end{array} = \begin{array}{c} \textcircled{a_1} \\ \textcircled{a_2} \\ \textcircled{a_3} \\ \textcircled{a_4} \end{array}, \quad (6.79)$$

We analyse all possible cases of the phase $\frac{a_3}{a_4}$.

If $\frac{a_3}{a_4} \in \mathcal{M}$, then either $\frac{a_3}{a_4} = \frac{0}{0}$, where clearly $U \in \mathcal{R}'$, or $\frac{a_3}{a_4} \in \{\frac{1}{2}, \frac{2}{1}\}$. In the latter case, by the commutation rule (K2), the copy rule (K1) and the colour change rules (H2) and (H2'), the red node $\frac{a_3}{a_4}$ can be pushed up through the node $\frac{a_1}{a_2}$, copied by v into connected edges with its neighbours, then colour-changed from red to green by Hadamard nodes and finally merged into the vertex operators of neighbours of v . Therefore the vertex operator U now is just a green node, thus belongs to the set \mathcal{R}' .

If $\frac{a_3}{a_4} \in \mathcal{N} = \{\frac{1}{0}, \frac{0}{1}, \frac{2}{0}, \frac{0}{2}\}$, then $\frac{a_3}{a_4} = \frac{p_1}{p_2} + \frac{m_1}{m_2}$, where $\frac{p_1}{p_2} \in \mathcal{P}$, $\frac{m_1}{m_2} \in \{\frac{1}{2}, \frac{2}{1}\}$. Thus by the commutation rule (K2),

$$\begin{array}{c} \boxed{U} \\ \hline \end{array} = \begin{array}{c} \textcircled{m_1} \\ \textcircled{m_2} \\ \textcircled{a_1} \\ \textcircled{a_2} \\ \textcircled{p_1} \\ \textcircled{p_2} \end{array}.$$

In a similar way as above, the node $\frac{m_1}{m_2}$ can be merged into the vertex operators of neighbours of v . Now U has the form

$$\begin{array}{c} \textcircled{a_1} \\ \textcircled{a_2} \\ \textcircled{p_1} \\ \textcircled{p_2} \end{array}, \quad (6.80)$$

We need to consider all the possible cases of $\frac{\bar{a}_1}{\bar{a}_2}$ now. If $\frac{\bar{a}_1}{\bar{a}_2} = \frac{0}{0}$, then applying 1-local complementations to v , the red node $\frac{p_1}{p_2}$ can be removed, so U is changed to the identity, which belongs to set \mathcal{R}' . If $\frac{\bar{a}_1}{\bar{a}_2} \in \{\frac{1}{2}, \frac{2}{1}\}$, then

$$\begin{array}{c} \boxed{U} \\ \hline \end{array} = \begin{array}{c} \textcircled{a_1} \\ \textcircled{a_2} \\ \textcircled{p_1} \\ \textcircled{p_2} \end{array} \stackrel{K2}{=} \begin{array}{c} \textcircled{a_1} \\ \textcircled{a_2} \\ \textcircled{p_1} \\ \textcircled{p_2} \end{array} \stackrel{S1}{=} \begin{array}{c} \textcircled{m_1} \\ \textcircled{m_2} \\ \textcircled{p_1} \\ \textcircled{p_2} \\ \textcircled{a_1} \\ \textcircled{a_2} \end{array}$$

where $\frac{n_1}{n_2} \in \mathcal{N}$, $\frac{\bar{m}_1}{\bar{m}_2} \in \{\frac{1}{2}, \frac{2}{1}\}$, $\frac{\bar{p}_1}{\bar{p}_2} \in \mathcal{P}$. As we did above, the red node $\frac{\bar{m}_1}{\bar{m}_2}$ merged into the vertex operators of neighbours of v , and the red node $\frac{\bar{p}_1}{\bar{p}_2}$ can be removed by applying 1-local complementations to v . So U is changed to be just the green node $\frac{\bar{a}_1}{\bar{a}_2}$, which clearly

belongs to the set \mathcal{R}' . To sum up, for $\frac{\bar{a}_1}{\bar{a}_2} \in \mathcal{M}$ in the case of (6.80), the vertex operator U can be changed to have no red nodes. For the remaining case where $\frac{\bar{a}_1}{\bar{a}_2} \in \mathcal{Q}$, it is clear that the vertex operator U in form (6.80) now belongs to the set \mathcal{R}' .

Therefore, for $\frac{a_3}{a_4} \in \mathcal{N}$ in the form of (6.79), the vertex operator U can be brought into a form of \mathcal{R}' .

Now the remaining case of $\frac{a_3}{a_4}$ in the form of (6.79) is that $\frac{a_3}{a_4} \in \mathcal{P}$, this case is exactly the same as (6.80), which has already been proved. Therefore, for

$$U = \begin{array}{c} \text{green } \frac{a_1}{a_2} \\ \text{red } \frac{a_3}{a_4} \end{array}$$

U can always be brought into the form of \mathcal{R}' .

Secondly we consider that U has the form (6.37):

$$U = \begin{array}{c} \text{red } \frac{p_1}{p_2} \\ \text{green } \frac{a_1}{a_2} \\ \text{red } \frac{a_3}{a_4} \end{array}$$

We first apply 1-local complementations to v , then the red node $\frac{p_1}{p_2}$ is removed, thus we are back to the case (6.79), which has already been proved.

Thirdly we consider that U has the form (6.38):

$$U = \begin{array}{c} \text{green } \frac{m_1}{m_2} \\ \text{red } \frac{a_1}{a_2} \\ \text{H} \\ \text{H} \end{array}$$

Here we can push the two Hadamard nodes up by property (6.7), then apply the graphical transformation $\circ_2 v$, the two Hadamard nodes can be removed by theorem 6.3.5 and property (6.7). Therefore we get back to the case (6.79), which has already been proved.

So far we are done with the chosen node v in the first step of the proof strategy. To proceed to deal with other nodes than v in the GS-LC diagram, we need to consider the impact on v 's neighbours whose vertex operators belong to the set \mathcal{R}' during the above operations on v . First note that in the above process of proof, there is not any red node added to any neighbour of v , only a green node $\frac{p_1}{p_2}$ or $\frac{m_1}{m_2}$ is possibly added to v 's neighbours, where $\frac{p_1}{p_2} \in \mathcal{P}$, $\frac{m_1}{m_2} \in \{\frac{1}{2}, \frac{2}{1}\}$. If it is the green node $\frac{m_1}{m_2}$ that is added to v 's neighbours, then their vertex operators still belong to the set \mathcal{R}' . If the green node $\frac{p_1}{p_2}$ is added to v 's neighbours,

then the resulted vertex operator that beyond the set \mathcal{R}' must be the sub-case of (6.80) where $\frac{\bar{a}_1}{\bar{a}_2} \in \mathcal{M}$, which we have shown that the red node can be removed. Therefore, each time when we have brought a vertex operator in to an element of \mathcal{R}' , we need to check whether the vertex operators of neighbours of the operand vertex are still belong to \mathcal{R}' . If not, then the red node will be removed. Since each vertex operator needs to be considered at most twice, the process will eventually terminate. Therefore all vertex operators must belong to the set \mathcal{R}' after finite steps.

By now we have finished the first step of the proof strategy: we have proved that any stabilizer state diagram is equal to some GS-LC diagram such that all vertex operators belong to the set \mathcal{R}' .

For the second step of the strategy, we are going to prove that each GS-LC diagram with vertex operators all belonging to \mathcal{R}' can be further brought into a form where any two adjacent vertices must not both have vertex operators including red nodes, with all vertex operators being still in \mathcal{R}' .

Suppose there are two adjacent qutrits a and b which have red nodes in their vertex operators, i.e. there is a subdiagram of the form

$$(6.81)$$

where $\frac{p_1}{p_2}, \frac{p_3}{p_4} \in \mathcal{P}, \frac{q_1}{q_2}, \frac{q_3}{q_4} \in \mathcal{Q}$. We operate on the vertex b to remove the red node from its vertex operator. Firstly,

$$(6.82)$$

where $\frac{m_1}{m_2} \in \mathcal{M}$ and we used local complementations about a to remove the green node $\frac{p_5}{p_6}$ on the output of b for the second equality. Below we analyse all possible values of $\frac{m_1}{m_2}$ in (6.82).

If $\frac{m_1}{m_2} = \frac{0}{0}$, then we can apply local complementations about b to remove the red node

$\frac{p_3}{p_4}$, and we have

$$(6.83)$$

Now we proceed on simplifying the vertex operator of a :

$$(6.84)$$

where $\frac{p_j}{p_i} \in \mathcal{P}$, $\frac{m_3}{m_4}, \frac{m_5}{m_6} \in \{\frac{1}{2}, \frac{2}{1}\}$ or $\frac{m_3}{m_4} = \frac{m_5}{m_6} = \frac{0}{0}$. By lemma 6.2.9, the first three nodes on the top of the output of a can be rewritten in one of two forms. If we use the rewritten form with two Hadamard nodes, then we have

$$(6.85)$$

where we apply the graphical transformation $\circ_2 a$ and local complementations about a for the second equality, perform local complementations about a for the third equality, and make a copy of red node $\frac{m_5}{m_6}$ through a for the fourth equality. Obviously we get a desired

form at the end of (6.85). Otherwise we use the rewritten form without Hadamard node, then

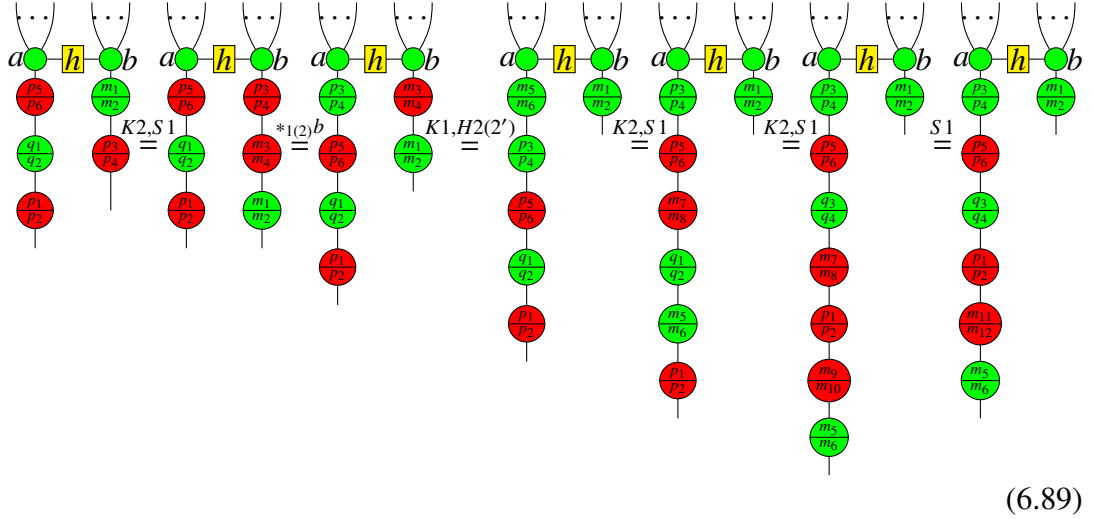
where $\frac{\bar{p}_5}{\bar{p}_6} \in \mathcal{P}$, $\frac{p_7}{p_8} + \frac{p_1}{p_2} = \frac{p_9}{p_{10}} \in \{0, \frac{1}{2}, 1\}$, and we apply local complementations about a for the second equality. Here we need to consider all the possible values of $\frac{p_9}{p_{10}}$ in (6.86). If $\frac{p_9}{p_{10}} = 0$, then

where $\frac{\bar{p}_5}{\bar{p}_6} + \frac{m_3}{m_4} = \frac{q_5}{q_6} \in \mathcal{Q}$, $\frac{q_7}{q_8} \in \mathcal{Q}$, $\frac{\bar{m}_5}{\bar{m}_6} \in \mathcal{M}$, and we make a copy of red node $\frac{m_5}{m_6}$ through a for the third equality. Otherwise $\frac{p_9}{p_{10}} \in \mathcal{P}$ in (6.86), then

where $\frac{q_9}{q_{10}} \in \mathcal{Q}$, $\frac{q_9}{q_{10}} + \frac{m_3}{m_4} = \frac{q_{11}}{q_{12}} \in \mathcal{Q}$, $\frac{q_{13}}{q_{14}} \in \mathcal{Q}$, $\frac{\bar{m}_5}{\bar{m}_6}, \frac{m_7}{m_8}, \frac{\bar{m}_7}{\bar{m}_8} \in \mathcal{M}$, and we make copies of red nodes $\frac{m_5}{m_6}$ and $\frac{m_7}{m_8}$ through a for the third equality and the sixth equality respectively.

By now, for $\frac{m_1}{m_2} = \frac{0}{0}$, we have proved that the resulting diagram in (6.82) can be brought into a form that at least one qutrit of a and b has no red nodes in its vertex operator while both a and b have vertex operators belonging to \mathcal{R}' .

The remaining case is that $\frac{m_1}{m_2} \in \{\frac{1}{2}, \frac{2}{1}\}$ in (6.82). In this case,



(6.89)

where $\frac{m_3}{m_4}, \frac{m_5}{m_6}, \frac{m_7}{m_8}, \frac{m_9}{m_{10}} \in \{\frac{1}{2}, \frac{2}{1}\}$, $\frac{m_7}{m_8} + \frac{m_9}{m_{10}} = \frac{m_{11}}{m_{12}} \in \mathcal{M}$, $\frac{q_3}{q_4} \in \mathcal{Q}$.

In the resulting diagram at the end of (6.89), the first four nodes on the top of the output of a are of the same type as the corresponding part of (6.83). So we can use the obtained results of (6.83), push the red node $\frac{m_{11}}{m_{12}}$ through green nodes and make it copied and added to vertex operators of a 's neighbours in green colour by the commutation rule (K2) and colour-change rules (H2) and (H2'). In this way, for $\frac{m_1}{m_2} \in \{\frac{1}{2}, \frac{2}{1}\}$ in (6.82), the resulting diagram can be brought into a form that at least one qutrit of a and b has no red nodes in its vertex operator, while both a and b have vertex operators belonging to \mathcal{R}' .

Therefore, the diagram (6.81) can always be brought into a form such that at least one qutrit of a and b has no red nodes in its vertex operator, while both a and b have vertex operators belonging to \mathcal{R}' . This finishes the second step of the proof strategy.

The third step of the proof strategy is to show that the vertex operators not only belong to \mathcal{R}' , but further resides in \mathcal{R} . To do this, it suffices to prove that the red node in the following diagram can be removed:



(6.90)

where the vertex operator of a belongs to the set

$$\mathcal{T} = \left\{ \begin{array}{cccccc} \textcircled{1} & \textcircled{0} & \textcircled{2} & \textcircled{2} & \textcircled{0} & \textcircled{1} \\ \textcircled{2} & \textcircled{2} & \textcircled{2} & \textcircled{1} & \textcircled{1} & \textcircled{1} \\ \textcircled{3} & \textcircled{2} & \textcircled{2} & \textcircled{1} & \textcircled{1} & \textcircled{1} \end{array} \right\}. \quad (6.91)$$

For the sake of conciseness, we just show one case, the others are similar:

$$\begin{array}{ccccccc} \textcircled{a} & \textcircled{h} & \textcircled{b} & & \textcircled{a} & \textcircled{h} & \textcircled{b} & & \textcircled{a} & \textcircled{h} & \textcircled{b} & & \textcircled{a} & \textcircled{h'} & \textcircled{b} \\ \textcircled{\frac{2}{3}} & & \textcircled{\frac{q_1}{q_2}} & & \textcircled{\frac{2}{3}} & & \textcircled{\frac{q_1}{q_2}} & & \textcircled{H} & & \textcircled{\frac{2}{3}} & & \textcircled{\frac{1}{1}} & & \textcircled{\frac{q_1}{q_2}} \\ \textcircled{\frac{1}{1}} & & \textcircled{\frac{1}{1}} & & \textcircled{\frac{1}{1}} & & \textcircled{\frac{1}{1}} & & \textcircled{\frac{1}{1}} & & \textcircled{\frac{1}{1}} & & \textcircled{\frac{1}{1}} & & \textcircled{\frac{q_1}{q_2}} \end{array} \quad (6.92)$$

where we apply 1-local complementations about a for the first equality, use equality (6.25) for the second equality, and apply the graphical transformation \circ_{2a} for the third equality.

Each time when we have brought a diagram of form (6.81) into a diagram that satisfies the conditions of rGS-LC diagram for the two connected nodes, we need to check whether the vertex operators of neighbours of the operand vertex are still belong to \mathcal{R} . If not, then the red node will be removed. Since the number of vertex operator beyond \mathcal{R} in such a diagram is always decreasing, all vertex operators must belong to the set \mathcal{R} after finite steps. Therefore, any GS-LC diagram is equal to some rGS-LC diagram within the ZX-calculus. \square

6.3.4 Transformations of rGS-LC diagrams

In this subsection we show how to transform one rGS-LC diagrams into another rGS-LC diagrams. Note that we call the graphical transformation \circ_{2v} a doubling-neighbour-edge transformation.

Lemma 6.3.18 *Suppose there is a rGS-LC diagram which has a pair of neighbouring qutrits a and b as follows:*

$$\begin{array}{ccc} \textcircled{a} & \textcircled{h} & \textcircled{b} \\ \textcircled{\frac{q_1}{q_2}} & & \textcircled{\frac{q_1}{q_2}} \\ \textcircled{\frac{p_1}{p_1}} & & \textcircled{\frac{1}{1}} \end{array} = \begin{array}{ccc} \textcircled{a} & \textcircled{h} & \textcircled{b} \\ \textcircled{\frac{m_1}{m_2}} & & \textcircled{\frac{q_1}{q_2}} \\ \textcircled{\frac{p_1}{p_1}} & & \textcircled{\frac{p_1}{p_1}} \end{array} \quad (6.93)$$

where $\frac{q_1}{q_2} \in \mathcal{A}$, $\frac{p_1}{p_1} \in \mathcal{P}$, $\frac{m_1}{m_2} \in \mathcal{M}$, $\frac{q_1}{q_2} = \frac{p_1}{p_1} + \frac{m_1}{m_2}$, h stands for either an H node or an H^\dagger node. Then a rGS-LC diagram with the following pair can be obtained by performing firstly a p_1 -local complementation about b , followed by a $(-p_1)$ -local complementation about a , and

possibly a further $(-p_1)$ -local complementation about b , in addition with some doubling-neighbour-edge operations $\circ_2 a(b)$ and copying operations on red nodes with phase angles in \mathcal{M} :

$$(6.94)$$

where $\frac{a_1}{a_2} \in \mathcal{A}$, $\frac{p_1}{p_1} \in \mathcal{P}$, $\frac{m_1}{m_2} \in \mathcal{M}$.

Proof: We first show the process of transformation from (6.93) to (6.94), then check that all the involved operations, including the two local complementations, doubling-neighbour-edge operations and copying operations, will transform all vertex operators to allowed ones.

Firstly consider the case that $\frac{m_1}{m_2} = \frac{0}{0}$, $\frac{a_1}{a_2} = \frac{m_3}{m_4} \in \mathcal{M}$ in (6.93). We have

$$(6.95)$$

where $\frac{m_i}{m_j} \in \mathcal{M}$, we applied a p_1 -local complementation about b for the first equality, then a $(-p_1)$ -local complementation about a for the second equality, and copied the red node $\frac{m_5}{m_6}$ in the last equality. The resulting diagram has the two properties in the definition of rGS-LC diagram.

Secondly consider the case that $\frac{m_1}{m_2} \in \mathcal{M}$, $\frac{a_1}{a_2} = \frac{m_3}{m_4} \in \mathcal{M}$ in (6.93). We have

$$(6.96)$$

where $\frac{m_i}{m_j} \in \mathcal{M}$, $\frac{m_{13}}{m_{14}} = \frac{m_7}{m_8} + \frac{m_1}{m_2}$, $\frac{m_{11}}{m_{12}} = \frac{m'_5}{m'_6} + \frac{m_3}{m_4}$, we copied the red node $\frac{m_5}{m_6}$ in the third equality. Now we can proceed base on the result of (6.95). That is

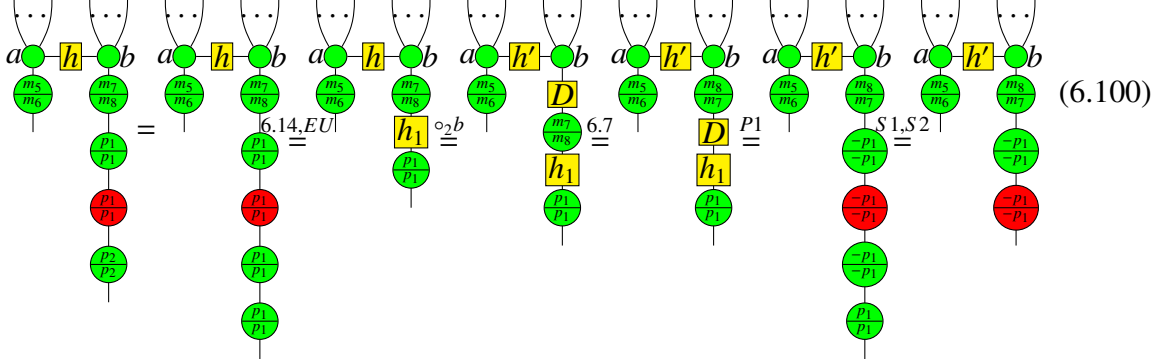
where $\frac{m_i}{m_j} \in \mathcal{M}$, $\frac{m_{19}}{m_{20}} = \frac{m_{13}}{m_{14}} + \frac{m_{15}}{m_{16}}$, $\frac{m_{23}}{m_{24}} = \frac{m_{17}}{m_{18}} + \frac{m_{21}}{m_{22}}$, we copied the red node $\frac{m_9}{m_{10}}$ in the third equality. The resulting diagram has the two properties in the definition of rGS-LC diagram.

Finally consider the case that $\frac{m_1}{m_2} \in \mathcal{M}$, $\frac{a_1}{a_2} = \frac{q_1}{q_2} = \frac{p_2}{p_2} + \frac{m_3}{m_4} \in \mathcal{M}$ in (6.93), where $\frac{p_2}{p_2} \in \mathcal{P}$, $\frac{m_3}{m_4} \in \mathcal{M}$. By (6.96) and (6.97), we have

where $\frac{m_i}{m_j} \in \mathcal{M}$. Note that either $p_1 = p_2$ or $p_1 = -p_2$ since $p_1 p_2 \neq 0$, $p_1, p_2 \in \mathbb{Z}_3$. If $p_1 = p_2$, we have

where $\frac{m_i}{m_j} \in \mathcal{M}$, we used the property (6.14) for the first equality, copied the red node $\frac{m_9}{m_{10}}$ in the third equality, and applied a $(-p_1)$ -local complementation about b for the last equality. The resulting diagram has the two properties in the definition of rGS-LC diagram.

If $p_1 = -p_2$, then $p_2 = -p_1 = 2p_1(\text{mod}3)$, and we have



where $h_1 = H$ or H^{-1} , and we used doubling-neighbour-edge operation $\circ_2 b$ for the third equality. The resulting diagram has the two properties in the definition of rGS-LC diagram.

Next we need to check that all the operations applied above will transform all vertex operators to allowed ones. First note that we can neglect all vertices which are not connected to a or b , since their vertex operators won't be changed under the transformation.

Besides, the neighbouring vertices of the operand vertex will gain some green phase operators through copying red nodes with phase angles in \mathcal{M} . Since the vertex operator of a neighbouring vertex either is merely a green phase or contains a green phase in the group \mathcal{M} , this copying operation preserves property 1 of rGS-LC diagrams.

As the doubling-neighbour-edge operation does not change any connectivity, but only add a D node to the vertex operator of the operand vertex whenever it is necessary, it helps for preserving the first property of rGS-LC diagrams.

Furthermore we consider the effect of local complementations. First, each vertex operator consisting of only green phases on a vertex other than a and b will continue to be a green phase under local complementations, since local complementations merely give green phases to such kind of vertex. Second, we consider vertices adjacent to a or b with vertex operator containing a red node. By the definition of rGS-LC diagram, such vertices must not be adjacent to a . Thus we can assume that w is a vertex whose vertex operator contains a red node and $\{w, b\}$ is an edge of the rGS-LC diagram before the transformation by local complementation. Then the p_1 -local complementation about b adds a phase $\begin{matrix} \text{green} \\ \frac{-p_1}{p_1} \end{matrix}$ to the vertex operator of w and produces an edge between w and a with weight $\Gamma'_{wa} = 0 + p_1\Gamma_{wb}\Gamma_{ab} = p_1\Gamma_{wb}\Gamma_{ab} \neq 0(\text{mod}3)$. And the $(-p_1)$ -local complementation about a adds $\begin{matrix} \text{red} \\ \frac{p_1}{p_1} \end{matrix}$ to w with the weight $\Gamma''_{wb} = \Gamma'_{wb} + (-p_1)\Gamma'_{wa}\Gamma'_{ab} = \Gamma_{wb} - (p_1)^2\Gamma_{wb}\Gamma_{ab}^2 = \Gamma_{wb} - \Gamma_{wb} = 0(\text{mod}3)$, where $\Gamma'_{wb} = \Gamma_{wb}$, $\Gamma'_{ab} = \Gamma_{ab}$, thus removes the edge between w and b . So if there further follows a $(-p_1)$ -local complementation about b , nothing will be added to the vertex

operator of w . Therefore the vertex operator of w still resides in the set \mathcal{R} , which means the transformation preserves the first property of the rGS-LC diagram.

Finally we consider two vertices v, w being adjacent to b which simultaneously have red nodes in their vertex operators. Since v, w lie in a rGS-LC diagram, there is no edge between v and w . After the p_1 -local complementation about b , there will be an edge between v and w and two edges $\{a, v\}$ and $\{a, w\}$ with weight $\Gamma'_{vw} = p_1\Gamma_{wb}\Gamma_{vb}$, $\Gamma'_{av} = p_1\Gamma_{wb}\Gamma_{ab}$, $\Gamma'_{aw} = p_1\Gamma_{vb}\Gamma_{ab}$ respectively. Also the $(-p_1)$ -local complementation about a results in $\Gamma''_{vw} = \Gamma'_{vw} + (-p_1)\Gamma'_{va}\Gamma'_{wa} = p_1\Gamma_{wb}\Gamma_{vb} - p_1(p_1)^2\Gamma_{wb}\Gamma_{vb}\Gamma_{ab}^2 = 0(\text{mod}3)$, which means the edge $\{v, w\}$ is removed, thus v and w are still non-adjacent. By the above calculation, the edges $\{v, b\}$ and $\{w, b\}$ are also removed, so if there further follows a $(-p_1)$ -local complementation about b , v and w will be non-adjacent. Clearly, edges connecting vertices which are not adjacent to a or b remain unchanged. Therefore the the second property of the rGS-LC diagram is also retained after transformation. To sum up, the resulting diagram is still a rGS-LC diagram. \square

6.4 Completeness

6.4.1 Comparing rGS-LC diagrams

In this subsection, we show that a pair of rGS-LC diagrams can be transformed into such a form that they are equal under the standard interpretation if and only if they are identical.

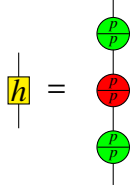
Definition 6.4.1 [5] *A pair of rGS-LC diagrams on the same number of qutrit is called simplified if there are no pairs of qutrits a, b , such that a has a red node in its vertex operator in the first diagram but not in the second, b has a red node in the second diagram but not in the first, and a and b are adjacent in at least one of the diagrams.*

Lemma 6.4.2 *Each pair of rGS-LC diagrams on the same number of qutrits can be made into a simplified form.*

Proof: The proof is same as that of the qubit case presented in [3, 5]. \square

Lemma 6.4.3 *Any component diagrams of a simplified pair of rGS-LC with an unpaired red node are unequal, where this red node resides as a vertex operator only in one of the pair of diagrams.*

where $\frac{a_i}{b_i} \in \mathcal{A}$, $h_i = H$ or H^{-1} , $i \in \{1, \dots, n\}$, $\frac{m_1}{m_2} \in \mathcal{M}$, $\frac{p}{p} \in \mathcal{P}$. Let



then $h_i = h^{a_i}$, $a_i \in \{1, -1\}$, $i \in \{1, \dots, n\}$.

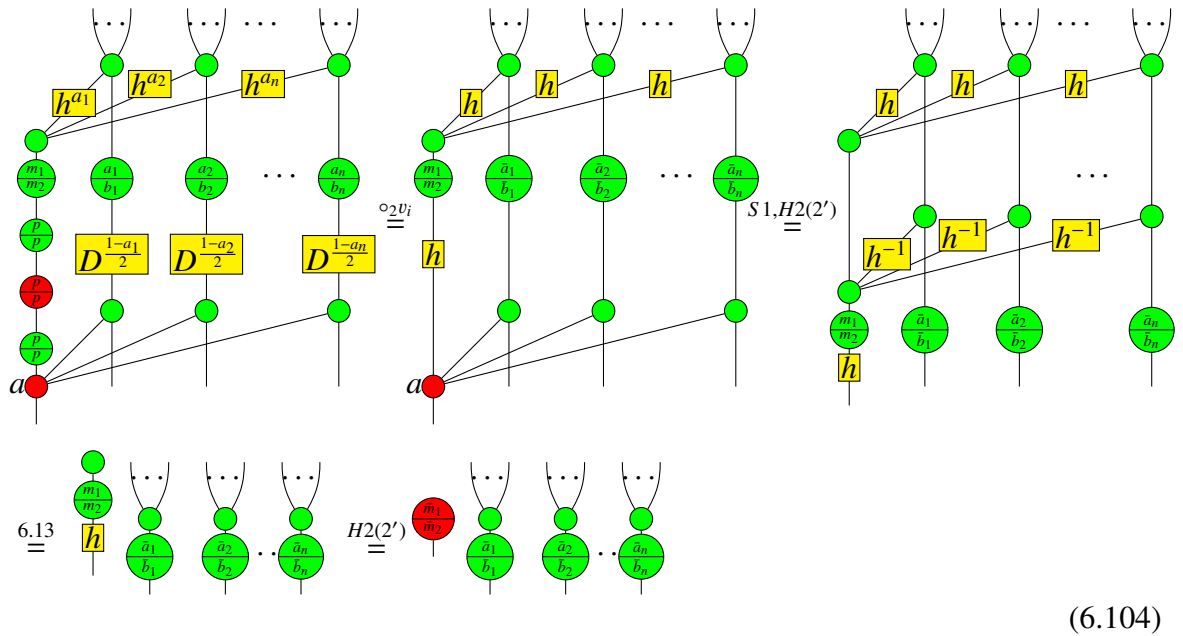
We now define an operation depending on D_1 as follows:

$$U_{D_1} = \left(\bigotimes_{v_i \in N_1} C_{X, v_i \rightarrow a} \right) \circ \left(R_{Z, a} \bigotimes_{v_i \in N_1} D^{\frac{1-a_i}{2}} \right) \quad (6.103)$$

where $D = H^2 = (H^{-1})^2$, $R_{Z, a}$ is the operation acting on a , and $C_{X, v_i \rightarrow a}$ is a generalized controlled-NOT gate with control v_i and target a . The operation U_{D_1} is well-defined as all the $C_{X, v_i \rightarrow a}$ commute with each other. Since each component is invertible, U_{D_1} must be invertible as well, therefore $U_{D_1} \circ D_1 = U_{D_1} \circ D_2 \Leftrightarrow D_1 = D_2$, which means if $U_{D_1} \circ D_1 \neq U_{D_1} \circ D_2$, then $D_1 \neq D_2$.

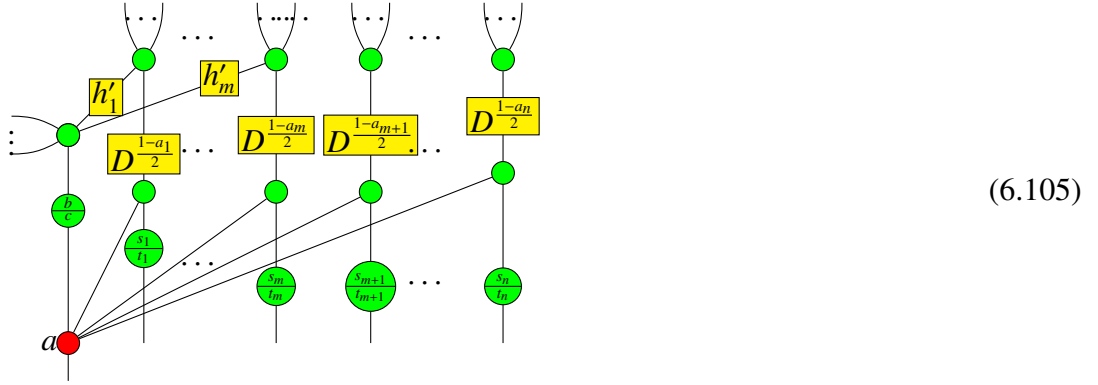
Below we will show that the qutrit a is in state in $U_{D_1} \circ D_1$, while being either entangled with other qutrits or in a state unequal to in $U_{D_1} \circ D_2$, where $\frac{\bar{m}_1}{\bar{m}_2} \in \mathcal{M}$. By the proof for the first two cases, this would entail that $U_{D_1} \circ D_1 \neq U_{D_1} \circ D_2$, thus $D_1 \neq D_2$.

First, for $U_{D_1} \circ D_1$, we have



where for the first equality, we applied the doubling-neighbour-edge operation to v_i whenever $a_i = -1$, and used the colour change rules (H2), (H2') for the second and the last equalities, the property (6.13) for the third equality.

Second, we consider $U_{D_1} \circ D_2$. There are three cases for vertices about their adjacency to a as well as application situation of controlled-NOT gates: 1) vertices are adjacent to a but have no controlled-NOT gates applied to them; 2) vertices are not adjacent to a but have controlled-NOT gates applied to them; 3) vertices are adjacent to a and also have controlled-NOT gates applied to them. Here we ignore edges not connected to a and edges without vertices in N_1 . Then we have

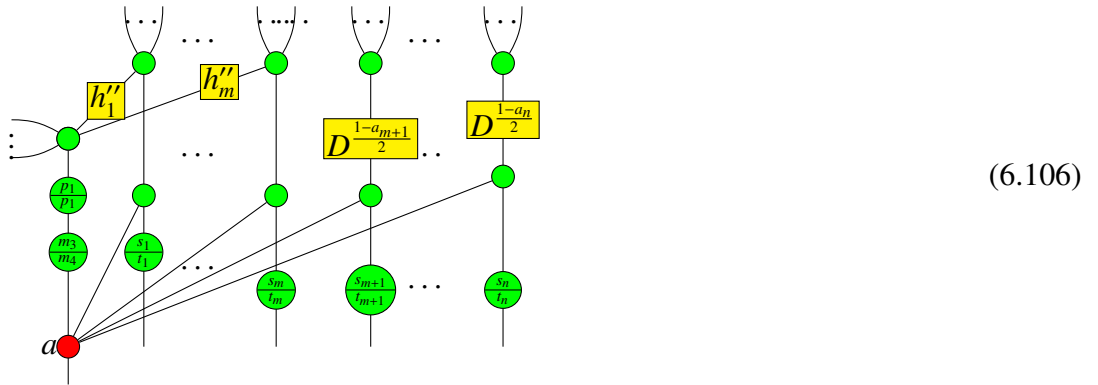


(6.105)

where the phase $\frac{b}{c} \in \mathcal{A}$ comes from the fusion of the vertex operator on a and the R_Z part of U_{D_1} .

To proceed, we investigate on different cases according to the value of $\frac{b}{c}$.

If $\frac{b}{c} = \frac{p_1}{p_1} + \frac{m_3}{m_4}$, where $\frac{p_1}{p_1} \in \mathcal{P}$, $\frac{m_3}{m_4} \in \mathcal{M}$, we apply the doubling-neighbour-edge operation to v_i for $a_i = -1$, $1 \leq i \leq m$. Then we have



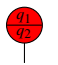
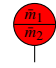
(6.106)

Furthermore, we apply p_1 -local complementation about a , then the vertex operator of a is

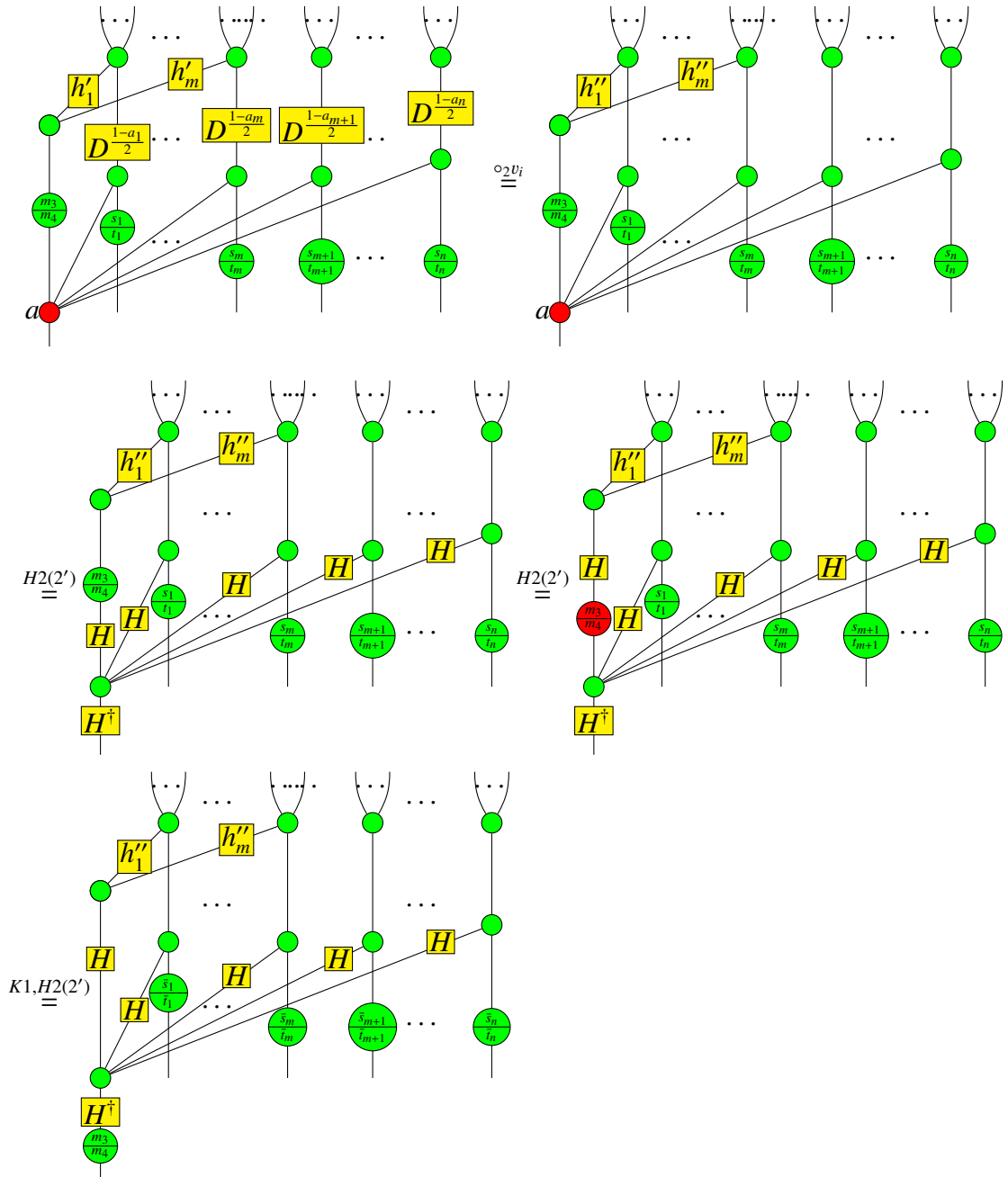
$$(6.107)$$

where $\frac{m_5}{m_6}, \frac{m_7}{m_8} \in \mathcal{M}$. The red node $\frac{m_5}{m_6}$ can be copied and changed in colour to fuse into vertex operators of a 's neighbours. So the diagram (6.106) is equal to

$$(6.108)$$

If $N_1 = N_2$, by property (6.13), a is either adjacent to some neighbours or in the state  where $\frac{q_1}{q_2} \in \mathcal{Q}$, which is clearly unequal to . Otherwise, a will always be connected to some neighbours after the application of U_{D_1} .

If $\frac{b}{c} = \frac{m_3}{m_4} \in \mathcal{M}$, there are two sub-cases. First, if $N_2 - N_1 \neq \emptyset$, then there exists $v \in N_2$ such that $v \notin N_1$. We apply a local complementation to this v , which will add a green phase $\frac{h_1}{h_1}$ to the vertex operator on a . The edges connected with a are changed as well, while there remains at least one vertex adjacent to a . Therefore we come back to the case $\frac{b}{c} = \frac{p_1}{p_1} + \frac{m_3}{m_4}$. Second, if $N_2 - N_1 = \emptyset$, since $N_2 \neq \emptyset$, it must be that $N_2 \subseteq N_1$, and thus $m = |N_2| > 0$. Not considering the edges unconnected to a , now the diagram is shown as follows:



(6.109)

where for the first equality, we applied the doubling-neighbour-edge operation to v_i whenever $a_i = -1$. Note that if $a_i = -1$ while v_i has no neighbours, then we just use the property that $\begin{array}{c} \bullet \\ | \\ \boxed{D} \end{array} = \begin{array}{c} \bullet \\ | \\ \bullet \end{array}$.

As we have mentioned exactly before dealing with $U_{D_1} \circ D_1$, to show that $D_1 \neq D_2$ it suffices to show that the qutrit a is either entangled with other qutrits or in a state unequal to $\begin{array}{c} \bullet \\ | \\ \frac{m_1}{m_2} \end{array}$ in $U_{D_1} \circ D_2$. For this purpose, we only need to pay attention to vertices a, v and the qutrit version of the controlled-Z gates between them. Also the last H^\dagger gate and the green phase $\frac{m_3}{m_4}$ on a are irrelevant here, so will be ignored. Therefore we have

$$(6.110)$$

where $\frac{m}{m} = \frac{1}{1}$ or $\frac{0}{0}$, we used the Euler decomposition rule (EU) and applied a 2-local complementation to v for the third equality, a 1-local complementation on a for the fourth equality, and the following property for the last equality which can be easily proved by rule (EU) and the property 6.62 :

$$(6.111)$$

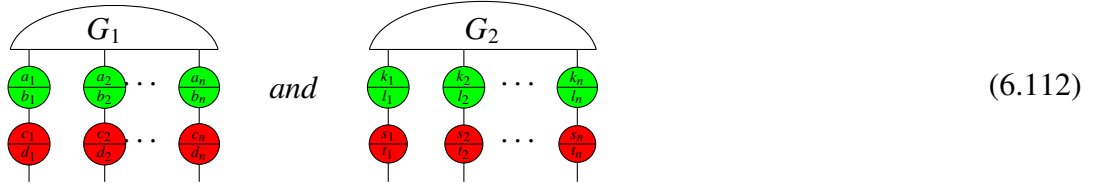
Now it is obvious that a is entangled with v . Thus for the second sub-case of the case $\frac{b}{c} = \frac{m_3}{m_4} \in \mathcal{M}$, we also proved $D_1 \neq D_2$.

So far we have shown in all cases that $D_1 \neq D_2$, hence finished the proof that any two component diagrams of a simplified pair of rGS-LC with an unpaired red node must be unequal.

□

Theorem 6.4.4 *The two component diagrams of any simplified pair of rGS-LC are equal under the standard interpretation if and only if they are identical.*

Proof: The necessity is obvious. We only prove the sufficiency. Denote the two component diagrams by D_1 and D_2 respectively. Suppose $D_1 = D_2$ in the sense that they represent the same quantum state. By lemma 6.4.3, $D_1 \neq D_2$ if there exists an unpaired red node. So we can assume that there are no unpaired red nodes in the simplified pair of rGS-LC under consideration. Let the graph underlying D_1 be $G_1 = (V, E_1)$, and the graph underlying D_2 be $G_2 = (V, E_2)$. Without loss of generality, assume that $V = \{1, 2, \dots, n\}$. Then D_1 and D_2 can be depicted as follows:

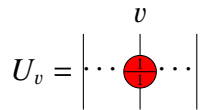


where $\frac{c_v}{d_v}, \frac{s_v}{t_v} \in \{0, 1, 2\}$,

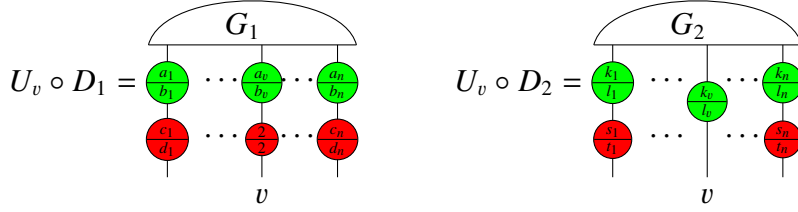
$$\frac{a_v}{b_v} \in \begin{cases} \mathcal{A}, & \text{if } \frac{c_v}{d_v} = 0 \\ \{1, 0, 2\}, & \text{if } \frac{c_v}{d_v} = 1 \\ \{2, 0, 1\}, & \text{if } \frac{c_v}{d_v} = 2 \end{cases} \quad \frac{k_v}{l_v} \in \begin{cases} \mathcal{A}, & \text{if } \frac{s_v}{t_v} = 0 \\ \{1, 0, 2\}, & \text{if } \frac{s_v}{t_v} = 1 \\ \{2, 0, 1\}, & \text{if } \frac{s_v}{t_v} = 2 \end{cases}$$

$1 \leq v \leq n$.

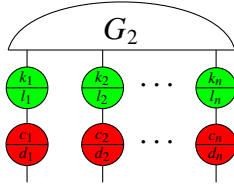
Since all red nodes are paired up, it follows that $\frac{c_v}{d_v} = 0 \Leftrightarrow \frac{s_v}{t_v} = 0$. If $\frac{c_v}{d_v} \neq 0, \frac{s_v}{t_v} \neq 0$, but $\frac{c_v}{d_v} \neq \frac{s_v}{t_v}$, w.l.o.g., assume $\frac{c_v}{d_v} = 1, \frac{s_v}{t_v} = 2$. Let



Since U_v is unitary, $U_v \circ D_1 = U_v \circ D_2 \Leftrightarrow D_1 = D_2$. Now



Clearly $U_v \circ D_1$ and $U_v \circ D_2$ are unpaired, so $U_v \circ D_1 \neq U_v \circ D_2$, thus $D_1 \neq D_2$. Therefore, $D_1 = D_2$ implies $\frac{c_v}{d_v} = \frac{s_v}{t_v}, \forall v \in \{1, 2, \dots, n\}$. Thus D_2 can be represented as



Define two operators

$$U = \bigotimes_{v \in V} R_{X,v}^{-1} \quad \text{and} \quad W = \bigotimes_{\{u,w\} \in E_1} C_{Z,uw}^{-1}, \quad (6.113)$$

where $R_{X,v} = \begin{matrix} \bullet \\ \frac{c_v}{d_v} \\ \bullet \end{matrix}$, $C_{Z,uw}$ is the edge $\begin{matrix} \bullet & \boxed{h} & \bullet \\ | & & | \end{matrix}$ connecting u and w in G_1 with $h = H$ or H^{-1} . Clearly, both U and W are invertible, Thus $(W \circ U) \circ D_1 = (W \circ U) \circ D_2 \Leftrightarrow D_1 = D_2$. After applying the operator U to D_1 and D_2 , all the red nodes are cancelled out, only green nodes left as vertex operators. Based on this operation, further composition with W will result in $(W \circ U) \circ D_1 = \begin{matrix} \bullet & \bullet \\ \frac{a_1}{b_1} & \frac{a_n}{b_n} \\ \bullet & \bullet \end{matrix}$. Since $D_1 = D_2$, it must be that $(W \circ U) \circ D_2 = \begin{matrix} \bullet & \bullet \\ \frac{a_1}{b_1} & \frac{a_n}{b_n} \\ \bullet & \bullet \end{matrix}$. If there is an edge in E_1 but not belong to E_2 , or an edge in E_2 but not belong to E_1 , then $(W \circ U) \circ D_2$ must be a entangled state. So $(E_1 - E_2) \cup (E_2 - E_1) = \emptyset$, i.e., $E_1 = E_2$. Furthermore, the weight of each edge in G_1 should be the same as that of the corresponding edge in G_2 , otherwise $(W \circ U) \circ D_2$ is impossible to be a product of single qutrit states. Therefore we have $G_1 = G_2$. It follows immediately that $(W \circ U) \circ D_2 = \begin{matrix} \bullet & \bullet \\ \frac{k_1}{l_1} & \frac{k_n}{l_n} \\ \bullet & \bullet \end{matrix}$. Again by $D_1 = D_2$, we have $\frac{a_v}{b_v} = \frac{k_v}{l_v}, \forall v \in V$. Thus D_1 and D_2 are identical. This completes the proof. \square

6.4.2 Completeness for qutrit stabilizer quantum mechanics

To achieve the proof of completeness for qutrit stabilizer QM, we will proceed in two main steps. Firstly, we show the completeness for stabilizer states.

Theorem 6.4.5 *The ZX-calculus is complete for pure qutrit stabilizer states.*

Proof: We only need to show that any two ZX-calculus diagrams that represent the same qutrit stabilizer state can be rewritten from one to the other by the ZX rules. Suppose D_1 and D_2 are such two diagrams. By theorem 6.3.17, D_1 and D_2 can be rewritten into rGS-LC diagrams D'_1 and D'_2 respectively. Clearly D'_1 and D'_2 are a pair of rGS-LC diagrams on the same number of qutrits. Then by lemma 6.4.2, they can be transformed to a simplified pair of rGS-LC diagrams D''_1 and D''_2 in the ZX-calculus while still representing the same quantum state. Now it follows from theorem 6.4.4 that D''_1 and D''_2 are identical diagrams, we denote this diagram by D'' . As described above, we have show the steps of rewriting D_1 and D_2 into D'' respectively. If we invert the rewriting processes from D_2 to D'' and compose with the rewriting processes from D_1 to D'' , then we get the rewriting processes from D_1 to D_2 . This completes the proof. \square

Secondly, we use the following map-state duality to relate quantum states and linear operators:

$$(6.114)$$

Then by theorem 6.4.5 and the map-state duality (6.114), we have the main result:

Theorem 6.4.6 *The ZX-calculus is complete for qutrit stabilizer quantum mechanics.*

A natural question arises at the end of this chapter: is there a general proof of completeness of the ZX-calculus for arbitrary dimensional (qudit) stabilizer QM? This is the problem we would like to address next, but we should also mention some challenges we may face. With exception of the increase of the order of local Clifford groups, the main difficulty comes from the fact that that it is not known whether any stabilizer state is equivalent to a graph state under local Clifford group for the dimension d having multiple prime factors [37]. As far as we know, stabilizer states are equivalent to graph states under local Clifford group for the dimension d which has only single prime factors [48]. Furthermore, the sufficient and necessary condition for two qudit graph states to be equivalent under local Clifford group in terms of operations on graphs is unknown in the case that d is non-prime. Finally, the generalised Euler decomposition rule for the generalised Hadamard gate can not be trivially derived, and other uncommon rules might be needed for general d .

Chapter 7

Some applications of the ZX-calculus

In the previous chapters, we mainly explored the theoretical aspects of the ZX-calculus: giving complete axiomatisations for the entire qubit quantum mechanics and other fragments of the QM. Now we turn to the application side of the ZX-calculus. Since its invention, the ZX-calculus has been applied to quantum foundations, such as non-locality [16, 17], and quantum computing [27, 36, 13, 24]. It has also been incorporated into the Quantomatic software for automatic reasoning [47]. However, none of these applications use any of the rules involved with the new generators—triangle and λ box.

In this chapter, we show some applications of the ZX-calculus with rules involving the new generators. These include four parts: proof of the generalised supplementarity, equivalent forms of 3-entanglement qubit states, representation of Toffoli gate, and equivalence-checking for the UMA gate.

7.1 Proof of the generalised supplementarity

In Chapter 3, the λ box is restricted to be parameterised by a non-negative real number. However, we can define green and red spiders parameterised by arbitrary complex numbers in terms of generators of the ZX_{full} -calculus. In fact, for any complex number a , let $a = \lambda e^{i\alpha}$, where $\lambda \geq 0, \alpha \in [0, 2\pi)$. Let $\begin{array}{c} | \\ \lambda \end{array} := \begin{array}{c} \square \lambda \\ \bullet \end{array}$. Then by rules (S1), (L1) and (L5) of the ZX_{full} -calculus, the following definition is well-defined:

$$\begin{array}{c} \dots \\ \diagup \quad \diagdown \\ \square a \\ \diagdown \quad \diagup \\ \dots \end{array} := \begin{array}{c} \dots \\ \diagup \quad \diagdown \\ \bullet a \\ \diagdown \quad \diagup \\ \dots \end{array} \begin{array}{c} | \\ \lambda \end{array} \tag{7.1}$$

Thus by the spider rule (S1) and the rules (L1), (L4) and (L5), we have the generalised green spider rule:



where a, b are arbitrary complex numbers.

By the colour change rule (H), the generalised red spider can be defined as follows:

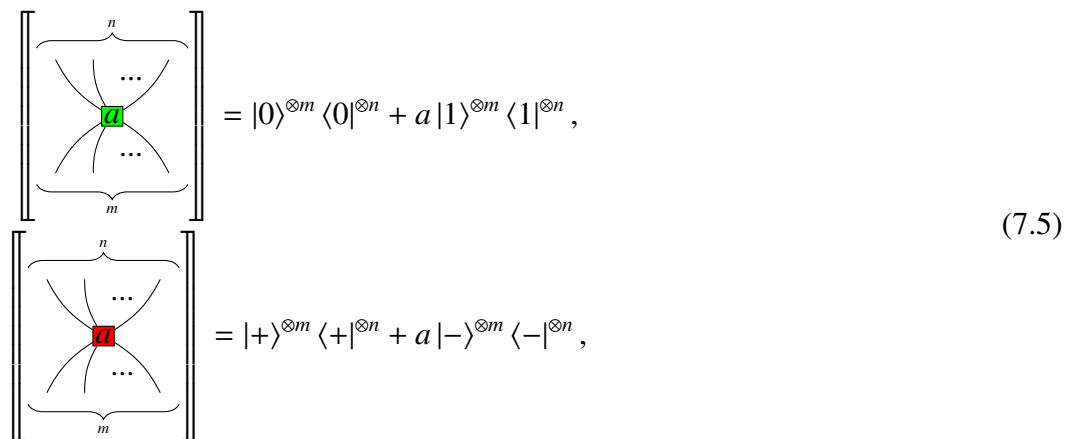


Therefore, we have the generalised red spider rule:



where a, b are arbitrary complex numbers.

The generalised green and red spiders have the following interpretation in Hilbert spaces:



where a is an arbitrary complex number.

Now we consider the generalised supplementarity— also called cyclotomic supplementarity, with supplementarity as a special case—which is interpreted as merging n subdiagrams if the n phase angles divide the circle uniformly [45]. The diagrammatic form of the

generalised supplementarity is as follows:

$$(7.6)$$

where there are n parallel wires in the diagram at the right-hand side.

Next we show that the generalised supplementarity can be seen as a special form of the generalised spider rule as shown in (7.4). For simplicity, we ignore scalars in the rest of this section.

First, it can be directly calculated that

where $a \in \mathbb{C}, a \neq -1$.

Then by the completeness of the ZX_{full} -calculus, we have

$$(7.7)$$

In particular,

$$(7.8)$$

where $\alpha \in [0, 2\pi), \alpha \neq \pi$. For $\alpha = \pi$, we can use the π copy rule directly.

Then

$$(7.9)$$

where we used the following formula given in [45]:

$$\prod_{j=0}^{n-1} (1 + e^{i(\alpha + \frac{j}{n}2\pi)}) = 1 + e^{i(n\alpha + (n-1)\pi)} \quad (7.10)$$

Note that if n is odd, then

$$\boxed{\frac{1-e^{in\alpha}}{1+e^{i(n\alpha+(n-1)\pi)}}} = \boxed{\frac{1-e^{in\alpha}}{1+e^{i(n\alpha)}}} \stackrel{7.8}{=} \begin{array}{c} \bullet \\ \diagup \quad \diagdown \\ \bullet \quad \bullet \end{array} \stackrel{5.2}{=} \begin{array}{c} \bullet \\ | \end{array} \quad (7.11)$$

If n is even, then

$$\boxed{\frac{1-e^{in\alpha}}{1+e^{i(n\alpha+(n-1)\pi)}}} = \boxed{1} \stackrel{L3}{=} \begin{array}{c} \bullet \\ | \end{array} \quad (7.12)$$

It is not hard to see that if we compute the parity of n in the right diagram of (7.6) not considering the scalars, then by Hopf law we get the same result as shown in (7.11) and (7.12).

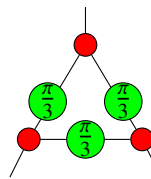
7.2 3-entanglement qubit states

It is well known that there are two SLOCC (Stochastic Local Operations and Classical Communication) equivalent classes of 3-entanglement qubit states [29] with representative members $|GHZ\rangle = |000\rangle + |111\rangle$, $|W\rangle = |100\rangle + |010\rangle + |001\rangle$. In fact, we have

Theorem 7.2.1 [29] *Two n -partite states $|\psi\rangle$ and $|\phi\rangle$ are SLOCC equivalent if and only if there exist invertible linear maps L_1, L_2, \dots, L_n such that*

$$|\psi\rangle = (L_1 \otimes L_2 \otimes \dots \otimes L_n) |\phi\rangle \quad (7.13)$$

In [18], Coecke and Edwards have represented the W state with phases in the ZX-calculus as follows:



$$\quad (7.14)$$

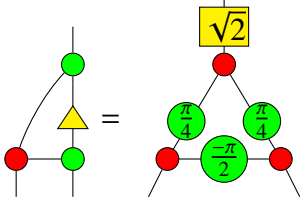
While another representation of the W state by a triangle was essentially given in [42], and explicitly given in [56]:



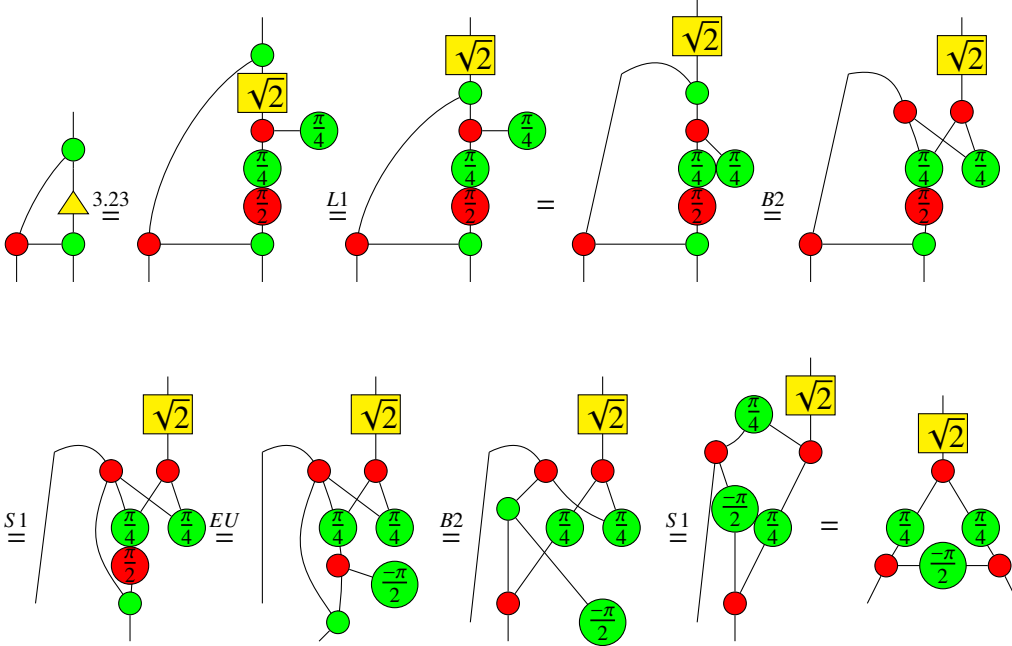
$$\quad (7.15)$$

Here we build a bridge between these two representations of the W state by λ box.

Lemma 7.2.2 For the W state, up to non-zero scalars, we have



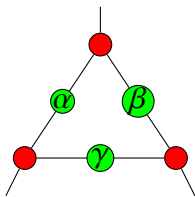
Proof:



□

Furthermore, Coecke and Edwards give explicit conditions for a GHZ-class state:

Lemma 7.2.3 [18] The following diagram



(7.16)

represents a GHZ-class state if α, β, γ violate one of the following equalities:

$$\begin{aligned} \alpha + \beta + \gamma &= \pi \\ \alpha + \beta - \gamma &= \pi \\ \alpha - \beta + \gamma &= \pi \\ \alpha - \beta - \gamma &= \pi \end{aligned}$$

However, if we use the generalised spiders defined in the previous section, then we can obtain an exact solution for transformation of GHZ-class state into simpler form. Note that

we will use standard interpretations for deriving diagrammatical identities in the following proofs because of the completeness of the ZX_{full} -calculus.

Lemma 7.2.4 *For GHZ state, we have*



$$(7.17)$$

where λ_i and x_i are complex numbers, $(1 + \lambda_1\lambda_2\lambda_3)(\lambda_1 + \lambda_2\lambda_3)(\lambda_2 + \lambda_1\lambda_3)(\lambda_3 + \lambda_1\lambda_2) \neq 0$,

$$x_1 = \pm \sqrt{\frac{(\lambda_2 + \lambda_1\lambda_3)(\lambda_1 + \lambda_2\lambda_3)}{(1 + \lambda_1\lambda_2\lambda_3)(\lambda_3 + \lambda_1\lambda_2)}}, x_2 = \pm \sqrt{\frac{(\lambda_1 + \lambda_2\lambda_3)(\lambda_3 + \lambda_1\lambda_2)}{(1 + \lambda_1\lambda_2\lambda_3)(\lambda_2 + \lambda_1\lambda_3)}},$$

$$x_3 = \pm \sqrt{\frac{(\lambda_2 + \lambda_1\lambda_3)(\lambda_3 + \lambda_1\lambda_2)}{(1 + \lambda_1\lambda_2\lambda_3)(\lambda_1 + \lambda_2\lambda_3)}}.$$

Proof: The matrix of the left-hand side of (7.17) is

$$\begin{pmatrix} 1 + \lambda_1\lambda_2\lambda_3 & 0 \\ 0 & \lambda_2 + \lambda_1\lambda_3 \\ 0 & \lambda_1 + \lambda_2\lambda_3 \\ \lambda_3 + \lambda_1\lambda_2 & 0 \end{pmatrix}.$$

The matrix of the right-hand side of (7.17) is

$$\begin{pmatrix} 1 & 0 \\ 0 & x_1x_3 \\ 0 & x_1x_2 \\ x_2x_3 & 0 \end{pmatrix}.$$

These two matrices are equal up to a scalar, thus

$$x_1x_3 = \frac{\lambda_2 + \lambda_1\lambda_3}{1 + \lambda_1\lambda_2\lambda_3}, x_1x_2 = \frac{\lambda_1 + \lambda_2\lambda_3}{1 + \lambda_1\lambda_2\lambda_3}, x_2x_3 = \frac{\lambda_3 + \lambda_1\lambda_2}{1 + \lambda_1\lambda_2\lambda_3}.$$

Then

$$(x_1x_2x_3)^2 = \frac{(\lambda_2 + \lambda_1\lambda_3)(\lambda_1 + \lambda_2\lambda_3)(\lambda_3 + \lambda_1\lambda_2)}{(1 + \lambda_1\lambda_2\lambda_3)^3},$$

i.e.,

$$x_1x_2x_3 = \pm \sqrt{\frac{(\lambda_2 + \lambda_1\lambda_3)(\lambda_1 + \lambda_2\lambda_3)(\lambda_3 + \lambda_1\lambda_2)}{(1 + \lambda_1\lambda_2\lambda_3)^3}}.$$

Therefore,

$$x_1 = \frac{x_1 x_2 x_3}{x_2 x_3} = \pm \sqrt{\frac{(\lambda_2 + \lambda_1 \lambda_3)(\lambda_1 + \lambda_2 \lambda_3)}{(1 + \lambda_1 \lambda_2 \lambda_3)(\lambda_3 + \lambda_1 \lambda_2)}}, x_2 = \frac{x_1 x_2 x_3}{x_1 x_3} = \pm \sqrt{\frac{(\lambda_1 + \lambda_2 \lambda_3)(\lambda_3 + \lambda_1 \lambda_2)}{(1 + \lambda_1 \lambda_2 \lambda_3)(\lambda_2 + \lambda_1 \lambda_3)}},$$

$$x_3 = \frac{x_1 x_2 x_3}{x_1 x_2} = \pm \sqrt{\frac{(\lambda_2 + \lambda_1 \lambda_3)(\lambda_3 + \lambda_1 \lambda_2)}{(1 + \lambda_1 \lambda_2 \lambda_3)(\lambda_1 + \lambda_2 \lambda_3)}}.$$

□

As an example, we have

Lemma 7.2.5


(7.18)

where

$$A = \begin{pmatrix} 1 & 0 \\ 0 & \pm \sqrt{3}i \end{pmatrix}, B = \begin{pmatrix} 1 & 0 \\ 0 & \mp \sqrt{\frac{1}{3}}(\sqrt{2} + i) \end{pmatrix}, C = \begin{pmatrix} 1 & 0 \\ 0 & \pm \sqrt{\frac{1}{3}}(1 + \sqrt{2}i) \end{pmatrix}.$$

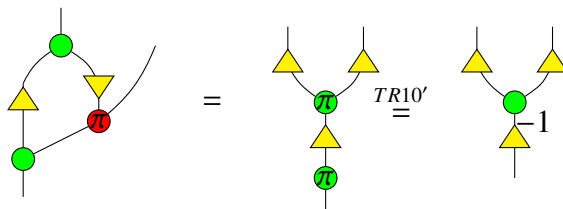
Proof: The matrix of the left-hand side of (7.18) is

$$\begin{pmatrix} 1 & 0 \\ 0 & -\sqrt{2} + i \\ 0 & 1 - \sqrt{2}i \\ -i & 0 \end{pmatrix}.$$

Then the result follows from Lemma 7.2.4. □

Finally, we have two more equivalent transformations of GHZ states from a loop form to a non-loop form like the bialgebra rule (B2), which can be verified by matrix calculations:

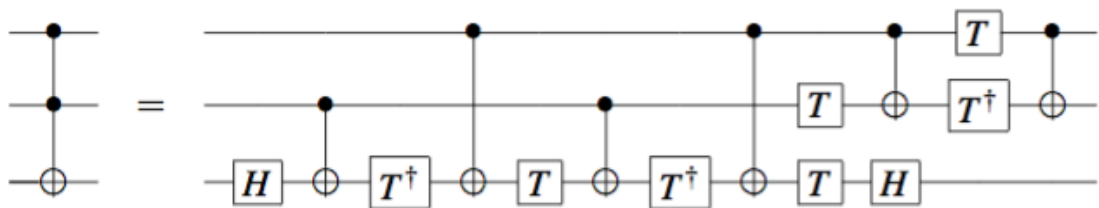

(7.19)


(7.20)

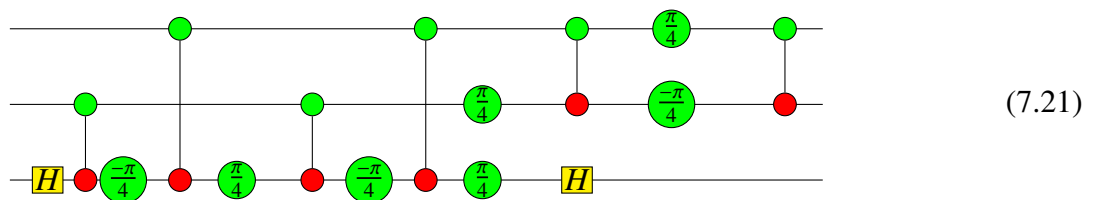
It is interesting to point out that the first diagram in (7.20) has been used by Jeandel, Perdrix, and Vilmart to construct the Toffoli gate [42], while the third diagram in (7.20) was used in (7.25) in this chapter and in [57] to construct the same gate. The equalities of (7.20) were obtained before the upload of the paper [57], we only choose the third diagram to construct the Toffoli gate because we think it makes the Toffoli gate simpler—there is no loop in the construction—and is easy to generalise to a multiple control Toffoli gate of form (7.29).

7.3 Representation of Toffoli gate

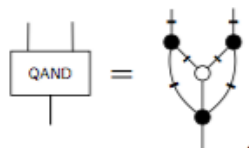
The Toffoli gate is known as the “controlled-controlled-not” gate [58]. The standard circuit form of Toffoli gate is given in [65] as follows:



We express the circuit form of Toffoli gate in ZX-calculus as follows:



In contrast to circuit form, the Toffoli gate can be expressed by the new generator–triangle—in a nice way (without phases). Here we follow the way of section 12.1.3 in [20] to construct the Toffoli gate. First, we need to specify the AND gate in ZX-calculus. The AND gate was given by a GHZ/W-pair in [35] as follows:



The right-side diagram above is a GHZ/W-calculus diagram [19]. If we translate this diagram into ZX-calculus, then we get

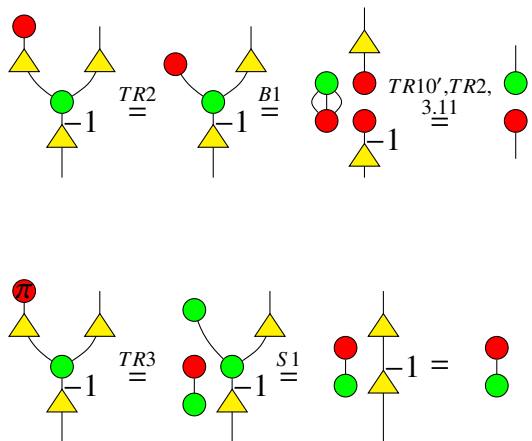

(7.22)

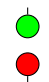
By further calculation, we have


(7.23)

where the triangle with a -1 on the top-left corner is the inverse of the normal triangle.

We check the correctness of the AND gate as follows:


(7.24)

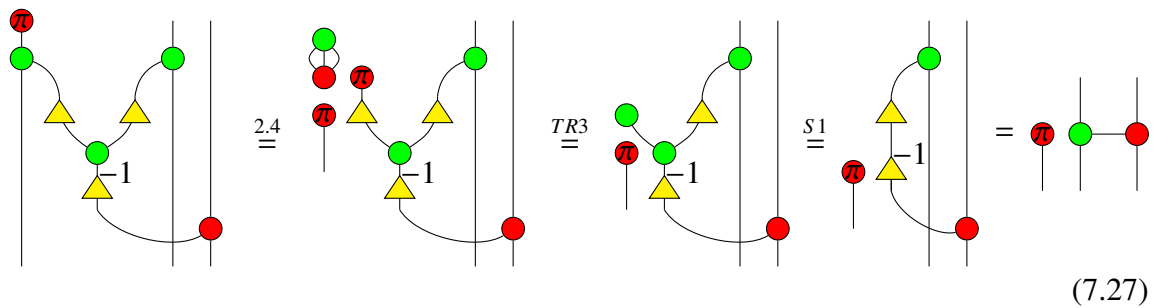
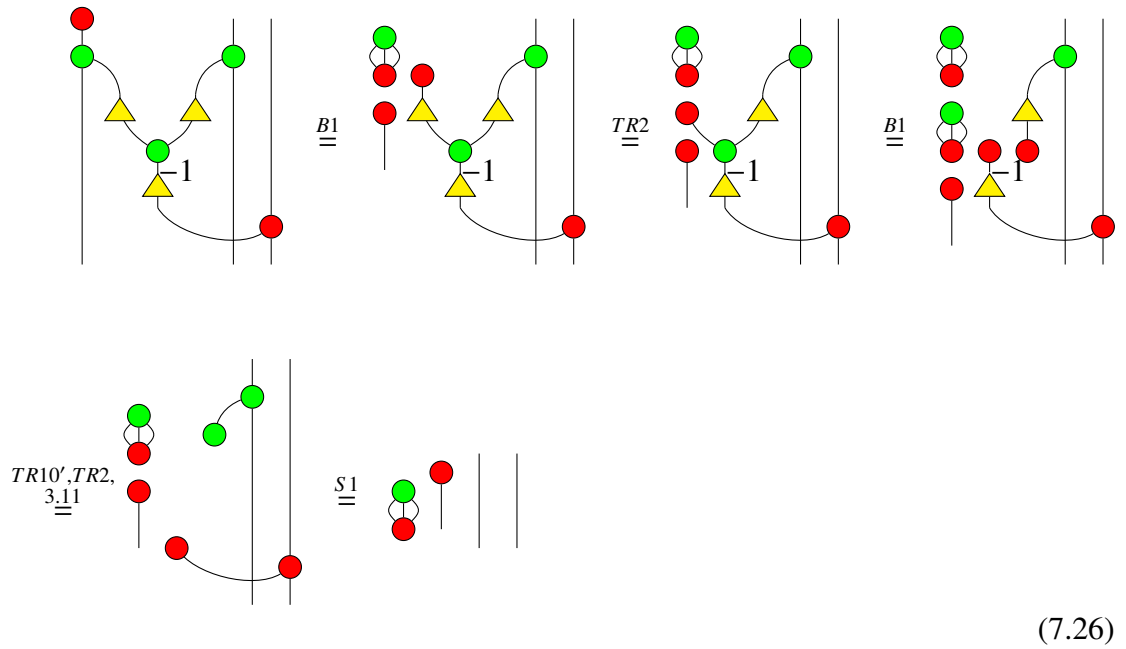
Note that the matrix form of the diagram  in (7.24) is $\sqrt{2}|0\rangle(\langle 0| + \langle 1|)$, which means the two rows of diagrammatic equalities of (7.24) have the same scalars under the standard basis. Therefore we prove the correctness of (7.23) for the AND gate.

It turns out that the “/” box (Exercise 12.10 in [20]) has the same matrix form as the new generator triangle (up to a scalar), thus the AND gate there is in a form similar to (7.23).

Then the Toffoli gate can be constructed as



Now we prove the correctness of the Toffoli gate. The key point to remember here is that the Toffoli gate is a “controlled-CNOT” gate [20].



The matrix form of $\text{green circle} \text{---} \text{red circle}$ is $\frac{1}{\sqrt{2}}(|00\rangle\langle 00| + |01\rangle\langle 01| + |11\rangle\langle 10| + |10\rangle\langle 11|)$, which means the final diagrams of (7.26) and (7.27) have the same scalars under the standard basis. Therefore we prove the correctness of (7.25) for the Toffoli gate.

It is easy to see that the AND gate can be generalised as follows:

$$QAND_n = \text{[Diagram: Green circle with } - \text{ and } n \text{ yellow triangles on inputs and one on output]} \quad (7.28)$$

Therefore the multiple control Toffoli gate (up to a scalar) can be represented as:

$$\text{[Diagram: Multiple control Toffoli gate with green and red circles and yellow triangles]} \quad (7.29)$$

We end this section with pointing out that it is not easy to find an efficient way to prove in the ZX-calculus the equivalence of the two forms of Toffoli gate (7.21) and (7.25), although this can, in principle, be done by rewriting them into normal forms induced from the ZW-calculus.

7.4 Equivalence-checking for the UMA gate

In this section, we consider applying the ZX-calculus to equivalence-checking [71] for two special quantum circuits. These two circuits are two forms of the so-called “UnMajority and Add” (UMA) quantum gate given in [22] as follows:

(a) 2-CNOT version

(b) 3-CNOT version

We check the equivalence of the two kind of UMA gate diagrammatically in terms of the representation of Toffoli gate (7.25). The translation from the UMA gate into ZX-calculus is direct: Toffoli gate in UMA translated to diagram (7.25), CNOT gate in UMA to CNOT in ZX, and NOT gate in UMA to the red π gate in the ZX-calculus.

Proposition 7.4.1 *The two versions of the UMA gate can be proved to be equal in the*

ZX-calculus:

(7.30)

Proof:

(7.31)

where for the second equality we used lemma 7.4.2, and for the fourth equality we used the bialgebra rule. □

Lemma 7.4.2

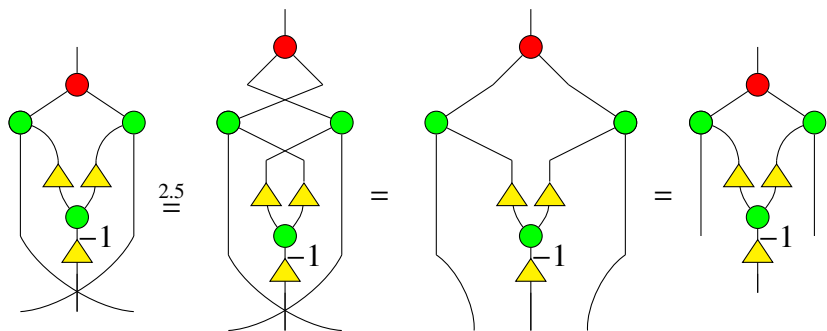
(7.32)

Proof:

(7.33)

where for the third equality we used the rule (TR11), for the last equality we made the following transformation by commutativity of the red and green spiders as well as the

naturality of diagrams (free move without changing any connections):



(7.34)

□

Chapter 8

Conclusions and further work

In this thesis, we first show that the ZX-calculus is complete for the overall pure qubit QM, with the aid of completeness of ZW-calculus for the whole qubit QM. Thus qubit quantum computing can be done purely diagrammatically in principle.

Based on this universal completeness, we directly obtain a complete axiomatisation of the ZX-calculus for the Clifford+T quantum mechanics by restricting the ring of complex numbers to its subring corresponding to the Clifford+T fragment resting on the completeness theorem of the ZW-calculus for arbitrary commutative ring.

Furthermore, we prove the completeness of the ZX-calculus (with just 9 rules) for 2-qubit Clifford+T circuits by verifying the complete set of 17 circuit relations in diagrammatic rewriting. This is an important step towards efficient simplification of general n-qubit Clifford+T circuits.

In addition to completeness results within the qubit related formalism, we extend the completeness of the ZX-calculus for qubit stabilizer quantum mechanics to the qudit stabilizer system. This generalisation is far from trivial as one can see that, for example, the local Clifford group for qubits has only 24 elements, while the local Clifford group for qudits has 216 elements.

Finally, we show by some examples the application of the ZX-calculus to the proof of generalised supplementarity, the representation of entanglement classification and Toffoli gate, as well as equivalence-checking for the UMA gate.

The results of this chapter has been published in the paper [21], with the coauthor Bob Coecke.

Further work

An obvious next step is to generalise the completeness of the ZX-calculus for qubit to that for qudit with arbitrary dimension d . One possible way to do this is to establish a com-

pleteness result for the qudit version of the ZW-calculus. Though there is a ZW-calculus universal for qudit quantum mechanics [33], it is not sure whether the completeness result for qudit can be finally obtained. To be honest, we have tried very hard along this direction, but have not succeeded in the end. Another way to have the completeness of the qudit ZX-calculus is to prove it directly without any resort to the completeness of the ZW-calculus. There is already a proof of completeness of the qubit ZX-calculus independent of the completeness of the ZW-calculus [44], however we have no idea on how to generalise this result from qubit to qudit. Furthermore, we would like to mention that a normal form of qubit ZX diagrams can be obtained if we resort to elementary transformations represented in ZX-calculus and the map-state duality, thus completeness could follow up. But no elegant ZX rewriting rules have been found in this way to date, so continuous work is still required, including generalisation to qudit case.

The standard interpretation of the ZX-calculus maps diagrams to matrices in a category with objects being tensor powers of a fixed finite dimensional Hilbert space. But in quantum computing, we often deal with the category **FdHilb**, whose objects could be Hilbert space of arbitrary finite dimension. So it is natural to construct a ZX-calculus that can deal with quantum computing for various dimensions in the same framework. In fact, we could have such a ZX-calculus by indicating each dimension of the type of a system and introducing the isomorphism between composite space and its component spaces. Once this mixed version of ZX-calculus is obtained, then one could fill in all the boxes that one usually encounters in categorical quantum mechanics with these kind of ZX diagrams. However, the completeness problem of this mixed version of ZX-calculus keeps open. Even more, one could try to generalise the ZX-calculus to the case of infinite dimension.

Since now we have a set of complete ZX rules for Clifford+T quantum mechanics, it would be of great interest to develop efficient strategies in the ZX-calculus for optimising Clifford+T quantum circuits. One simple idea for this direction is to firstly take the ZX-calculus as a learning machine to learn existing excellent strategies and algorithms by encoding everything in the language of the ZX-calculus, and then try to improve the results obtained.

As we demonstrated in Section 7.3, the Toffoli gate has a simple representation in the ZX-calculus. Then it would be interesting to apply this version of Toffoli gate to the field of Toffoli based quantum circuits, for example, quantum boolean circuits [41]. Meanwhile, Toffoli and Hadamard are universal for quantum computation [66], so one could employ the ZX version of Toffoli gate to explore on Toffoli+H quantum circuits instead of Clifford+T circuits.

The completeness of ZX-calculus for 2-qubit Clifford+T circuits depends on the proof of complete relations given in [64]. It is unknown whether one can derive a direct proof from the universal completeness of the ZX-calculus. Furthermore, can we obtain the completeness of ZX-calculus for 3-qubit Clifford+T circuits, or even arbitrary n-qubit Clifford+T circuits?

As for the stabilizer formalism, it is natural to ask whether there is a general proof of completeness of the ZX-calculus for arbitrary dimensional (qudit) stabilizer quantum mechanics. As in the qubit case, we can't expect to use a triangle as a generator to have a complete axiomatisation of the qudit stabilizer quantum mechanics, so the techniques from qudit graph states may still be needed.

Another question suggested by Bob Coecke is to embed the qubit ZX-calculus into qudit ZX-calculus, which is not obvious since a representation of some special non-stabilizer phase is involved.

Lastly, it is also interesting to incorporate the rules of the universally complete ZX-calculus in the automated graph rewriting system Quantomatic [47].

Bibliography

- [1] <http://cqm.wikidot.com/zx-completeness>.
- [2] Samson Abramsky and Bob Coecke. A categorical semantics of quantum protocols. In *Proceedings of the 19th Annual IEEE Symposium on Logic in Computer Science, LICS '04*, pages 415–425, Washington, DC, USA, 2004. IEEE Computer Society. doi:10.1109/LICS.2004.1.
- [3] Miriam Backens. The ZX-calculus is complete for stabilizer quantum mechanics. *New Journal of Physics*, 16(9):093021, September 2014. doi:10.1088/1367-2630/16/9/093021.
- [4] Miriam Backens. The ZX-calculus is complete for the single-qubit Clifford+T group. *Electronic Proceedings in Theoretical Computer Science*, 172:293–303, 2014. doi:10.4204/eptcs.172.21.
- [5] Miriam Backens. *Completeness and the ZX-calculus*. PhD thesis, February 2016. arXiv:1602.08954.
- [6] Miriam Backens, Simon Perdrix, and Quanlong Wang. A Simplified Stabilizer ZX-calculus. *EPTCS*, 236:1–20, January 2017. doi:10.4204/EPTCS.236.1.
- [7] John C. Baez, Brandon Coya, and Franciscus Rebro. Props in network theory. arXiv:1707.08321, 2017.
- [8] Mohsen Bahramgiri and Salman Beigi. Graph states under the action of local clifford group in non-binary case. arXiv:quant-ph/0610267.
- [9] Xiaoning Bian and Quanlong Wang. Graphical calculus for qutrit systems. *IEICE Transactions on Fundamentals of Electronics, Communications and Computer Sciences*, E98.A(1):391–399, 2015. doi:10.1587/transfun.E98.A.391.

- [10] Filippo Bonchi, Paweł Sobociński, and Fabio Zanasi. Interacting Hopf algebras. *Journal of Pure and Applied Algebra*, 221(1):144 – 184, 2017. doi:<https://doi.org/10.1016/j.jpaa.2016.06.002>.
- [11] Francis Borceux. *Handbook of Categorical Algebra*, volume 2 of *Encyclopedia of Mathematics and its Applications*. Cambridge University Press, 1994. doi:10.1017/CBO9780511525865.
- [12] P. O. Boykin, T. Mor, M. Pulver, V. Roychowdhury, and F. Vatan. On universal and fault-tolerant quantum computing: a novel basis and a new constructive proof of universality for shor’s basis. In *40th Annual Symposium on Foundations of Computer Science (Cat. No.99CB37039)*, pages 486–494, 1999. doi:10.1109/SFFCS.1999.814621.
- [13] Nicholas Chancellor, Aleks Kissinger, Joschka Roffe, Stefan Zohren, and Dominic Horsman. Coherent parity check construction for quantum error correction. arXiv:1611.08012.
- [14] Bob Coecke and Ross Duncan. Interacting quantum observables. In *Automata, Languages and Programming*, volume 5126, pages 298–310. Springer Berlin Heidelberg, 2008. https://doi.org/10.1007/978-3-540-70583-3_25.
- [15] Bob Coecke and Ross Duncan. Interacting quantum observables: categorical algebra and diagrammatics. *New Journal of Physics*, 13(4):043016, 2011. doi:10.1088/1367-2630/13/4/043016.
- [16] Bob Coecke, Ross Duncan, Aleks Kissinger, and Quanlong Wang. Strong complementarity and non-locality in categorical quantum mechanics. In *Proceedings of the 2012 27th Annual IEEE/ACM Symposium on Logic in Computer Science, LICS ’12*, pages 245–254. IEEE Computer Society, 2012. doi:10.1109/LICS.2012.35.
- [17] Bob Coecke, Ross Duncan, Aleks Kissinger, and Quanlong Wang. *Generalised Compositional Theories and Diagrammatic Reasoning*, pages 309–366. Springer Netherlands, 2016. doi:10.1007/978-94-017-7303-4-10.
- [18] Bob Coecke and Bill Edwards. Three qubit entanglement within graphical z/x-calculus. 52:22–33, 01 2010. doi: 10.4204/EPTCS.52.3.
- [19] Bob Coecke and Aleks Kissinger. The compositional structure of multipartite quantum entanglement. In Samson Abramsky, Cyril Gavoille, Claude Kirchner, Friedhelm

- Meyer auf der Heide, and Paul G. Spirakis, editors, *Automata, Languages and Programming*, pages 297–308, Berlin, Heidelberg, 2010. Springer Berlin Heidelberg. doi:10.1007/978-3-642-14162-1_25.
- [20] Bob Coecke and Aleks Kissinger. *Picturing quantum processes*. Cambridge University Press, 2017.
- [21] Bob Coecke and Quanlong Wang. ZX-rules for 2-qubit Clifford+T quantum circuits. In *Proceedings of the 10th International Conference, Reversible Computation 2018*, LNCS, pages 144–161, 2018. doi:10.1007/978-3-319-99498-7_10.
- [22] Steven A. Cuccaro, Thomas G. Draper, Samuel A. Kutin, and David Petrie Moulton. A new quantum ripple-carry addition circuit. arXiv:quant-ph/0410184, June 2004.
- [23] Shawn X. Cui and Zhenghan Wang. Universal quantum computation with metaplectic anyons. *Journal of Mathematical Physics*, 56(3):032202, 2015. doi:10.1063/1.4914941.
- [24] Niel de Beaudrap and Dominic Horsman. The zx calculus is a language for surface code lattice surgery. 06 2017. arXiv:1704.08670.
- [25] Ross Duncan and Maxime Lucas. Verifying the steane code with quantomatic. In *Proceedings of the 10th International Workshop on Quantum Physics and Logic, QPL 2013, Castelldefels (Barcelona), Spain, July 17-19, 2013.*, pages 33–49, 2013. doi:10.4204/EPTCS.171.4.
- [26] Ross Duncan and Simon Perdrix. Graph states and the necessity of Euler decomposition. *Mathematical Theory and Computational Practice*, 5635:167–177, 2009. doi:10.1007/978-3-642-03073-4_18.
- [27] Ross Duncan and Simon Perdrix. Rewriting measurement-based quantum computations with generalised flow. In *Automata, Languages and Programming*, volume 6199, pages 285–296. Springer Berlin Heidelberg, Berlin, Heidelberg, 2010. doi:10.1007/978-3-642-14162-1_24.
- [28] Ross Duncan and Simon Perdrix. Pivoting makes the ZX-calculus complete for real stabilizers. *Electronic Proceedings in Theoretical Computer Science*, 171:50–62, December 2014. doi:10.4204/EPTCS.171.5.
- [29] W. Dur, G. Vidal, and J. I. Cirac. Three qubits can be entangled in two inequivalent ways. *Phys. Rev.*, A62:062314, 2000. doi:10.1103/PhysRevA.62.062314.

- [30] Brett Giles and Peter Selinger. Exact synthesis of multiqubit Clifford+T circuits. *Phys. Rev. A*, 87:032332, Mar 2013. doi:10.1103/PhysRevA.87.032332.
- [31] Xiaoyan Gong and Quanlong Wang. Equivalence of local complementation and Euler decomposition in the qutrit ZX-calculus. arXiv:1704.05955.
- [32] Amar Hadzihasanovic. A diagrammatic axiomatisation for qubit entanglement. In *2015 30th Annual ACM/IEEE Symposium on Logic in Computer Science*, pages 573–584, July 2015. doi:10.1109/LICS.2015.59.
- [33] Amar Hadzihasanovic. *The algebra of entanglement and the geometry of composition*. PhD thesis, University of Oxford, 2017. arXiv:1709.08086.
- [34] Amar Hadzihasanovic, Kang Feng Ng, and Quanlong Wang. Two complete axiomatisations of pure-state qubit quantum computing. In *Proceedings of the 33rd Annual ACM/IEEE Symposium on Logic in Computer Science, LICS '18*, pages 502–511. ACM, 2018. doi:10.1145/3209108.3209128.
- [35] Michael Herrmann. Models of multipartite entanglement. *Master thesis, University of Oxford*, 2010. <http://www.cs.ox.ac.uk/people/bob.coecke/Michael.pdf>.
- [36] Clare Horsman. Quantum picturalism for topological cluster-state computing. *New Journal of Physics*, 13(9):095011, 2011. doi:10.1088/1367-2630/13/9/095011.
- [37] Erik Hostens, Jeroen Dehaene, and Bart De Moor. Stabilizer states and clifford operations for systems of arbitrary dimensions and modular arithmetic. *Phys. Rev. A*, 71:042315, Apr 2005. doi:10.1103/PhysRevA.71.042315.
- [38] Mark Howard, Eoin Brennan, and Jiri Vala. Quantum contextuality with stabilizer states. *Entropy*, 15(6):2340–2362, 2013. doi:10.3390/e15062340.
- [39] Dan Hu, Weidong Tang, Meisheng Zhao, Qing Chen, Sixia Yu, and C. H. Oh. Graphical nonbinary quantum error-correcting codes. *Phys. Rev. A*, 78:012306, Jul 2008. doi:10.1103/PhysRevA.78.012306.
- [40] Cambridge Quantum Computing Inc. <https://cambridgequantum.com/2017/10/20/collaboration-with-university-of-oxford-computer-science-department/>.
- [41] K. Iwama, Y. Kambayashi, and S. Yamashita. Transformation rules for designing cnot-based quantum circuits. In *Proceedings 2002 Design Automation Conference (IEEE Cat. No.02CH37324)*, pages 419–424, June 2002. doi:10.1109/DAC.2002.1012662.

- [42] Emmanuel Jeandel, Simon Perdrix, and Renaud Vilmart. A complete axiomatisation of the ZX-calculus for Clifford+T quantum mechanics. arXiv:1705.11151v1.
- [43] Emmanuel Jeandel, Simon Perdrix, and Renaud Vilmart. Diagrammatic reasoning beyond Clifford+T quantum mechanics. arXiv:1801.10142.
- [44] Emmanuel Jeandel, Simon Perdrix, and Renaud Vilmart. A generic normal form for ZX-diagrams and application to the rational angle completeness. arXiv:1805.05296.
- [45] Emmanuel Jeandel, Simon Perdrix, Renaud Vilmart, and Quanlong Wang. ZX-calculus: Cyclotomic supplementarity and incompleteness for Clifford+T quantum mechanics. In *42nd International Symposium on Mathematical Foundations of Computer Science, MFCS 2017, August 21-25, 2017 - Aalborg, Denmark*, pages 11:1–11:13, 2017. doi:10.4230/LIPIcs.MFCS.2017.11.
- [46] Andre Joyal and Ross Street. The geometry of tensor calculus, I. *Advances in Mathematics*, 88:55–112, 1991. doi:10.1016/0001-8708(91)90003-P.
- [47] Aleks Kissinger, Alex Merry, Ben Frot, Bob Coecke, David Quick, Lucas Dixon, Matvey Soloviev, Ross Duncan, and Vladimir Zamdzhiev. Quantomatic. <https://quantomatic.github.io/>.
- [48] Shiang Yong Looi and Robert B. Griffiths. Tripartite entanglement in qudit stabilizer states and application in quantum error correction. *Phys. Rev. A*, 84:052306, Nov 2011. doi:10.1103/PhysRevA.84.052306.
- [49] Shiang Yong Looi, Li Yu, Vlad Gheorghiu, and Robert B. Griffiths. Quantum-error-correcting codes using qudit graph states. *Phys. Rev. A*, 78:042303, Oct 2008. doi:10.1103/PhysRevA.78.042303.
- [50] Saunders Mac Lane. *Categories for the Working Mathematician*, volume 5. Springer New York, 1978. <http://dx.doi.org/10.1007/978-1-4757-4721-8>.
- [51] Saunders MacLane. Categorical algebra. *Bulletin of the American Mathematical Society*, 71(1):40–106, 01 1965. <https://projecteuclid.org:443/euclid.bams/1183526392>.
- [52] Mehul Malik, Manuel Erhard, Marcus Huber, Mario Krenn, Robert Fickler, and Anton Zeilinger. Multi-photon entanglement in high dimensions. In *Frontiers in Optics 2016*, page FW3F.1. Optical Society of America, 2016. doi:10.1364/FIO.2016.FW3F.1.

- [53] Anne Marin, Damian Markham, and Simon Perdrix. Access Structure in Graphs in High Dimension and Application to Secret Sharing. In Simone Severini and Fernando Brandao, editors, *TQC 2013 - 8th Conference on the Theory of Quantum Computation, Communication and Cryptography*, volume 22 of *Leibniz International Proceedings in Informatics (LIPIcs)*, pages 308–324, Guelph, Canada, May 2013. Schloss Dagstuhl. 18 pages, 2 figures.
- [54] Ashok Muthukrishnan and C. R. Stroud. Multivalued logic gates for quantum computation. *Phys. Rev. A*, 62:052309, Oct 2000. doi:10.1103/PhysRevA.62.052309.
- [55] Nāgārjuna. *The Fundamental Wisdom of the Middle Way*. Oxford University Press, 1995. Translated by Garfield, Jay L.
- [56] Kang Feng Ng and Quanlong Wang. A universal completion of the ZX-calculus. 2017. arXiv:1706.09877.
- [57] Kang Feng Ng and Quanlong Wang. Completeness of the ZX-calculus for pure qubit clifford+t quantum mechanics. 2018. arXiv:1801.07993.
- [58] Michael A. Nielsen and Isaac L. Chuang. *Quantum Computation and Quantum Information*. Cambridge University Press, Cambridge, 2010. doi:10.1017/CBO9780511976667.
- [59] Simon Perdrix and Quanlong Wang. Supplementarity is Necessary for Quantum Diagram Reasoning. In *41st International Symposium on Mathematical Foundations of Computer Science (MFCS 2016)*, volume 58 of *LIPIcs*, pages 76:1–76:14, 2016. doi:10.4230/LIPIcs.MFCS.2016.76.
- [60] Andre Ranchin. Depicting qudit quantum mechanics and mutually unbiased qudit theories. In *Electronic Proceedings in Theoretical Computer Science*, volume 172 of *EPTCS*, pages 68–91, 2014. doi:10.4204/EPTCS.172.6.
- [61] Christian Schröder de Witt and Vladimir Zamdzhiev. The ZX-calculus is incomplete for quantum mechanics. *EPTCS*, 172:285–292, December 2014. doi:10.4204/EPTCS.172.20.
- [62] Peter Selinger. Autonomous categories in which $A \cong A^*$: (Extended Abstract). *Proceedings of the 7th International Workshop on Quantum Physics and Logic (QPL 2010)*, pages 151–160, 2010.

- [63] Peter Selinger. Finite dimensional hilbert spaces are complete for dagger compact closed categories (extended abstract). *Electronic Notes in Theoretical Computer Science*, 270(1):113 – 119, 2011. <https://doi.org/10.1016/j.entcs.2011.01.010>.
- [64] Peter Selinger and Xiaoning Bian. Relations for Clifford+T operators on two qubits. *Quantum Programming and Circuits Workshop*, June 2015. https://www.mathstat.dal.ca/~xbian/talks/slides_cliffordt2.pdf.
- [65] Vivek V. Shende and Igor L. Markov. On the cnot-cost of TOFFOLI gates. *Quantum Information & Computation*, 9(5):461–486, 2009. <http://www.rintonpress.com/xxqic9/qic-9-56/0461-0486.pdf>.
- [66] Yaoyun Shi. Both toffoli and controlled-not need little help to do universal quantum computing. *Quantum Info. Comput.*, 3(1):84–92, January 2003.
- [67] A. Smith, B. E. Anderson, H. Sosa-Martinez, C. A. Riofrío, Ivan H. Deutsch, and Poul S. Jessen. Quantum control in the $6S_{1/2}$ ground manifold using radio-frequency and microwave magnetic fields. *Phys. Rev. Lett.*, 111:170502, Oct 2013. doi:10.1103/PhysRevLett.111.170502.
- [68] Celso Vieira. Which is more fundamental: processes or things? *Aeon*, 2017. <https://aeon.co/ideas/which-is-more-fundamental-processes-or-things>.
- [69] Quanlong Wang. Qutrit ZX-calculus is complete for Stabilizer Quantum Mechanics. *Electronic Proceedings in Theoretical Computer Science*, 266:58–70, 2018. doi:10.4204/EPTCS.266.3.
- [70] Quanlong Wang and Xiaoning Bian. Qutrit Dichromatic Calculus and Its Universality. *EPTCS*, June 2014. doi:10.4204/EPTCS.172.7.
- [71] Shigeru Yamashita and Igor L. Markov. Fast equivalence - checking for quantum circuits. *Quantum Information & Computation*, 10(9&10):721–734, 2010. <http://www.rintonpress.com/xxqic10/qic-10-910/0721-0734.pdf>.